



Theses and Dissertations

---

2010-09-02

## Axial Temperature Gradients in Gas Chromatography

Jesse Alberto Contreras  
*Brigham Young University - Provo*

Follow this and additional works at: <https://scholarsarchive.byu.edu/etd>



Part of the [Biochemistry Commons](#), and the [Chemistry Commons](#)

---

### BYU ScholarsArchive Citation

Contreras, Jesse Alberto, "Axial Temperature Gradients in Gas Chromatography" (2010). *Theses and Dissertations*. 2645.

<https://scholarsarchive.byu.edu/etd/2645>

This Dissertation is brought to you for free and open access by BYU ScholarsArchive. It has been accepted for inclusion in Theses and Dissertations by an authorized administrator of BYU ScholarsArchive. For more information, please contact [scholarsarchive@byu.edu](mailto:scholarsarchive@byu.edu), [ellen\\_amatangelo@byu.edu](mailto:ellen_amatangelo@byu.edu).

Axial Temperature Gradients in Gas Chromatography

Jesse Alberto Contreras Miranda

A dissertation submitted to the faculty of  
Brigham Young University  
in partial fulfillment of the requirements for the degree of

Doctor of Philosophy

Milton L. Lee  
Steven R. Goates  
H. Dennis Tolley  
David V. Dearden  
Aaron R. Hawkins

Department of Chemistry and Biochemistry

Brigham Young University

December 2010

Copyright © 2010 Jesse Alberto Contreras Miranda

All Rights Reserved

## ABSTRACT

### Axial Temperature Gradients in Gas Chromatography

Jesse Alberto Contreras Miranda

Department of Chemistry and Biochemistry

Doctor of Philosophy

The easiest and most effective way to influence the separation process in gas chromatography (GC) is achieved by controlling the temperature of the chromatographic column. In conventional GC, the temperature along the length of the column is constant at any given time,  $T(t)$ . In my research, I investigated the effects of temperature gradients on GC separations as a function of time and position,  $T(t,x)$ , along the column. This separation mode is called thermal gradient GC (TGGC). The research reported in this dissertation highlights the fundamental principles of axial temperature gradients and the separation potential of the TGGC technique. These goals were achieved through the development of mathematical models and instrumentation that allowed study of the effects of axial temperature gradients. The use of mathematical models and computer simulation facilitated evaluation of different gradient profiles and separation strategies prior to development of the instrumentation, providing theoretical proof of concept. Three instruments capable of generating axial temperature gradients, based on convective cooling and resistive heating, were developed and evaluated. Unique axial temperature gradients, such as nonlinear and moving sawtooth temperature gradients with custom profiles were generated and evaluated. The results showed that moving sawtooth temperature gradients allowed continuous analysis and were well-suited for comprehensive GC×GC separations. The use of custom temperature profiles allowed unique control over the separation power of the system, improving separations, as well as selectively increasing the peak capacity and signal-to-noise. A direct comparison of TGGC with conventional GC methods showed that TGGC produces equivalent separations to temperature programmed GC. This technology holds great promise for performing smart separations in which the column volume is most efficiently utilized and optimum separations can be quickly achieved. Moreover, precise control of the elution of compounds can be used to greatly reduce method development time in GC. This feature can be automated using feedback to develop efficient separations with minimum user intervention. This technology is of special interest in micro-GC systems, which allows relatively easy incorporation of resistive heating elements in the micro-column design.

Keywords: gas chromatography, chromathermography, axial temperature gradient, feedback control, thermal gradient, resistive heating.

## ACKNOWLEDGEMENTS

The accomplishments in life are always greatly influenced by the help and support of others. This dissertation is no exception. I am very grateful for all of the encouragement that I have received from family, friends, and faculty. I express my gratitude to all who have made this journey joyful and possible.

To my advisor, Dr. Milton Lee, I am forever grateful for giving me the opportunity to be part of his research group and allowing me to explore my own ideas. I thank him for sharing his wisdom and always being supportive and kind. His work ethic and humbleness will always be a model to follow. I also thank past and present members of Dr. Lee's group for providing a nice, friendly environment that allowed good discussions and research. I especially thank Anzi Wang for his hard work during these last months gathering data and learning the techniques and instrumentation; he will continue this exciting research and, hopefully, enjoy the next phase of the journey.

I want to thank, as well, Dr. Dennis Tolley, whose words of encouragement and advice kept my outlook always on the bright side. It has been a pleasure working with him. I thank my committee members, Dr. Steven Goates, Dr. David Dearden and Dr. Aaron Hawkins for their encouragement, suggestions, and advice during my annual reviews.

Many professors and staff members at BYU have contributed to solutions to problems encountered during my research. Without Dr. Matt Asplund's advice in Matlab programming and use of the supercomputer, the simulations would still be running. I thank Dr. Dan Maynes for lending me the infrared camera and sharing his experience in fluid dynamics to improve the most recent system design. I appreciate the help and friendship of Therin Garrett from the Precision Machining Lab for helping me build the instrument parts quickly and precisely.

Special thanks go to Valco VICI, particularly to Chris Bishop, whose work on resistive heating technology made my work possible. I thank him for his help and willingness to share his technology and experience. I am very grateful for the funding provided by Torion Technologies and the knowledge I gained by being part of that team. I appreciate the work and time that Randy Waite and Scott Losee put on the development of the custom temperature circuit board controllers, as well as to Tony Rands for help in designing the instrumentation developed in this

work. I also appreciate the Chemistry & Biochemistry Department for providing a good environment to do research.

This journey would not have been possible without being introduced to the exciting world of gas chromatography. For this, I thank Wayne Rubey and Richard Striebitch at the University of Dayton. Their insightful discussions about thermal gradient gas chromatography definitely grabbed my attention.

During this journey, I have made many good friends, especially Jacolin Murray. I thank her for her encouragement, support and friendship; my family and I will miss her. I greatly appreciate the proofreading she did for me, and cherish our many discussions. We had great times during this journey, and I hope to share more successes in the future. I greatly appreciate Dr. Andres Fullana from the University of Alicante, Spain, whose discussions and clever suggestions made a difference in this work. I thank him for teaching me not only science, but also a different way of looking at life that has helped me overcome moments of doubt. I am grateful for his wisdom, kindness and friendship.

Finally and most importantly, I thank my family. My father has been a great inspiration to me. As a professor, he never slowed in his endeavors. While many have benefitted from his passion of learning and teaching, no person has benefitted from this more than me. I thank you, Dad, and love you for instilling in me a good foundation of moral values. My mother has cheered for me since day one. Her faith and confidence in my abilities have helped me reach this point in my life. This work is a result of her encouragement. I hope to be as good to my children as she has been to me. I thank you, Mom, and I love you. Thank you Marites and Michelle, my sisters, for cheering for me and being there to offer support and help whenever I needed it. My wife Evelyn has been an enduring source of strength and encouragement. Thank you, Nene, for your support, especially during these last months which you endured alone with the babies while I finished writing this dissertation. This achievement has been a team effort; the success is ours. I thank you for your patience and for always being there for me. I love you. I dedicate this dissertation to you and our babies, Kevin and David.

Brigham Young University

SIGNATURE PAGE

of a dissertation submitted by

Jesse Alberto Contreras Miranda

The dissertation of Jesse Alberto Contreras Miranda is acceptable in its final form including (1) its format, citations, and bibliographical style are consistent and acceptable and fulfill university and department style requirements; (2) its illustrative materials including figures, tables, and charts are in place; and (3) the final manuscript is satisfactory and ready for submission.

\_\_\_\_\_  
Date

\_\_\_\_\_  
Milton L. Lee, Committee Chair

\_\_\_\_\_  
Date

\_\_\_\_\_  
Steven R. Goates, Committee Member

\_\_\_\_\_  
Date

\_\_\_\_\_  
H. Dennis Tolley, Committee Member

\_\_\_\_\_  
Date

\_\_\_\_\_  
David V. Dearden, Committee Member

\_\_\_\_\_  
Date

\_\_\_\_\_  
Aaron R. Hawkins, Committee Member

\_\_\_\_\_  
Date

\_\_\_\_\_  
Matthew R. Linford, Graduate Coordinator

\_\_\_\_\_  
Date

\_\_\_\_\_  
Thomas W. Sederberg  
Associate Dean, College of Physical and  
Mathematical Sciences

# TABLE OF CONTENTS

<b>LIST OF FIGURES.....</b>	<b>XVI</b>
<b>LIST OF TABLES.....</b>	<b>XXV</b>
<b>LIST OF ABBREVIATIONS.....</b>	<b>XXVII</b>
<b>LIST OF SYMBOLS.....</b>	<b>XXVIII</b>
<b>1 INTRODUCTION.....</b>	<b>1</b>
1.1 IMPORTANCE OF TEMPERATURE IN GC SEPARATIONS.....	4
1.2 HEAT TRANSFER FUNDAMENTALS .....	6
1.3 HEATING METHODS IN GC .....	8
1.3.1 Vapor Jacket.....	9
1.3.2 Dewar Flask.....	10
1.3.3 Oil Bath.....	10
1.3.4 Heat Exchanger.....	12
1.3.5 Air Bath Oven.....	13
1.3.6 Resistive Heating.....	17
1.3.7 Infrared Heating.....	19
1.3.8 Microwave Heating.....	20
1.3.9 Inductive Heating.....	22
1.4 COOLING METHODS IN GC.....	23
1.4.1 Forced Air Convection.....	24
1.4.2 Cooling Fixture .....	24
1.4.3 Cryogenic Fluids.....	24
1.4.4 Vortex Cooler.....	26
1.4.5 Peltier Cooler.....	27
1.5 RESISTIVE HEATING IN GC .....	29
1.5.1 Overview .....	29

1.5.1.1	Direct Resistive Heating.....	32
1.5.1.2	On-column Wire Resistive Heating.....	33
1.5.1.3	Resistively Heated Column Fixtures .....	35
1.5.2	<i>Commercially Available Resistive Heating Systems</i> .....	36
1.5.3	<i>Direct Resistive Heating of Metal Capillary Columns</i> .....	40
1.5.4	<i>Resistive Heating in Microcolumn GC Systems</i> .....	42
1.6	THERMAL GRADIENT GC (TGGC) .....	43
1.7	AXIAL TEMPERATURE GRADIENTS IN GC .....	49
1.7.1	<i>Controversy Around TGGC</i> .....	58
1.8	MODERN TRENDS AND CHALLENGES IN GC .....	60
1.9	DISSERTATION OVERVIEW.....	61
1.10	REFERENCES .....	62
<b>2</b>	<b>DEVELOPMENT OF A SIMPLE MATHEMATICAL PLATE MODEL FOR SIMULATING THE EFFECT OF AXIAL TEMPERATURE GRADIENTS IN GAS CHROMATOGRAPHY .....</b>	<b>73</b>
2.1	INTRODUCTION .....	73
2.2	MATHEMATICAL MODEL.....	75
2.3	EXPERIMENTAL.....	82
2.4	RESULTS AND DISCUSSION .....	84
2.5	CONCLUSIONS .....	98
2.6	REFERENCES .....	99
<b>3</b>	<b>MATHEMATICAL SOLUTION TO PEAK POSITION IN MOVING THERMAL GRADIENT GAS CHROMATOGRAPHY.....</b>	<b>101</b>
3.1	INTRODUCTION .....	101
3.2	PRELIMINARY CONSIDERATIONS.....	103
3.3	MODEL.....	106
3.4	DETERMINATION OF THE CHARACTERISTIC EQUILIBRIUM TEMPERATURE .....	107



3.5	PEAK LOCATION AND WIDTH UNDER GRADIENT CONDITIONS.....	109
3.6	VALIDATION OF THE MODEL .....	113
3.7	APPLICATIONS OF THE EQUATIONS .....	114
3.8	CONCLUSIONS .....	119
3.9	REFERENCES .....	120
<b>4</b>	<b>PEAK SWEEPING AND GATING USING THERMAL GRADIENT GAS</b>	
	<b>CHROMATOGRAPHY .....</b>	<b>122</b>
4.1	INTRODUCTION .....	122
4.2	MATERIALS AND METHODS .....	123
4.3	RESULTS AND DISCUSSION .....	128
	4.3.1 Generation of Axial Temperature Gradients.....	128
	4.3.2 Peak Sweeping.....	130
4.4	EXPERIMENTAL COMPARISON OF THE DIFFERENT GC SEPARATION MODES.....	134
4.5	PEAK GATING.....	140
4.6	APPLICATION OF TGGC TO A COMPLEX SAMPLE.....	143
4.7	CONCLUSIONS .....	145
4.8	REFERENCES .....	148
<b>5</b>	<b>MOVING THERMAL GRADIENT GAS CHROMATOGRAPHY .....</b>	<b>150</b>
5.1	INTRODUCTION .....	150
5.2	MATERIALS AND METHODS .....	152
	5.2.1 Construction and Operation of the Moving TGGC System.....	152
	5.2.2 Construction and Operation of the Comprehensive GC×TGGC System .....	160
5.3	RESULTS AND DISCUSSION .....	162
	5.3.1 TGGC System Development .....	162
	5.3.2 Generation of Axial Temperature Gradients.....	163
	5.3.3 Continuous Analysis of Normal Alkanes .....	167

5.3.4	<i>Use of Moving TGGC as Modulator and Second Dimension Separation Technique in Comprehensive GC×GC Separations</i> .....	172
5.4	CONCLUSIONS .....	176
5.5	REFERENCES .....	178
<b>6</b>	<b>MOVING THERMAL GRADIENT GC WITH CUSTOM TEMPERATURE PROFILES .....</b>	<b>180</b>
6.1	INTRODUCTION .....	180
6.2	MATERIALS AND METHODS .....	183
6.2.1	<i>Construction and Operation of the Moving TGGC System</i> .....	183
6.2.2	<i>Development of a Resistively Heated TPGC Column Assembly</i> .....	190
6.3	RESULTS AND DISCUSSION .....	193
6.3.1	<i>Generation of Temperature Gradients</i> .....	193
6.3.2	<i>Testing of the Moving TGGC System</i> .....	199
6.3.3	<i>Effect of Axial Temperature Gradients on Separation</i> .....	201
6.3.4	<i>Use of Custom Gradient Profiles</i> .....	210
6.3.5	<i>Experimental Comparison of Moving TGGC with TPGC Separations</i> .....	213
6.4	CONCLUSIONS .....	222
6.5	REFERENCES .....	224
<b>7</b>	<b>CONCLUSIONS AND FUTURE WORK .....</b>	<b>226</b>
7.1	CONCLUSIONS .....	226
7.2	RECOMMENDATIONS FOR FUTURE RESEARCH .....	228
7.2.1	<i>Effects of Axial Temperature Gradient Resolution and Stationary Phase Film Thickness on Peak Width</i> .....	228
7.2.2	<i>Retention Indices in TGGC for the Identification of Analytes</i> .....	229
7.2.3	<i>Improvement of the Simulation Model</i> .....	231
7.2.4	<i>Use of Feedback Control with Moving TGGC</i> .....	231
7.2.5	<i>Use of Moving TGGC as Modulator and Second Dimension Separation in Comprehensive GC×GC Separations</i> .....	234

7.2.6	<i>Application of Moving TGGC in Micro-GC Technology</i> .....	235
7.2.7	<i>Lab-size TGGC System for Long Columns</i> .....	242
7.2.8	<i>Extended Moving TGGC: a Leap into the Future of Portable GC Systems</i> .....	243
7.2.9	<i>Applications of Axial Temperature Gradients in Other Separation Areas</i> .....	247
7.3	REFERENCES .....	255

## LIST OF FIGURES

Figure 1-1. Vapor jacket heating system for packed GC columns. ....	10
Figure 1-2. Dewar flask for maintaining the GC column at constant temperature. ....	11
Figure 1-3. Oil bath system for heating coiled packed chromatographic columns. ....	12
Figure 1-4. Heat exchanger system for capillary GC columns. ....	13
Figure 1-5. Diagram of a convective oven illustrating its different components. ....	16
Figure 1-6. Diagram of a resistively heated fused-silica column inserted through a coaxial metal sheath. ....	18
Figure 1-7. Cross section diagram of an infrared heating oven. ....	20
Figure 1-8. Schematic of a microwave heated coated column. ....	21
Figure 1-9. Diagram of an inductively heating column fixture. ....	23
Figure 1-10. Diagram illustrating the operation of a vortex cooler. ....	27
Figure 1-11. Classification of heating and cooling methods by heat transfer mechanism. ....	28
Figure 1-12. Three-dimensional views of the operational modes of GC. <sup>25, 32</sup> ....	47
Figure 1-13. Focusing mechanism of migrating zone. <sup>29, 36, 165</sup> ....	48
Figure 2-1. Retention factors determined from isothermal separations at various temperatures between 40°C and 210°C. ....	85
Figure 2-2. Retention time differences for alkanes versus number of segments used in the model, and simulation time for a temperature programmed separation from 40°C (1 min hold) to 210°C (1 min hold) at a heating rate of 20°C/min. ....	87
Figure 2-3. Plot of measured isothermal retention time versus predicted value. ....	89
Figure 2-4. Peak width of nonane (n-C <sub>9</sub> ) versus number of segments/m and simulation time. ....	91
Figure 2-5. Predicted and measured van Deemter plots for n-dodecane using a 130°C using a 3 m x 0.1 mm x 0.4 µm DB-5 column. ....	92

Figure 2-6.	Comparison of predicted and experimentally obtained chromatograms. Simulations were performed using 1500 segments/m. Conditions: as described in the experimental section; (A) Isothermal separation at 150°C. (B) Temperature programmed from 40°C (60 s hold) to 210°C (60 s hold) at 20°C/min. ....	93
Figure 2-7.	Peak areas of n-alkanes from the experimental temperature programmed chromatogram in Figure 2-6A. ....	94
Figure 2-8.	Experimental chromatograms resulting from two different moving sawtooth axial temperature gradient profiles for continuous sampling of three n-alkanes from headspace. Separation conditions: 60 psig head pressure, 2.28 mL/min He mobile phase flow, and 2.22 cm/s (45 s/rev) gradient linear velocity. ....	95
Figure 2-9.	Comparison of predicted and experimentally obtained chromatograms from TGGC separations. Conditions: 2.22 cm/s gradient velocity; 2.28 mL/min mobile phase flow rate; (A) 5.75°C/cm gradient slope; (B) 0.77°C/cm gradient slope of. Simulations were performed with 1500 segments/m. ....	96
Figure 2-10.	Snapshots of n-alkanes as they travel and separate along the column during moving sawtooth temperature gradient operation with continuous sample injection. The temperature gradient profile is also plotted. ....	97
Figure 3-1.	Diagram showing a moving linear temperature gradient with slope $b$ at time $t > 0$ , describing the different variables of the model. ....	106
Figure 3-2.	Temperature profiles of a moving sawtooth axial temperature gradient and resultant repetitive chromatograms for continuous sampling of normal alkane vapors performed under different conditions. (A) $u_m = 96.3$ cm/s, $w = 9.09$ cm/s, (B) $u_m = 155.1$ cm/s, $w = 22.2$ cm/s. (C) $u_m = 138.3$ cm/s, $w = 22.2$ cm/s. ....	115
Figure 3-3.	Retention factor and mobile phase velocity as a function of $T_{eq}$ for normal alkanes. ....	118
Figure 3-4.	Effect of the mobile phase linear velocity on calculations of the $T_{eq}$ values for various normal alkane compounds for $u_m = 120$ cm/s. ....	118
Figure 4-1.	Configuration for resistively heating the fused silica capillary column. ....	124
Figure 4-2.	Heat exchanger configuration for generating (A) concave down and (B) concave up profiles. ....	126
Figure 4-3.	Power circuit that controlled the voltage of the resistively heated Ni sleeve through a custom LabVIEW program. ....	127

Figure 4-4. TGGC system for generating concave down axial temperature gradient profiles. ....	128
Figure 4-5. Example of axial temperature gradient profiles generated with the TGGC heat exchanger system. Concave down profile: 8 L/min room temperature nitrogen while 2.5 V was applied to the Ni sleeve. Concave up profile: 8 L/min preheated nitrogen gas with no resistive heating of the Ni sleeve.....	129
Figure 4-6. Thermal field showing heating of a concave down axial temperature gradient. Cold nitrogen at a flow of 10 L/min in combination with 4 V potential applied to the Ni sleeve. Heating at 2300°C/min was achieved by turning off the nitrogen flow and increasing the voltage to 12 V.....	130
Figure 4-7. TGGC separations of n-alkanes using a concave down profile and sweeping operation at different different times (A and B) (arrows represent the times when the column was heated at 130°C/min to release the analytes). The gradient profile used is shown in Figure 4-5. The mobile phase flow rate was 0.35 mL/min.....	132
Figure 4-8. TGGC separation of n-alkanes using a concave up profile and sweeping operation (arrow represents the time when the column was heated to release the analytes at a heating rate of 130°C/min). The temperature profile used is shown in Figure 4-5. The mobile phase flow rate was 0.35 mL/min.....	133
Figure 4-9. GC analysis of normal alkanes using different separation modes. The arrow indicates when the temperature gradient was increased (sweeping).....	138
Figure 4-10. Resolution comparison of the different separation modes. ....	139
Figure 4-11. GC analyses of a 26 component EPA Method 624 volatile halocarbon mixture using different separation modes. The red arrow indicates when the gradient was heated in B. Peak identifications: (1) 1,1-dichloroethane, (2) methylene chloride, (3) trans-1,2-dichloroethene, (4) 1,1-dichloroethane, (5) chloroform, (6) 1,2-dichloroethane, (7) 1,1,1-trichloroethene, (8) benzene, (9) carbon tetrachloride, (10) 1,2-dichloropropane, (11) trichloroethylene, (12) bromodichloromethane, (13) 2-chloroethylvinyl ether, (14) <i>cis</i> -1,3-dichloropropene, (15) <i>trans</i> -1,3-dichloropropene, (16) toluene, (17) 1,1,2-trichloroethene, (18) dibromochloromethane, (19) tetrachloroethene, (20) chlorobenzene, (21) ethyl benzene, (22) bromoform, (23) 1,1,2,2-tetrachloroethane, (24) 1,3-dichlorobenzene, (25) 1,4-dichlorobenzene, (26) 1,2-dichlorobenzene. ....	141
Figure 4-12. Concave down thermal field for a typical peak gating operation, where heating and cooling rates as high as 4000 and 3500°C/min, respectively, can be achieved. ....	142

Figure 4-13. Application of TGGC gating to selectively separate the n-alkanes. Red and blue arrows indicate when the gradient was heated and cooled, respectively. Peak identifications: (1) n-C <sub>9</sub> , (2) n-C <sub>10</sub> , (3) n-C <sub>11</sub> , (4) n-C <sub>12</sub> , and (5) n-C <sub>13</sub> .	144
Figure 4-14. Application of different TGGC operations for separation of a 26 component EPA Method 624 volatile halocarbon mixture. The red and blue arrows indicate when the gradient was heated and cooled at a heating rate of 4000 and 3500°C/min, respectively. The red brackets indicate static gradient separation of the analytes. For peak identifications, see Figure 4-11.	146
Figure 5-1. Diagram of the movement of an analyte in a moving temperature gradient. $T_{eq}$ = characteristic equilibrium temperature, $v_{peak}$ = peak linear velocity and $w$ = gradient linear velocity.	151
Figure 5-2. Configuration for resistively heating the fused silica capillary column.	153
Figure 5-3. Diagram illustrating the generation of a moving temperature gradient by the application of a liquid CO <sub>2</sub> jet stream. $t_0$ = initial column status at high temperature (red dotted line), $t_1$ = nitrogen jet stream on (dashed line), $t_2$ & $t_3$ = moving jet stream and formation of the moving temperature gradient (green and blue lines, respectively).	154
Figure 5-4. System configuration for generating a moving sawtooth temperature gradient for TGGC.	155
Figure 5-5. Diagram of temperature gradient generation for a sawtooth type profile by simultaneously cooling two resistively heated loops. $t_0$ = initial column status at high temperature (dotted line), $t_1$ = the two nitrogen jet streams on (dashed line), $t_2$ = moving jet stream and formation of the saw-tooth profile along the column (blue line).	156
Figure 5-6. Cad drawing of the moving TGGC system.	157
Figure 5-7. Photograph of the column support structure.	157
Figure 5-8. Photograph of the moving TGGC system.	159
Figure 5-9. Configuration of the continuous head space sampling system.	159
Figure 5-10. Diagram of the comprehensive GC×TGGC system.	161
Figure 5-11. Snapshots at two different times from a simulation of the separation of normal alkanes as they travelled and separated along the column during a concave down moving sawtooth temperature gradient operation with continuous sample injection. The temperature gradient profile is also plotted.	164

Figure 5-12. Diagram of the moving sawtooth temperature gradient GC process. ....	165
Figure 5-13. Moving sawtooth temperature gradient profile. Ni sleeve voltage of 15.3 V, 11 s/loop or 9.09 cm/s gradient linear velocity. ....	165
Figure 5-14. Moving sawtooth temperature gradient profile. 3.8 V Ni sleeve voltage, 11 s/loop or 9.09 cm/s gradient linear velocity. ....	166
Figure 5-15. Thermal field of a moving sawtooth axial temperature gradient. ....	166
Figure 5-16. Temperature profile of a moving sawtooth axial temperature gradient (i.e., thermal wave) and resultant repetitive chromatograms for continuous sampling of normal alkane vapors. The pink dashed line represents the characteristic equilibrium temperature of C <sub>11</sub> . The average resolutions are C <sub>11</sub> -C <sub>12</sub> = 6.4, C <sub>12</sub> -C <sub>13</sub> = 5.6, and C <sub>13</sub> -C <sub>14</sub> = 4.1. The separation conditions were: 52.6 psig head pressure, 1.44 mL/min mobile phase flow, 9.09 cm/s gradient linear velocity and 15 V Ni sleeve voltage. ....	168
Figure 5-17. Isothermal separations of normal alkanes for different injection times. The column temperature was 170°C. ....	170
Figure 5-18. Three dimensional view of a GCxTGGC separation of kerosene. ....	175
Figure 5-19. 2D chromatogram of a GCxTGGC kerosene separation, showing the one-dimensional chromatogram separation on top and a second dimension chromatogram obtained at a retention time of 59.6 min (segmented line) on the right. ....	176
Figure 6-1. Diagram illustrating analytes traveling in a moving temperature gradient. ....	181
Figure 6-2. Diagram showing the unique separation potential of the moving TGGC technique that allows optimization of separations by customizing the gradient profile. ....	182
Figure 6-3. Diagram illustrating the generation of a moving temperature gradient by resistively heating individual sections of the column with forced convection cooling. Grey lines represent the separation between individual resistively heated sections. t <sub>0</sub> = initial column status at a low temperature (red dotted line), t <sub>1</sub> = gradually resistively heating the first segments of the column (dashed line), t <sub>2</sub> & t <sub>3</sub> = fully developed moving temperature gradient (green and blue lines, respectively). ....	184
Figure 6-4. Diagram illustrating the generation of a moving sawtooth temperature gradient by simultaneously heating two column loops using individually resistively heated segments in combination with forced convection cooling. Grey lines represent the separation between individual resistively heated sections. t <sub>0</sub> = initial column status at a low temperature	



	(red dotted line), $t_1$ = beginning of the formation of the temperature gradients (dashed line), $t_2$ = fully developed moving sawtooth temperature gradient (blue line).....	185
Figure 6-5.	Configuration of the individual resistively heated coils with pulse modulation control for the generation of custom temperature gradient profiles. ....	186
Figure 6-6.	Photograph of the tightly wind Nichrome 80 wires, showing the individual resistively heated sections.....	186
Figure 6-7.	System configuration for generating custom moving sawtooth temperature gradient profiles. ....	188
Figure 6-8.	Photograph of the moving TGGC system with individual resistively heated sections for the generation of custom temperature gradients. ....	189
Figure 6-9.	Diagram of the resistively heated assembly for TPGC and ITGC separations.....	192
Figure 6-10.	Photographs showing (A) 5 m commercially available LTM-GC assembly, (B) 3.5 m resistive heating assembly described in this work, and (C) close up showing both columns side by side. ....	192
Figure 6-11.	Heating and cooling capabilities of the resistively heated sections with continuous forced air convection cooling. A heating rate of 1200°C/min and cooling from 300 to 50°C in less than 6 s was typical. ....	194
Figure 6-12.	Sawtooth linear temperature gradient profiles with different slopes. (a) 0.73°C/cm, (b) 1.44°C/cm, (c) 2.07°C/cm and (d) 2.75°C/cm. The gradient velocity was 2.22 cm/s (45 s/rev). ....	195
Figure 6-13.	Sawtooth linear temperature profiles as a function of gradient linear velocity; the heating voltage and times for heating and cooling were kept constant. (A) 25 s/rev, (B) 15 s/rev, (C) 10 s/rev and (D) 5 s/rev.....	195
Figure 6-14.	Different sawtooth temperature gradient profiles generated with the moving TGGC system. (A) Linear, (B) two slopes low-high, (C) two slopes high-low (D) concave down, (E) concave up, and (F) combination of concave up and down profiles. A gradient velocity of 2.22 cm/s (45 s/rev) was used. ....	197
Figure 6-15.	Infrared photographs of the moving TGGC system showing a linear temperature gradient moving around the column loop. The white arrows indicate the clockwise rotation direction of the moving gradient.....	198
Figure 6-16.	Continuous analysis of n-alkane vapors using a moving sawtooth temperature profile, with resultant repetitive chromatograms. Zoom of	

the chromatogram shows the temperature gradient profile used. The average resolution values are  $C_{12}-C_{13} = 4.1$ , and  $C_{13}-C_{14} = 3.8$ . The separation conditions were: 70 psig head pressure, 2.88 mL/min mobile phase flow, 2.22 cm/s (45 s/rev) gradient velocity, and 1.64°C/cm gradient slope for the largest linear temperature region. ....200

Figure 6-17. Peak width of  $C_{13}$  as a function of the amount of sample injected for two different gradient slopes. To the right of the horizontal line in the plots, the effect of a larger amount of sample is shown. Separation conditions: 60 psig head pressure, 2.28 mL/min mobile phase flow, and 2.22 cm/s (45 s/rev) gradient velocity. ....202

Figure 6-18. Peak width of polar (decylamine) and nonpolar ( $n-C_{13}$ ) compounds as a function of the gradient slope. Separation conditions: 60 psig head pressure, 2.28 mL/min mobile phase flow, and 2.22 cm/s (45 s/rev) gradient velocity.....204

Figure 6-19. Peak symmetry of polar (decylamine) and nonpolar ( $n-C_{13}$ ) compounds as a function of gradient slope for a column coated with a slightly polar stationary phase (5% diphenyl, 95% dimethyl polysiloxane). Separation conditions: 60 psig head pressure, 2.28 mL/min mobile phase flow rate, and 2.22 cm/s (45 s/rev) gradient velocity. ....205

Figure 6-20. Peak shape comparison of isothermal and moving TGGC separations of nonylamine and decylamine. For the isothermal separation,  $As_{\text{nonylamine}} = 6.3$  and  $As_{\text{decylamine}} = 6.8$ , with a resolution of 1.5. For the moving TGGC separation,  $As_{\text{nonylamine}} = 1.0$  and  $As_{\text{decylamine}} = 0.9$ , with a resolution of 5.1. Separation conditions: 195°C for the isothermal separation, 20 psig head pressure, 0.34 mL/min mobile phase flow, 3.28°C/cm gradient slope, and 2.22 cm/s (45 s/rev) gradient velocity. ....206

Figure 6-21. Peak width as a function of the mobile phase linear velocity for constant gradient slope and velocity. Separation conditions: 60 psig head pressure, 2.28 mL/min mobile phase flow, 2.22 cm/s (45 s/rev) gradient velocity, and 2.75°C/cm gradient slope. The linear sawtooth profile used is plot d in Figure 6-12.....208

Figure 6-22. Van Deemter plot for  $C_{13}$  where HETP is the height equivalent to a theoretical plate.<sup>10</sup> For isothermal separations, the entire TGGC column length was held constant at 125°C. ....208

Figure 6-23. Resolution of 2 normal alkane pairs ( $C_{12}-C_{13}$  and  $C_{13}-C_{14}$ ) as a function of the mobile phase linear velocity for a constant moving TGGC gradient slope. Separation conditions: 2.22 cm/s (45 s/rev) gradient velocity and 2.75°C/cm gradient slope. The linear sawtooth profile used is plot d in Figure 6-12.....209

Figure 6-24. Separation of normal alkanes (C <sub>12</sub> -C <sub>14</sub> ) using different gradient slopes. Linear sawtooth profiles were used. Separation conditions: 60 psig head pressure, 2.28 mL/min mobile phase flow, 2.22 cm/s (45 s/rev) gradient velocity.....	211
Figure 6-25. Resolution of two pairs of normal alkanes (C <sub>12</sub> -C <sub>13</sub> and C <sub>13</sub> -C <sub>14</sub> ) as a function of the temperature gradient slope. Separation conditions: 20 psig head pressure, 0.34 mL/min mobile phase flow, 2.22 cm/s (45 s/rev) gradient velocity, and 2.75°C/cm gradient slope. ....	212
Figure 6-26. Chromatograms resulting from four different custom moving sawtooth axial temperature gradient profiles for continuous sampling of three normal alkane vapors. The chromatograms show the unique control of selectivity using the TGGC technique. Separation conditions: 60 psig head pressure, 2.28 mL/min mobile phase flow, and 2.22 cm/s (45 s/rev) gradient velocity. The <i>T<sub>eq</sub></i> for the alkanes were C <sub>12</sub> = 77.7°C, C <sub>13</sub> = 90.0°C, and C <sub>14</sub> = 99.3°C. ....	214
Figure 6-27. Separation of normal alkanes (C <sub>12</sub> -C <sub>14</sub> ) using a custom gradient profile for maximizing resolution and S/N. Separation conditions: 20 psig head pressure, 0.34 mL/min mobile phase flow, 8.2°C/cm gradient slope where the <i>T<sub>eq</sub></i> values of the peaks were located, and 2.22 cm/s (45 s/rev) gradient velocity. The <i>T<sub>eq</sub></i> for the alkanes were C <sub>12</sub> = 99°C, C <sub>13</sub> = 111°C, and C <sub>14</sub> = 128°C. Resolution: C <sub>12</sub> -C <sub>13</sub> = 46.5 and C <sub>13</sub> -C <sub>14</sub> = 41.5. ....	215
Figure 6-28. Heating and cooling temperature ramp of the new 1 m resistively heated TPGC assembly with heating rates as high as 2100°C/min and a cooling rate from 200 to 50°C in 32 s. ....	216
Figure 6-29. Reproducibility of the separation of normal alkanes (C <sub>12</sub> -C <sub>14</sub> ) using the new resistively heated TPGC column assembly. ....	217
Figure 6-30. GC analysis of normal alkanes (C <sub>12</sub> -C <sub>14</sub> ) using different separation modes. Separation conditions for TGGC: 20 psig head pressure (for both methods), 0.34 mL/min mobile phase flow, and 2.22 cm/s (45 s/rev) gradient velocity. For the TPGC separations, no hold times for the initial and final temperatures were used. ....	218
Figure 6-31. GC analysis of the headspace of frankincense (India) essential oil using different separation modes. Separation conditions for TGGC: 20 psig head pressure, 0.34 mL/min mobile phase flow, 180-32°C linear gradient, 2.39°C/cm gradient slope, and 2.22 cm/s (45 s/rev) gradient velocity. For TPGC: initial temperature 28°C (0 s hold) to 180°C (0 s hold) @ 70°C/min, 20 psig head pressure. ....	220
Figure 6-32. GC analysis of the head space of frankincense (India) essential oil by moving TGGC with a custom temperature profile and by TPGC. The brackets indicate the areas where the separation was improved.	

Separation conditions for TGGC: 20 psig head pressure, 0.34 mL/min mobile phase flow, 180-32°C linear gradient, 2.39°C/cm gradient slope, and 2.22 cm/s (45 s/rev) gradient velocity. For TPGC: initial temperature 88°C (0 s hold) to 120°C (0 s hold) @ 26°C/min, 20 psig head pressure.....	221
Figure 7-1. Linearity of measured $T_{eq}$ values with respect to the carbon number of n-alkanes, demonstrating that they could be used for the calculation of retention indices. The $T_{eq}$ values were obtained from separations shown in Chapter 6. (A) Values from Figure 6-27. (B) Values from Figure 6-26. (C) Values from Figure 6-16.....	231
Figure 7-2. Schematic diagram showing how different temperature gradient profiles result in different chromatographic resolution. The right chromatogram shows the optimum profile.....	233
Figure 7-3. Schematic diagram showing computer control of the feedback system for optimizing a separation. ....	233
Figure 7-4. Diagram of a microfabricated GC column design that incorporates resistively heated sections to implement the TGGC technique for improving the separation performance of current micro-GC systems.....	238
Figure 7-5. Diagram showing a temperature gradient profile that may result from a microfabricated GC column design that incorporates the use of resistively heated sections to implement the TGGC technique. ....	239
Figure 7-6. Diagram of a multichannel microfabricated GC system to improve the sample capacity and sensitivity of the system. ....	240
Figure 7-7. Diagram showing different views of a micro-GC column.....	241
Figure 7-8. Diagram showing a micro-GC assembly including Peltier cooler.....	242
Figure 7-9. Diagram of a TGGC instrument to accommodate a 30 m capillary column.....	243
Figure 7-10. Diagram of the TGGC virtual column concept.....	244
Figure 7-11. Simulations showing the effect on resolution of using temperature gradients equivalent to longer column lengths. ....	246

## LIST OF TABLES

Table 1-1. Overview of resistive heating instrumentation development in gas chromatography. ....	44
Table 1-2. Overview of the instrumentation development of TGGC .....	55
Table 2-1. Normal alkane thermodynamic properties determined from various isothermal experiments. ....	86
Table 2-2. Retention time comparison of normal alkanes for four different isothermal temperatures ( $\Delta t_r = (\text{measured} - \text{predicted}) / \text{measured} \times 100$ ). ....	88
Table 2-3. Retention time comparison of temperature programmed separations of normal alkanes for four different heating rates ( $\Delta t_r = (\text{measured} - \text{predicted}) / \text{measured} \times 100$ ). ....	90
Table 3-1. Normal alkane thermodynamic properties determined from various isothermal experiments. ....	105
Table 3-2. Characteristic equilibrium temperatures for alkanes separated with sawtooth moving gradients, and their experimental and calculated $T_{eq}$ values. ....	116
Table 4-1. Relative standard deviations obtained from three separations performed for each GC operation mode. ....	135
Table 4-2. Peak capacities obtained from n-alkane separations using different GC operation modes. ....	139
Table 5-1. Average characteristic equilibrium temperatures for alkanes separated with the sawtooth moving gradient, and their $T_{eq}$ values. ....	168
Table 5-2. Peak widths and standard deviations obtained from continuous analysis of normal alkanes. ....	169
Table 6-1. Peak widths and percent relative standard deviations obtained from continuous analysis of normal alkanes. ....	200
Table 6-2. Peak widths and relative standard deviations obtained for n-tridecane at two different gradient slopes and various concentrations. ....	202
Table 6-3. Peak widths, resolution, peak capacity and relative standard deviations obtained for the normal alkanes ( $C_{12}$ - $C_{14}$ ) separated using different gradient profiles. ....	215

Table 6-4. Peak widths, resolution and peak capacities of the normal alkanes using different separation methods.....219

Table 7-1. Resolution of simulated separations showing the comparison between the virtual column length of a 1 m column with respect to separations obtained with actual column lengths.....247

## LIST OF ABBREVIATIONS

CEC	Capillary electrochromatography
GC	Gas chromatography
GC×GC	Comprehensive gas chromatography
GC-FID	Gas chromatography with a flame ionization detector
GC-MSD	Gas chromatography with a mass spectrometry detector
GC-TCD	Gas chromatography with a thermal conductivity detector
GEP	General elution problem
HETP	Height equivalent to a theoretical plate
HPLC	High performance liquid chromatography
ITGC	Isothermal gas chromatography
LC	Liquid chromatography
LTM	Low thermal mass
MDGC-MS	Multidimensional gas chromatography mass spectrometry
ppm	Parts per million, concentration units
PWM	Pulse-width modulation
%RSD	Percent relative standard deviation
SFC	Supercritical fluid chromatography
S/N	Signal-to-noise
TGF	Temperature gradient focusing
TGGC	Thermal gradient gas chromatography
TPGC	Programmed temperature gas chromatography
VICI	Valco Instruments Co. Inc.

## LIST OF SYMBOLS

$a_o$	Velocity of the peak at the reference position $z_o$
$b$	Slope of the temperature gradient
$C$	Specific heat capacity
$C_M$	Concentration of analyte in the mobile phase
$C_S$	Concentration of analyte in the stationary phase
$C_M^*$	Concentration of analyte in the mobile phase after equilibrium
$C_S^*$	Concentration of analyte in the stationary phase after equilibrium
$D_A$	Dispersion term due to resistance to mass transfer
$D_C$	Diffusion constant that depends on molecular masses and structural and volume increments of the analyte
$D_{eff}$	Effective diffusion
$d_f$	Stationary phase film thickness
$D_M$	Diffusion coefficient in the mobile phase
$D_S$	Diffusion coefficient in the stationary phase
$D_T$	Total dispersion
$F$	Volumetric flow rate
$H$	Plate height
$I$	Current
$I$	Retention index
ID	Inner diameter
$j$	Local segment in the mathematical model
$J$	Diffusion flux
$k$	Retention factor



$K$	Partition coefficient or distribution factor
$L$	Column length
$m$	Mass of material
OD	Outer diameter
$P$	Pressure
$P_i$	Pressure at the inlet of the column
$P_o$	Pressure at the outlet of the column
$Q$	Energy
$r$	Column radius
$R$	Electrical resistance
$R$	Universal gas constant
$t$	Time
$t_m$	Dead time or time it takes for an unretained compound to elute from the column
$t_R$	Retention time of analyte
$T$	Temperature
$T(t)$	Column temperature as a function of time
$T(t,x)$	Column temperature as a function of time and position
$T^*$	Temperature at the reference position $z_o$
$T_{eq}$	Characteristic equilibrium temperature
$T_o$	Temperature at the column outlet
$T_{ref}$	Reference temperature
$u_M$	Mobile phase velocity
$\bar{u}_M$	Average mobile phase velocity
$u_Z$	Velocity of analyte relative to the temperature gradient

$V$	Voltage
$V$	Volume
VAC	Alternating current voltage
VDC	Direct current voltage
$V_b$	Back side peak velocity
$V_c$	Center peak velocity
$V_f$	Front side peak velocity
$V_M$	Volume of the mobile phase
$V_S$	Volume of the stationary phase
$w$	Velocity of the temperature gradient
$W$	Watts
$w_b$	Peak width at the base
$x$	Position of analyte from the column inlet
$X$	Number of moles that transfer to reach equilibrium
$z$	Position of the analytes respect to reference point on the temperature gradient
$z$	Carbon number of a normal alkane
$z_o$	Reference position on the temperature gradient

### **Greek Letters**

$\beta$	Phase ratio of a column
$\delta$	Constant for the determination of the peak velocity in the temperature gradient
$\Delta C$	Concentration change
$\Delta G^\circ$	Standard Gibbs energy change
$\Delta H^\circ$	Standard enthalpy change

$\Delta S^\circ$	Standard entropy change
$\Delta T$	Temperature difference
$\gamma_1$	Longitudinal diffusion constant
$\gamma_2$	Resistance to mass transfer constant
$\eta$	Mobile phase gas viscosity
$\sigma_t$	Spread of a Gaussian peak at time t
$\mu_t$	Position of the peak apex relative to the temperature gradient at time t

# 1 INTRODUCTION

Gas chromatography (GC) is one of the most important and widely applied analytical techniques in modern analytical chemistry for the analysis of volatile and semi-volatile organic compounds due to its sensitivity, separation efficiency, reasonable analysis time, and simplicity.<sup>1-2</sup> The three basic operations necessary to perform GC are sampling, separation, and detection. A typical GC system consists of a sample concentrator and injector, a separation column, a detector, and electronics for control and data analysis. Although each component is important for GC analysis, the heart of the GC system is the chromatographic column where the separation occurs.

In GC, the variables that produce the greatest effects on separation efficiency and analysis time are the stationary phase, internal column diameter, operating column temperature, carrier gas, and carrier gas velocity. However, controlling the column temperature is the easiest and most effective way to influence the separation process. Currently, the two major operational modes in GC are isothermal GC (ITGC) and temperature programmed GC (TPGC). For both methods, the entire column is maintained at a constant temperature at any given time,  $T(t)$ . It is well known that ITGC can produce higher resolution than TPGC; unfortunately, this advantage comes at the cost of prohibitively long analysis time for a relatively narrow volatility range of compounds.<sup>3</sup> In TPGC the column temperature increases at a given rate, allowing the analysis of mixtures with a wide range of molecular weights at the expense of some losses in separation power, especially when high heating rates are used.<sup>4-5</sup> Despite the excellent separation efficiency that modern GC methods offer, peak coelution is still a concern, especially with complex samples.

In GC, there has always been an interest in developing new methods for improving separation performance, selectivity and analysis time. Methods that improve separation performance include, backflushing,<sup>6-8</sup> heart cutting,<sup>9</sup> multidimensional GC,<sup>10</sup> pressure tunable selectivity,<sup>11-13</sup> comprehensive GC×GC,<sup>14</sup> flow modulation,<sup>15</sup> narrow band injection,<sup>16-19</sup> vacuum operation<sup>20-22</sup> and resistive heating,<sup>23-24</sup> especially for fast separations. These methods have in common the use of either ITGC or TPGC in combination with changes in the flow pressure, flow direction, injection band width, or column stationary phase (i.e., multi-dimensional techniques).

Since the column temperature is the variable that has the greatest effect on separation, changing the temperature not only in time but also in position along the column,  $T(t,x)$ , offers an appealing approach for optimizing separations. This is achieved in thermal gradient GC (TGGC) where a negative temperature gradient is applied in the axial direction of the chromatographic column, with the ability to modify the gradient with time.<sup>25</sup> Decreasing the column temperature from the injector to the detector will cause the front of the peak to move slower than the tail of the peak, causing the peak to focus. In a moving negative gradient, the peaks not only focus but they also move with the gradient at characteristic equilibrium temperatures.<sup>26</sup> This behavior is markedly different from what is experienced in ITGC and TPGC modes, where the axial length of a migrating solute zone continually increases with migration distance. The use of temperature gradients in GC was first introduced by Zhukhovitskii in 1951<sup>27</sup> and more recently explored by Rubey<sup>25, 28</sup> and Phillips<sup>29-30</sup> in the 1990s, and by Zhao<sup>31</sup> and Contreras<sup>32</sup> in the early 2000s.

TGGC has the potential to improve the peak capacity (maximum number of resolved peaks per time)<sup>33-35</sup> of the column due to axial compression of the peaks along the column.<sup>28</sup> The sensitivity of the system is also enhanced, as the focusing effect creates taller and narrower peaks. In addition, the compounds being separated interact more with the stationary phase at decreased temperatures, which results in an increase in selectivity. Moreover, since the peaks travel with the gradient at characteristic equilibrium temperatures, separation efficiency and selectivity can be optimized by customizing the gradient profiles. These attributes make TGGC a highly attractive alternative for improving GC separations.

Understanding the effects that different temperature gradients have on separation performance is of great importance for instrumental design and operational aspects of this separation technique. To the best of our knowledge, previous TGGC studies only utilized linear<sup>30, 36</sup> and concave down<sup>25</sup> temperature gradients with limited control over the profile shape. Because of this, the separation potential of TGGC has not been exploited. Currently, the main challenge in TGGC is development of instrumentation for generating and controlling desired temperature gradient profiles. Lack of suitable instrumentation has limited the use and evaluation of TGGC. This dissertation describes the design, development, and testing of three instruments capable of generating unique axial temperature gradients to evaluate their separation performance. Furthermore, TGGC computer simulations were developed as a means to provide useful insights into the effects of different axial temperature gradient profiles, with the ultimate goal of predicting the best operating conditions.

## 1.1 IMPORTANCE OF TEMPERATURE IN GC SEPARATIONS

The variable that produces the greatest effect on separation performance in GC is the column temperature.<sup>28, 36-37</sup> Separation in chromatography relies on differences in the distribution of compounds between a stationary phase and a mobile phase, which is continuously thermodynamically driven towards equilibrium.<sup>35, 38-39</sup> In the early days of the development of GC, it became clear that the proper use of temperature can considerably extend the applications of the GC technique.<sup>40</sup>

During the chromatographic process, the sample moves between the mobile and the stationary phases, resulting in a concentration distribution at equilibrium between the two phases. The ratio of the concentration of an analyte in the stationary phase to its concentration in the mobile phase at equilibrium is the partition coefficient or distribution constant ( $K$ ) of the analyte.

$$K = \frac{\text{concentration in stationary phase}}{\text{concentration in mobile phase}} \quad (1.1)$$

The distribution constant differs from component to component and is independent of the amount of the two phases in the column.<sup>41</sup> The effect of temperature in GC separations can be understood through its effect on the distribution constant. At equilibrium,  $K$  is related to the standard Gibbs energy change by the following equation

$$\Delta G^\circ = -RT \ln(K) \quad (1.2)$$

where  $\Delta G^\circ$  is the standard Gibbs energy change,  $R$  is the universal gas constant, and  $T$  is the absolute temperature. From thermodynamics, the standard Gibbs energy change is represented by

$$\Delta G^\circ = \Delta H^\circ - T\Delta S^\circ \quad (1.3)$$

where  $\Delta H^\circ$  is the standard enthalpy change, and  $\Delta S^\circ$  is the standard entropy change.

Substituting equation 1 into 2, we obtain

$$-RT \ln(K) = \Delta H^\circ - T\Delta S^\circ \quad (1.4)$$

which can be rearranged to give

$$K = \exp\left(-\frac{\Delta H^\circ}{RT} + \frac{\Delta S^\circ}{R}\right) \quad (1.5)$$

Equation 1.5, shows that by increasing or decreasing the temperature of the chromatographic column, one can significantly change the distribution of compounds between the stationary and mobile phases. This effect is used to maximize the difference in displacement between analytes, which ultimately leads to separation.

The time an analyte resides in the stationary phase versus the time it spends in the mobile phase is known as the retention factor,  $k$ . This parameter is widely used to describe the migration rates of analytes in the column.<sup>41</sup>

$$k = \frac{t_r - t_m}{t_m} \quad (1.6)$$

where  $t_r$  is the retention time of the analyte and  $t_m$  is the dead time or the time it takes for an unretained compound to elute from the column. The retention factor can be related to the distribution factor by the following equation

$$K = \beta k \quad (1.7)$$

where  $\beta$  is the phase ratio determined by

$$\beta = \frac{V_M}{V_S} \quad (1.8)$$

where  $V_M$  and  $V_S$  are volumes of the mobile and stationary phases, respectively. The influence of temperature on GC becomes evident from equations 1.5, 1.6 and 1.7,



showing how changes in temperature can produce exponential shifts in the distribution constant and, thus, in the retention time of analytes, affecting their separation.

The importance of temperature in GC has been known since the beginning of its development, when different column temperatures were used to separate different mixtures.<sup>42-43</sup> Isothermal GC, which was the first separation mode, showed that lower temperatures allowed the separation of volatile compounds; however, less volatile compounds took a long time to elute, and were broad and widely separated. This behavior is known as the general elution problem (GEP), i.e., early eluting peaks are sharp and clustered together, while later peaks are broad and spread out.<sup>25, 44</sup> As a result, isothermal GC proved to be inadequate for the separation of samples with wide volatility range. The effect of temperature on separation was further demonstrated when Griffiths *et al.*<sup>45</sup> in 1952 suggested that an improvement in separation was possible by programming the temperature of the column. However, it was not until the late 1950s when TPGC finally was noticed, thanks to Dal Nogare who showed the instrumentation, theory and advantages of this technique.<sup>39, 46-49</sup> The TPGC technique proved to be a solution to the general elution problem, and it subsequently became the primary separation mode in GC.

## **1.2 HEAT TRANSFER FUNDAMENTALS**

In GC, the separation column is the heart of the system. Thus, it is important to understand how heat transfer is used to adequately control the column temperature for development of new gas chromatographic systems and techniques.

From the second law of thermodynamics, we learn that energy always flows from a higher temperature object to a lower temperature one (heat flow). The greater the difference in temperature between two objects, the faster heat flows between them, until

it stops when the objects reach thermal equilibrium, which is when both objects reach the same temperature. Heat transfer between objects at different temperatures, or an object and its surroundings, can never be stopped, but it can be decreased. Heat can be transferred by conduction, convection, radiation, or a combination of them.<sup>50</sup>

In conduction, heat transfer takes place when there is direct contact of particles of matter. This mechanism is commonly seen in solid materials. In convection, the transfer of heat occurs by the movement of molecules from one part of the material to another. This mechanism is typical of fluids, and increases with an increase in fluid motion. There are two types of convective heat transfer: natural convection, in which the movement of the fluid is due to buoyancy forces as a result of variations in density due to variations in temperature of the fluid, and forced convection, where the movement of fluid is achieved by an external force such as a fan or a pump. In radiative heat transfer, the thermal energy is transferred through electromagnetic waves, such as the heat radiated from the sun. In any of the heating mechanisms, the surface area of the objects plays an important role in the heat transfer rate, i.e., the more the area exposed, the faster the energy can be exchanged.

To increase or decrease the temperature of an object, it is necessary to provide or remove a certain amount of energy. The energy required to change the temperature of a substance by an increment ( $\Delta T$ ) can be written as<sup>50</sup>

$$Q = m C \Delta T \quad (1.9)$$

where  $Q$  is the energy as heat (Joules),  $C$  is the specific heat capacity of the material (joules per gram Celsius), and  $m$  is the mass of the material (grams). It is important to note that heat has the units of energy and heat flow has the units of power. From equation

1.9, it is clear that objects of larger mass require more energy over a given time period to reach a certain temperature. However, not only is the mass important, but one must also take into account the specific heat capacity of the material in order to determine the energy required.

The thermal mass is the capacity of storing thermal energy and it is related to the specific heat capacity of the substance and its mass ( $m C$ ). The thermal mass of an object provides inertia against temperature fluctuations. A high thermal mass system implies that it takes a large amount of energy to change its temperature. Such systems react slowly to temperature variations, which is the case with bulky GC ovens. Materials with low thermal mass, such as fused-silica columns, can rapidly follow temperature variations. The heating and cooling rates of a system are strongly dependent on its thermal mass.

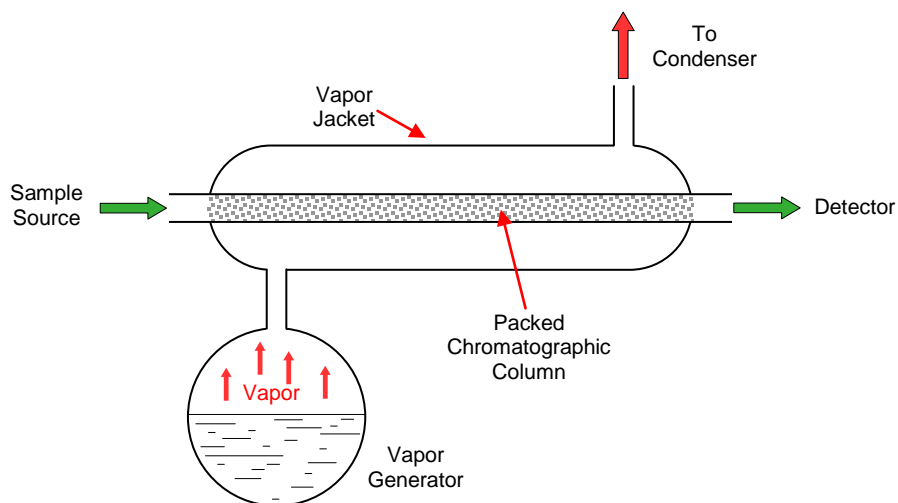
### **1.3 HEATING METHODS IN GC**

The need for controlling the column temperature was known since the introduction of the GC technique in the early 1950s.<sup>43</sup> The ineffectiveness of low temperatures for the separation of high boiling compounds was quickly realized; therefore, heating the column became important to broaden the separation capability of the technique.<sup>43</sup> Furthermore, temperature uniformity along the column was recognized to be important when temperature fluctuations during the day and night produced non-reproducible retention times, to the extent that qualitative analysis was not possible.<sup>51</sup> The first commercial GC instruments did not have an oven; the column temperature varied with the room temperature.<sup>52</sup> The dependence of retention time upon column temperature is exponential, and small changes in the column temperature can produce

significant shifts in the retention time.<sup>37, 53</sup> As a result, adequate control and uniformity of the temperature along the GC separation column was required to achieve reproducible results and perform quantitative analysis.<sup>37, 42, 54</sup> This was one of the first problems encountered during the development of GC systems.<sup>54-56</sup> There was a need to create and adapt different heating methods for regulating the column temperature. Following is an overview of the different heating methods to control and maintain a uniform temperature along the separation column that have been used since the GC technique was introduced. Knowledge of the heating techniques used in GC is of great importance when developing GC systems. At the end of the section (Figure 1-11), the heating and cooling methods are classified by heat transfer mechanism.

### **1.3.1 Vapor Jacket**

The first GC separations were performed with the column heated using a vapor jacket (Figure 1-1).<sup>43, 52, 57</sup> The vapor jacket system consisted of placing the GC column inside a vapor bath of a boiling pure substance, such as water (b.p. 100°C) or ethylene glycol (b.p. 200°C). The column temperature was maintained relatively constant at the boiling point of the pure substance. To reduce any temperature gradients along the column, the vapor jacket was placed horizontally. By changing the pressure inside the vapor jacket, the column temperature was modified to some extent; however, greater variations in temperature required replacing the pure substance.<sup>58</sup> In any case, changing the temperature using this technique was time-consuming and cumbersome.



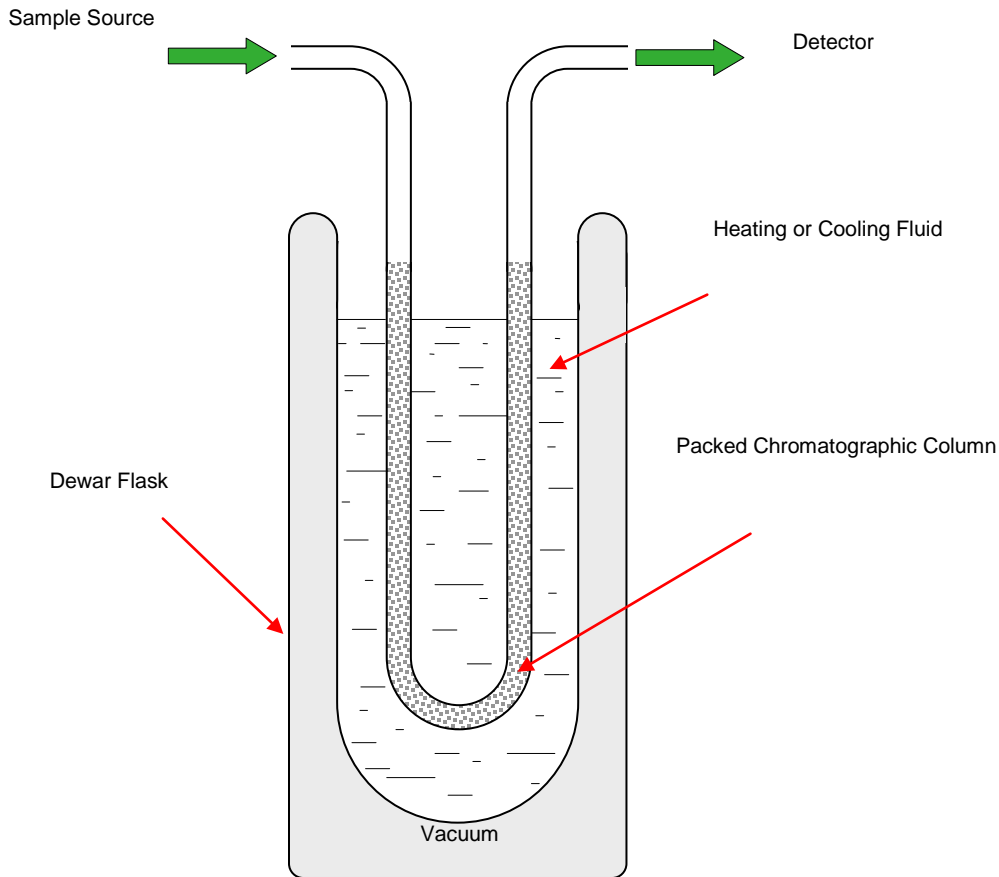
**Figure 1-1. Vapor jacket heating system for packed GC columns.**

### 1.3.2 Dewar Flask

After the introduction of the GC technique in the early 1950s,<sup>43, 57</sup> most of the first gas chromatographs were home-built following the Janák-type chromatograph.<sup>59-60</sup> This system became very popular because it was simple to construct using standard laboratory hardware. A uniform temperature along the column was achieved by placing the column inside a liquid thermostat Dewar flask (Figure 1-2).<sup>61</sup> The temperature range of the system was restricted between sub-ambient to 60°C, limiting its application to the separation of inorganic gases and C1-C4 hydrocarbons.<sup>59</sup> These systems were gradually replaced with the introduction of more versatile commercial chromatographs.

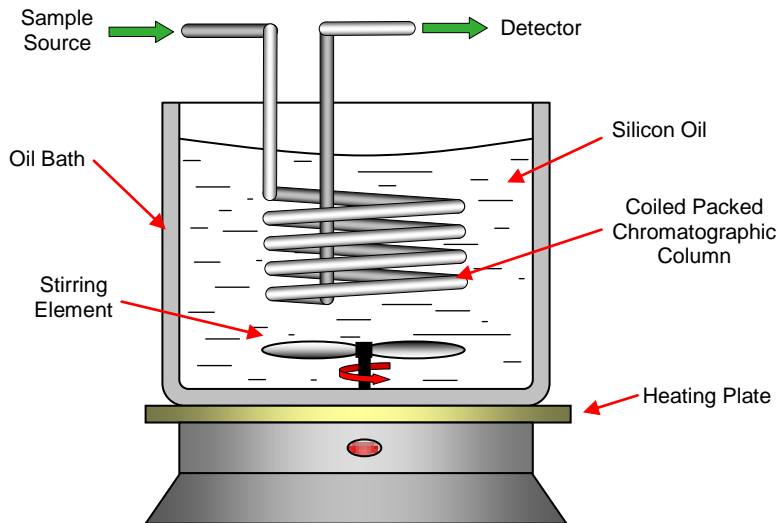
### 1.3.3 Oil Bath

In the mid-1950s, oil baths were employed to thermostat the column.<sup>62-63</sup> This method was based on forced convection, in which a moving fluid (silicon oil) was used to



**Figure 1-2. Dewar flask for maintaining the GC column at constant temperature.**

efficiently transfer heat (Figure 1-3). A uniform temperature along the column was achieved through proper stirring of the oil, combined with its good temperature stability and heat-transfer characteristics. The oil bath was able to cover a wide temperature range between 40°C and 300°C, and could even be programmed at a slow heating rate due to the high thermal mass of the oil.<sup>63</sup> Although the method provided better thermal flexibility than vapor jackets, having oil around the column was inconvenient and messy.

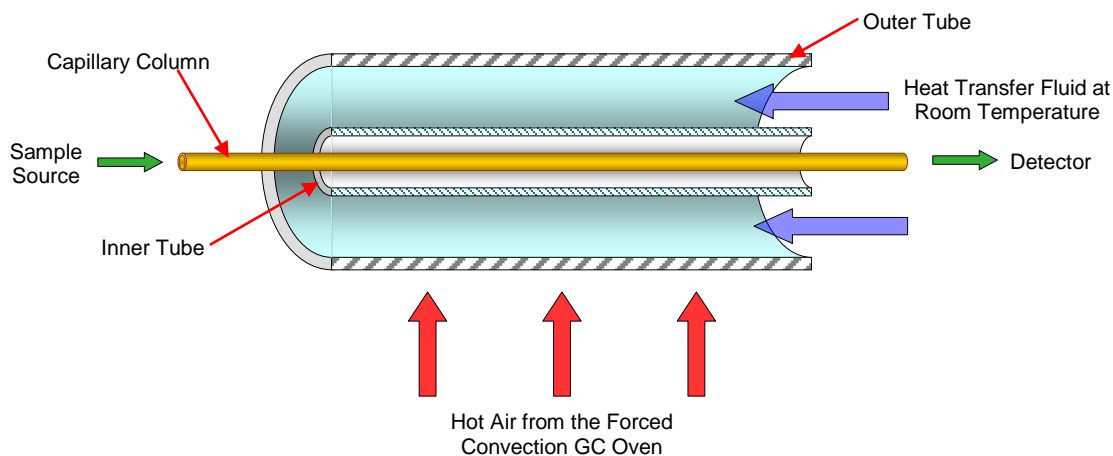


**Figure 1-3. Oil bath system for heating coiled packed chromatographic columns.**

### 1.3.4 Heat Exchanger

Using this approach, a device is used to facilitate the transfer of heat from one fluid to another, where the fluids are usually separated by a solid wall to prevent them from mixing. Recently, researchers have designed a heating and cooling GC module (heat exchanger) that allows for ballistic heating (heating rates  $>1^{\circ}\text{C/s}$ <sup>64</sup>) and ultrafast cooling (cooling rates  $\approx 100^{\circ}\text{C/s}$ ) for short (2.5 m) capillary columns, where paraffin oil was used to regulate the column temperature.<sup>65</sup> The heat exchanger consisted of a 2.5 m coaxial stainless steel tubing that was placed inside an air bath oven. The air bath oven was kept at a high temperature ( $350^{\circ}\text{C}$ ) and room temperature paraffin oil was used as the cooling medium. The heat transfer was between the hot oven air and the paraffin oil. The column was placed in the inner tube and heat was transferred to the column by conduction (Figure 1-4). The column was maintained at room temperature when the paraffin oil flowed between the coaxial tubing. Heating was achieved when the paraffin oil flow was stopped, and the column was brought to the air bath oven temperature. Heating rates of

330°C/min and cooling rates as high as 6000°C/min were achieved with this system.<sup>65</sup> Fast cooling was obtained when the flow of oil was reestablished. A limitation of this system is that the heating rate is difficult to control, because it becomes a function of the air bath oven temperature, and the heat capacity and linear velocity of the cooling medium (paraffin oil). With heat exchangers, the temperature changes with position along the fluid motion; therefore, it is possible that a temperature gradient was actually established in the previous work. The system temperature was determined by the resistance of a wire placed along the heat exchanger, so only an average temperature was obtained.<sup>65</sup> Heat exchanger systems have been used before for generating negative axial temperature gradients.<sup>28, 32</sup> In these systems, the heat exchanger did not have an inner tube (Figure 1-4), and heat was transferred by convection.



**Figure 1-4. Heat exchanger system for capillary GC columns.**

### 1.3.5 Air Bath Oven

The first commercial gas chromatographs in the mid-1950s implemented this method for heating the column.<sup>52</sup> With this method, heat is provided by the motion of air



over the column (forced convection), bringing or carrying energy with it. Easy access for replacing the column combined with fast temperature change and wide temperature range from room temperature to over 300°C made it an ideal heating technique for GC systems.

The early air bath oven design exhibited a significant temperature lag between the set and actual column temperatures (thermal lag).<sup>66</sup> Long times (hours) were required for the oven temperature to equilibrate and reach its set point, due to the low heat capacity of air and the relatively high thermal mass of U-shaped packed columns.<sup>55</sup> This effect became more pronounced when programmed temperature operations were introduced. Another design drawback was the presence of undesired temperature gradients along the column due to the use of long air bath ovens to accommodate the U-shaped columns.<sup>59, 63</sup>

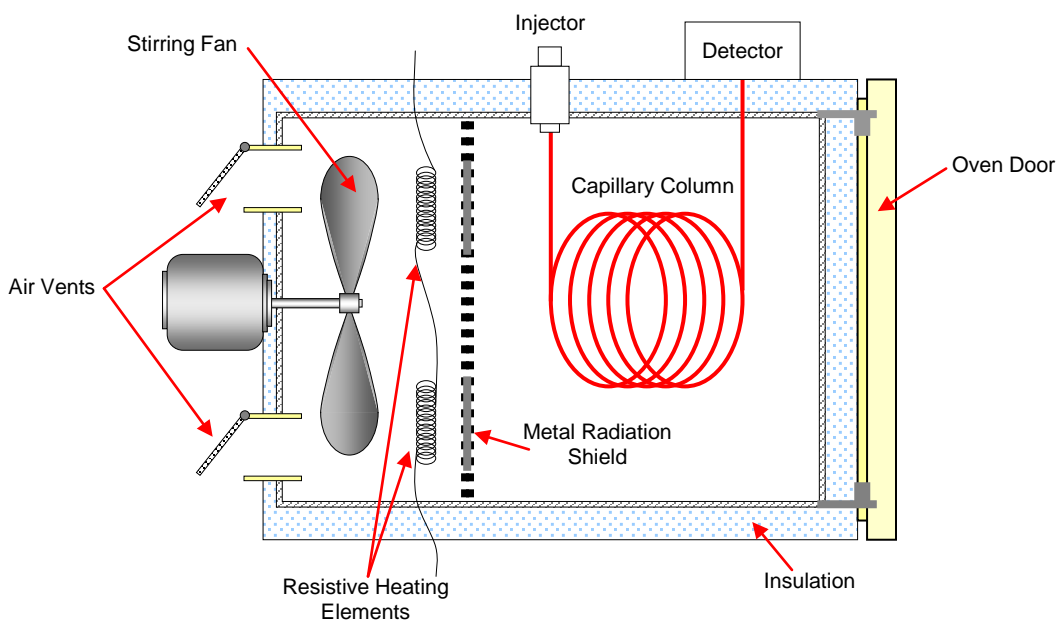
A suggested solution for these problems was to use fluidized solids to increase the heat capacity of the fluid, reducing the time for the temperature to reach equilibrium, while maintaining the cleanliness and ease of replacing the column as in air bath ovens.<sup>67</sup> Although this idea had its merits, it was not pursued in the GC field. The solution came in the 1960s with improvements in the air bath oven design. More powerful heaters to increase the temperature programming rates, stronger fans to minimize thermal gradients across the oven, and more efficient insulation materials to reduce heat losses to the environment resulted in a decrease in the temperature equilibration time. Moreover, the introduction of a new column technology, thin-wall stainless steel capillary columns, helped to further minimize thermal lag problems.<sup>68</sup> Coiled capillary columns allowed the use of smaller ovens which in turn facilitated better heating designs for programmed temperature operations.<sup>52, 58</sup> The response of capillary columns to temperature changes in the oven was improved by the lower thermal mass of the column and its coil

arrangement. The columns were wound on wire frame supports where most of the capillary column area was exposed to the heated air, providing rapid temperature equilibration.<sup>69</sup>

A typical air bath oven consists of a metallic box covered with insulation in which the column is heated through forced air convection (Figure 1-5). Turbulent airflow is achieved by a fan located at the back of the oven. The air in the oven is resistively heated by electric coil wire elements placed in front of the fan. A metal shield placed between the heaters and the column prevents radiated heat from unevenly heating the column. Adequate temperature control as well as rapid cooling of the instrument is achieved by regulating an ambient air vent intake and an exhaust vent that are normally placed at the rear wall of the oven. The entire oven cavity and its components are subjected to heating and cooling, thus requiring the generation and dissipation of a large amount of energy, which consumes a considerable amount of power and time.

Currently, air-bath ovens are the method of choice for laboratory bench-top GC systems, providing a controlled, uniform temperature along the GC column. The operating temperature range of current ovens is between room temperature to 450°C. However, lower temperatures down to -99°C can be achieved with the help of cryogenic cooling fluids.<sup>70-71</sup> Actual GC ovens are large in volume, and most of the thermal energy is needed to heat the oven itself.<sup>72-73</sup> Conventional air bath ovens typically consume power on the order of kilowatts (~2 KW). The large thermal mass of the conventional GC oven helps to stabilize the temperature, but dramatically retards the rate at which the column can be heated and cooled.<sup>58</sup> The possible linear heating rate of most conventional GC ovens declines from 75°C/min to 20°C/min as the oven temperature increases.<sup>74</sup> At

higher temperatures, the heating rate decreases due to heat losses to the surrounding air.<sup>70-71, 75</sup> Higher heating rates up to a maximum of 120°C/min for fast separations can be achieved by using a high power input (>200 V AC), a dual electric heating source,<sup>74</sup> or by using accessories to reduce the heating volume of the oven.<sup>70, 76-78</sup> Another way of addressing this problem is by decreasing the size of the convective oven, which allows increasing the heating rate up to a maximum of 240°C/min.<sup>79</sup> Fast turn around times for conventional air bath gas chromatographs is limited by the cooling time. In current air bath ovens, the cool down time from 350 to 50°C is between 2 to 6 min, depending on the model.<sup>70-71, 73, 75, 77-78, 80</sup>



**Figure 1-5. Diagram of a convective oven illustrating its different components.**

Air bath ovens have gained broad acceptance in GC systems due to their flexibility, accurate control of the column temperature, and easy access and replacement of the column. However, GC air bath ovens have reached their practical limit; their high

thermal mass limits their heating and cooling rates as well as their use in portable instrumentation.

### 1.3.6 Resistive Heating

Resistive heating involves the use of an electrical current to heat a conductive material in close contact with the column (Figure 1-6). In resistive heating, heat is transferred to the column mostly by conduction. Resistive heaters come in the form of conductive coatings,<sup>29, 81-83</sup> wires that are wrapped around or lie beside the column,<sup>24, 48, 83-89</sup> metal fixtures with the column wrapped around or placed within,<sup>52, 58, 90-93</sup> metal tubes that contain the column,<sup>82-83, 85, 94</sup> or the column itself.<sup>16, 48, 66, 86, 94-96</sup> Resistive heating is based on the principle that the temperature of a conductive material increases when current passes through it (Joule's law)

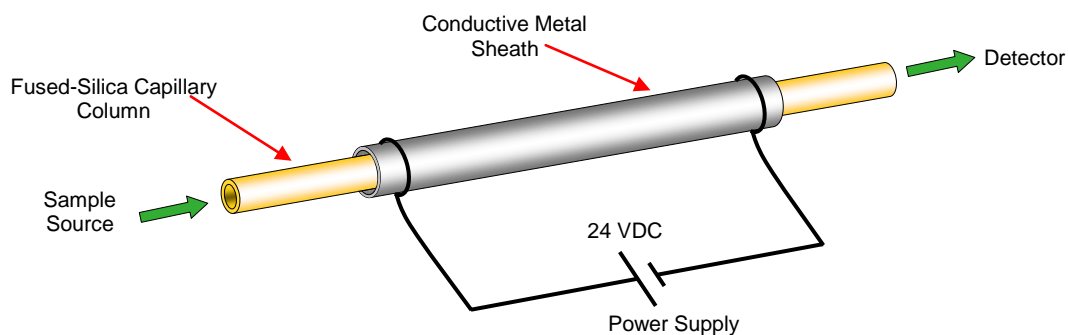
$$Q = I^2 R t \quad (1.10)$$

where  $Q$  is the heat generated (Joules) for time  $t$  (seconds),  $I$  is the current through the conductor (amperes), and  $R$  is the electrical resistance of the conductor (ohms). From Ohm's law ( $V=I \cdot R$ ), equation 1.10 can be rewritten as

$$Q = V I t \quad (1.11)$$

where  $V$  is the potential voltage difference measured across the conductor (volts). From equation 1.11, it is apparent that the degree of heating of a conductor and, hence, its temperature (see equation 1.9) for a given time is proportional to the increase in voltage or current. This physical property of conductors was well known and used in electrical heating systems before the GC was introduced. Therefore, it was chosen as one method for heating the column. There are three approaches for resistively heating the column. One involves resistively heating an element or fixture that conducts the heat to the

column. Another uses the column itself as the resistive heating element, also known as direct resistive heating. The third uses a resistive heating wire wrapped or placed along the column. Higher heating rates are achieved with direct resistive heating, since the thermal mass is very low and there is no temperature sensor or heating element that must be heated as well. Heating rates on the order of  $1000^{\circ}\text{C}/\text{min}$ <sup>81, 83</sup> are common in resistive heating applications, and they can even reach  $240^{\circ}\text{C}/\text{s}$  ( $14,400^{\circ}\text{C}/\text{min}$ ).<sup>97</sup> Cooling is achieved by blowing ambient air (forced convection) with cooling rates on the order of  $200^{\circ}\text{C}/\text{min}$ .<sup>83, 85</sup> Power consumption for a resistively heated system is typically under 120 W,<sup>24, 87, 98</sup> which is over 15 times less than conventional air bath ovens ( $\approx 2\text{ kW}$ ).<sup>70-71</sup>



**Figure 1-6. Diagram of a resistively heated fused-silica column inserted through a coaxial metal sheath.**

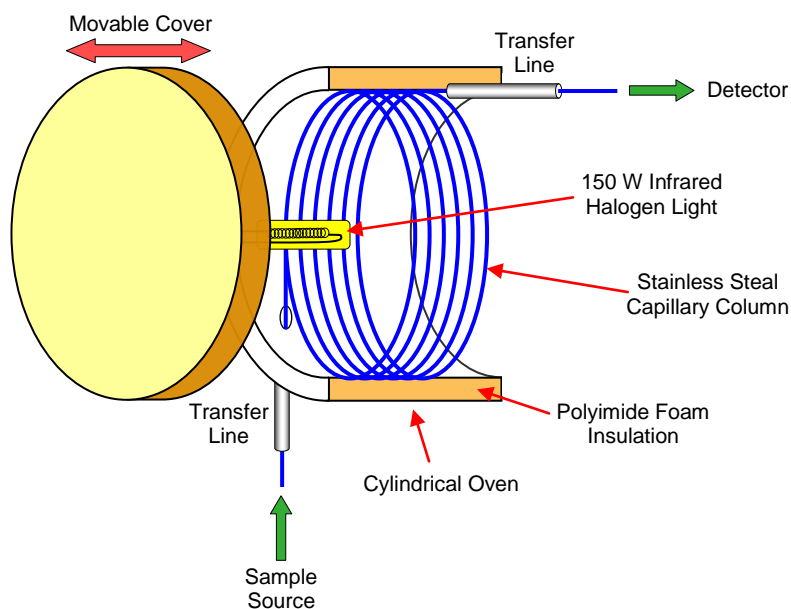
Resistive heating offers low thermal mass and fast heating rates, low power consumption and fast cooling times, which are highly desirable characteristics for achieving fast separations and for portable GC applications.

### 1.3.7 Infrared Heating

During infrared heating, thermal energy is transferred in the form of electromagnetic waves. A high temperature body emits radiation and an object can absorb the radiation at some wavelength. This absorbed radiation is what creates the heat within the object. Common infrared heaters are constructed with an electrically heated filament as the emitting body, and temperature can be regulated by the amount of current supplied to the filament. In the mid 1990s, Matz and coworkers from the Technical University of Hamburg developed an infrared heated gas chromatograph for field applications and fast heating rates.<sup>99-100</sup> In their proposed system, a 3 m x 0.25 mm x 1  $\mu\text{m}$  stainless steel column wound in a cylindrical arrangement was placed against the inner wall of a cylindrical oven that was heated with a 150 W infrared halogen lamp placed in the middle of the oven (Figure 1-7). The low thermal mass of the system permitted a maximum heating rate of 1000°C/min in a temperature range up to 300°C. With the chamber open on both sides, it could be cooled down in 60 s by blowing air using a fan. To improve heating efficiency, the oven chamber was small and made of polyimide foam insulation with an inner diameter of 5 cm and a wall thickness of 3 cm. The inner walls were covered with aluminum foil to reflect the infrared radiation and improve the heating efficiency. During heating, the two sides of the cylinder chamber were closed with polyimide foam covers.<sup>101</sup> Although this heating method proved to be simple in design for achieving high heating rates, no follow up work has been performed in this area.

Another approach for infrared heating was suggested by Rounbeheler<sup>102</sup> in which a laser would be used as the infrared source, and heating would be accomplished by using

the column as a light path. This approach would produce very fast heating rates by rapidly heating the stationary phase within the column by absorption of some of the laser energy. However, this idea has not yet been tested.

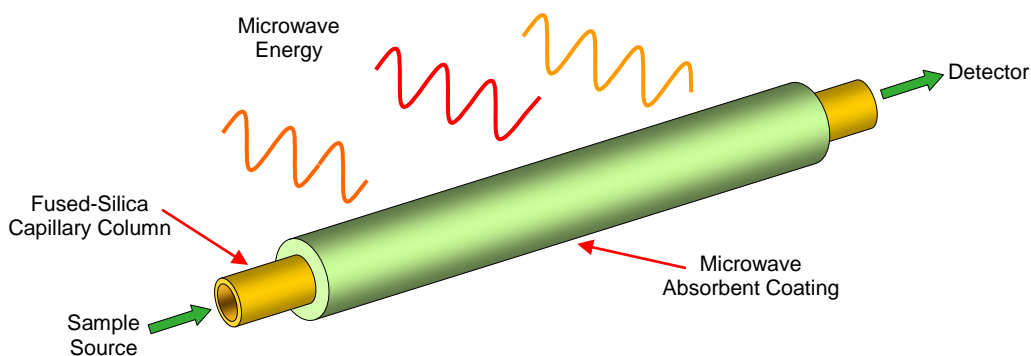


**Figure 1-7. Cross section diagram of an infrared heating oven.**

### 1.3.8 Microwave Heating

An alternative for heating capillary GC columns is the use of microwave radiation. In 1962, Brashear suggested the use of microwave heating for heating fluids inside a glass column.<sup>103</sup> Current fused-silica columns do not absorb microwave energy at an appreciable rate, therefore, the columns used in microwave ovens must be coated with a microwave-absorbent material, such as iron-filled epoxy that converts microwave energy to thermal energy which heats the column (Figure 1-8).<sup>104-105</sup> A microwave GC oven has been engineered to generate a uniform microwave field around the column,

eliminating cold spots, and evenly heating the capillary column.<sup>106-107</sup> Heating rates in excess of 10°C/s (600°C/min), and 30 s cool-down times from 350 to 35°C (10°C/s) were attained with this system.<sup>108</sup> The authors claim that microwave energies at the frequencies used are not appreciably absorbed by organic molecules, thus, their integrity is maintained during the separation.<sup>108</sup> This technology allows the oven to be small enough to be held in the palm of the hand, and stay cold during the heating cycle. Only the column thermal mass and coating is heated inside the oven. However, conductive materials such as metal capillary columns cannot be used because they will reflect the electromagnetic energy, shorting out the electric field. Currently, Petroleum Analyzer Company (PAC), a provider of analytical instruments, is marketing this technology as the Radian UltraFast GC<sup>®</sup> system.<sup>109</sup> This instrument can achieve heating rates up to 360°C/min and can cool down in seconds. However, no power consumption data was provided. A drawback of this system is the potential for temperature gradients and hot spots along the column due to non-homogeneous coatings.



**Figure 1-8. Schematic of a microwave heated coated column.**

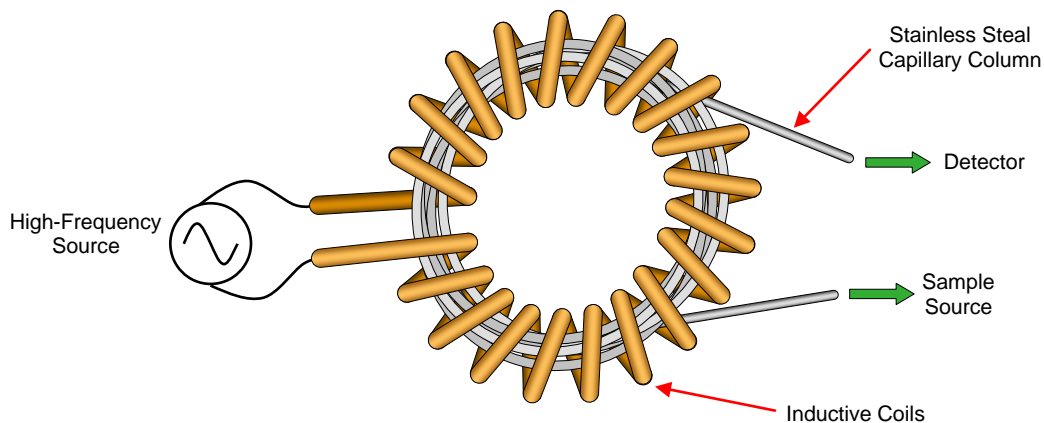


### 1.3.9 Inductive Heating

An electric conductor can be heated by inducing an electric current through the use of an alternating magnetic field according to Faraday's Law. This magnetic field can be generated in the center of a coil when a high-frequency alternating current is applied. The material to be heated needs to be placed in the middle of the coils where the magnetic field strength is high.<sup>110</sup> The induced current increases the material temperature due to Joule heating from the electrical resistance of the material (see equation 1.10). Since the conductive piece is electrically isolated, the induced current dissipates in the form of heat, resulting in a rapid temperature increase. The temperature reached in the conductive material can be precisely controlled by regulating the frequency and strength of the alternating field. This heating technique has been applied in different areas since the 1920s, and was first suggested to heat packed chromatographic columns in the early 1960s by Brashear<sup>103</sup> and by Loyd.<sup>111</sup> In their proposed system, coils around the column were used for inductively heating the packed column. Brashear even suggested the use of conductive particles as packing material in a glass column to inductively heat the column from the inside out. In this technique, the column is not in contact with the inductive coils, maintaining its low thermal mass for fast heating rates (Figure 1-9). Although a gas chromatographic system with this heating technique has not been developed, inductive heating has been used in high performance liquid chromatography (HPLC) in the last decade, with columns containing conductive particles.<sup>112-114</sup>

This heating technique has the potential to be applied to commercial metal and metal-clad fused silica capillary columns, producing a low thermal mass system that can have fast heating and cooling rates. However, the power consumption of a prototype

inductively heated HPLC system was considerably high (1 kW) for portable applications.<sup>112</sup> The thermal mass of metal capillary columns is only a fraction of packed HPLC columns. Thus, the heating efficiency of inductively heated capillary columns must be first determined experimentally with an optimized system before drawing further conclusions.



**Figure 1-9. Diagram of an inductively heating column fixture.**

## 1.4 COOLING METHODS IN GC

The cooling techniques in GC usually involve either blowing a cold fluid over the column or coupling the column to an element that can be quickly cooled. Cooling in gas chromatography operations becomes very important when sub-ambient temperatures and high speed separations are required. A true high speed GC separation not only involves rapid heating of the column, but it also requires fast cooling to decrease the analysis cycle and, hence, increase sample throughput. To accomplish this, the thermal mass of the column heating assembly (oven and heating elements) must be kept as small as possible. Another factor that plays an important role during cooling is the column arrangement.

The amount of column area exposed to the cooling mechanism will dictate the cooling rate as well as the amount of power consumed during heating. In any cooling method, care must be taken when working below the water freezing temperature; condensation of the surrounding water vapor over the column assembly or the cryogenic cooling system can have a profound effect on the heating and cooling rates, which can affect the separation performance of the GC system.

#### **1.4.1 Forced Air Convection**

The main cooling method in GC is forced convection. This is commonly achieved by blowing ambient or cold air over the column. Cooling of the column can be optimized by either improving the flow of air around the column assembly, increasing the flow of air, or by rearranging the column assembly to increase the exposed column area.

#### **1.4.2 Cooling Fixture**

Cooling can also be achieved by cooling an element in close contact with the column by either flowing a cold fluid or a cryogenic fluid through the cooling element, or by using a Peltier cooler.<sup>58, 65</sup>

#### **1.4.3 Cryogenic Fluids**

Sub-ambient temperatures can be reached by using cryogenic fluids such as liquid nitrogen and liquid CO<sub>2</sub>. High cooling rates can be achieved as a result of their very low temperatures: -196°C for liquid nitrogen and -78°C for compressed liquid CO<sub>2</sub> when it expands. In current forced convection ovens, cooling to sub-ambient temperatures is performed by direct injection of cryogenic fluids into the oven stirring fan, providing a uniform column temperature.<sup>70</sup> Cooling with cryogenic fluids can also be achieved by

directly spraying the column assembly; however, temperature control is difficult, and uneven temperatures along the column can be created.

When working with liquid nitrogen, proper insulation of the plumbing is required to reduce nitrogen consumption and to allow effective transfer from the Dewar to the usage point in the system with minimal vaporization or loss. Jacketed vacuum pipes are available that provide the best insulation, although foam insulation can be used as well. In any case, the need for insulation makes the tubes bulky and cumbersome to work with. When pumping liquid nitrogen, a two phase (liquid-gas) fluid can form from boiling of the liquid nitrogen that produces a very irregular flow that is hard to control. A solution is to use the cold nitrogen headspace gas boiling off the liquid nitrogen, which can be achieved with some liquid nitrogen Dewar containers. Nitrogen gas can be cooled by bubbling liquid nitrogen gas through it or by using a coil heat exchanger tube submerged in a Dewar with liquid nitrogen. The pressure drop of the heat exchanger must be kept low to avoid condensation of the gas and formation of a two-phase fluid. Care must be taken to avoid blockage inside the heat exchanger from water condensation; the use of a pressure relief valve placed before the heat exchanger can prevent risk of high pressure build-up. Liquid nitrogen allows the use of high flows and volumes for cooling of large areas. A downside of using cryogenic liquid nitrogen is that this approach is not compatible with portable applications.

On the other hand, handling pressurized liquid CO<sub>2</sub> is easier because the plumbing used can be smaller diameter and it does not need to be insulated. Cooling only takes place at the end of the plumbing where the liquid CO<sub>2</sub> expands, cooling itself by the Joule-Thompson effect. Small areas (0.5 in<sup>2</sup>) can be cooled with liquid CO<sub>2</sub> by directly

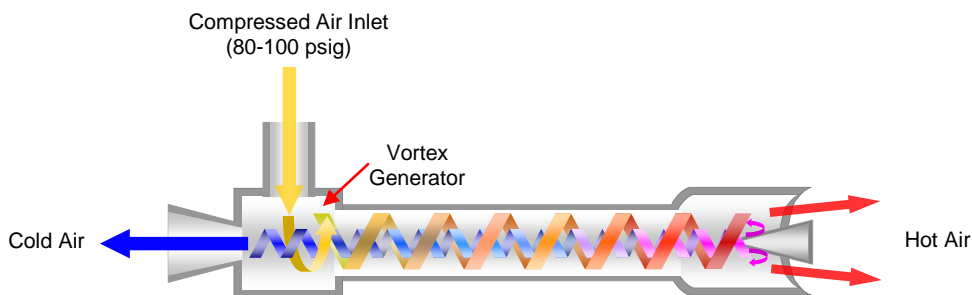
spraying from a nozzle. Larger areas can be cooled as well by releasing the liquid CO<sub>2</sub> into a fan that will uniformly distribute the cold. Temperature quickly increases as the gas moves away from the nozzle; therefore, cryogenic temperatures are obtained from direct exposure to the liquid CO<sub>2</sub> expansion. Liquid CO<sub>2</sub> has the potential for use in cryogenic cooling applications for portable GC systems because it can be carried into the field in small, disposable, pressurized cylinder cartridges.

Well ventilated areas and protective gear must be used when working with cryogenic fluids to avoid cold burns and asphyxiation, which may result from the displacement of oxygen in the air.

#### **1.4.4 Vortex Cooler**

Another way to obtain sub-ambient temperatures is by using a vortex cooler.<sup>115-116</sup> This device is a heating and cooling system that employs no moving parts, and only requires a stream of compressed air. The compressed air is injected tangentially into the system, and a vortex generated inside causes the air flow to be separated into a cold and a hot stream (Figure 1-10). Air at a pressure of 80-100 psig with a flow between 1-150 ft<sup>3</sup>/min is adequate. The fraction of air that is cooled can be regulated between 80-20% of the total air flow with maximum cooling obtained for the lowest fraction. The cold temperature can reach down to -46°C, while the hot side approaches 126°C. This cooling device has been previously used to reach sub-ambient temperatures in an air bath oven, and as an alternative method for cold trapping in GC×GC separations.<sup>115, 117</sup> The practicality of this cooling approach increases with smaller column assemblies and when compressed air is available, such as from in-house compressed air commonly found in

laboratories. The downside of its application is the high amount of air required and the noise level produced from the release of compressed air.



**Figure 1-10. Diagram illustrating the operation of a vortex cooler.**

### 1.4.5 Peltier Cooler

Thermoelectric heat pumps, also known as Peltier coolers, can be used to cool down a column to sub-ambient temperatures. When a DC current is applied to the Peltier cooler, heat transfers from one side of the device to the other side against a temperature gradient from cold to hot. The effectiveness of the Peltier cooler at moving heat away from the cold side is a function of the amount of current provided and how well heat is removed from the hot side. This characteristic allows Peltier coolers to be stacked one on top of another to achieve lower temperatures. Heat is typically removed from the hot side of the device with a heat sink. Temperatures as low as  $-20^{\circ}\text{C}$  and as high as  $200^{\circ}\text{C}$  can be achieved, with heating rates that can reach up to  $7000^{\circ}\text{C}/\text{min}$ .<sup>118-119</sup> Typical Peltier coolers are a few millimeters thick and a few centimeters square; however, new microPeltier coolers can be as thin as  $460\ \mu\text{m}$ . They are best suited for smaller cooling applications, such as microchip GC systems<sup>119-120</sup> because of their compact size, no moving parts and low maintenance. Peltier coolers can be used to cool down conventional capillary columns by either arranging the column in a flat format or by

cooling a larger element that is in close contact with the column.<sup>91</sup> Even though Peltier coolers can work as heaters when the current is reversed, they are mostly used as coolers, since there are more efficient ways for heating. When combined with a heating element, a thin coating of insulating material may be used between the Peltier cooler and the heating element to optimize both the power required to heat and the time required to cool.

Reducing the thickness of the insulation decreases the cooling time, but increases the power that must be applied to the system to overcome heat loss to the Peltier cooler. The downside of such heat pumps is that they are not very efficient, requiring considerable power. However, recent work by Lewis *et al.*<sup>120</sup> has demonstrated a microcolumn GC system that can provide temperature control between 10-200°C with a peak power demand of only 25 W.

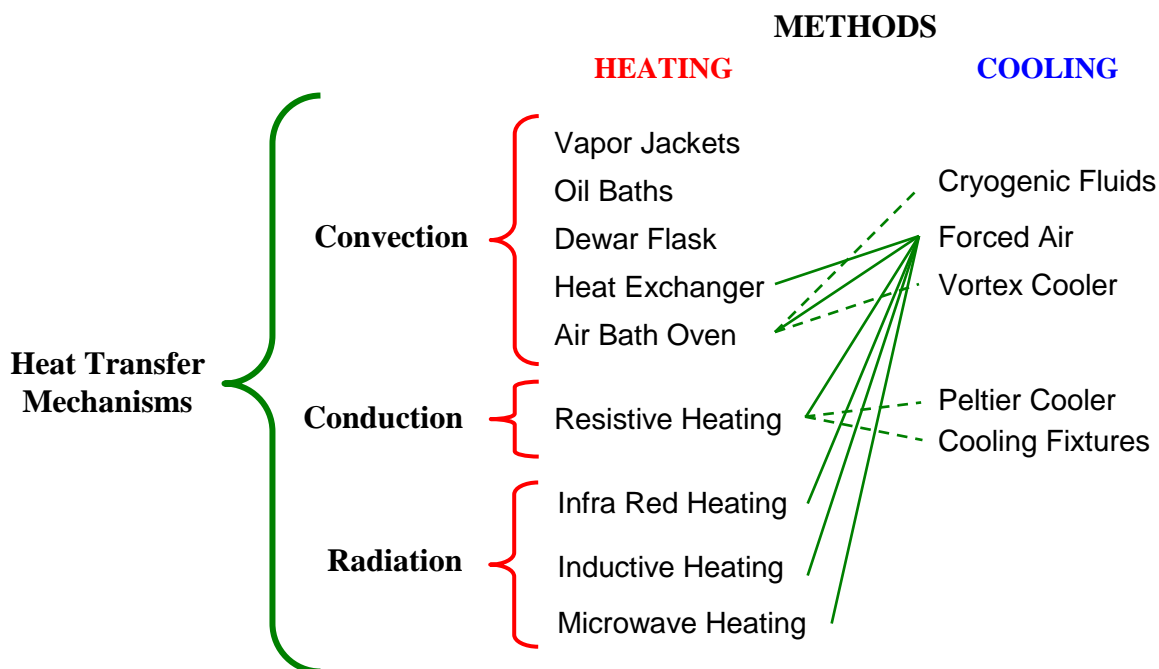


Figure 1-11. Classification of heating and cooling methods by heat transfer mechanism.

From Figure 1-11, it can be clearly seen that the cooling method of choice is forced air convection, and that convection heat transfer is involved in most of the heating and cooling approaches. However, it is important to mention that heating of fluids by convection is commonly achieved using resistive heating elements. Thus, conduction and convection are very important heat transfer mechanisms to consider when developing GC systems.

## **1.5 RESISTIVE HEATING IN GC**

Even though the accepted standard for heating in GC systems is forced convection air bath ovens, resistive heating techniques have gained considerable interest over the past decades. Currently, resistive heating is the heating method of choice to achieve fast GC separations and for portable GC applications. In the following overview, I describe the different resistive heating strategies that have been developed since the introduction of gas chromatography in the early 1950s.

### **1.5.1 Overview**

The first GC that implemented resistive heating was introduced in the mid-1950s, in which a resistive heating wire wrapped around the column was used for heating.<sup>52, 54</sup> In the late 1950s, Dal Nogare used resistive heating methods to demonstrate the separation power of programmed temperature operation. Resistive heating was preferred over air bath ovens because the method offered a low thermal mass system with no thermal lag problems during programmed temperature operations.<sup>86, 121</sup> Dal Nogare tested direct resistive heating using a stainless steel U-shaped packed column as the heating element.<sup>86</sup> However, this approach was abandoned because direct resistive heating required



electrical isolation of the column from the detector, which at the time was difficult to achieve. Furthermore, the low resistance of the stainless steel column required high-current, low voltage step-down transformers that were bulky. Dal Nogare ended up using insulated heating wire that provided equivalent performance to direct resistive heating. In his chromatographic system, the U-shaped packed column was uniformly wrapped with insulated resistance heating wire.<sup>52, 86, 121-122</sup> The column temperature was regulated by voltage applied to the heating wire, and cooling was achieved by blowing ambient air over the column. In the early 1960s, Perkin-Elmer introduced the 222 and 222P GC models for temperature programmed operation. In these systems, the U-shaped stainless steel packed columns were directly resistively heated, and program rates as high as 52°C/min were possible. Other resistively heated GC systems for temperature programming operation and with different sample introduction systems were proposed in patents in the 1960s.<sup>55, 122-125</sup>

The introduction of open-tubular capillary columns with superior separation performance in the late 1950s by Golay slowly replaced the U-shaped packed columns and, with it, the need for resistive heating.<sup>126</sup> By the late 1960s and during the 1970s, metal and glass capillary columns became commonly used, and GC systems with redesigned air bath ovens successfully performed temperature programmed operations without thermal lag problems.<sup>126</sup> The simpler design of the air bath ovens quickly took over the resistive heating design, especially the challenging direct resistive heating of long metal capillary columns. Avoiding the shorting of the heating circuit in metal capillary columns was difficult, since each metal column coil needed to be electrically insulated from adjacent coils as well as from column supports and other parts of the

system.<sup>58</sup> The introduction of glass and later fused-silica capillary columns in the 1970s further limited the use of resistive heating methods. The only exception was the Model 226 GC by Perkin-Elmer, which was a resistively heated system marketed from 1962 to 1967.<sup>52, 58</sup> This system had a flat helically coiled metal capillary column that was sandwiched between two aluminum plates, which were clamped between two resistively heated metal blocks. Heating rates up to 50°C/min were possible with this system, and cooling was achieved by forced air or by using a cryogenic fluid.<sup>58</sup> A drawback of the system was that its configuration made column replacement cumbersome.

During the 1960s and 1970s, fast heating rates were achieved with resistive heating methods and, hence, shorter analysis times were experienced compared to air bath ovens.<sup>58</sup> During this period, a significant amount of time was consumed in sample preparation and quantitative evaluation of the chromatogram; the separation step only represented a small portion of the total analysis.<sup>127</sup> Thus, reduction in the separation time was not important. However, with the introduction of microprocessors and personal computers in the late 1970s, new GC system designs and software made data collection and analysis easier and faster by the 1980s. Resistive heating methods were emphasized again by Lee, Yang and Bartle in their 1984 book, by describing the significant advantages of direct resistively heating a metallic coated fused-silica capillary column.<sup>37</sup> The authors suggested that because of the low thermal mass of the fused-silica columns, ultrafast heating and cooling with no thermal lag problems could be achieved with minimum power consumption. Furthermore, the authors predicted that this technology would facilitate the miniaturization of gas chromatographic systems.

By the 1980s, fused-silica columns were widely used; however, resistively heating this type of column was not straightforward. Three different approaches were developed in the following years to resistively heat capillary columns: direct resistive heating, on-column wire resistive heating and resistively heated column fixtures.

#### ***1.5.1.1 Direct Resistive Heating***

In 1986, a solution to resistively heat capillary columns came with the development of fused-silica columns coated with a thin aluminum cladding for high temperature separations.<sup>128-130</sup> In 1989, Hail and Yost demonstrated direct resistive heating of aluminum-clad capillary columns.<sup>83, 131-132</sup> A 3 m long column was wrapped around a Teflon spool and insulated with Nextel glass braid to prevent electrical shorting between the coils. The column temperature was sensed by measuring the resistance of the column itself, and the temperature was controlled by changing the voltage across the column. The low thermal mass of the column allowed for fast heating and cooling rates of 524°C/min and 165°C/min, respectively, reaching a maximum of 2400°C/min for both cases. The power requirement for the resistive heating systems was 35 watts, which was 500 times less than conventional air bath ovens.<sup>83</sup> The low resistance of the commercial aluminum-clad fused-silica capillary columns combined with uneven aluminum film thickness hampered their use in direct resistive heating applications.<sup>58, 66</sup> Controlling the temperature of the low resistance system and eliminating the uneven temperature along the column proved to be difficult.<sup>81</sup>

Jain and Phillips in 1995 provided a different solution for direct resistive heating of fused-silica columns by painting them with a thin layer of conductive paint.<sup>29-30, 81</sup> The electrically conductive paint was intended for use in repairing electrical heating elements

on automobile glass windows.<sup>17</sup> The columns used in the experiments were all less than 1 m long, and they were laid along a laboratory bench top or hung from a support. Heating rates as high as 1300°C/min were possible with these columns.<sup>29-30, 81</sup> Separation of five normal alkanes (C<sub>6</sub>-C<sub>10</sub>) was achieved within 2 s using this heating system.<sup>81</sup> However, the column coating process was time-consuming and non-reproducible. Uneven temperatures along the length of the column were possible. Although Phillips first showed the application of direct resistive heating to an entire column in the mid 1990s, he started using this coating technique in the mid 1980s to construct on-column thermal modulators to introduce narrow sample bands into capillary columns, especially for comprehensive two-dimensional GC applications.<sup>133-135</sup>

#### ***1.5.1.2 On-column Wire Resistive Heating***

The drawback of direct resistive heating of fused-silica columns with metal coatings is the mechanical instability of the conductive coating due to differences in thermal expansion coefficients of the fused-silica and the conductive coating. Although direct resistive heating requires the least amount of power for heating, mechanical instability and uneven coating resulted in problems such as uneven heating, rupture of the conductive coating, and damage to the column itself.<sup>85</sup>

In 1996, Ehrmann and Overton offered another approach for resistive heating of fused-silica columns.<sup>85, 136-137</sup> In their design, the heating element was either a separate tube (coaxial heater) or a resistive heating wire placed along the column (collinear heater).<sup>85</sup> In both cases, a temperature sensor was placed along the column and a Teflon tube was used as an electrical insulator between column coils. The configurations were capable of accurately programming the column temperature from 50°C to 300°C. The

columns used were 3 m long, and linear heating rates of up to 600°C/min and cooling rates of 230°C/min were possible, with a peak power consumption of only 60 watts. Lower heating rates were expected with respect to previous direct resistive heating systems due to the higher thermal masses of the resistive heating element, temperature sensor and insulation. Both coaxial and linear heater designs performed similarly. However, the coaxial heater had some drawbacks. The nickel coating used to decrease the resistance of the coaxial heater came off, and the coaxial heater ends had the potential of breaking the fused-silica columns by abrasion.<sup>85</sup>

A similar colinear heating approach was suggested by Norem in 1961.<sup>84</sup> In his invention, a glass tube with three parallel holes was used to contain a heating wire, a temperature sensor and the separation column. Such a device would have had a very low thermal mass, but no temperature and separation data performance were provided. Another interesting collinear approach was demonstrated by Dubski in 1971.<sup>89</sup> In his approach, a coated metal wire running coaxially inside a column was resistively heated. Both metal and nylon columns were evaluated.

The work by Yost, Phillips and Overton in the 1990s renewed interest in resistance heating methods for fast separations and portable GC applications. After their work, other resistive heating approaches as well as commercial systems were developed. More recently in 2008, Tienpont *et al.*<sup>138</sup> developed a coaxial resistive heating jacket for capillary columns. The jacket consisted of polyimide tubing (0.5 mm ID) covered with densely braided thin metal wires that were then coated with a polyimide layer to serve as electrical insulation. For heating, the capillary column was inserted inside the heating jacket and the braided wires were resistively heated. Heating rates up to 100°C/min were

achieved for a 5 m column, although they were limited by the power supply, since the column was tested in a portable GC system.

### ***1.5.1.3 Resistively Heated Column Fixtures***

Another resistive heating approach for metal and non-metal capillary columns is to resistively heat a separate device that is in close contact with, and serves as, a structural support to the column. The increase in thermal mass as a result of the heating fixture can be observed by lower achievable heating rates compared to previously discussed direct resistive heating methods. An example of resistive heating through a heating fixture is the Perkin-Elmer Model 226 GC previously discussed in which the capillary column was sandwiched between two resistively heated metal plates.

In an invention described by Sides and Cates,<sup>91</sup> a capillary column was heated through a tubular (cylinder) heat conductor around which the column was wrapped. The resistive heating elements were placed in the inside wall of the heat conductor, and a fan mounted inside the tubular fixture was used for cooling. Heating rates as high as 210°C/min were achieved and cooling from 180-50°C was performed within two min (~65°C/min).

Another resistive heating design for capillary columns was described by Maswadeh and Snyder.<sup>92</sup> In their invention, the resistive metal column support was a flat ring oven which contained an internal and external groove. The internal groove was designed to contain a coiled capillary column, and the external groove was designed to contain a resistive heating wire to heat the metal ring fixture. A cooling fan in the middle of the ring oven was used for cooling. The small dimensions of the ring oven (3.8 x 2.5 x

0.64 cm) allowed it to reach a heating rate of 45°C/min and a cooling rate of 25°C/min with a power consumption of 15 W during heating and 9 W during cooling.

More recently in 2006, Roques<sup>90</sup> described a design in which a capillary column was constrained in a flat, ordered spiral pattern, encased between two thin opposing surfaces by an adhesive force or mechanical compression. The system was heated by resistive heating and cooled by means of a fan or a Peltier cooler. The resistive heating element was deposited as a thin conductive layer on top of one of the surfaces containing the spiral. The low thermal mass of this system allowed it to achieve heating rates as high as 300°C/min for a 1.7 m column with a power requirement of 91 W; however, the cooling time was not reported.<sup>90</sup>

### **1.5.2 Commercially Available Resistive Heating Systems**

The first commercially available resistive heating system for fused-silica capillary columns was the EZ Flash from Thermedics Detection introduced in 1998.<sup>58, 94</sup> The EZ Flash system followed the coaxial heater design of Overton in which a fused-silica capillary column was inserted into a metal sheath that was resistively heated. The heating tube was externally insulated and coiled into a radius that fit inside a conventional air bath oven. The column assembly was connected to the injector and detector through interface heaters that could be individually adjusted; the interface also served to electrically insulate the resistive heating tube. The columns were typically either 5 or 10 m long. The column assembly was powered using a 96 V computer-controlled power source, and the temperature was determined by resistance measurements of the heating tube. Heating rates as high as 1200°C/min and cool down times of approximately 1 min from 350°C to 40°C could be achieved.<sup>58, 64, 88, 94, 139</sup> The column arrangement was rapidly

cooled by activating the oven fan at the end of the run. This resistive heating technology was acquired by Thermo Scientific and replaced with a resistive heating wire to extend its use to capillary columns with broader range of lengths and diameters.<sup>64, 88</sup>

Another commercially successful resistive heating system for capillary columns was the low thermal mass (LTM) GC column from RVM Scientific. This resistive heating design was developed in the mid 1990s.<sup>140</sup> Currently, this technology is owned by Agilent Technologies.<sup>141</sup> The column assembly follows Overton's collinear heating approach in which a resistive heating wire and a temperature sensor are placed along the capillary column. In the LTM column design, the heating element is a Nickel wire electrically insulated with a ceramic fiber that is placed along the capillary column over its full length. The temperature of the assembly is sensed by measuring the resistance of a 2 m platinum wire that is electrically insulated and combined with the column.<sup>140</sup> The heating wire, column, and temperature sensor are bundled together. The bundle is then coiled in a toroidal geometry to maximize the heat exchange between the coils and to minimize the exposed surface area, reducing convective heat loss. Even though the heater, column, and temperature sensor are insulated with ceramic fibers, thermal conduction takes place because the fiber layer is very thin.<sup>142</sup> The torus assembly is wrapped with aluminum foil to conduct and contain the heat in the column bundle for temperature uniformity, and to conserve power.<sup>87</sup> The smaller the torus diameter, the greater the heating efficiency. However, optimized packing of the bundle requires a compromise in torus dimensions to allow enough surface area exposure for fast cooling. The column in the LTM GC assemblies are coiled to a 5-inch diameter torus.<sup>141</sup> For smaller torus diameters, the mechanical stability of the column should be considered. The



LTM column assembly allows heating rates up to 1800°C/min, depending on the column length and configuration.<sup>141</sup> A small fan placed in front of the column assembly is used for cooling by forced convection of ambient air. Cooling from 350 to 50°C can be achieved in 2 min or less, depending on the column length.<sup>24, 140-141</sup> Power consumption has been measured to be on the order of 1-5 W/m, depending on the heating rate.<sup>24, 87</sup> A transfer line is used at each end of the toroidal assembly to connect the column to the injector and detector with minimum cold spots. Moreover, temperature gradients between the transfer lines and the toroidal column assembly are eliminated by heating the transfer lines at the same time as the column assembly.<sup>140</sup> With this approach, the column length is not hindered and long capillary columns up to 30 m can be resistively heated.<sup>141</sup> Even metal capillary columns can be resistively heated using this technique, which is desirable for portable GC applications due to their robustness compare to fused-silica columns. With this method, there is no need to electrically isolate the injector and detector from the column assembly. The LTM column design is currently the most successful resistive heating technique on the market for fast GC separations and for portable applications.

Valco Instruments (VICI) is a well known company for its specialized valves and fittings for analytical applications. Among many other capabilities, VICI has technology for producing fused-silica capillary columns as well as for producing high quality electroformed nickel tubing. With this knowhow, VICI has been developing electroformed nickel columns, sleeves and Ni-clad fused silica columns for resistive heating applications since the mid 2000s. Nickel has the highest change in resistance vs. temperature of any metal. This allows nickel-clad fused silica to serve both as the heater and sensor without adding additional mass. The electroplating of pure nickel over the

fused-silica column allows a uniform coating along the tubing, which eliminates temperature gradients along the column, as well as cold and hot spots. The Ni-cladding provides robustness to the fused-silica columns and higher mechanical stability than previous metal coated fused-silica columns.

In 2005, VICI demonstrated a prototype miniature GC-TCD system based on resistive heating of a Ni sleeve over a fused-silica capillary column.<sup>143</sup> More recently in 2009, VICI introduced a Ni-clad polyimide-coated fused silica column that could be used for direct resistive heating applications and a Fast GC Module which contained a direct resistively heated column and a pulse discharge detector, showing the portability potential of their technology. For GC applications, the Ni-clad column is electrically insulated and then coiled in a small (2.5") torus bundle. The electrical insulation of the Ni-clad column is provided by coating the column with a polyimide layer or by using a thin ceramic fiber sleeve. Heating rates as high as 1200°C/min and cooling times from 200 to 70°C in less than 1 min for a 7 m column can be achieved with a small fan.<sup>82</sup> Resistive heating is performed with a 24 or 48 VDC power supply. Column lengths up to 30 m are available. This technology has great potential for developing direct resistive heating applications for portable GC instruments. An advantage of using the column as the heating element and temperature sensor is that there is no delay in temperature feedback, providing accurate temperature tracking and reduction in temperature overshoot during fast ramping, which could be a problem in other resistive heating systems.

Following a similar resistive heating design as Maswadeh and Snyder, C2V Incorporated (Concept to Volume) developed its Micro GC Technology in the mid 2000s.

This technology is now owned by Thermo Scientific which has recently introduced the C2V-200 micro GC product.<sup>93</sup> The fixture that supports the column consists of a flat metal ring with a groove in the inner circumference where the capillary column is coiled. The groove width is designed to be 3 times the column diameter to ensure maximum temperature conduction and uniformity in the coiled column.<sup>93</sup> Heat is provided by placing the ring housing between two circuit boards that contain conductive tracks that are resistively heated. Heating rates up to 240°C/min and cooling rates of 60°C/min for a 5 m column can be achieved with this system. The typical power consumption is 20 W with a maximum of 120 W.<sup>98</sup> The modular format of the C2V system is an appealing design, where the column, injector and detector are all together in a cartridge. Column exchange and maintenance in this system is easily performed. The down side of the system is the maximum operational temperature, which is only 180°C.

The zNose<sup>TM</sup> uses a chromatographic column that can be directly heated at rates up to 1080°C/min. The column is arranged in a flat spiral and kept in place between two thin surfaces.<sup>144-145</sup> Typical run times are in the 10's of seconds to achieve near real-time analysis.<sup>146</sup> This design allows the column to cool down quickly, but at the expense of less efficient heating. The zNose GC-SAW system is manufactured by Electronic Sensor Technology.<sup>147</sup>

### **1.5.3 Direct Resistive Heating of Metal Capillary Columns**

In 2007, Reid and Synovec reported direct resistively heating of commercially available stainless-steel capillary columns. Metal capillary columns were used in the 1960s; however, due to their high surface activity, they were replaced by glass and later fused-silica columns. The MXT columns from Restek are treated with Silcosteel, a

proprietary coating technology that greatly reduces the activity of the metal surface. The column used for the experiment was a 2.3 m x 0.18 mm x 0.4  $\mu\text{m}$  MXT-5 column. The column coils were electrically insulated from each other by threading the column into an insulating cage. Heating rates as high as 240°C/s (14,400°C/min) and cooling times between 30 s to 2 min were possible. The power supply used was a variable autotransformer (0-120 VAC). The heating rate was indirectly determined from previous isothermal data and assuming linear heating rates.<sup>148</sup> The purpose of the work was to perform temperature programmed separations in 1 s; thus, they needed heating rates of over 200°C/s to separate a wide boiling range sample.

More recently, Xu and coworkers<sup>95</sup> also used a metal capillary column from Restek to perform direct resistive heating. In their work, they addressed problems of temperature gradients and hot spots along the metal column due to uneven wall thicknesses. To reduce temperature variations along the column, they applied a current with pulse width modulation in cycles of 100 ms with a maximum duty cycle of 95%. The time interval of the pulse provided a time lag for the heat to transfer between column sections, maintaining a uniform temperature along the column. The metal column was electrically insulated with braided fiber glass. Temperature was measured with a type K thermocouple tightly bound to the outer surface of the column. The metal column was electrically isolated from the detector by using a union interface. Heating and cooling rates up to 600°C/min and 400°C/min, respectively, were obtained with this system. The power supply voltage applied was in the range of 42-125 VDC, with a maximum power requirement of 35 W/m, depending on temperature programming rates and column

length. A drawback of this heating system is that it is limited to short columns; 8-30 m long columns produce safety problems during operation.

#### **1.5.4 Resistive Heating in Microcolumn GC Systems**

Heating and cooling method development goes hand-in-hand with column technology. In the past decade, there has been an increased interest in miniaturization of analytical systems. In the case of GC, miniaturization involves reduction in size of the separation column. The use of photolithography and chemical etching techniques has allowed the development of microfabricated columns in a silicon wafer. This technology, although introduced in the late 1970s by Terry et al.,<sup>149</sup> has gained most interest in the past decade. Currently, there are several laboratories that are working towards miniaturizing the GC system.<sup>96, 150-156</sup> Although air bath ovens have been used as a means to evenly heat the silicon wafer to characterize the separation performance of microfabricated columns,<sup>150, 152, 157-158</sup> the use of bulky ovens defeats the micro fabrication purpose. The preferred method for heating microfabricated columns is resistive heating, either using a separate resistive heating element<sup>94</sup> or by direct deposition of a resistive heating tracing on the silicon itself.<sup>96, 120, 156, 159-160</sup> Furthermore, integration of the resistive heating and temperature sensing elements into the microfabricated column greatly reduces the thermal mass of the system and allows for accurate temperature measurements. Heating rates as high as 60°C/s (3600°C/min) can be achieved in microfabricated GC columns by resistive heating methods.<sup>96</sup> Thermoelectric heat pumps (Peltier coolers) in combination with resistive heating elements have been used with microfabricated columns to provide a wide temperature range from sub-ambient to

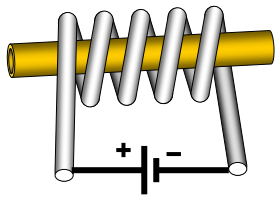
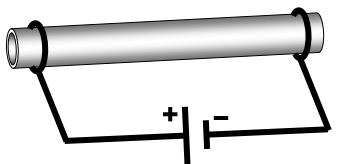

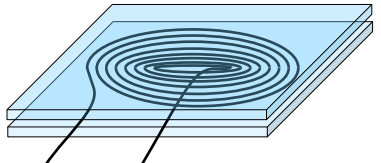


300°C.<sup>120, 161</sup> Peltier coolers also help to increase the cooling rate, and can be used as well for heating purposes.<sup>120, 162-163</sup>

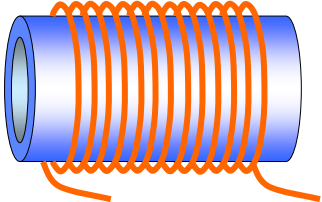

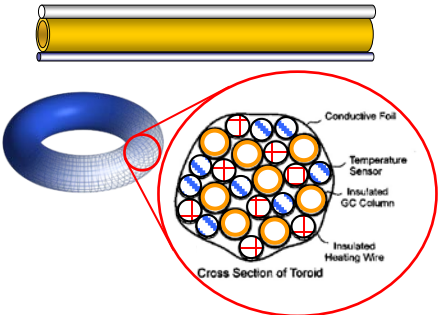

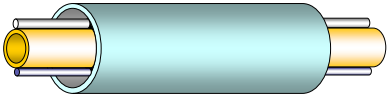
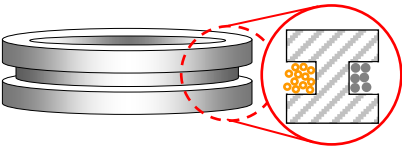
The small thermal mass of the microfabricated column and its resistive heating elements improves the thermal response and power consumption of these systems, which is important for portable applications. In Table 1-1, a chronological list of the different resistive heating methods is provided.

## **1.6 THERMAL GRADIENT GC (TGGC)**

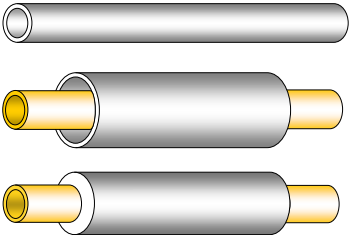
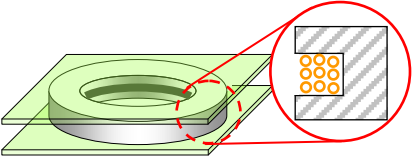
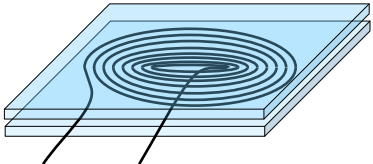
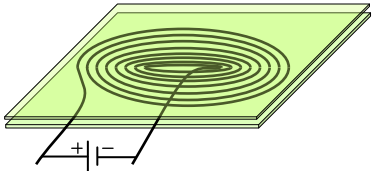
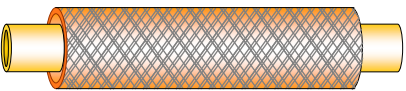
Currently, the two major operational modes in GC are isothermal GC (ITGC) and temperature programmed GC (TPGC). ITGC provides the highest resolution of any separation mode and it is very useful for the analysis of complex samples with a narrow range of boiling temperatures. On the other hand, TPGC is used to separate mixtures with a wide boiling point range. In both ITGC and TPGC methods, the temperature along the length of the column is constant at any given time,  $T(t)$ . Another mode of performing GC is by manipulating the column temperature as a function of time and position along the column,  $T(t,x)$ .<sup>164</sup> This novel operational mode is known as thermal gradient GC (TGGC).<sup>25, 29</sup> In TGGC, the temperature along the axial direction of the column always decreases from the injector to the detector in any given time and position.<sup>25, 28, 165</sup> TGGC can be easily understood by using three-dimensional temperature vs time and column length plots or thermal fields, as shown by Rubey (Figure 1-12), where the differences between the three separation modes can be clearly seen.<sup>25</sup> For instance, ITGC for which the column temperature is constant at any given time and position along the column can be represented by a horizontal plane (Figure 1-12A).

**Table 1-1. Overview of resistive heating instrumentation development in gas chromatography.**

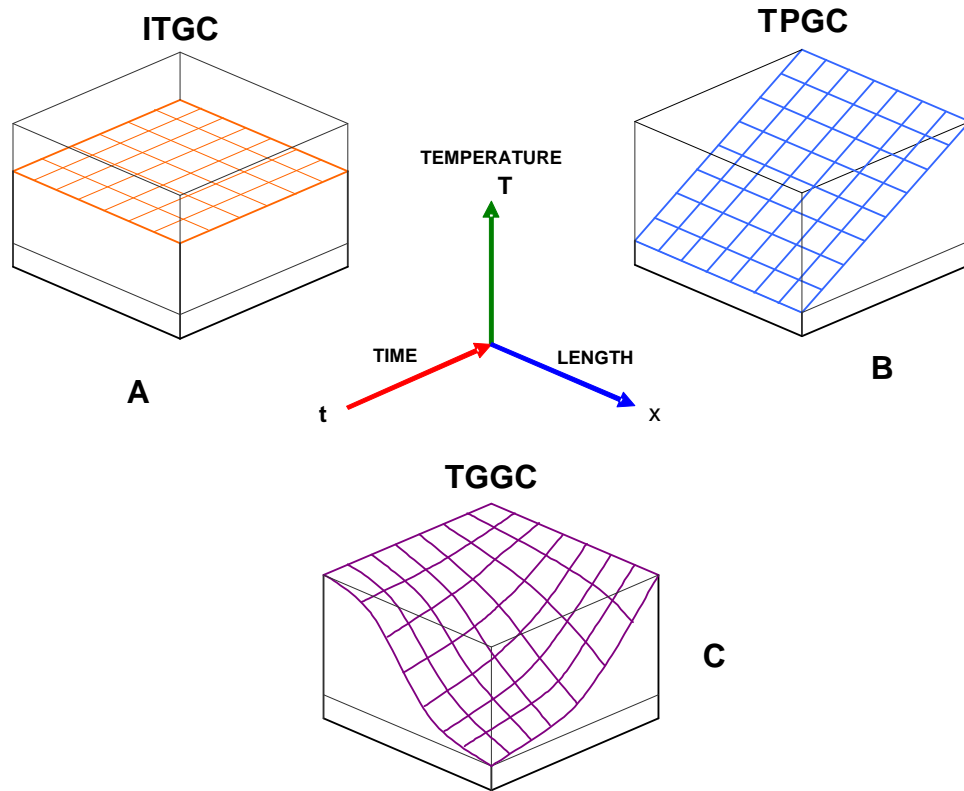
Year	Diagram	Description	Author
1957		Uniformly wrapped packed column with insulated heating wire	Burrell Kromo-Tog K-2 <sup>52, 54</sup>
1958			Dal Nogare <sup>84</sup>
1958		Direct resistive heating of metal packed column	Dal Nogare <sup>86</sup>
1960			Perkin-Elmer GC Model 222 and 222P <sup>66</sup>
1961		Three-hole glass tube with heating wire, temperature sensor and column	Norem <sup>84</sup>
1962		Resistive heating fixture Flat spiral metal column between two aluminum plates resistively heated by two metal blocks.	Perkin-Elmer Model 226 <sup>52, 58</sup>
1971		Resistive metal wire inside column	Dubski <sup>89</sup>
1989		Aluminum clad fused-silica column directly resistively heated	Hail and Yost <sup>83</sup>
Year	Diagram	Description	Author

1991		Tubular heater fixture. Fused silica is wrapped around and the resistive heating element is inside the cylinder	Sides and Cates <sup>91</sup>
1995		Conductive paint coating over fused-silica columns, direct resistively heated	Jain and Phillips <sup>81</sup>
1995		Low thermal mass (LTM) toroidal column with heating wire and temperature sensor in a collinear configuration. Ceramic fiber is used as electrical insulation. The system is then coiled in a toroidal arrangement	RVM now owned by Agilent Technologies <sup>24, 87, 140, 142</sup>
1996		Coaxial heater tube or metal sheath, resistively heated with Teflon tube insulation	Ehrmann and Overton <sup>85</sup> (first suggested this design)
1998		Collinear heating wire with temperature sensor cover with Teflon tube insulation	EzFlash system by Thermo Scientific uses this design <sup>58, 94</sup>
1999		Flat ring oven with internal and external grooves for column and heating wire, respectively	Maswadeh and Snyder <sup>92</sup>
<b>Year</b>	<b>Diagram</b>	<b>Description</b>	<b>Author</b>



2005		Electroformed nickel tube, sleeve, and Ni-clad fused silica column, directly resistively heated	Valco Instruments (VICI) <sup>82, 143</sup>
2005		Flat ring oven metal fixture with inner groove for column, heated by circuit boards with resistive heating elements	C2V micro-GC from Thermo Scientific <sup>98</sup>
2006		Flat ordered spiral column between heating surfaces	Roques <sup>90</sup>
2006		Metal column in a flat spiral arrangement, directly resistively heated	zNose <sup>™</sup> GC-SAW system manufactured by Electronic Sensor Technology <sup>144, 146</sup>
2008		Resistively heated capillary column with a braided wire Jacket	Tienpont <sup>138</sup>

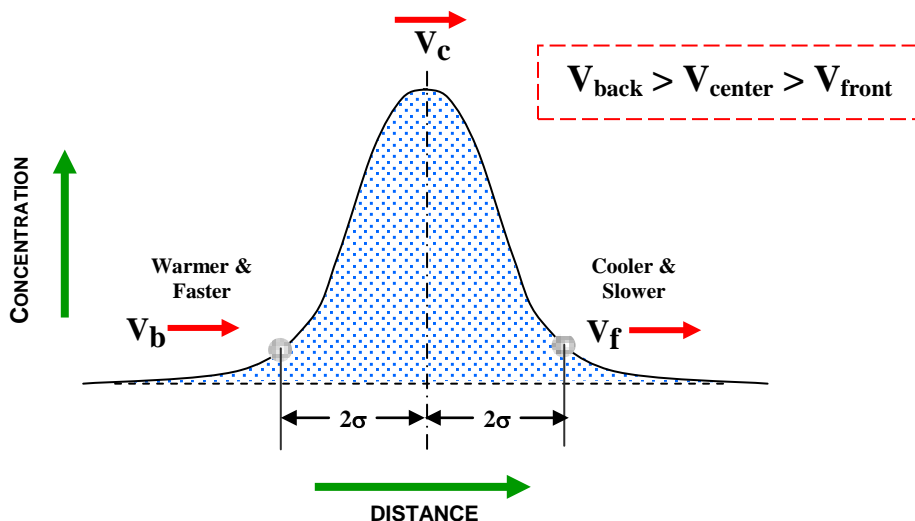
Temperature programmed operations, in which the entire column temperature experiences a gradual increase as a function of time (heating rate), is represented with an inclined plane (Figure 1-12B). However, three dimensions are needed to describe the temperature surface (thermal field) applied in the TGGC technique, since the column temperature varies in time and position along the column (Figure 1-12C). The three-dimension views of these different operational modes help to understand and clearly visualize the TGGC process.



**Figure 1-12. Three-dimensional views of the operational modes of GC.**<sup>25, 32</sup>

An important operational aspect of TGGC is that a solute zone will continually encounter a negative temperature gradient throughout its chromatographic axial migration.<sup>29, 36, 165</sup> Moving into regions of lower temperature leads to greater retention, resulting in lower axial velocity (see Figure 1-13). This effect causes the front of a peak

to move slower than the back of the peak, leading to a narrower focused peak. A negative thermal gradient provides a mechanism for solute zone axial compression and concentration similar to that produced by cryofocusing.<sup>166-167</sup>



**Figure 1-13. Focusing mechanism of migrating zone.**<sup>29, 36, 165</sup>

This behavior is clearly different from that experienced in other GC modes, such as ITGC and TPGC, in which the axial length of a migrating solute zone continually increases with migration distance. With axial compression provided by TGGC operation, the longitudinal spread of a migrating solute zone actually diminishes as depicted in Figure 1-13. Furthermore, with the large number of variables associated with TGGC, there are correspondingly more operational variables available for obtaining increased selectivity for closely spaced solute zones, such as gradient length, slope, temperature difference between the inlet and outlet of the gradient, gradient profile, linear velocity, starting heating time and heating rate. Moreover, the TGGC operational mode has demonstrated its use for separating substances that differ greatly in volatility or polarity.<sup>32, 168</sup> Although peaks are narrower in TGGC, the distance between the centroids of adjacent peaks is also smaller, usually less than in TPGC. This effect must be taken

into consideration with regard to the peak capacity and chromatographic resolution.<sup>25, 29, 165, 168</sup>

## 1.7 AXIAL TEMPERATURE GRADIENTS IN GC

The first application of temperature gradients was performed in 1951 by Zhukhovitskii *et al.*<sup>27, 169-171</sup> In this work, a moving negative gradient along the longitudinal axis of a gas-solid partition chromatography column was used to decrease severe tailing of peaks.<sup>172</sup> The negative temperature gradient was generated by using a furnace in which the highest temperature was at the head of the column and a lower temperature was at some distance down the column. This variant of GC was called chromathermography.<sup>27, 173</sup> In chromathermography, the gradient was used in either a stationary or non-stationary manner. In 1956, Zhokhovitskii introduced the heat dynamic method in which frontal chromatography and a non-stationary gradient were combined, allowing semi-continuous analysis of samples.<sup>36</sup> In the 1950s, gas chromatographs in the Soviet Union were designed for chromathermography. In 1958, the model KhT-2 and later the KhT-2M gas chromathermograph were introduced in a large scale.<sup>174-176</sup> In this instrument the moving thermal field was produced by contact heating of the spiral chromatographic column and by blowing air along it, opposite to the direction of the carrier-gas flow.<sup>172, 174</sup> Outside the Soviet Union, there were few publications on chromathermography. One of the first publications was in 1960 by Zhukhovitskii describing the applications of the technique.<sup>177</sup> Several other publications from Russian journals were reviewed by A. P. Tudge, who further elaborated on the theory of the technique.<sup>26</sup> The chromathermography method was later explored by Nerheim<sup>178</sup> in the early 1960s in which he suggested that an improved separation in GC may be achieved

with a moving temperature gradient. In his system, a 1ft glass sleeve covered with heating tape produced a temperature gradient of 2°C/min. The oven was passed several times over the packed column, increasing the temperature with each pass and separating individual peaks. However, it was not until 1963 with Ohline's work that a detailed theoretical study of this technique in gas-liquid partition chromatography was performed.<sup>27, 173</sup> Ohline and DeFord employed a moving negative gradient oven. The oven consisted of a 15" aluminum bar that contained two heat exchanging compartments located at each extreme of the bar. One heat exchanger used tap water and the other used steam to form the temperature gradient along the aluminum bar. Gradient slopes between 1 and 8.5°C/cm were achievable with this system. In 1968, Kaiser<sup>179</sup> described the use of chromathermography with a moving oven to perform semi-continuous analysis of a sample, and to serve as a concentration technique for the analysis of trace substances in gases.

In the 1970s, a new way of performing chromathermography was studied; instead of moving a furnace, the gradient was generated through the whole column. Vergnaud *et al.*<sup>8, 180-181</sup> at the University of Saint-Etienne, France, used electrically insulated resistance heating wire wound around the column. The number of wire windings per unit length of the column was varied to generate a linear temperature gradient. A number of options were then available; a constant stationary gradient could be employed or the gradient temperature could be increased with time. Vergnaud applied axial temperature gradients in combination with different GC techniques, such as isothermal, programmed temperature and backflushing,<sup>7-8, 182-183</sup> as approaches for improving separations and reducing analysis time.

In 1973, Kaiser<sup>184</sup> used a static gradient in a sorbing bed for enriching volatile organic compounds from gases for environmental analysis. The focusing of compounds on the trap collected the sample components at different places within the gradient, thus preventing chemical reaction of the enriched traces with each other. The gradient was generated in a coaxial heat exchanger tube in which the middle was filled with the absorbent material and the outer shell was used to introduce cold nitrogen. Preheated nitrogen gas was used for heating.

All of the above studies were performed using conventional packed gas chromatographic columns. In 1975, Fenimore<sup>164</sup> applied axial temperature gradients to capillary columns. The system used for creating the temperature gradient consisted of individual heating sections in intimate contact with the capillary column. The heating segments consisted of 4.45 cm OD x 7.62 cm long brass tubes with a resistive heating element placed inside and with an outer spiral groove where the column was wrapped. The system was flexible enough to generate temperature gradients with different gradient slopes as well as various operating modes, such as temperature programming.<sup>164</sup>

In the early 80s, the principles of chromathermography were summarized by Vigdergauz, who discussed the early periods of GC in the USSR.<sup>185-187</sup> A more detailed description of the various techniques developed from the 1950s to the 80s employing a thermal gradient along the separation column was given by Berezkin *et al.* in the mid 1980s.<sup>36, 188-189</sup> In the 1990s, renewed interest in the application of axial temperature gradients was observed. In 1991, Rubey used a column sheath assembly based on a counter-current heat exchanger principle for establishing temperature gradients along the column. The fused-silica capillary column was wrapped on the outside of a coaxial heat

exchanger where cold nitrogen and preheated in-line nitrogen gas was used to change the temperature over distance and time within the heat exchanger. Improved separation times and efficiencies were claimed by rapid change in a curvilinearly-shaped negative temperature gradient profile.<sup>25, 30, 165, 190</sup> Moreover, Rubey introduced a novel way of visualizing the use of axial temperature gradients by incorporating the column length as a third dimension in conventional temperature vs time plots, establishing the concept of thermal fields or three-dimensional temperature surfaces.<sup>25</sup> Phillips and Jain demonstrated fast separations in less than 2 s for a series of alkanes from heptane to decane by applying negative temperature gradients.<sup>29-30, 81</sup> The temperature gradients were generated by resistively heating fused-silica capillary columns that were coated with varying layers of electrically resistive coating. The resistance of the coating was proportional to the temperature.<sup>30</sup>

Several instrumentation patents during the 1990s were designed to create axial temperature gradients along the separation column to perform chromathermographic separations, which demonstrated renewed interest in this technique. In 1991, Rubey<sup>191-192</sup> introduced a system that created axial temperature gradients by controlling the temperature of a heat transfer fluid by resistive heating, with the capability of rapidly modifying the gradient with time. The column was placed coaxially inside a heat exchanger system where resistive heating elements placed on the inside walls regulated the temperature of the heat transfer fluid. Hiller introduced a patent in 1993 describing the use of a coaxial heat exchanger to establish negative temperature gradients for improving chromatographic analysis. Rounbehler *et al.* introduced a patent in 1998 in which several heating techniques to achieve axial temperature gradients in capillary

columns were described. Among their ideas, they suggested resistively heating metal columns with variable cross section, and also removing heat from a uniformly resistively heated column at different rates along the length of the column by using circumferential fins with varying diameters.<sup>102</sup> However, chromatograms showing separations using these systems were not provided.

In 1996 Weihong, *et al.*,<sup>193</sup> and in 1999, Xiaoyan *et al.*<sup>194</sup> reported a different type of static gradient. In their approach, the gradient formed was not in temperature, but instead it was in the thickness of the stationary phase along the column. A 3 m long by 3 mm ID column was divided into 4 sections that contained packing materials with four different stationary phase thicknesses, increasing or decreasing in thickness along the column. Xiaoyan tested a gradient that followed a cosine thickness profile.<sup>194</sup> Separation with this column was compared with a homogeneous packed column containing the average stationary phase thickness of the gradient column. The sample used was a mixture of normal alkanes from C6 to C9, and the results showed narrower peaks obtained when gradient film thicknesses were employed.

In 2002, Zhao *et al.* evaluated the use of TGGC as a separation mode in a mini-size gas chromatograph for the analysis of natural gas. A different approach was used for generating an axial temperature gradient along a short 70 cm micro packed capillary column. In their system, a static temperature gradient was generated on a 20 cm diameter by 0.5 mm thick circular brass plate, which was heated with a smaller circular heating plate in the center. The column covered with different thickness asbestos sheaths was then placed on top of the brass plate following an Archimedes spiral arrangement, forming the temperature gradient along the column, and the column inlet was located at

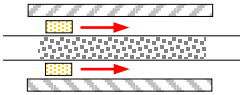
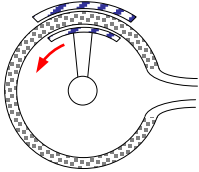
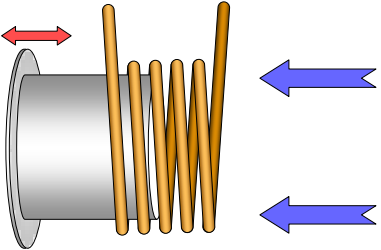
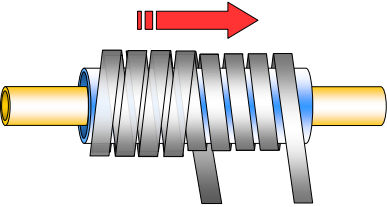
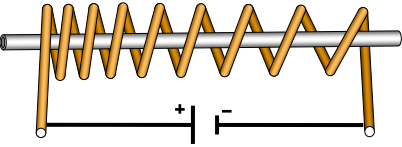


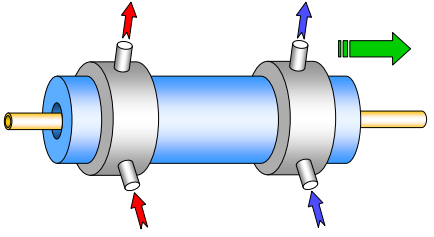
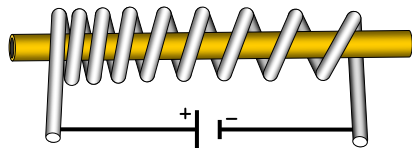
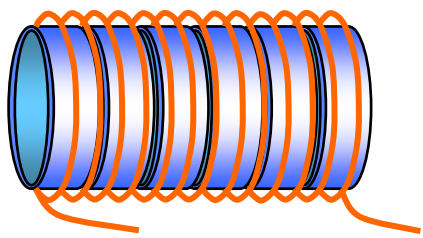

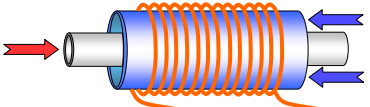
the center of the brass plate. A mixture of four alcohols (methanol, ethanol, propanol and butanol) was used to compare the different GC separation modes of ITGC, TPGC and TGGC. Results showed that the temperature gradient slope ( $^{\circ}\text{C}/\text{cm}$ ) played an important role in resolution, and that faster and narrower peaks were achieved with the TGGC technique compared to the ITGC and TPGC modes.


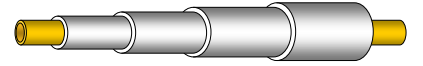
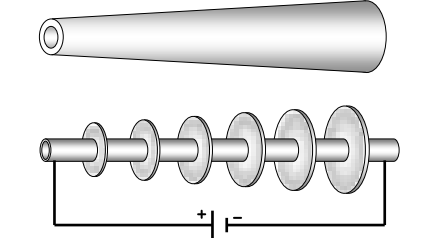
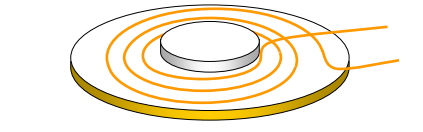
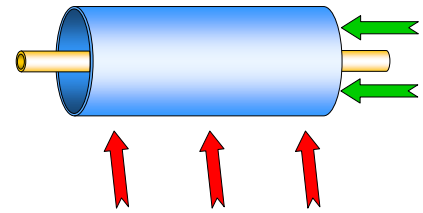
More recently in 2004, Contreras used a heat exchanger approach to generate axial temperature gradients along a 1 m commercial fused-silica capillary column.<sup>32</sup> The heat exchanger system consisted of a low thermal mass, hand-made  $\frac{1}{4}$ " diameter polyimide tube in which the capillary column was placed coaxially. The gradient was generated when cold nitrogen gas was increasingly heated as it flowed through the polyimide tube, which was placed inside a hot ( $250^{\circ}\text{C}$ ) GC oven. The peaks inside the temperature gradient slowed down, therefore, heating of the cold side of the gradient was required to release the focused peaks into the detector. Heating and cooling rates as high as  $33^{\circ}\text{C}/\text{s}$  ( $1980^{\circ}\text{C}/\text{min}$ ) and  $200^{\circ}\text{C}/\text{s}$  ( $12,000^{\circ}\text{C}/\text{min}$ ), respectively, were achieved with this column assembly, allowing TGGC separations every 15 s for the second dimension of a multidimensional gas chromatography-mass spectrometry (MDGC-MS) system. The use of TGGC allowed faster separations in longer second dimension columns, eliminating wrap-around problems and improving the separation in the second dimension of the MDGC-MS system.

Table 1-2 shows the chronological development of the TGGC techniques to date.

**Table 1-2. Overview of the instrumentation development of TGGC**

Year	Diagram	Description	Author
1951	 A schematic diagram of a packed column. The column is shown as a horizontal tube with a central core of packing material. A smaller, shaded rectangular oven is positioned around the column, with red arrows indicating its movement along the length of the column.	Chromathermography in which a packed column is placed inside a large isothermal oven combined with a smaller oven moving along the column	Zhukhovitskii <sup>27</sup>
1956	 A cross-sectional diagram of a circular column. A central sample is shown being introduced into the column. A furnace with a temperature gradient is shown rotating around the column, with a red arrow indicating the direction of rotation.	Thermal dynamic method in which a sample is continuously introduced into a circular column where a furnace with a gradient rotates, allowing semi-continuous analysis	Zhukhovitskii <sup>36</sup>
1958	 A diagram showing a coil of orange rods. A red double-headed arrow above the coil indicates the displacement direction of the resistive heating fixture. Two blue arrows point from the right towards the coil, representing the flow of air for convection.	Moving conductive heater over a column coil for contact heating with forced air convection in the opposite direction for generating the gradient  Blue arrows: flow of air Red arrow: displacement direction of the resistive heating fixture	Model KhT-2 and KhT-2M gas chromathermographs <sup>185</sup>
1960	 A diagram of a glass sleeve (yellow cylinder) with a heating tape (grey) wrapped around it. A red arrow above the tape indicates its movement along the length of the sleeve.	Glass sleeve with heating tape for generating the gradient which is moved along the column	Nerheim <sup>178</sup>
1962	 A diagram of a coil of orange rods wrapped around a central grey tube. A red arrow above the coil indicates its movement along the tube. A battery symbol with '+' and '-' signs is shown below the coil, connected to the ends of the coil.	Patent suggesting induction heating through a coil with a decreasing wrapping density which is moved along the column	Brashear <sup>103</sup>
Year	Diagram	Description	Author

1963		<p>Aluminum bar with two heat exchanger chambers used to generate the gradient over the column</p> <p>Red arrow: steam water Blue arrow: tap water</p>	Ohline and DeFord <sup>173</sup>
1970		Resistive heating wire with decreasing wrapping density providing a static gradient	Vergnaud <sup>8, 180-181</sup>
1975		Individual resistive heating section to generate the axial temperature gradient	Fenimore <sup>164</sup>
1991		Heat exchanger using resistive heating to heat cold nitrogen as it advances along the column	Rubey <sup>25, 28</sup>
1992		Heat exchanger with column externally wrapped	
<b>Year</b>	<b>Diagram</b>	<b>Description</b>	<b>Author</b>

1993		Coaxial heat exchanger	Hiller <sup>195</sup>
1995		Conductive paint coatings in resistive layers for generating the gradient by direct resistive heating	Jain and Phillips <sup>29-30</sup>
1998		<p>Direct resistive heating of a metal column with a variable cross section</p> <p>Removing heat from a uniformly resistively heated column at different rates by using circumferential fins with varying diameters</p>	Rounbehler <sup>102</sup>
2002		Gradient in a circular brass plate with resistive heater in the center and with the capillary column coiled around	Zhao <sup>31</sup>
2004		<p>Heat exchanger with a capillary column placed coaxially along a low thermal mass polyimide tube that is positioned inside a GC oven</p> <p>Green arrows: cold nitrogen gas Red arrows: hot convective air from GC oven</p>	Contreras <sup>32</sup>

### 1.7.1 Controversy Around TGGC

Even though TGGC was first introduced in 1951, it is still considered to be in its early stages. The complexity of the instrumentation compared to isothermal and programmed temperature separations has made its implementation and, hence, its study difficult. Over the years, the idea of changing the temperature along the chromatographic column to produce a focusing effect has intrigued gas chromatographers. Several studies on the use of axial temperature gradients in GC have highlighted the appealing characteristics of the technique, such as reduced tailing, narrow peaks, better detection of trace components and fast analysis. However, considerable controversy has emerged over the separation capabilities of TGGC compared to programmed temperature separations regarding resolution and speed of analysis.<sup>196</sup> Previous work has suggested that TGGC can provide superior performance with respect to conventional GC separation modes.<sup>25, 28-30, 178</sup> The assumption comes from the focusing effect observed in TGGC, which produces narrow peaks believed to aid in separation performance compared to the continuous broadening observed in conventional ITGC and TPGC separation modes. However, the gradient not only focuses the bands, but it also moves them closer together.

Theoretical studies from Blumberg and Ohline<sup>168, 173, 197</sup> have shown that under ideal chromatographic conditions, an increase in the gradient slope for a moving linear gradient produces an overall resolution decrease relative to isothermal separations. Therefore, a linear moving gradient cannot enhance the theoretical performance obtained in conventional ITGC and TPGC. However, TGGC proponents<sup>25, 29-30, 196</sup> claim that in a more realistic situation, theoretical analysis becomes extremely complex and, thus, does not provide all the answers. Because the capacity factor, a measure of the retention of a

compound in the column, is larger and more consistent throughout the separation in TGGC than in TPGC (*i.e.*, retention in TPGC decreases as compounds migrate through the column), better separations should be obtained in TGGC.<sup>28, 196</sup> The reasoning behind this is that substances that do not interact much with the stationary phase are not resolved from each other. Furthermore, the maintenance of constant capacity factors throughout the separation resembles ITGC separations, which is the separation mode that provides the maximum separation power.

Regarding speed of analysis, compounds are focused at the beginning of the column in TPGC and remain in place until the temperature is high enough for them to move, which is not optimum for separation speed. On the other hand in TGGC, compounds are injected at a high temperature at which the more volatile compounds move immediately down the column where the retention factor is higher, improving separation speed.<sup>196</sup> Nevertheless, Blumberg mentions that the TGGC technique can be a great tool for improving losses of resolution or speed of analysis resulting from non-ideal chromatographic conditions, such as poor sample introduction, column overloading, and dead volumes.<sup>168, 196</sup> TGGC can represent a solution to these problems, which are commonly found in GC systems, especially in micro GC systems where sample introduction, dead volumes, non-uniformities of the stationary phase and active sites are present.

From the previous discussion, one can assume that TGGC is still in its infancy. The instrumentation to generate axial temperature gradients is still a major challenge; however, current technology can facilitate its development, closing this gap. Controversy and instrumentation difficulties have placed this technique on the sidelines, which has not

encouraged its further development. In this work, we demonstrate some unique applications that can be performed using this technique, and shed further light on the controversy surrounding this technique.

## **1.8 MODERN TRENDS AND CHALLENGES IN GC**

In GC, there has always been an interest in developing new methods for improving separation performance, selectivity and analysis time. Presently, this is being achieved by using short, narrow diameter columns with narrow band injections<sup>16-19</sup> and fast heating rates,<sup>23-24</sup> modulating the flow (pressure tunable selectivity),<sup>11-13, 15</sup> and/or moving a sample or fraction between columns with different stationary phases and even column diameters (GC×GC).<sup>9-10, 14</sup> Currently, there is an interest in miniaturization for developing portable systems including microfabricated GC systems because of the inherent performance gains that arise when analytical systems are downsized to the micron scale.<sup>198</sup> The benefits include, but are not limited to, parallel manufacturing for low production cost, small thermal mass for low power consumption, compact and robust systems, short analysis times and field applicability. One of the goals is to produce micro-GC systems that are small enough to be placed inside cell phones to be used for early-warning chemical detection.<sup>199</sup> However, miniaturization of the column comes with reduced sample capacity, need for pre-concentration, wider than desired injection bands and detectors with less than adequate detection limits.

TGGC can aid in overcoming these hurdles. In TGGC, the bands are focused as they travel through the column, allowing on-column concentration and less stringent sample introduction and detection requirements. Furthermore, since TGGC is a focusing technique, it also reduces band broadening due to non-uniform stationary phase coatings,

extra-column effects and dead volumes along the column. Moreover, TGGC offers a separation flexibility that cannot be found in any other separation method, allowing for unique selectivity and fast feedback control for optimizing separations. The use of the TGGC technique in a micro-GC system will allow the maximum potential performance of microfabricated columns, bringing closer to reality the total miniaturization of a GC system.

## 1.9 DISSERTATION OVERVIEW

In this chapter, the importance of temperature in GC separations is established. Then, an overview of the column heating methods is provided to aid in the design and development of TGGC instrumentation. Current challenges and future trends in GC are also discussed. In Chapter 2, a mathematical model to simulate GC separations in axial temperature gradients is presented. A custom-written computer program of the model proved to be very flexible and allowed unique insights on the separation occurring inside the column, which helped in the design of the TGGC instruments presented in Chapters 5 and 6. Chapter 3 shows an analytical approach for understanding the effect of axial temperature gradients in GC. The equations developed provided an accurate method for determining the  $T_{eq}$  of compounds. In Chapter 4, the application of TGGC is shown and a new method for the selective separation of compounds (gating) is introduced. A comparison of TGGC with ITGC and TPGC is also presented in this chapter. Chapter 5 describes the design, fabrication, and evaluation of a moving TGGC instrument capable of creating sawtooth temperature gradient profiles for continuous analysis. This instrument uses a resistive heating nickel sleeve and a moving cold jet stream to form the moving temperature gradient. Application of this instrumentation for the analysis of



normal alkanes, and as a modulator and second dimension separation in a GC×GC analysis of kerosene is demonstrated. Chapter 6 describes the design, fabrication and evaluation of a TGGC instrument capable of generating moving temperature gradients with customized profiles. The instrument is based on continuous forced air convection and individually resistively heated sections. The flexibility of the system for customizing temperature profiles allowed exploring the separation potential of the technique, providing unique control of the movement and elution of compounds. Moreover, a new resistively heated assembly for TPGC operations is also presented, which allows the comparison between TGGC and TPGC methods. In Chapter 7, general conclusions of the work and recommendations for future applications of this technique are given.

## 1.10 REFERENCES

1. Bartle, K. D.; Myers, P., History of Gas Chromatography. *Trends Anal. Chem.* **2002**, *21*, 547-557.
2. Ettre, L. S., Gas Chromatography - Past, Present, and Future. *LC-GC* **2001**, *19*, 120-123.
3. Blumberg, L. M.; Klee, M. S., Quantitative Comparison of Performance of Isothermal and Temperature-Programmed Gas Chromatography. *J. Chromatogr. A* **2001**, *933*, 13-26.
4. Grall, A., *et al.*, Peak Capacity, Peak-Capacity Production Rate, and Boiling Point Resolution for Temperature-Programmed GC with Very High Programming Rates. *Anal. Chem.* **2000**, *72*, 591-598.
5. Harris, W. E.; Habgood, H. W., *Programmed Temperature Gas Chromatography*. John Wiley & Sons: New York, 1966; p 305.
6. Vergnaud, J. M., Gas Phase Chromatography: The Application of Gas Flow Variation and Backflushing. *J. Chromatogr. A.* **1965**, *19*, 495-503.
7. Bellabes, R., *et al.*, Gas Chromatography with Backflushing: Isothermal during the First Step, Programming of Longitudinal Temperature Gradient during the Second Step. *Sep. Sci. Technol.* **1982**, *17* (9), 1177-1182.
8. Le Parlouer, P., *et al.*, Gas Chromatography with Backflushing, with Linear Temperature Programming in the First Direction and a Programmed Longitudinal Positive Temperature Gradient During the Opposite Direction of Gas Flow. *J. Chromatogr. A.* **1977**, *133* (2), 253-261.
9. Deans, D. R., A New Technique for Heart Cutting in Gas Chromatography. *Chromatographia* **1968**, *1* (1-2), 18-22.

10. Marriott, P. J., *et al.*, Emerging Opportunities for Flavor Analysis through Hyphenated Gas Chromatography†. *J. Agric. Food Chem.* **2009**, *57* (21), 9962-9971.
11. Hinshaw, J. V.; Ettre, L. S., Selectivity Tuning of Serially Connected Open-tubular (Capillary) Columns in Gas Chromatography. Part I: Fundamental Relationships *Chromatographia* **1986**, *21* (10), 561-572.
12. Hinshaw, J. V.; Ettre, L. S., Selectivity Tuning of Serially Connected Open-tubular (Capillary) Columns in Gas Chromatography. Part II. Implementation *Chromatographia* **1986**, *21* (12), 669-680.
13. Akard, M.; Sacks Richard, D., Pressure-Tunable Selectivity for High-Speed Gas Chromatography. *Anal. Chem.* **1994**, *66*, 3036-3041.
14. Liu, Z. Y.; Phillips, J. B., Comprehensive Two-Dimensional Gas Chromatography Using an On-Column Thermal Modulator Interface. *J. Chromatogr. Sci.* **1991**, *29*, 227-231.
15. Examining Comprehensive Flow-Modulated Two-Dimensional Gas Chromatography. [www.agilent.com](http://www.agilent.com).
16. Reid, V. R., *et al.*, Investigation of High-Speed Gas Chromatography Using Synchronized Dual-Valve Injection and Resistively Heated Temperature Programming. *J. Chromatogr. A* **2007**, *1148*, 236-243.
17. Phillips, J. B., *et al.*, Multiplex Gas Chromatography by Thermal Modulation of a Fused Silica Capillary Column. *Anal. Chem.* **1985**, *57* (14), 2779-2787.
18. Jinno, K., *et al.*, Thermal Desorption Modulator for Capillary Liquid Chromatography. *Anal. Chem.* **1986**, *58* (6), 1248-1251.
19. Phillips, J. B.; Ledford, E. B., Thermal Modulation: A Chemical Instrumentation Component of Potential Value in Improving Portability. *Field Analytical Chemistry and Technology* **1996**, *1* (1), 23-29.
20. Grall, A. J.; Sacks, R. D., Column Performance and Stability for High-Speed Vacuum-Outlet GC of Volatile Organic Compounds Using Atmospheric Pressure Air as Carrier Gas. *Anal. Chem.* **1999**, *71* (22), 5199-5205.
21. Grall, A. J., *et al.*, High Speed Analysis of Complex Indoor VOC Mixtures by Vacuum-outlet GC with Air Carrier Gas and Programmable Retention. *Environ. Sci. & Tech.* **2001**, *35* (1), 163-169.
22. Smith, H., *et al.*, High-Speed, Vacuum-Outlet GC Using Atmospheric-Pressure Air as Carrier Gas. *Anal. Chem.* **1999**, *71* (8), 1610-1616.
23. Sloan, K. M., *et al.*, Development and Evaluation of a Low Thermal Mass Gas Chromatograph for Rapid Forensic GC-MS Analyses. *Field Anal. Chem. & Tech.* **2001**, *5* (6), 288-301.
24. Mustacich, R., *et al.*, Fast GC: Thinking Outside the Box. *American Lab.* **2003**.
25. Rubey, W. A., A Different Operational Mode for Addressing the General Elution Problem in Rapid Analysis Gas Chromatography. *J. High Res. Chromatogr.* **1991**, *14*, 542-548.
26. Tudge, A. P., Studies in Chromatographic Transport III. Chromathermography. *Can. J. Phy.* **1961**.
27. Zhukhovitskii, A. A., *et al.*, New Method of Chromatographic Analysis. *Doklady Akademii Nauk SSSR* **1951**, *77*, 435-8.

28. Rubey, W., Operational Theory and Instrumental Implementation of the Thermal Gradient Programmed Gas Chromatography (TGPGC) Mode Analysis. *J. High Resol. Chromatogr.* **1992**, *15*, 795-799.
29. Phillips, J. B.; Jain, V., On-Column Temperature Programming in Gas Chromatography Using Temperature Gradients Along the Capillary Column. *J. Chromatogr. Sci.* **1995**, *33*, 543-550.
30. Jain, V.; Phillips, J. B., High-Speed Gas Chromatography Using Simultaneous Temperature Gradient in Both Time and Distance along Narrow-Bore Capillary Columns. *J. Chromatogr. Sci.* **1995**, *33*, 601-605.
31. Zhao, H., *et al.*, Characteristics of TGPGC on Short Micro Packed Capillary Column. *Anal. Sci.* **2002**, *18* (1), 93-95.
32. Contreras, J. A. Design and Application of Thermal Gradient Programming Techniques for Use in Multidimensional Gas Chromatography-Mass Spectrometry (MDGC-MS) University of Dayton, Dayton, 2004.
33. Giddings, J. C., *Anal. Chem.* **1984**, *56*, 1258A.
34. Bertsch, W., Two-Dimensional Gas Chromatography. Concepts, Instrumentation, and Applications – Part 1: Fundamentals, Conventional Two-Dimensional Gas Chromatography, Selected Applications *J. High Resol. Chromatogr.* **1999**, *22*, 647-665.
35. Giddings, J. C., *Unified Separation Science*. Wiley Interscience New York, 1991.
36. Berezkin, V. G., *et al.*, Temperature Gradients in Gas Chromatography. *J. Chromatogr.* **1986**, *373*, 21-44.
37. Lee, M. L., *et al.*, *Open Tubular Column Gas Chromatography* Wiley-Interscience: New York, 1984.
38. Scott, R., Principles and Practice of Chromatography. Library4science.com, Ed. 2002. <http://www.chromatography-online.org/Principles/Introduction/rs2.html>.
39. Harris, W. E.; Habgood, H. W., *Programmed Temperature Gas Chromatography*. J. Wiley: New York, 1966; p 309.
40. Dal Nogare, S.; Langlois, W. E., Programmed Temperature Gas Chromatography. *Anal. Chem.* **1960**, *32* (7), 767-770.
41. Ettre, L. S.; Hinshaw, J. V., *Basic Relationships of Gas Chromatography*. Advanstar Communications: Cleveland, 1993.
42. James, A. T.; Martin, A. J. P., Gas-liquid Partition Chromatography: The Separation and Micro-estimation of Volatile Fatty Acids from Formic Acid to Dodecanoic Acid. *Biochem. J.* **1952**, *52*, 242-247.
43. James, A. T., *et al.*, Gas-liquid partition Chromatography. Separation and Microestimation of Ammonia and the Methylamines. *Biochem. J.* **1952**, *52*, 238-4.
44. Kirkland, J. J., *Modern Practice of Liquid Chromatography*. John Wiley & Sons: New York, 1971.
45. Griffiths, J. H., *et al.*, Adsorption and Partition Methods. *Analyst* **1952**, *77*, 897.
46. Giddings, J. C., In *Gas Chromatography*, Brenner, N.; Callen, J. E.; Weiss, M. D., Eds. Academic Press: New York, 1962; p 57.
47. Nogare, S. D.; Bennett, C. E., Programmed Temperature Gas Chromatography. *Anal. Chem.* **1958**, *30*, 1157-1158.

48. Nogare, S. D.; Harden, J. C., Programmed Temperature Gas Chromatography Apparatus. *Anal. Chem.* **1959**, *31*, 1829-1832.
49. Teranishi, R., *et al.*, Gas-Liquid Chromatography Programmed Temperature Control of the Capillary Column. *Anal. Chem.* **1960**, *32*, 1384-1386.
50. Bird, R. B., *Transport Phenomena*. John Wiley & Sons: New York, 1966; p 780.
51. McNair, H., A History of Gas Chromatography: My Early Experiences. *LC GC North America* **2010**, *28* (2), 138-144.
52. Ettre, L. S., American Instrument Companies and the Early Development of Gas Chromatography. *J. Chromatogr. Sci.* **1977**, *15*, 90-110.
53. Dimbat, M., *et al.*, Apparatus Requirements for Quantitative Applications. *Anal. Chem.* **1956**, *28* (3), 290-297.
54. Ettre, L. S., Fifty Years of GC Instrumentation. *LC GC Europe* **2005**, *18* (7), 416-421.
55. Winters, J. C. Gas Chromatography Apparatus US Patent 3115766, 1963.
56. Ettre, L. S., The Early Development and Rapid Growth of Gas Chromatographic Instrumentation in the United States. *J. Chromatogr. Sci.* **2002**, *40* (8), 458-472.
57. James, A. T.; Martin, A. J. P., Gas-liquid Partition Chromatography: The Separation and Microestimation of Volatile Fatty Acids From Formic Acid to Dodecanoic Acid. *Biochem. J.* **1952**, *50*, 679-90.
58. Hinshaw, J. V., GC Ovens A Hot Topic. *LC-GC* **2000**, *18* (11), 1142-1147.
59. Ettre, L. S., *Chapters in the Evolution of Chromatography*. Imperial Collage Press: 2008; p 473.
60. Ettre, L. S., The Janák-Type Gas Chromatographs of the 1950s. *Lc Gc Europe* **2002**, *15* (12), 2-6.
61. Ettre, L. S., Early Evolution of Gas Adsorption Chromatography - Part II: Elution Chromatography Matures. *Chromatographia* **2002**, *55* (9-10), 625-631.
62. Eggertsen, F. T., *et al.*, Gas Chromatography Use of Liquid-Modified Solid Adsorbent to Resolve C5 and C6 Saturates. *Anal. Chem.* **1956**, *28* (3), 303-306.
63. Fredericks, E. M.; Brooks, F. R., Gas Chromatography Analysis of Gaseous Hydrocarbons by Gas-Liquid Partition Chromatography. *Anal. Chem.* **1956**, *28* (3), 297-303.
64. Bicchi, C., *et al.*, Direct Resistively Heated Column Gas Chromatography (Ultrafast Module-GC) for High-speed Analysis of Essential Oils of Differing Complexities. *J. Chromatogr. A.* **2004**, *1024*, 195-207.
65. Krkošová, Ž., *et al.*, Gas Chromatography with Ballistic Heating and Ultrafast Cooling of Column. *Chem. Pap.* **2008**, *62* (2), 135-140.
66. Ettre, L. S., Some Comments on Temperature Programming by Resistive Heating. *Am. Lab.* **1999**, *31* (14), 30-33.
67. Adams, C. E., *et al.*, Heating Small Reactors - High Temperature Fluidized Solids Bath for Continuous Systems. *Ind. & Eng. Chem.* **1954**, *46* (12), 2458-2460.
68. Teranishi, R., *et al.*, Gas-Liquid Chromatography. Programmed Temperature Control of the Capillary Column. *Anal. Chem.* **1960**, *32* (11), 1384-1386.
69. McEwen, D. J., Temperature Programmed Capillary Columns in Gas Chromatography. *Anal. Chem.* **1963**, *35* (11), 1636-1640.
70. Agilent 7890A Network Gas Chromatograph Data Sheet [www.chem.agilent.com](http://www.chem.agilent.com).
71. Varian 450-GC Specifications Guide. [www.varianinc.com](http://www.varianinc.com).

72. Abdel-Rahman, M. F.; Firor, R. L. Oven Housing Module in an Analytical Instrument. US Patent 6248158 B1, 2001.
73. Botelho, J., *et al.* Chromatography Oven with Heat Exchange and Method of Use. US Patent 7361208 B2, 2008.
74. MacDonald, S. J. Gas Chromatography Oven Heaters. US Patent 6485543, 2002.
75. Agilent 6890N Network Gas Chromatograph Data Sheet. [www.chem.agilent.com](http://www.chem.agilent.com).
76. Installing the Agilent 6890 Oven Insert for Fast Chromatography (Kit G2646-60500). [www.chem.agilent.com](http://www.chem.agilent.com).
77. Perkin Elmer Clarus 680 Gas Chromatograph Specifications. [www.perkinelmer.com](http://www.perkinelmer.com).
78. Thermo Scientific FOCUS™ GC Gas Chromatograph Product Specifications. [www.thermo.com](http://www.thermo.com).
79. Agilent 6850 Series II Network GC system Specifications. [www.agilent.com](http://www.agilent.com).
80. Shimadzu Gas Chromatograph GC-2010. [www.shimadzu.com](http://www.shimadzu.com).
81. Jain, V.; Phillips, J. B., Fast Temperature Programming on Fused-Silica Open-Tubular Capillary Columns by Direct Resistively Heating. *J. Chromatogr. Sci.* **1995**, *33*, 55-59.
82. Fast GC Module from VICI Valco Instruments Co. Inc. . [www.VICI.com](http://www.VICI.com).
83. Hail, M. E.; Yost, R. A., Compact Gas Chromatograph Probe for Gas Chromatography/mass Spectrometry Utilizing Resistively Heated Aluminum-clad Capillary Columns. *Anal. Chem.* **1989**, *61* (21), 2410-2416.
84. Norem, S. D. Heating Apparatus for Chromatographic Column. US Patent 3159996, 1961.
85. Ehrmann, E. U., *et al.*, Novel Column Heater for Fast Capillary Gas Chromatography. *J. Chromatogr. Sci.* **1996**, *34* (12), 533-539.
86. Nogare, S. D.; Bennett, C. E., Programmed Temperature Gas Chromatography. *Anal. Chem.* **1958**, *30* (6), 1157-1158.
87. Mustacich, R. V.; Everson, J. F. Reduced Power Consumption Gas Chromatograph System. US Patent 6217829, 2001.
88. Thermo Scientific UltraFast TRACE GC Ultra Configuration. [www.thermo.com](http://www.thermo.com).
89. Dubsky, H., Step Programmed Temperature GC. *J. Chromatogr. Sci.* **1971**, *9*, 356-358.
90. Roques, N. J. Flat Spiral Capillary Column Assembly with Thermal Modulator. US Patent 2006/0283324 A1, 2006.
91. Sides, G. D.; Cates, M. Continuous Air Monitoring Apparatus and Method. US Patent 5014541, 1991.
92. Maswadeh, W. M.; Snyder, A. P. Hand-Held Temperature Programmable Modular Gas Chromatograph 5856616, 1999.
93. Burger, G.-J., *et al.* Device for Capillary Chromatography and Method for Manufacturing Such a Device. US 2008/0185342 A1, 2008.
94. MacDonald, S. J.; Wheeler, D., Fast Temperature Programming by Resistive Heating with Conventional GCs. *Am. Lab.* **1998**, *30* (22), 27-28, 37-40.
95. Xu, F., *et al.*, Fast Temperature Programming on a Stainless-steel Narrow-bore Capillary Column by Direct Resistive Heating for Fast Gas Chromatography. *J. Chromatogr. A* **2008**, *1186* (1-2), 183-188.

96. Stadermann, M., *et al.*, Ultrafast Gas Chromatography on Single-Wall Carbon Nanotube Stationary Phases in Microfabricated Channels. *Anal. Chem.* **2006**, 78 (15), 5639-5644.
97. Reid, V. R., *et al.*, Investigation of High-Speed Gas Chromatography Using Synchronized Dual-Valve Injection and Resistively Heated Temperature Programming. *J. Chromatogr. A* **2007**, 1148 (2), 236-243.
98. C2V-200 Micro GC from Thermo Scientific. [www.c2v.nl](http://www.c2v.nl).
99. Matz, G., *et al.*, Fast Analysis of Hazardous Organics in Fire and Chemical Accidents by Mobile GC/MS. *Field Anal. Methods Hazard. Wastes Toxic Chem., Proc. Spec. Conf.* **1997**, 290-296.
100. Matz, G. Peak-Hopping: A New Technique to Increase Analysis Speed in Short Column GC/MS. [www.tu-harburg.de](http://www.tu-harburg.de).
101. Walte, A., *et al.* Procedures for the Separation of Selected Substances in a Gas Chromatograph and Gas Chromatograph for Implementing the Process German Patent DE 19707114, 1998.
102. Rounbehler, D. P., *et al.* High Speed Gas Chromatography. US Patent 5808178, 1998.
103. Brashear, R. T. Thermochromatographic Analyzer Heater. US Patent 3023835, 1962.
104. Walters, D. L.; Gaisford, S. G. Chromatographic Column for Microwave Heating. 6029498, 2000.
105. Sacks, G.; Brenna, T., Comparison of Microwave and Conventionally Heated Columns for Gas Chromatography of Fatty Acid Methyl Esters. *Am. Lab.* **2003**, 35 (18), 22-+.
106. Crnko, J. S.; Warren, S. K. Negative Temperature Profiling Using Microwave GC Apparatus. US Patent 7291203, 2007.
107. Gaisford, S. G.; Walters, D. L. Microwave Heating Apparatus for Gas Chromatographic Columns. US Patent 6316759, 2001.
108. Gaisford, S., A Microwave Oven for Gas Chromatography. *Am. Lab.* **2002**, 34 (15), 10-10.
109. Radian UltraFast GC<sup>®</sup> by AC Analytical Controls. [www.paclp.com](http://www.paclp.com).
110. Rudney, V., *et al.*, *Handbook of Induction Heating*. Marcel Dekker: New York, 2003.
111. Loyd, R. J. Thermal Chromatography Temperature Gradient. US Patent 3146616, 1964.
112. Yagi, H., *et al.*, New Liquid Chromatography Method Combining Thermo-responsive Material and Inductive Heating Via Alternating Magnetic Field. *J. Chromatogr. B* **2008**, 876 (1), 97-102.
113. Ma, M., *et al.*, Size Dependence of Specific Power Absorption of Fe<sub>3</sub>O<sub>4</sub> Particles in AC Magnetic Field. *J. Magnetism and Magnetic Mat.* **2004**, 268 (1-2), 33-39.
114. Wakamatsu, H., *et al.*, Preparation and Characterization of Temperature-responsive Magnetite Nanoparticles Conjugated with N-isopropylacrylamide-based Functional Copolymer. *J. Magnetism and Magnetic Mat.* **2006**, 302 (2), 327-333.
115. Bruno, T. J., Vortex Cooling for Subambient Temperature Gas Chromatography. *Anal. Chem.* **1986**, 58 (7), 1595-1596.

116. Bruno, T. J., Laboratory Applications of the Vortex Tube. *J. Chem. Edu.* **1987**, *64* (11), 987.
117. Górecki, T., *et al.* In *Cryogen-Free Thermal Modulator: Development and Applications*, 32<sup>nd</sup> International Symposium on Capillary Chromatography and 5<sup>th</sup> GC×GC Symposium, Rival del Gard, Italy, May 26-30; 2008.
118. Bottner, H., *et al.*, New Thermoelectric Components Using Microsystem Technologies. *Journal of Microelectromechanical Systems* **2004**, *13* (3), 414-420.
119. Peltier Coolers from TE Technology Inc [www.tetech.com](http://www.tetech.com).
120. Lewis, A. C., *et al.*, Microfabricated Planar Glass Gas Chromatography with Photoionization Detection. *J. Chromatogr. A* **2010**, *1217* (5), 768-774.
121. Nogare, S. D.; Harden, J. C., Programmed Temperature Gas Chromatography Apparatus. *Anal. Chem.* **1959**, *31* (11), 1829-1832.
122. Nerheim, A. G. Sample Introduction System for Gas Chromatography Apparatus US Patent 3063286, 1962.
123. Burow, F. H., *et al.* Gas Chromatography Apparatus. US Patent 3232093, 1966.
124. Burow, F. H. Sample Preparation and Collection Means for Gas Chromatographic Columns. US Patent 3225520, 1965.
125. Burow, F. H. Serially Connected Thermochromatographic Columns. US Patent 3225521, 1965.
126. Ettre, L. S., Open-Tubular Columns: Past, Present and Future. *Chromatographia* **1992**, *34* (9-10), 513-528.
127. Ettre, L. S., Gas chromatography - Past, Present, and Future. *LC GC North America* **2001**, *19* (2), 120-123.
128. Lipsky, S. R.; Duffy, M. L., High-Temperature Gas-Chromatography - The Development of New Aluminum Clad Flexible Fused-Silica Glass-Capillary Columns Coated with Thermostable Nonpolar Phases .1. *J. High Res. Chromatogr. Chromatogr. Commun.* **1986**, *9* (7), 376-382.
129. Lipsky, S. R.; Duffy, M. L., High-Temperature Gas-Chromatography - The Development of New Aluminum Clad Flexible Fused-Silica Glass-Capillary Columns Coated with Thermostable Nonpolar Phases .2. *J. High Res. Chromatogr. Chromatogr. Commun.* **1986**, *9* (12), 725-730.
130. Aluminum-clad Fused Silica Columns, Quadrex Corporation. [www.quadrexcorp.com](http://www.quadrexcorp.com).
131. Hail, M. E., *et al.*, Gas Chromatographic Sample Introduction Into The Collision Cell of a Triple Quadrupole Mass Spectrometer for Mass-selection of Reactant Ions for Charge Exchange and Chemical Ionization. *Anal. Chem.* **1989**, *61* (17), 1874-1879.
132. Yost, R. A.; Hail, M. E. Direct Resistive Heating and Temperature Measurement of Metal-Clad Capillary Columns in Gas Chromatography and Related Separation Techniques. 5114439, May 19, 1992.
133. Liu, Z.; Phillips, J. B., Sample Introduction Into a 5- $\mu$ m i.d. Capillary Gas Chromatography Column Using an On-column Thermal Desorption Modulator. *J. Microcol. Sep.* **1989**, *1* (3), 159-162.
134. Liu, Z.; Phillips, J. B., High-speed Gas Chromatography Using an On-column Thermal Desorption Modulator. *J. Microcol. Sep.* **1989**, *1* (5), 249-256.

135. Liu, Z.; Phillips, J. B., Large-volume Sample Introduction Into Narrow-bore Gas Chromatography Columns Using Thermal Desorption Modulation and Signal Averaging. *J. Microcol. Sep.* **1990**, 2 (1), 33-40.
136. Overton, E. B. Portable Gas Chromatograph. US Patent 5611846, 1997.
137. Overton, E. B., *et al.*, Fast GC Instrumentation and Analysis for Field Applications. *Field Anal. Chem. Tech.* **2001**, 5 (1-2), 97-105.
138. Tienpont, B., *et al.*, Features of a Micro-gas Chromatograph Equipped with Enrichment Device and Microchip Plasma Emission Detection ( $\mu$ PED) for Air Monitoring. *Lab on a Chip* **2008**, 8 (11), 1819-1828.
139. Dalluge, J., *et al.*, Fast Temperature Programming in Gas Chromatography using Resistive Heating. *J. High Resolut. Chromatogr.* **1999**, 22 (8), 459-464.
140. Sloan, K. M., *et al.*, Development and Evaluation of a Low Thermal Mass Gas Chromatograph for Rapid Forensic GC-MS Analyses. *Field Anal. Chem.* **2001**, 5 (6), 288-301.
141. Agilent Low Thermal Mass (LTM) System for Gas Chromatography Data Sheet. [www.agilent.com](http://www.agilent.com).
142. Mustacich, R. V.; Richards, J. P. Electrically Insulated Gas Chromatograph Assembly and Method of Fabricating Same. US Patent 6209386, 2001.
143. Miniature GC-TCD System with a Resistively Heated Ni Column and a Miniature Thermal Conductivity Detector (TCD) Valco Instruments Co. Inc. 28<sup>th</sup> *International Symposium on Capillary Chromatography, Las Vegas, NV* **2005**.
144. ZNOSE<sup>®</sup> Product Line by Electronic Sensor Technology. [www.estcal.com](http://www.estcal.com).
145. Staples, E. J. Portable Chemical Profiling. [www.sensorsmag.com](http://www.sensorsmag.com).
146. Gross, G. M., *et al.*, Recent Advances in Instrumentation for Gas Chromatography. *Current Anal. Chem.* **2005**, 1 (2), 135-147.
147. zNose<sup>™</sup> GC-SAW system, by Electronic Sensor Technology. [www.estcal.com](http://www.estcal.com).
148. Akporhonor, E. E., *et al.*, Calculation of Programmed Temperature Gas-Chromatography Characteristics from Isothermal Data .1. Theory and Computational Procedures. *J. Chromatogr.* **1987**, 405, 67-76.
149. Terry, S. C.; Herman, J. C., A Gas Chromatographic Air Analyzer Fabricated on a Silicon Wafer. *IEEE Trans. Electron Devices* **1979**, 26, 1880-1886.
150. Bhushan, A., *et al.*, Fabrication and Preliminary Results for LiGA Fabricated Nickel Micro Gas Chromatograph Columns. *J. Microelectromech. Syst.* **2007**, 16 (2), 383-393.
151. Bhushan, A., *et al.*, Fabrication of Micro-gas Chromatograph Column for Fast Chromatography. *Microsyst. Technol.* **2007**, 13, 361-368.
152. Lambertus, G., *et al.*, Design, Fabrication, and Evaluation of Microfabricated Column for Gas Chromatography. *Anal. Chem.* **2004**, 76, 2629-2637.
153. Lambertus, G., *et al.*, Silicon Microfabricated Column with Microfabricated Differential Mobility Spectrometer for GC Analysis of Volatile Organic Compounds. *Anal. Chem.* **2005**, 77 (23), 7563-7571.
154. Lu, C.-J., *et al.*, First-Generation Hybrid MEMS Gas Chromatograph. *Lab Chip* **2005**, 5, 1123-1131.
155. Pai, R. S., *et al.* In *Microfabricated Gas Chromatograph for Trace Analysis*, Technologies for Homeland Security, Waltham, MA, 12-13 May; 2008; pp 150-154.



156. Reid, V. R., *et al.*, High-Speed, Temperature Programmable Gas Chromatography Utilizing a Microfabricated Chip With an Improved Carbon Nanotube Stationary Phase. *Talanta* **2009**, *77*, 1420-1425.
157. Serrano, G., *et al.*, Assessing the Reliability of Wall-coated Microfabricated Gas Chromatographic Separation Columns. *Sensors and Actuators B-Chemical* **2009**, *141* (1), 217-226.
158. Radadia, A. D., *et al.*, Partially Buried Microcolumns for Micro Gas Analyzers. *Anal. Chem.* **2009**, *81* (9), 3471-3477.
159. Reidy, S., *et al.*, Temperature-programmed GC Using Silicon Microfabricated Columns with Integrated Heaters and Temperature Sensors. *Anal. Chem.* **2007**, *79* (7), 2911-2917.
160. Manginell, R. P.; Frey-Mason, G. C. Temperature Programmable Microfabricated Gas Chromatography Column US Patent 6666907, 2003.
161. Lieshout, M. v., *et al.*, Fast Capillary Gas Chromatography, Comparison of Different Approaches. *J. High Res. Chromatogr.* **1998**, *21* (11), 583-583.
162. Robinson, A. L.; Anderson, L. F. Sub- to Super-Ambient Temperature Programmable Microfabricated Gas Chromatography Column. US Patent 6706091, 2004.
163. Hastings, M. R., *et al.* Separation Column for a Gas Chromatograph. US Patent 6607580, 2003.
164. Fenimore, D. C., Gradient Temperature Programming of Short Capillary Columns. *J. Chromatogr.* **1975**, *112*, 219-227.
165. Rubey, W. A., Theory of Constrained Migration Behavior in Open-Tubular Gas Chromatography Columns with Various Operational Modes. In *23<sup>rd</sup> International Symposium on Capillary Chromatography*, Riva del Garda, Italy 2000.
166. Phillips, J. B., *et al.*, Multiplex Gas Chromatography by Thermal Modulation of a Fused Silica Capillary Column *Anal. Chem.* **1985**, *57*, 2779-2787.
167. Somenath, M.; Phillips, J. B., Use of Thermal Desorption Modulators in Gas Chromatograph/Mass Spectrometer. *Anal. Chem.* **1988**, *59* (8), 1427-1428.
168. Blumberg, L. M., Outline of a Theory of Focusing in Linear Chromatography. *Anal. Chem.* **1992**, *64*, 2459-2460.
169. Zhukhovitskii, A. A., *et al.*, Theory of Chromathermography. *Doklady Akademii Nauk SSSR* **1953**, *88*, 859-62.
170. Zhukhovitskii, A. A., *et al.*, The Spreading of Bands During Chromathermographic and Thermal Separation. *Doklady Akademii Nauk SSSR* **1954**, *96*, 303-6.
171. Zhukhovitskii, A. A.; Turkel'taub, N. M., Adsorption Spectral Analysis. *Doklady Akademii Nauk SSSR* **1954**, *94*, 77-80.
172. Etre, L. S.; Berezkin, V. G., A. A. Zhukhovitskii - A Russian Pioneer of Gas Chromatography. *LC-GC* **2000**, *18*, 1148-1155.
173. Ohline, R. W.; DeFord, D. D., Chromathermography, the Application of Moving Thermal Gradients to Gas Liquid Partition Chromatography. *Anal. Chem.* **1963**, *35* (2), 227-234.
174. Moshinskaya, M. B.; Vigdergauz, M. S., The Evolution of the Construction and Manufacturing of Gas Chromatographs in the Soviet Union. *J. Chromatogr. Sci.* **1978**, *16*, 351-357.

175. Starshov, I. M., Analysis of the Gases Produced by Pyrolytic Cracking with a HT-2M Chromathermograph. *Akad. Nauk SSSR, Tr. Vtoroi Vses. Konf.* **1964**, 470-473.
176. Arutyunov, Y. I.; Breshchenko, V. Y., Continuous Analysis of Raw Materials and of Pyrolysis Products by Chromathermography with Stabilized Parameters and Separation Program. *Akad. Nauk SSSR, Tr. Vtoroi Vses. Konf.* **1964**, 335-344.
177. Zhukhovitskii, A. A., Some Developments in Gas Chromatography in the U.S.S.R. In *Gas Chromatography 1960*, Scott, R. P. W., Ed. Butterworths: Edinburgh, 1960; pp 293-300.
178. Nerheim, A. G., Gas-Liquid Chromathermography. *Anal. Chem.* **1960**, 32.
179. Kaiser, R., Temperature Gradient Chromatography. *Chromatographia* **1968**, 1, 199-207.
180. Fastcher, M., *et al.*, Method Using a [Chromatography] in which the Column Temperature is Constant with Time and Varies Exponentially Along the Longitudinal Abscissa. *Sciences Chimiques* **1971**, 273, 1042-1046.
181. Fastcher, M.; Vergnaud, J. M., Use in Quantitative Analysis of Gas Chromatography Methods with Established Longitudinal Temperature Gradient with or without Temperature Programming. *Analisis* **1972**, 1, 231-234.
182. Guermouche, M. H., *et al.*, Étude Des Paramètres de la Chromatographie en Phase Gazeuse Réalisée en Couplant un Gradient Longitudinal et Une Programmation de Température. *J. Chromatogr. A* **1970**, 52, 9-20.
183. Coudert, M., *et al.*, Chromatographie en Phase Gazeuse Réalisée Simultanément Avec Une Programmation de Température et Une Programmation Du Gradient Longitudinal Négatif de Température : Théorie de la Rétention et Influence Des Paramètres. *J. Chromatogr. A* **1971**, 58, 159-167.
184. Kaiser, R. E., Enriching Volatile Compounds by a Temperature Gradient Tube. *Anal. Chem.* **1973**, 45 (6), 965-967.
185. Vigdergauz, M. S., The Early Period of the Development of Gas Chromatography in the U.S.S.R. *Chromatographia* **1978**, 11 (11), 627-633.
186. Badger, C. M. A., *et al.*, Heater-Displacement Chromatography. *J. Chromatogr.* **1976**, 126, 11-18.
187. Horrocks, J. P., *et al.*, Quantitative Aspects of Heater Displacement Chromatography. *J. Chromatogr.* **1980**, 197, 109-119.
188. Berezkin, V. G.; Starostina, N. G., Application of Chromatography for the Determination of Impurities. *Chromatographia* **1975**, 8 (8), 395-398.
189. Cantuti, V.; Cartoni, G. P., Chromathermography: Uses in the Analysis of Trace Amounts. *Chimica e l'Industria* **1968**, 50 (4), 449-50.
190. Rubey, W. Gas Chromatography Methods and Apparatus. US 4923486, 1990.
191. Rubey, W. A. Gas Chromatography Methods and Apparatus US Patent 4923486, 1990.
192. Rubey, W. A. Gas Chromatography Methods and Apparatus US Patent 5028243, 1991.
193. Weihong, Y., *et al.*, Study of Linear Gradient Loaded Column of Gas Chromatography. *Hunan Daxue Xuebao* **1996**, 23 (4), 51-55.
194. Xiuyan, Y., *et al.*, Study on Cosine Gradient Loaded Column in Gas Chromatography. *Hunan Daxue Xuebao* **1999**, 26 (3), 21-24.

195. Hiller, J. F., *et al.* Apparatus and Method for Establishing a Temperature Gradient in a Chromatography Column. US 5215556, 1993.
196. Blumberg, L. M., Focusing Cannot Enhance Resolution or Speed Limit of a GC Column. *J. Chromatogr. Sci.* **1997**, 35 (9), 451-454.
197. Blumberg, L. M., Limits of Resolution and Speed of Analysis in Linear Chromatography With And Without Focusing. *Chromatographia* **1994**, 39 (11-12), 719-728.
198. Manz, A., *et al.*, Miniaturized Total Chemical Analysis Systems: A Novel Concept for Chemical Sensing. *Sens. Actuators B* **1990**, 1, 244-248.
199. Department of Homeland Security Science and Technology Directorate, Cell-All: Super Smartphones Sniff Out Suspicious Substances.  
[http://www.dhs.gov/files/programs/gc\\_1268073038372.shtm](http://www.dhs.gov/files/programs/gc_1268073038372.shtm).

## **2 DEVELOPMENT OF A SIMPLE MATHEMATICAL PLATE MODEL FOR SIMULATING THE EFFECT OF AXIAL TEMPERATURE GRADIENTS IN GAS CHROMATOGRAPHY**

### **2.1 INTRODUCTION**

Contrary to uniform column temperatures used in isothermal and temperature programmed gas chromatography (TPGC) operations, in thermal gradient gas chromatography (TGGC), axial temperature gradients are applied along the column. The temperature along the column is not static, instead it is simultaneously changed in time and position to control the movement and elution of compounds in unique ways.<sup>1</sup> For example, a negative temperature gradient from the injector to the detector will cause the front of the peak to move slower than the rear of the peak, leading to a narrower, focused peak.<sup>2</sup> In a moving negative gradient in the direction of mobile phase flow, the peaks will not only focus, but they will also travel with the gradient at their characteristic equilibrium temperatures ( $T_{eq}$ ).<sup>2-3</sup> This behavior is markedly different from what is experienced in isothermal GC (ITGC) and TPGC and, thus, can be used for developing new approaches for optimizing separations. The main challenge in performing TGGC is the instrumentation. Generating axial temperature gradients along the column with the capability of controlling the temperature gradient profile with time is difficult. The limitation imposed by available instrumentation has hindered the application and

development of TGGC. As a result, the maximum separation potential that this technique can offer has not yet been realized.

The development of a computer program for simulating axial temperature gradients in GC is desirable to study the separation potential of TGGC, without instrumentation constraints. Simulations can be used to determine not only the optimal temperature gradients but also to evaluate new separation strategies by manipulating the temperature and gradient profile along the column. The data obtained from the simulations provide the operating parameters required for the development and design of TGGC instrumentation. Various methods have been suggested for predicting the retention time<sup>4-5</sup> and peak width in isothermal and temperature programmed operations,<sup>6-18</sup> however, simulations of GC separations with axial temperature gradients have not been performed. Simulation models that have been used for estimating peak width are based on summation of the local peak variance as the peak travels along the column. This approach does not allow for consideration of focusing effects and, thus, cannot be used for TGGC.<sup>7, 14</sup> Therefore, a simple plate model was developed to predict the retention times and peak widths when axial temperature gradients are applied. The simple plate model described in this work is founded on a thermodynamic model of GC separations.<sup>19-</sup>

20

A numerical procedure that uses the thermodynamic values of entropy and enthalpy, obtained from isothermal separations, to predict retention times and peak widths is presented. For validating the model, the measured and predicted retention times and peak widths are compared for both ITGC and TPGC separations of an alkane mixture. The absolute mean relative error between the predicted and measured retention

times for isothermal and temperature programmed operations was less than 2%. For peak widths, small absolute relative errors down to 10% between observed and simulated peak widths were attainable at the expense of considerable simulation time (hours). On the other hand, the retention time relative error was small, even with much less computation. The reduced time simulations, although, accurate for retention times, yielded peak widths 3 to 5 times wider than experimentally observed. The simple plate model proved to be flexible, and allowed the simulation of different axial gradient profiles. Even though the predicted peak widths were wider, the band broadening behaviors of the peaks under ITGC, TPGC, and TGGC operations were predicted accurately. Furthermore, the computer simulations provided a unique visualization of the effect of axial temperature gradients on the separation of analytes as they traveled along the column. This feature offered useful insights for development and design of new separation strategies and GC systems described in this dissertation.

## **2.2 MATHEMATICAL MODEL**

The simple plate mathematical model considers both plate theory and rate models to predict the effect of axial temperature gradients on separation. In the simple plate model, the column is divided into a series of small segments where separation takes place. Each segment is considered to have a constant temperature, pressure and mobile phase velocity. The analytes move along the column as they are transferred from segment to segment by the mobile phase, however, they can also move between segments by diffusion. An effective diffusion parameter is introduced based on Golay's rate theory equation to take into account the band broadening due to longitudinal diffusion and resistance to mass transfer.<sup>20</sup> Following is a detailed description of the model.

Chromatographic separation is performed in the axial direction along the column segments where analyte is distributed between the mobile and the stationary phases according to the distribution coefficient,  $K$ .<sup>19-20</sup>

$$K = \frac{\text{Concentration in stationary phase}}{\text{Concentration in mobile phase}} = \frac{C_S}{C_M} \quad (2.1)$$

The distribution of the analyte is driven by thermodynamics where  $K$  is only a function of temperature, and independent of pressure, column diameter and film thickness. Assuming that equilibrium occurs in each segment and knowing the  $K$  for the analyte, the concentrations of the analyte in the mobile and stationary phases can be determined.

When an analyte is carried by the mobile phase into a segment, a fraction,  $\Delta C$ , will transfer between the two phases to reach equilibrium in accordance to the constant  $K$ . To illustrate, at each specific column segment, the only analyte that moves is the analyte contained in the mobile phase, which is transferred to the next segment downstream. Thus, after a transfer, the instantaneous concentration in a segment prior to equilibrium adjustment is  $C_S$  for the stationary phase and  $C_M$  for the mobile phase. Equilibrium in the segment is adjusted by transferring a fraction,  $\Delta C$ , to satisfy equation 2.1. This can be expressed by

$$K = \frac{C_S - \Delta C}{C_M + \Delta C} \quad (2.2)$$

Making the transfer fraction a function of the number of moles ( $X$ ), Equation 2.2 can be rewritten as

$$K = \frac{C_S - \frac{X}{V_S}}{C_M + \frac{X}{V_M}} \quad (2.3)$$

where  $V_M$  and  $V_S$  are the volumes of the mobile and stationary phases respectively. Solving for  $X$  produces an equation for calculating the number of moles transferred between both phases to reach equilibrium.

$$X = \frac{(C_M - K C_S)}{\left(\frac{1}{V_M} + \frac{K}{V_S}\right)} \quad (2.4)$$

In GC, analytes move along the column only with the mobile phase, since longitudinal diffusion in the stationary phase is negligible. Applying this principle in the simple plate model, the resulting equation for determining  $X$  for each segment is given as

$$X_j = \frac{(C_{M(j-1)} - K_j C_{S(j)})}{\left(\frac{1}{V_{M(j)}} + \frac{K_j}{V_{S(j)}}\right)} \quad (2.5)$$

where the index  $j$  refers to a local segment, and  $j-1$  refers to the previous segment. After calculating  $X_j$ , the mobile and stationary phase concentrations,  $C_S^*$  and  $C_M^*$ , after equilibrium can be determined by

$$C_{S(j)}^* = C_{S(j)} + \frac{X_j}{V_{S(j)}} \quad (2.6)$$

$$C_{M(j)}^* = C_{M(j-1)} - \frac{X_j}{V_{M(j)}} \quad (2.7)$$

The analytes in the mobile phase at equilibrium are then transferred to the next segment where the calculation cycle starts over again to calculate  $X_j$ . This procedure is repeated as the analyte moves along the column until it elutes. The retention time of an analyte is determined by multiplying the number of mobile phase transfers required to elute the peak. The transfer time between segments is determined by dividing the



segment length by the average carrier gas linear velocity, which may be calculated using the Hagen-Poiseuille equation<sup>19</sup>

$$\bar{u}_M = \frac{3 r^2}{32 \eta L} \frac{(P_i^2 - P_o^2)^2}{(P_i^3 - P_o^3)} \quad (2.8)$$

where  $\bar{u}_M$  is the average mobile phase linear velocity at the column temperature,  $P_i$  is the inlet column pressure,  $P_o$  is the outlet column pressure,  $L$  is the column length,  $r$  is the column inner diameter and  $\eta$  is the mobile phase gas viscosity at the column temperature. For a temperature gradient along the column, the average column temperature can be used to estimate  $\bar{u}_M$ . However, experimental measurements of the linear velocity are required to provide more accurate results because of discrepancies between the actual column diameter and the nominal values reported by the manufacturer. A chromatogram is obtained by plotting the analyte mobile phase concentration in the last column segment as a function of time.

Because the mobile phase is compressible, the amount of analyte that moves between segments varies along the column. The fraction of analyte that moves into a consecutive segment is pressure and temperature dependent and can be determined using the ideal gas law with the following correction factor

$$\frac{C_{M(j+1)}}{C_{M(j)}} = \frac{P_{(j+1)} T_j}{P_{(j)} T_{(j+1)}} \quad (2.9)$$

where  $j+1$  represents a consecutive segment,  $P$  is the pressure, and  $T$  is the temperature of the corresponding segment  $j$ . To determine the pressure drop along the column, the Hagen-Poiseuille flow equation is used<sup>19</sup>

$$F = \frac{\pi r^4}{16\eta L} \left( \frac{P_i^2 - P_o^2}{P_o} \right) \quad (2.10)$$

where  $F$  is the volumetric flow at the column temperature. Applying the Hagen-Poiseuille equation for a position  $x$  along the column from the inlet, we obtain

$$F = \frac{\pi r^4}{16\eta_{Tx} x} \left( \frac{P_i^2 - P_x^2}{P_x} \right) \quad (2.11)$$

where  $P_x$  is the local pressure at position  $x$  from the inlet, and  $\eta_{Tx}$  is the viscosity of the mobile phase at the temperature of position  $x$ . The values at position  $x$  will be those of segment  $j$  in which  $x$  falls. From mass balance, the mass flow along the column is constant; therefore, using the ideal gas law, the mass flow in the column can be determined by

$$\text{Mass Flow} = F \left( \frac{P}{RT} \right) \quad (2.12)$$

where  $R$  is the ideal gas constant. Combining Equations 2.10, 2.11 and 2.12, rearranging and solving for  $P_x$ , we obtain

$$P_x = \sqrt{P_i^2 - \frac{x \eta_{Tx} T_x}{L \eta_{To} T_o} (P_i^2 - P_o^2)} \quad (2.13)$$

where  $\eta_{To}$  is the viscosity of the mobile phase at the outlet temperature. Equation 2.13 allows the local pressure along the column to be determined when an axial temperature gradient is applied. This equation assumes that the overall effect of the temperature gradient in the column flow is small. The viscosity,  $\eta$ , for a temperature,  $T$ , can be determined using the equation<sup>19, 21</sup>

$$\eta_T = \eta_{ref} \left( \frac{T}{T_{ref}} \right)^{x_\eta} \quad (2.14)$$

where  $x_\eta$  is an exponent specific to the type of mobile phase and  $\eta_{ref}$  is the viscosity at a reference temperature.

Diffusion is incorporated in the model through Fick's equation<sup>22</sup>

$$J = -D_{eff} \left( \frac{\partial C}{\partial x} \right) \quad (2.15)$$

where  $J$  is the diffusion flux,  $\partial C$  is the difference in concentration between consecutive segments,  $\partial x$  is the distance between segments, and  $D_{eff}$  is the effective diffusion coefficient, which is a function of the longitudinal diffusion and resistance to mass transfer dispersion in the column.<sup>20</sup> Using Fick's equation, the amount of analyte that transfers between consecutive segments as a function of diffusion can be determined. The effective diffusion can be calculated from

$$D_{eff} = \left( \frac{\bar{u}_M}{2} \right) H \quad (2.16)$$

where  $H$  is the height equivalent to a theoretical plate, which can be determined from the Golay equation<sup>19-20</sup>

$$H = \frac{2D_M}{\bar{u}_M} + \left[ \frac{(1 + 6k + 11k^2)r^2}{24(1+k)^2 D_M} + \frac{2k d_f^2}{3D_S(1+k)^2} \right] \bar{u}_M \quad (2.17)$$

where  $D_M$  and  $D_S$  are the diffusion coefficients of the analytes in the mobile and stationary phases, respectively,  $d_f$  is the stationary phase film thickness and  $k$  is the retention factor. The diffusion coefficient for the mobile phase can be calculated using the Fuller-Schettler-Giddings equation<sup>19, 23</sup>

$$D_M = D_C \left( \frac{T_x^{1.75}}{P_x} \right) \quad (2.18)$$

where  $D_c$  is a constant that depends on the molecular masses and structural and volume increments of the analyte and mobile phase molecules. There is no model that can accurately determine  $D_S$ ; however, it can be estimated using the approximation<sup>7</sup>

$$D_S = \frac{D_M}{5 \times 10^4} \quad (2.19)$$

The retention factor can be calculated for a specific temperature in an isothermal separation<sup>19</sup> from

$$k = \frac{t_R - t_M}{t_M} \quad (2.20)$$

where  $t_R$  is the retention time of the analyte, and  $t_M$  is the elution time of a non-retained compound (or dead time), which may be determined by dividing the column length,  $L$ , by the average mobile phase linear velocity,  $\bar{u}_M$ . However, the dependence of the retention factor on temperature can be determined from its relationship to the distribution coefficient<sup>19</sup>

$$k = \frac{K}{\beta} \quad (2.21)$$

where  $\beta$  is the column phase ratio, which can be calculated from

$$\beta = \frac{V_M}{V_S} = \frac{r}{2d_f} \quad (2.22)$$

The distribution coefficient can be calculated from<sup>20</sup>

$$\ln(K) = \frac{\Delta H}{RT} + \frac{\Delta S}{R} \quad (2.23)$$

where  $\Delta H$  and  $\Delta S$  are the molar enthalpy and entropy terms, respectively, which are independent of temperature. These constants can be determined for each analyte

experimentally by performing isothermal separations. The dependence of  $k$  on temperature can be determined by combining Equations 2.21 and 2.23<sup>7</sup> to give

$$\ln(k) = \frac{\Delta H}{RT} + \ln \frac{a}{\beta} \quad (2.24)$$

where

$$a = \exp \frac{\Delta S}{R} \quad (2.25)$$

From retention factors determined at different isothermal temperatures,  $\ln(k)$  vs  $1/T$  can be plotted, where the slope of the linear relation is  $\Delta H/R$ , and the intercept is  $\ln(a/\beta)$ .

The most attractive feature of this model for simulating GC separations is that the analyte band can be monitored as it travels along the column, which is important in TGGC, since the effect of different axial temperature gradients on the band can be visualized. The simple plate model was programmed in Matlab 7.4 (Natic, MA, USA). All separations were performed under constant column head pressure. The simple mathematical model provided enough flexibility to simulate custom temperature gradient profiles, as well as isothermal and temperature programmed separations. Furthermore, the column segment approach allowed for plotting the movement of the analytes as they traveled and separated along the column.

## 2.3 EXPERIMENTAL

Isothermal and program temperature separations were performed using an Agilent 6890 GC system equipped with a split-splitless injector, a flame ionization detector (FID), and a 7883 autosampler injector (Santa Clara, CA, USA). The column used in this study was a 4.8 m x 0.1 mm x 0.4  $\mu\text{m}$  MXT-5 (5% diphenyl 95% dimethyl polysiloxane)

from Restek (Bellefonte, PA, USA). Isothermal separations were used to determine the thermodynamic terms ( $\Delta H$  and  $\Delta S$ ) for the analytes. The mixture used in the separation was composed of eight normal alkanes from n-nonane to n-pentadecane (n-C<sub>9</sub> to n-C<sub>15</sub>). The mixture was prepared in methanol at a concentration of 100 ppm. Injections of 0.2  $\mu\text{L}$  were performed in the split mode (1:100), and both injector and detector were maintained at 250°C during the experiments. Separations were performed in the constant pressure mode with helium as the carrier gas. Isothermal separations were performed between 40°C and 210°C. For temperature programmed separations, the column was held at 40°C for 1 min and then ramped to 210°C and held for 1 min. The heating rates used were 5, 10, 15 and 20°C/min. The chromatographic data were analyzed using Agilent ChemStation software (Santa Clara, CA, USA).

TGGC separations were performed using a home-built system with a 3 m x 0.1 mm x 0.4  $\mu\text{m}$  DB-5 fused silica column from Agilent (Santa Clara, CA, USA) of which 2 m of the column were coiled in a 1-m perimeter loop, and the rest of the column was used as transfer lines connecting the column to the injector and detector. The 1-m perimeter loop coil was divided into 40 individually resistively heated sections. Each of these sections were heated using tightly coiled resistively heated Nichrome 80 wire from Pelikan Wire (Naples, FL, USA). The coils were independently heated under computer control,<sup>24</sup> making the design flexible for generating a wide variety of temperature gradient profiles along the column. A fan was used in conjunction with the section heaters to provide rapid cooling for generating a moving sawtooth temperature profile. Details of the TGGC system design are given in the next chapters.

All chemicals used were commercially available. n-Nonane (99%) was obtained from Acros (Morris Plains, NJ, USA). n-Decane (99%) was obtained from Spectrum Chemicals (Gardena, CA, USA). n-Octane (99%), n-undecane (99%), n-dodecane (99%), n-tridecane (99%), n-tetradecane (99%), n-pentadecane (99%), and methanol (99.9%) were obtained from Sigma-Aldrich (Milwaukee, WI, USA).

## **2.4 RESULTS AND DISCUSSION**

Isothermal separations of the mixture of normal alkanes were performed to determine the thermodynamic coefficients as described previously. The retention factors obtained for the alkanes under isothermal conditions can be seen in Figure 2-1A, illustrating that small changes in temperature can produce exponential changes in the retention of the analytes and, at low temperatures, this retention can be very high. The natural log of the retention factor versus the inverse of temperature can be observed in Figure 2-1B where the lines represent the best fit linear regression (after the log transformation) for each analyte obtained from Excel. The analyte thermodynamic parameters, which are given by the slope and intercept of the line equations, are listed in Table 3-1. The thermodynamic values were used in the mathematical model to determine the temperature dependence of the distribution factor and to calculate variations in retention and peak width due to temperature changes along the column.

In the simple plate model, the column is divided into segments where equilibrium occurs and separation takes place. Thus, the greater the number of segments along the column, the more accurate the calculations. However, this comes at the expense of simulation time. Figure 2-2 shows the relative error for retention time as a function of the number of segments used per meter and the time required for the simulation to be

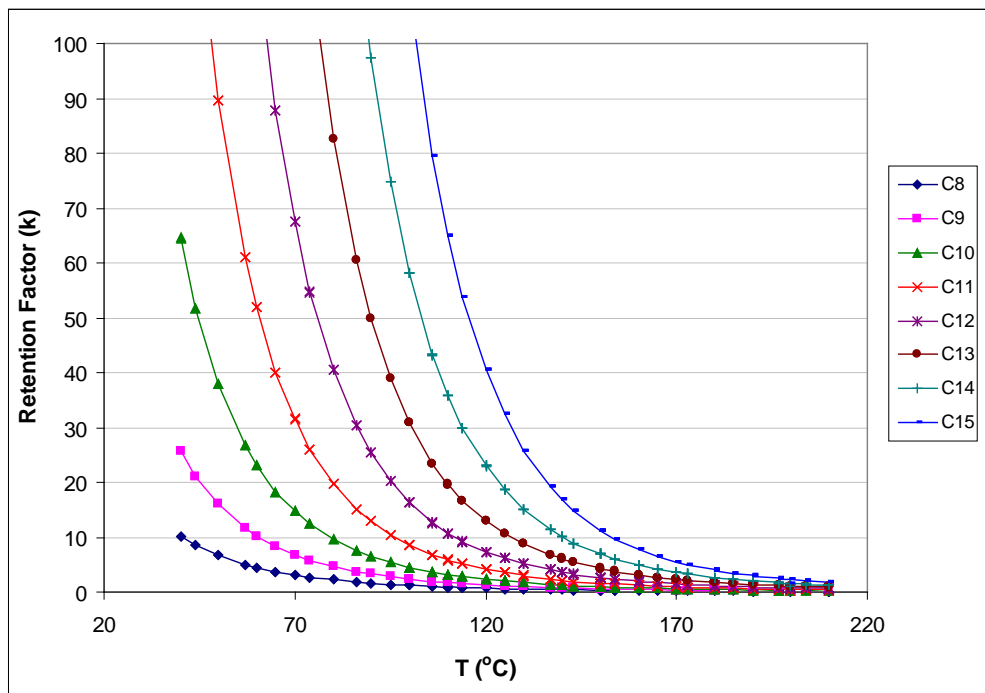
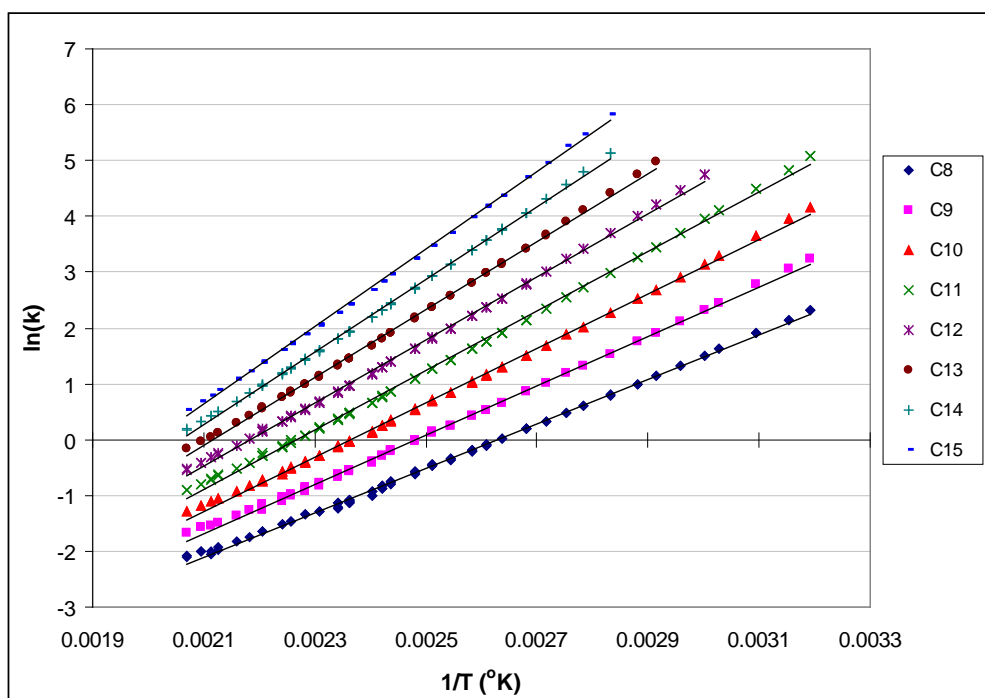
**A****B**

Figure 2-1. Retention factors determined from isothermal separations at various temperatures between 40°C and 210°C.

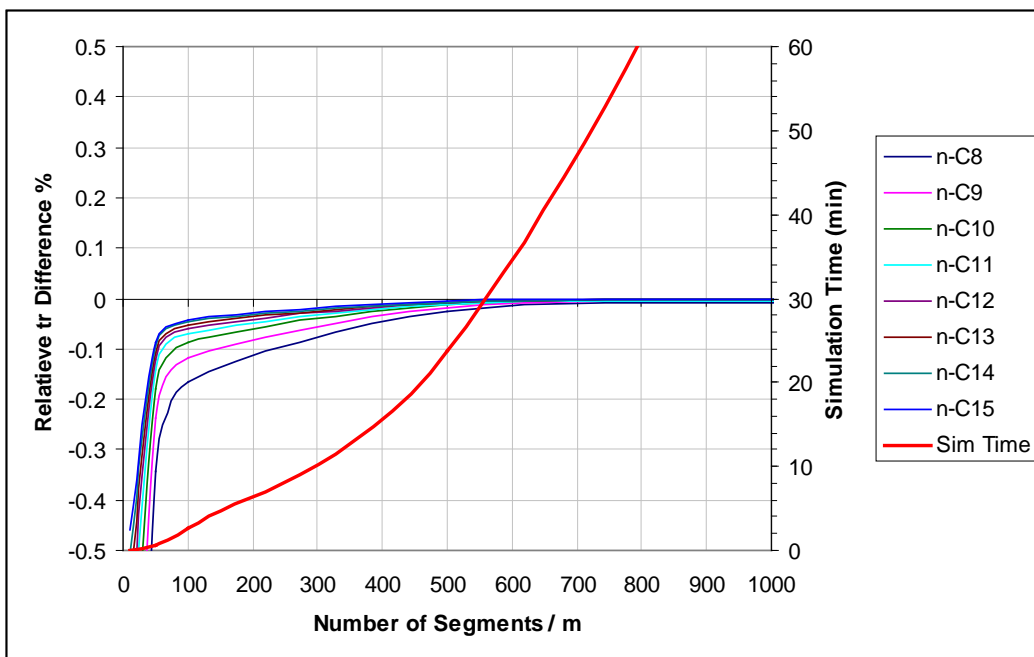


**Table 2-1. Normal alkane thermodynamic properties determined from various isothermal experiments.**

<b>Compound</b>	$\Delta H/R$ (K)	$\ln(a/\beta)$
<i>n</i> -C8	3983.25	-10.469
<i>n</i> -C9	4419.45	-10.966
<i>n</i> -C10	4866.27	-11.501
<i>n</i> -C11	5318.40	-12.058
<i>n</i> -C12	5672.75	-12.397
<i>n</i> -C13	6088.61	-12.892
<i>n</i> -C14	6500.43	-13.382
<i>n</i> -C15	6966.95	-14.001

performed. From this plot, it can be observed that the error for retention time becomes negligible when 600 or more segments/m are used; however, the simulation takes 35 min for all of the alkanes. This is not practical when the actual experiment can be performed in less than 8 min. The relative error remains small until fewer than 100 segments/m are used, at which point it quickly increases. Therefore, to perform fast simulations with minimum relative error, the number of segments/m chosen for the calculation of retention times was 100.

Using the thermodynamic parameters, predicted retention times for isothermal separations were compared with measured values to validate the model. Table 2-2 lists retention time comparisons of predicted and experimental values for four isothermal separations. Good agreement was observed between the predicted and measured values, with a maximum relative difference of -4.3% and a maximum absolute average error of 1.95%. The apparent random values for the errors observed in Table 2-2 indicate that they are not a result of a systematic error introduced by the model. These errors are small and can be attributed to how well the linear regression equation fit the experimental



**Figure 2-2. Retention time differences for alkanes versus number of segments used in the model, and simulation time for a temperature programmed separation from 40°C (1 min hold) to 210°C (1 min hold) at a heating rate of 20°C/min.**

retention factors. An average  $R^2$  of 0.998 was obtained for the regression, indicating that small discrepancies in the retention times can be expected. Accurate measurements of dead times and retention times are required to provide more precise retention factors to reduce the variation of the predicted retention times. Figure 2-3 shows a graphical comparison of the retention times measured and predicted for the various isothermal separation conditions performed. A slope of 0.9812 indicates an overall discrepancy in the predicted values. However, the absolute mean error for all predicted values in Figure 2-3 was only 1.2%, which indicates that the model can be used for predicting isothermal retention times.

Evaluation of the mathematical model for predicting retention times in temperature programmed separations was also performed. The measured retention times

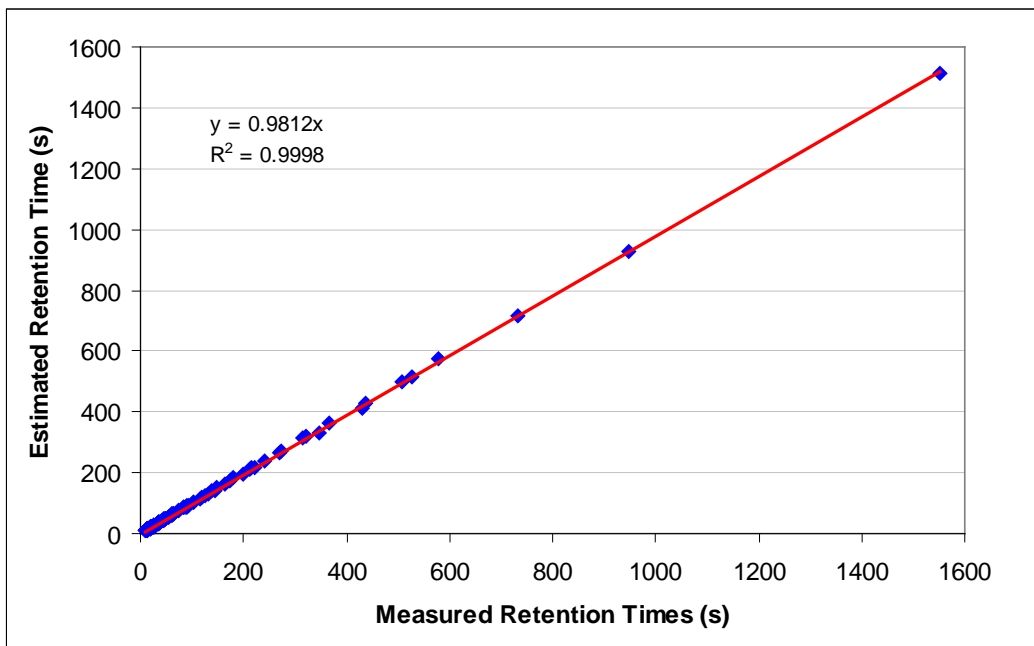
**Table 2-2. Retention time comparison of normal alkanes for four different isothermal temperatures ( $\Delta t_r = (\text{measured} - \text{predicted}) / \text{measured} \times 100$ ).**

Compounds	50 °C			100 °C		
	Measured	Predicted	$\Delta t_r\%$	Measured	Predicted	$\Delta t_r\%$
n-C <sub>8</sub>	62.28	64.2	3.08	19.08	19.1	0.10
n-C <sub>9</sub>	137.76	139.1	0.97	28.8	29.2	1.39
n-C <sub>10</sub>	316.02	313.1	-0.92	47.28	48.7	3.00
n-C <sub>11</sub>	733.98	715.3	-2.55	82.26	85.8	4.30
n-C <sub>12</sub>	1550.52	1515.8	-2.24	148.5	150.8	1.55
n-C <sub>13</sub>				273.84	272.8	-0.38
n-C <sub>14</sub>				507.96	496.8	-2.20
n-C <sub>15</sub>				946.56	925.9	-2.18
Mean Difference %	1.95			1.89		
	$t_M = 0.139$ min			$t_M = 0.143$ min		

Compounds	150 °C			200 °C		
	Measured	Predicted	$\Delta t_r\%$	Measured	Predicted	$\Delta t_r\%$
n-C <sub>8</sub>	12.48	12.25	-1.85	11.16	11.47	2.77
n-C <sub>9</sub>	14.7	14.48	-1.49	12	12.17	1.41
n-C <sub>10</sub>	18.36	18.17	-1.06	13.14	13.19	0.38
n-C <sub>11</sub>	24.3	24.22	-0.32	14.76	14.68	-0.56
n-C <sub>12</sub>	33.84	34.00	0.47	17.04	16.97	-0.41
n-C <sub>13</sub>	49.2	49.66	0.94	20.34	20.16	-0.87
n-C <sub>14</sub>	74.16	74.89	0.98	25.02	24.80	-0.88
n-C <sub>15</sub>	114.3	115.73	1.25	31.8	31.28	-1.62
Mean Difference %	1.04			1.11		
	$t_M = 0.157$ min			$t_M = 0.182$ min		

and predicted values were compared for four different heating rates in Table 2-3. The maximum relative retention time difference and absolute average error were -3.92% and 1.62%, respectively. These errors are similar in magnitude to those observed for the isothermal predictions, which was expected since the same thermodynamic values were used. However, the small retention time errors suggest that any calculation errors introduced by the model are negligible and, therefore, the model can be used for predicting retention times in temperature programmed separations. In general, the low relative error obtained for the predicted retention times demonstrates that the mathematical model can be used for accurately predicting retention times for both isothermal and temperature programmed operations.



**Figure 2-3. Plot of measured isothermal retention time versus predicted value.**

The predicted peak widths were in general 5 to 3 times wider than the experimental values when 100 and 500 segments/m were used, respectively (see Figure 2-4). For improved prediction of the peak widths, a higher number of segments is required. Figure 2-4 illustrates how the predicted peak width of n-C<sub>9</sub> becomes closer to its measured value as the number of segments increases. However, the time required to calculate the peak width within 10% of its measured value was over 6 h. Because of this time constraint, only when accurate peak width measurements were required, the column was divided into a greater number of segments. Plotting the height equivalent to a theoretical plate (HETP) versus mobile phase linear velocity (van Deemter plot) provides insight for the band broadening mechanisms.<sup>20</sup> At lower linear velocities in GC, broadening is governed by longitudinal diffusion, and at higher velocities, broadening

**Table 2-3. Retention time comparison of temperature programmed separations of normal alkanes for four different heating rates ( $\Delta t_r = (\text{measured} - \text{predicted}) / \text{measured} \times 100$ ).**

Compounds	5 °C/min			10 °C/min		
	measured	predicted	$\Delta t_r\%$	measured	predicted	$\Delta t_r\%$
n-C <sub>8</sub>	89.28	89	-0.31	88.56	88.63	0.08
n-C <sub>9</sub>	185.94	180.5	-2.93	169.14	164.99	-2.45
n-C <sub>10</sub>	326.46	319.8	-2.04	262.98	259.78	-1.22
n-C <sub>11</sub>	490.68	489.9	-0.16	357.9	359.39	0.42
n-C <sub>12</sub>	660.54	655.1	-0.82	449.52	449.40	-0.03
n-C <sub>13</sub>	826.92	826.2	-0.09	536.4	538.49	0.39
n-C <sub>14</sub>	986.34	989.8	0.35	618.54	622.06	0.57
n-C <sub>15</sub>	1137.72	1149.3	1.02	696.36	702.08	0.82
Mean Difference %	0.96			0.75		

$t_M = 0.144 \text{ min @ } 40 \text{ } ^\circ\text{C}$

Compounds	15 °C/min			20 °C/min		
	measured	predicted	$\Delta t_r\%$	measured	predicted	$\Delta t_r\%$
n-C <sub>8</sub>	87.9	86.72	-1.34	87.3	85.79	-1.72
n-C <sub>9</sub>	157.8	152.13	-3.59	149.46	143.59	-3.92
n-C <sub>10</sub>	229.08	224.23	-2.12	207.42	202.18	-2.53
n-C <sub>11</sub>	296.64	294.92	-0.58	260.1	257.18	-1.12
n-C <sub>12</sub>	359.82	357.06	-0.77	308.58	304.80	-1.22
n-C <sub>13</sub>	419.1	417.41	-0.40	353.7	350.49	-0.91
n-C <sub>14</sub>	474.84	473.58	-0.27	396.06	392.82	-0.82
n-C <sub>15</sub>	527.4	526.89	-0.10	436.02	432.74	-0.75
Mean Difference %	1.15			1.62		

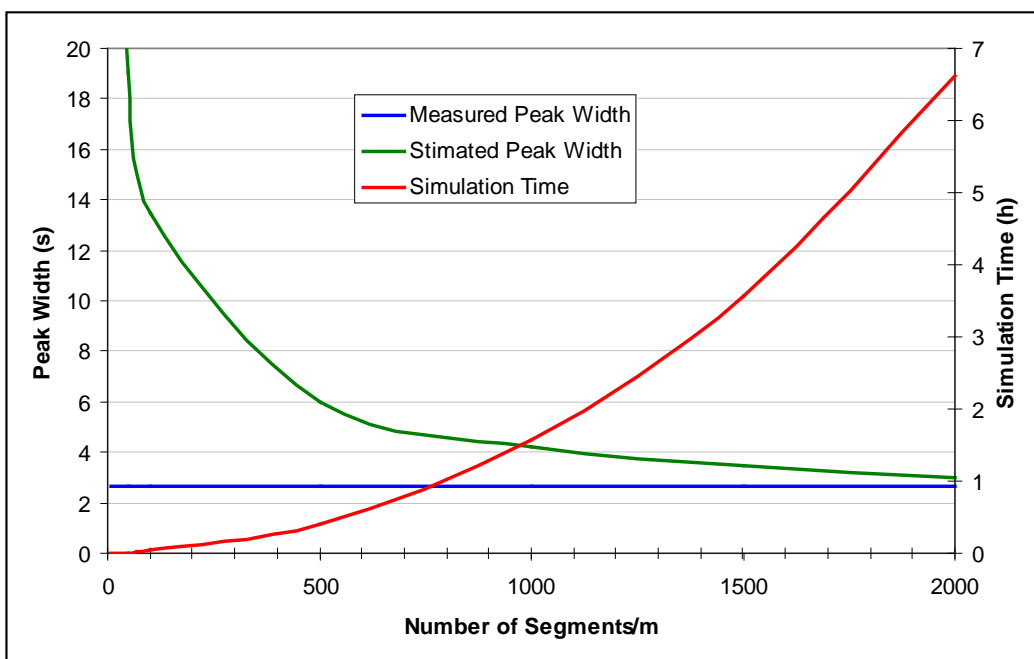
$t_M = 0.144 \text{ min @ } 40 \text{ } ^\circ\text{C}$

occurs due to resistance to mass transfer. The van Deemter plot for n-dodecane was predicted and compared with experimentally obtained values. For the predicted van Deemter plot, the peak width for n-C<sub>12</sub> was calculated for a series of isothermal separations at various mobile phase linear velocities at 130°C. The HETP values were then calculated from the retention times and peak widths obtained for the different isothermal separations from

$$HETP = 16 * \left( \frac{t_r}{w_b} \right)^2 \quad (2.26)$$

where  $w_b$  is the peak width at the base. Figure 2-5 shows van Deemter plots obtained for measured and simulated values for n-dodecane. The higher predicted HETP values at

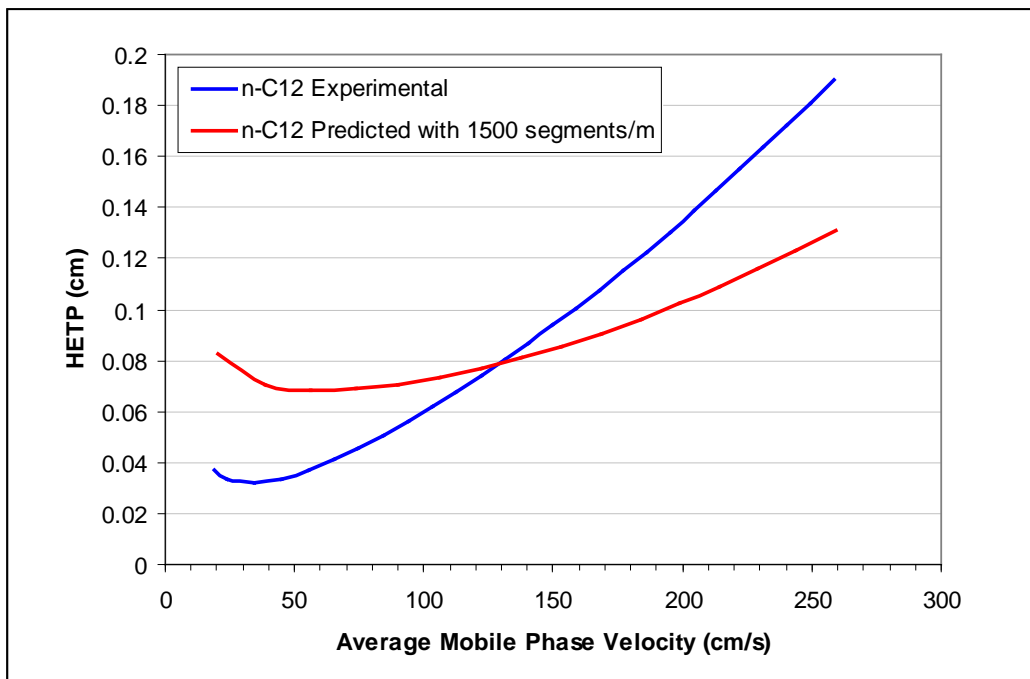
lower velocities were expected due to the broader bands obtained from the simulation. Higher HETP values would have been observed as well for the entire velocity range if the van Deemter plot profile was steeper at the end. The differences observed for the simulated values at higher velocities, where resistance to mass transfer is predominant, can be attributed to the lack of accurate prediction of the diffusion coefficients of analytes in the stationary phase.



**Figure 2-4. Peak width of nonane (n-C<sub>9</sub>) versus number of segments/m and simulation time.**

Overall, even though there are some differences between the profiles, the predicted band broadening behavior is consistent with the experimental van Deemter plot. This can be visualized in Figure 2-6, which shows the predicted and measured chromatograms for isothermal and temperature programmed separations of the n-alkane mixture.

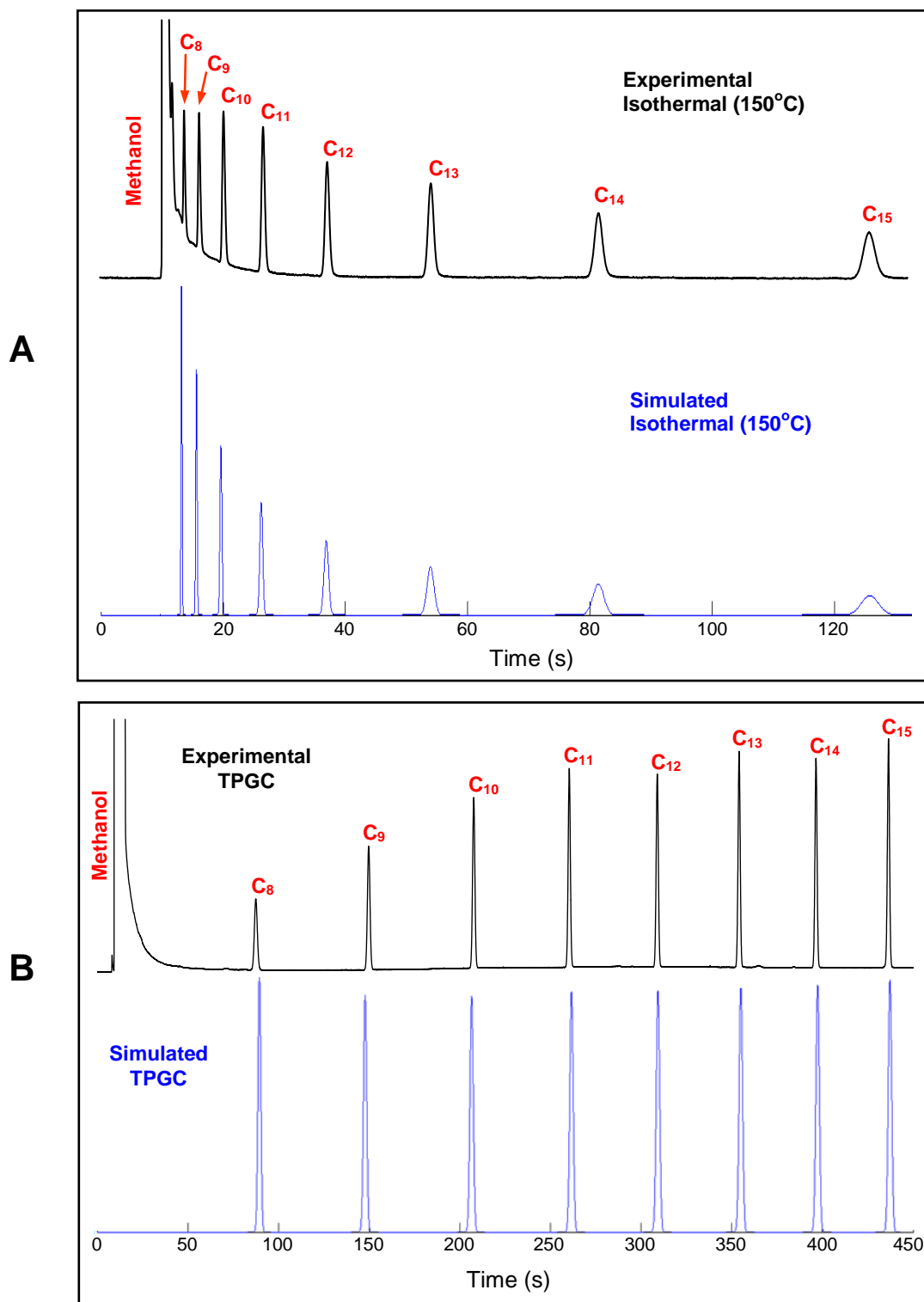
In Figure 2-6, accurate retention time predictions as well as consistent band spreading behavior can be observed. The differences observed in the peak heights in the



**Figure 2-5. Predicted and measured van Deemter plots for n-dodecane using a 130°C using a 3 m x 0.1 mm x 0.4  $\mu$ m DB-5 column.**

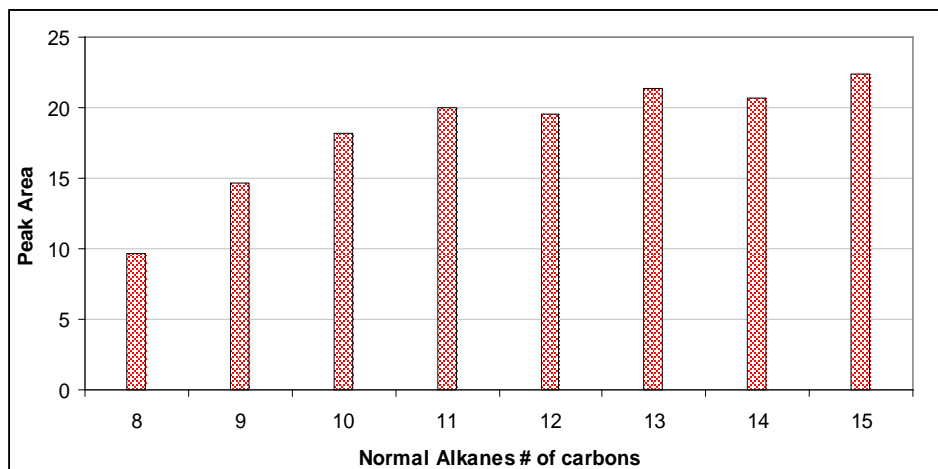
experimental chromatograms compared to those in the predicted chromatogram are a result of variations in the analyte concentrations in the sample. For the simulations, all analytes were assumed to have equal concentrations. However, this was not the case for the actual alkane test mixture.

The peak areas in a chromatogram are proportional to the concentrations of the analytes injected. Figure 2-7 shows the n-alkane peak areas for the experimental chromatogram in Figure 2-6A, showing that injected analytes did not have equal concentrations. This explains the differences between the predicted and experimentally obtained chromatograms in Figure 2-6A. Furthermore, the profile in Figure 2-7 resembles the peak height profile observed in the experimental chromatogram in Figure 2-6B. This



**Figure 2-6. Comparison of predicted and experimentally obtained chromatograms. Simulations were performed using 1500 segments/m. Conditions: as described in the experimental section; (A) Isothermal separation at 150°C. (B) Temperature programmed from 40°C (60 s hold) to 210°C (60 s hold) at 20°C/min.**

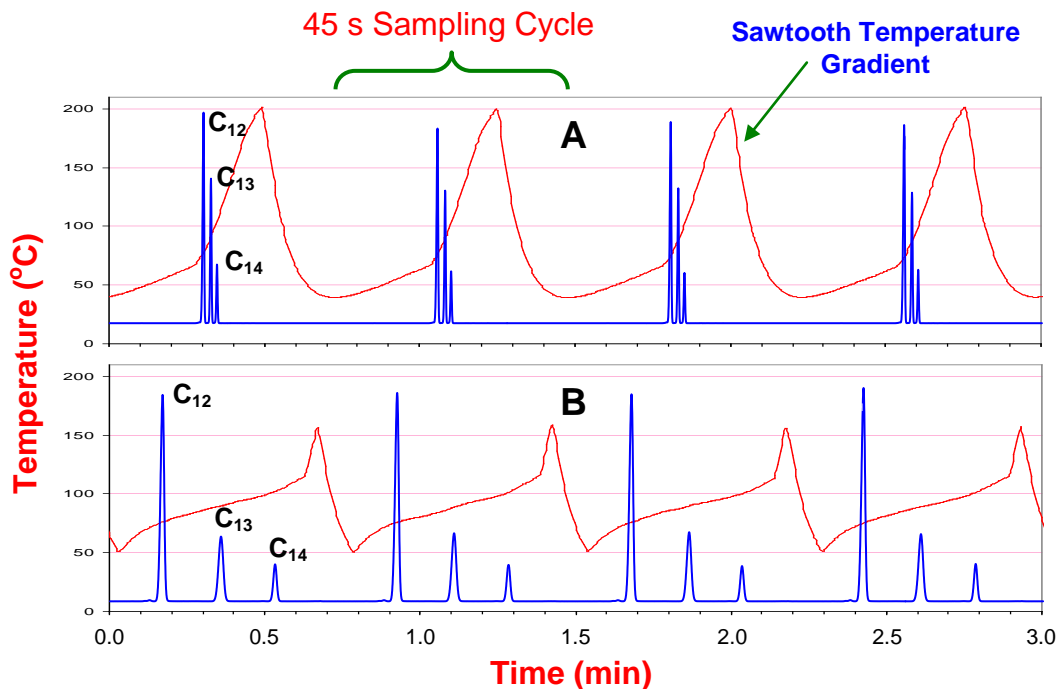




**Figure 2-7. Peak areas of n-alkanes from the experimental temperature programmed chromatogram in Figure 2-6A.**

reaffirms that if the concentrations of n-alkanes had been the same, the experimental chromatogram would have looked nearly the same as the predicted chromatogram. The particularly low values for n-C<sub>8</sub> and n-C<sub>9</sub> explain the smaller peaks obtained in the experimental chromatogram in Figure 2-6B. These results clearly show the ability of the model to predict retention times and band broadening behavior for isothermal and TPGC operations.

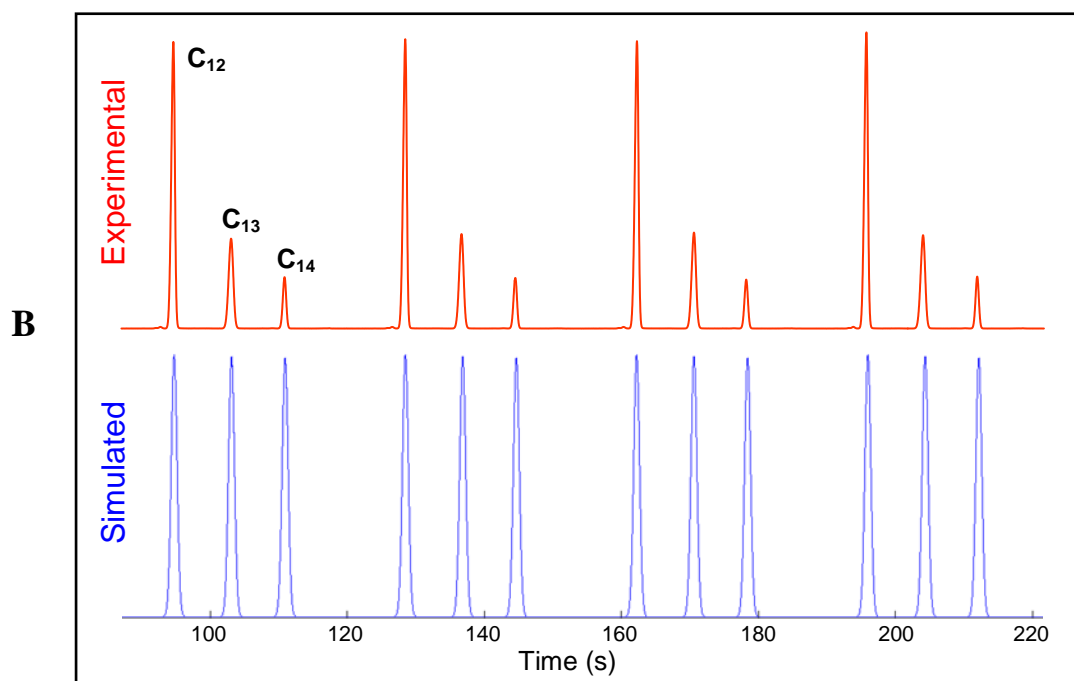
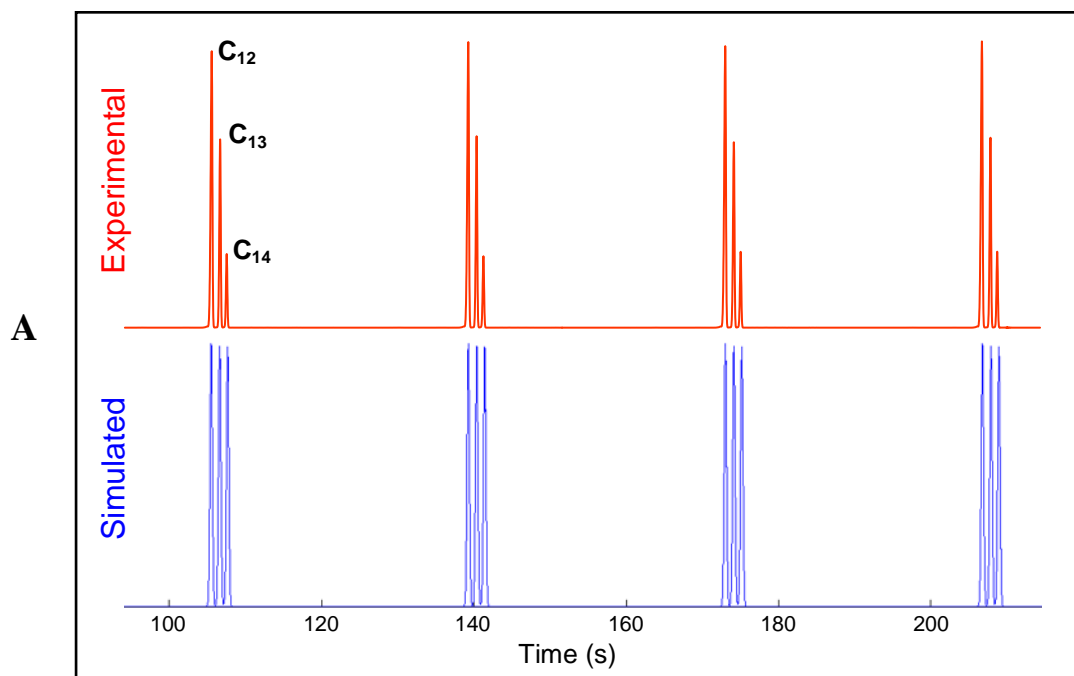
A home-built TGGC system was used to evaluate the effect of axial temperature gradients along the column. The head space of a mixture of three normal alkanes (n-C<sub>12</sub>-C<sub>14</sub>) was continuously injected and separated every 45 s using a moving sawtooth temperature profile (Figure 2-8). The temperature profile in Figure 2-8 is obtained by measuring the temperature at a fixed point on the column and then plotting it versus time. The compounds were separated using two different gradients with slopes of 5.75 and 0.77°C/cm, respectively. A comparison between the predicted and experimentally obtained chromatogram is shown in Figure 2-9. As can be seen, the peaks in the predicted



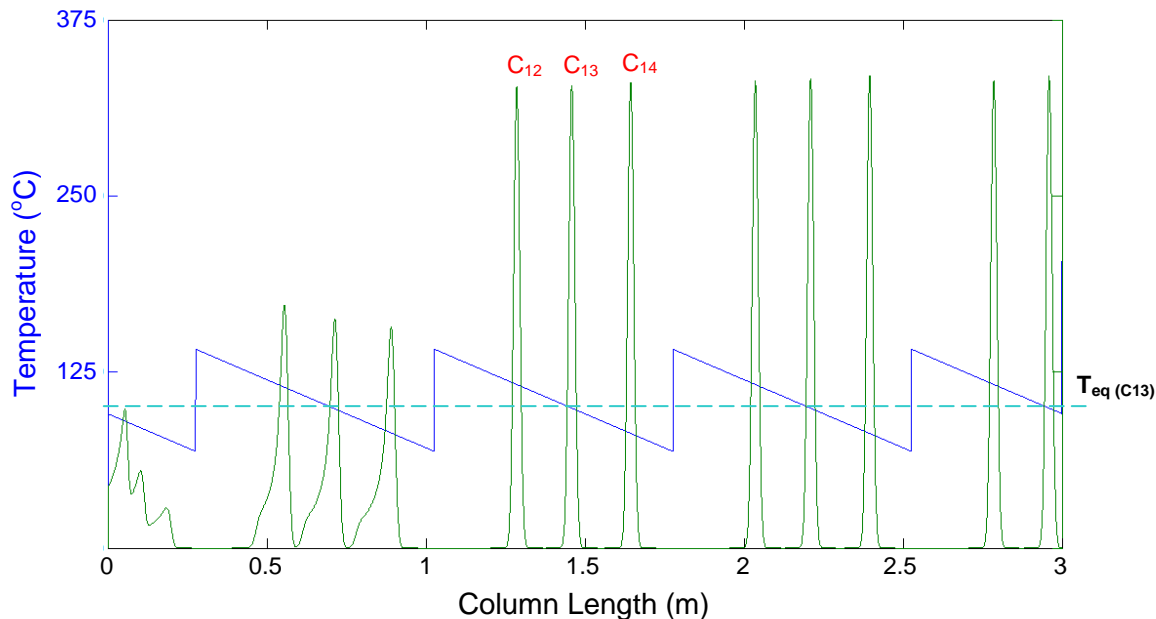
**Figure 2-8. Experimental chromatograms resulting from two different moving sawtooth axial temperature gradient profiles for continuous sampling of three n-alkanes from headspace. Separation conditions: 60 psig head pressure, 2.28 mL/min He mobile phase flow, and 2.22 cm/s (45 s/rev) gradient linear velocity.**

chromatograms share the same retention times as in the experimental separations for both temperature gradient slopes. The different peak heights observed in the experimental separations correspond to differences in the vapor pressures of the compounds, with tetradecane being the smallest and least volatile component in the mixture. The concentrations of alkanes in the simulation were set to be equal.

Broader peak widths in the simulated separation compared to the observed experimental values were expected because only 1500 segments/m were used. However, the narrow peaks indicate that the model can be used for predicting the focusing effect when negative axial temperature gradients are applied along the column. These results demonstrate that the simple plate model can be used to predict the effects of axial temperature gradients in GC separations. Furthermore, the computer model allowed a



**Figure 2-9. Comparison of predicted and experimentally obtained chromatograms from TGGC separations. Conditions: 2.22 cm/s gradient velocity; 2.28 mL/min mobile phase flow rate; (A) 5.75°C/cm gradient slope; (B) 0.77°C/cm gradient slope. Simulations were performed with 1500 segments/m.**



**Figure 2-10. Snapshots of n-alkanes as they travel and separate along the column during moving sawtooth temperature gradient operation with continuous sample injection. The temperature gradient profile is also plotted.**

unique view of how the separations progressed in distance by plotting the bands as they traveled and developed along the column. This can be seen in Figure 2-10 where the simulated separation of the n-alkanes described in Figure 2-9B is shown. The sawtooth temperature profile is overlaid with the chromatogram to facilitate visualization of the effects that result from changes in optimization of the temperature profile. Since the temperature profile is plotted as a function of length, the direction is opposite to the temperature profile plotted in Figure 2-8, which is plotted as a function of time.

The view in Figure 2-10 is of particular interest for TGGC operation because it aids in understanding the TGGC process. The advantage of this view is a clear visualization of how the bands develop along the column. The first tooth of the temperature profile shows sample introduction and how the bands begin to separate. The second tooth shows the focusing process where the broad tailing bands resulting from continuous injection

concentrate around their respective equilibrium temperatures. The bands are completely separated and developed by the third tooth, and no gain in separation is further observed. This insight provides key information for the development of new separation strategies and for the design of new TGGC systems.

## **2.5 CONCLUSIONS**

A simple mathematical plate model was developed and a computer program was written for the determination of the effects of axial temperature gradients on GC separations. The model was capable of predicting retention times with an absolute relative error of less than 2%. Predicted peak widths were generally wider. However, lower relative deviations were achieved at the cost of long calculation times (hours). Overall, the model was capable of accurately predicting the band spreading behavior observed in ITGC, TPGC and TGGC separations. The computer program allowed the visualization of the analytes as they traveled along the column, providing unique insight into separations when axial temperature gradients are applied. With the aid of the simulation program, the maximum potential of the TGGC technique can be explored, improving the performance and scope of the technique without instrumentation limitations. The simulation program proved to be an important tool in this dissertation for testing new separation strategies and for the development and design of new TGGC systems as described in the following chapters. However, further program optimization should be performed to improve the peak width predictions and required calculation times.

## 2.6 REFERENCES

1. Rubey, W. A., A Different Operational Mode for Addressing the General Elution Problem in Rapid Analysis Gas Chromatography. *J. High Res. Chromatogr.* **1991**, *14*, 542-548.
2. Ohline, R. W.; DeFord, D. D., Chromathermography, the Application of Moving Thermal Gradients to Gas Liquid Partition Chromatography. *Anal. Chem.* **1963**, *35* (2), 227-234.
3. Zhukhovitskii, A. A., Some Developments in Gas Chromatography in the U.S.S.R. In *Gas Chromatography 1960*, Scott, R. P. W., Ed. Butterworths: Edinburgh, 1960; pp 293-300.
4. Gonzalez, F. R.; Nardillo, A. M., Theoretical and Practical Aspects of Flow Control in Programmed-temperature Gas Chromatography. *J. Chromatogr. A.* **1997**, *757* (1-2), 97-107.
5. Gonzalez, F. R.; Nardillo, A. M., Integration of the Equation of Peak Motion in Programmed-pressure and -Temperature Gas Chromatography. *J. Chromatogr. A.* **1997**, *766* (1-2), 147-152.
6. Hinshaw, J. V., Strategies for GC Optimization, Part III - Software. *LC GC North America* **2000**, *18* (10), 1040-1047.
7. Snijders, H., *et al.*, Optimization of Temperature-Programmed Gas Chromatographic Separations I. Prediction of Retention Times and Peak Widths from Retention Indices. *J. Chromatogr. A* **1995**, *718*, 339-355.
8. Akporhonor, E. E., *et al.*, Calculation of Programmed Temperature Gas-Chromatography Characteristics from Isothermal Data .2. Predicted Retention Times and Elution Temperatures. *J. Chromatogr.* **1989**, *463* (2), 271-280.
9. Gonzales, F. R.; Nardillo, A. M., Retention in Multistep Programmed-Temperature Gas Chromatography and Flow Control Linear Head Pressure Programs. *J. Chromatogr. A.* **1997**, *757*, 109-118.
10. Staerk, D. U., *et al.*, Use of the Equilibrium-dispersive Model of Nonlinear Gas Chromatography for the Modelling of the Elution Band Profiles in the Preparative-scale Gas Chromatographic Separation of Enantiomers. *J. Chromatogr. A.* **1996**, *734* (2), 289-296.
11. Özdural, A. R., *et al.*, Modeling Chromatographic Columns: Non-equilibrium Packed-bed Adsorption with Non-linear Adsorption Isotherms. *J. Chromatogr. A.* **2004**, *1041* (1-2), 77-85.
12. Cavalli, E. J.; Guinchard, C., Forecasting Retention Times in Temperature-Programmed Gas Chromatography: Experimental Verification of the Hypothesis on Compound Behavior. *J. Chromatogr. Sci.* **1996**, *34*, 547-549.
13. Aldaeus, F., *et al.*, Prediction of Retention Times and Peak Widths in Temperature-programmed Gas Chromatography Using the Finite Element Method. *J. Chromatogr. A.* **2009**, *1216* (1), 134-139.
14. Castello, G., *et al.*, Retention Models for Programmed Gas Chromatography. *J. Chromatogr. A.* **2009**, *1216* (10), 1607-1623.
15. Dorman, F. L., *et al.*, Predicting Gas Chromatographic Separation and Stationary-Phase Selectivity Using Computer Modeling. *Anal. Chem.* **2002**, *74* (9), 2133-2138.

16. Dorman, F. L., *et al.*, Using Computer Modeling to Predict and Optimize Separations for Comprehensive Two-dimensional Gas Chromatography. *J. Chromatogr. A.* **2008**, *1186* (1-2), 196-201.
17. Bautz, D. E., *et al.*, Computer Simulation as an Aid in Method Development for Gas Chromatography : I. The Accurate Prediction of Separation as a Function of Experimental Conditions. *J. Chromatogr. A.* **1991**, *541*, 1-19.
18. Moler, G. F., *et al.*, Estimation of the variance of the area of a single chromatography peak. *Anal. Chem.* **1983**, *55* (6), 842-847.
19. Ettre, L. S.; Hinshaw, J. V., *Basic Relationships of Gas Chromatography*. Advanstar Communications: Cleveland, 1993.
20. Giddings, J. C., *Unified Separation Science*. Wiley Interscience New York, 1991.
21. Hawkes, S. J., Viscosities of Carrier Gases at Gas Chromatograph Temperatures. *Chromatographia* **1993**, *37* (7/8), 399-401.
22. Bird, R. B., *Transport Phenomena*. John Wiley & Sons: New York, 1966; p 780.
23. Karaiskakis, G.; Gavril, D., Determination of Diffusion Coefficients by Gas Chromatography. *J. Chromatogr. A.* **2004**, *1037*, 147-189.
24. Fenimore, D. C., Gradient Temperature Programming of Short Capillary Columns. *J. Chromatogr.* **1975**, *112*, 219-227.

# **3 MATHEMATICAL SOLUTION TO PEAK POSITION IN MOVING THERMAL GRADIENT GAS CHROMATOGRAPHY**

## **3.1 INTRODUCTION**

In gas chromatography (GC), the column temperature is the variable that has the greatest effect on separation. Therefore, the separation modes in GC are based on how temperature is applied to the column. Among the separation modes in GC, the superiority of the isothermal mode for compounds with similar retention times is widely known. The fact that any modification of the operating temperature during separation cannot increase resolution and decrease the time for separation simultaneously has been elegantly proven in a series of papers by Blumberg and colleagues.<sup>1-5</sup> Consequently, although temperature programming methods are often used to greatly decrease separation time relative to isothermal separations, these are used at a cost of decreased resolution, especially when high programming rates are used.<sup>6-7</sup>

An alternative to temperature programming methods is temperature gradient methods, such as thermal gradient GC (TGGC).<sup>8-14</sup> In TGGC, axial temperature gradients are applied along the column instead of uniformly heating the whole column as in isothermal and temperature programming methods. Separations in TGGC are performed in a decreasing column temperature from the injector to the detector, producing a focusing effect on the peaks since the fronts of the peaks are at lower temperature and move slower than the backs of the peaks. Blumberg's theoretical work has also shown that axial temperature gradients cannot enhance resolution beyond ideal basic



separations, such as isothermal and temperature programmed separations.<sup>3,5</sup> However, Blumberg also found that improvements in separation can be obtained with axial temperature gradients as a result of focusing recovery due to non-ideal sample introduction, which in practice is typically the case.<sup>1-2,5</sup> Blumberg's conclusions were experimentally investigated in this dissertation (see Chapters 4-6), from which it was found that the TGGC method produced approximately equivalent separations to TPGC. However, the separation potential of the moving TGGC technique relies on unique control over the movement and elution of compounds.

In moving TGGC, peaks travel along the column with the moving temperature gradient at their characteristic temperatures of equilibrium ( $T_{eq}$ ). As the analytes travel along the negative gradient into lower temperatures, they slow down as they become more retained. However, since the gradient moves along the column, higher temperatures continue to push analytes until equilibrium is reached ( $T_{eq}$ ).

Adequate control of the temperature gradient profile allows unparalleled control over the movement and elution of analytes, which has not been fully explored. Knowing the positions of analytes in the temperature gradient is required to establish the temperature profile that provides optimum separation. Consequently, the purpose of this chapter is to present a mathematical analysis of the moving TGGC method to provide a foundation for explicitly examining the unique capabilities of the technique. The goal is to provide the mathematical tools to rapidly determine the characteristic temperatures of equilibrium of the analytes and their respective peak widths and locations inside the temperature gradient, based on approximating the dynamics of the moving TGGC technique.

## 3.2 PRELIMINARY CONSIDERATIONS

Analyte transport is assumed to be essentially a one-dimensional model, since in moving TGGC the analyte moves in one direction along the column with the temperature gradient. To facilitate the mathematical development, and make the model clear, the dynamics of the analyte were studied relative to the temperature gradient. Thus, the positions of the analytes with respect to the beginning of the column are referred to as  $x$ -values, while the positions of the analytes with respect to the beginning of the gradient ( $z_o$ ) are referred to as  $z$ -values (Figure 3-1).

For this model, the following notation is employed:

$x$  = coordinate along the capillary, starting at  $x = 0$  for the beginning and  $x = L$  for the end.

$u_m(x, T)$  = velocity of an analyte in the mobile phase at point  $x$  in the column and at temperature  $T$ . This is assumed to be the same as the bulk flow velocity at  $x$  and  $T$ .

$w$  = velocity of the temperature gradient along the capillary.

$T^*$  = fixed temperature for an isothermal separation, where peak velocity is time invariant.

$u(t)$  = velocity of the peak at time  $t$  relative to the fixed coordinate system ( $x$ ).

$-b$  = slope of the temperature gradient, where  $|b| > 0$ .

$z_o$  = fixed reference point along the moving temperature gradient. This point moves as the temperature gradient moves. For simplicity, we use the beginning of the temperature gradient, *i.e.*, the point where the temperature increases above  $T^*$ , as the reference point,  $z_o$ . As the temperature gradient moves from point  $x = 0$  to point  $x = L$ , the point  $z_o$  also moves between these two points, and can be determined by  $z_o = w * t$ .

$z$  = point in the capillary relative to point  $z_o$ . Note that for a fixed point in the capillary, the  $z$ -value for the point changes as the reference point  $z_o$  moves from  $x = 0$  to  $x = L$ .

$T_{(z)}$  = temperature at point  $z$ .

$\mu_t$  = peak center, relative to  $z_o$  at time  $t$ .

$K(T)$  = distribution coefficient, which expresses how strong an analyte is retained in the stationary phase relative to the mobile phase.<sup>15</sup> This coefficient is specific to the analyte and to the stationary and mobile phases. This coefficient can be determined by<sup>16</sup>

$$\ln(K) = \frac{\Delta H}{RT} + \frac{\Delta S}{R} \quad (3-1)$$

where  $R$  is the ideal gas constant, and  $\Delta H$  and  $\Delta S$  are the molar enthalpy and entropy terms, respectively, which are independent of temperature. These constants, as well as the retention factor ( $k$ ), can be determined for each analyte ( $i$ ) experimentally by performing isothermal separations. The retention factor can be calculated for a specific temperature in an isothermal separation<sup>15</sup> from

$$k = \frac{t_R - t_M}{t_M} \quad (3-2)$$

where  $t_R$  is the retention time of the analyte, and  $t_M$  is the elution time of a non-retained compound (or dead time), which may be determined by dividing the column length,  $L$ , by the average mobile phase linear velocity,  $\bar{u}_M$ . The retention factor is related to the distribution coefficient by<sup>15</sup>

$$k = \frac{K}{\beta} \quad (3-3)$$

where  $\beta$  is the column phase ratio (mobile phase to stationary phase). The dependence of  $k$  on temperature can be determined by combining Equations 3-1 and 3-5<sup>17</sup> to give

$$\ln(k) = \frac{\Delta H}{RT} + \ln \frac{a}{\beta} \quad (3-4)$$

where

$$a = \exp \frac{\Delta S}{R} \quad (3-5)$$

From retention factors determined at different isothermal temperatures,  $\ln(k)$  vs  $1/T$  can be plotted, where the slope of the line is  $\Delta H/R$  and the intercept is  $\ln(a/\beta)$ . From Chapter 2, the values of  $\Delta H/R$  and  $\ln(a/\beta)$  for a series of normal alkanes are listed in Table 3-1.

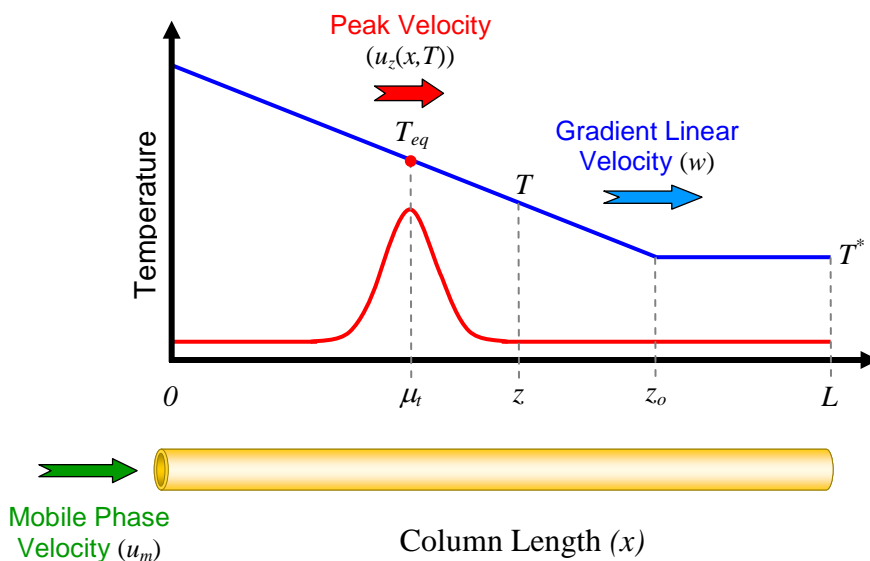
**Table 3-1. Normal alkane thermodynamic properties determined from various isothermal experiments.**

Compound	$\Delta H/R$ (K)	$\ln(a/\beta)$
<i>n</i> -C8	3983.25	-10.47
<i>n</i> -C9	4419.45	-10.97
<i>n</i> -C10	4866.27	-11.50
<i>n</i> -C11	5318.40	-12.06
<i>n</i> -C12	5672.75	-12.40
<i>n</i> -C13	6088.61	-12.89
<i>n</i> -C14	6500.43	-13.38
<i>n</i> -C15	6966.95	-14.00

In this model, we use point  $z_o$  as the reference point, and it is implicitly assumed that the temperature gradient is "long" enough for the separation considered, *i.e.*, the  $T_{eq}$  values are within the temperature range of the gradient.

### 3.3 MODEL

In the model, a moving linear temperature gradient travels down the capillary column at velocity  $w$  (Figure 3-1).



**Figure 3-1.** Diagram showing a moving linear temperature gradient with slope  $b$  at time  $t > 0$ , describing the different variables of the model.

One might think of an oven that surrounds the capillary and moves from point  $x = 0$  to  $x = L$ .<sup>18</sup> At time  $t = 0$ , the oven is at the beginning of the column, where the front of the gradient is at  $z_o = 0$  and the temperature of the whole column is assumed to be  $T^*$ . As the oven moves from  $x = 0$  to  $x = L$ , the temperature gradient moves with leading coordinate  $z_o$  down the column, and the temperature at each point in the column increases as the front of the oven moves past it (Figure 3-1). Assuming a linear gradient, the temperature at any point  $z < z_o$  is given by

$$T = T^* - b(z - z_o) \quad (3-6)$$

Implicit in this expression is that  $z - z_o < 0$ . Thus, the temperature at a point  $x$  in the capillary will be  $T^*$  until the oven reaches that point, and then it will increase at a constant rate of  $b$  per unit time.

### 3.4 DETERMINATION OF THE CHARACTERISTIC EQUILIBRIUM TEMPERATURE

From basic principles of GC, the velocity of an analyte ( $u$ ) in the capillary can be determined by<sup>15</sup>

$$u = \frac{u_m}{1+k(T)} = \frac{u_m}{1+K(T)/\beta} \quad (3-7)$$

The velocity at temperature  $T$  of the analyte at a point  $z$ , relative to the velocity at point  $z_o$  is defined as  $u_z(T)$ . Since the velocity of  $z_o$  is the velocity of the gradient  $w$ , we have

$$u_{z(T)} = \frac{u_m}{1+K(T)/\beta} - w \quad (3-8)$$

For points to the left of  $z$  the temperature is higher than  $T$  (Figure 3-1). Consequently, the distribution coefficient is smaller (Equation 3-1), making the velocity of the analyte larger. Points on the temperature gradient to the right of  $z$  have lower temperatures, making the partition coefficient larger and the velocity of the analyte smaller. It is of interest to determine if the center of the analyte peak is stationary relative to  $z_o$ .

Explicitly, is there a temperature,  $T_{eq}$ , such that the relative velocity,  $u_z(T_{eq})$ , is zero? This point is assumed to be to the left of  $z_o$  and, therefore, the value of  $T_{eq}$  must be larger than  $T^*$ . If  $\Delta H > 0$  then  $k(T_{eq}) < k(T^*)$ . Thus, at  $T_{eq}$

$$w = \frac{u_m}{1+k(T_{eq})} \quad (3-9)$$

$$w > \frac{u_m}{1 + k(T^*)} \quad (3-10)$$

To find the value of  $T_{eq}$ , we rearrange Equation 3-9

$$k(T_{eq}) = \left( \frac{u_m}{w} - 1 \right) \quad (3-11)$$

Substituting in the definition for  $k(T_{eq})$  (Equation 3-4) we obtain

$$\exp\left(\frac{\Delta H}{RT} + \ln \frac{a}{\beta}\right) = \left( \frac{u_m}{w} - 1 \right) \quad (3-12)$$

Now, provided the right hand side of Equation 3-11 is greater than zero we have

$$T_{eq} = \frac{\Delta H}{R \left( \ln(u_m - w) - \ln\left(\frac{a}{\beta} w\right) \right)} \quad (3-13)$$

Thus, there is a  $T_{eq}$  temperature if  $\ln(u_m - w) > \ln\left(\frac{a}{\beta} w\right)$

$$w < \frac{u_m}{1 + a/\beta} \quad (3-14)$$

It is important to note that if  $u_m/(1+a/\beta) < w < u_m$ , Equation 3-13 gives a negative temperature value as a solution. Combining Equations 3-10 and 3-14, we obtain

$$\frac{u_m}{1 + k(T^*)} < w < \frac{u_m}{1 + a/\beta} \quad (3-15)$$

These equations show that the moving TGGC method can only be applied if  $w$  satisfies Equation 3-15; if so, there exists a temperature,  $T_{eq} > T^*$ , such that the velocity of the peak at  $T_{eq}$  is the same as the velocity of the moving temperature gradient,  $w$ . In summary, for a given mobile phase velocity and minimum achievable gradient temperature ( $T^*$ ), there is a gradient velocity range where the analytes can reach their  $T_{eq}$

values. Consequently, if  $b > 0$ , there is a point along the temperature gradient, say  $z_{Teq}$ , where the temperature is  $T_{eq}$ , such that the analyte peak reaches zero velocity relative to the point  $z_o$ . If  $b = 0$ , then there is no point along the gradient where the velocity of the peak equals  $w$ . In this case, at all points,  $z < z_o$ , the velocity of the peak is lower than the velocity,  $w$ , of the point  $z_o$ .

Unless otherwise stated, we assume that the value of  $b$  is strictly positive,  $b > 0$ . For points to the right of  $z_T$ , the relative velocity,  $u_z(T)$ , of the peak is negative. Similarly, to the left of the point  $z_T$ , the relative velocity is positive, producing a focusing effect on the moving temperature gradient.

There are two opposing forces affecting the movement of the analyte. The first is bulk flow, represented by  $u_m$ . The second force is the force on the peak created by the movement of the temperature gradient and the propensity of the front of the peak to have a lower adsorption/desorption rate than the back of the peak, causing a differential velocity in the peak according to the relative position on the temperature gradient.

### **3.5 PEAK LOCATION AND WIDTH UNDER GRADIENT CONDITIONS**

Under common chromatographic conditions, the greatest sources of dispersion in a peak are due to longitudinal diffusion in the mobile phase and resistance to mass transfer due to random adsorption/desorption of molecules in the stationary phase. However, the differential effect of temperature in a moving temperature gradient acts to offset the effects of these sources of dispersion. This is explored next.

In effect, the analyte peak is in a temperature gradient relative to the moving point  $z_o$ . Consequently, as noted above, the peak will focus at a stationary point relative to the



point  $z_o$ . To explore this in the simplest case, we make the assumption that the velocity gradient is linear relative to  $z_o$ .

$$u_z(T) = a_o - b\delta(z - z_o) \quad (3-16)$$

where  $a_o$  is the velocity of the peak at the reference point  $z_o$ ,  $\delta$  is a function of the temperature  $T$ , partition coefficient  $K$ , and location  $z$  on the temperature gradient.

The condition that the velocity gradient is linear is based on the profile of the temperature gradient; for this model, it is assumed to be linear with slope  $-b$ . This is not the same as a linear change in the temperature as the point  $z_o$  moves at constant velocity from point  $x = 0$  to the point  $x = L$ . In addition, the velocity in the mobile phase increases as the analyte approaches the end of the column. Here we present an approximation to the linearity assumption. Explicitly, the velocity at point  $z$ , at temperature  $T$  is

$$u_z(T) = \frac{u_m}{1 + \exp\left(\frac{\Delta H_i}{RT(z)} + \ln\left(\frac{a}{\beta}\right)\right)} - w \quad (3-17)$$

We linearize this Equation 3-17 by expanding about the point  $z_o$  to obtain

$$u_z \approx u_{z_o} - b \delta (z - z_o), \quad (3-18)$$

where

$$\delta = \frac{u_m \Delta H_i \exp\left(\frac{\Delta H_i}{RT^*} + \ln\left(\frac{a}{\beta}\right)\right)}{R(T^*)^2 \left(1 + \exp\left(\frac{\Delta H_i}{RT^*} + \ln\left(\frac{a}{\beta}\right)\right)\right)^2} = \frac{u_m \Delta H_i k(T^*)}{R(T^*)^2 (1 + k(T^*))^2} \quad (3-19)$$

Note that this first order approximation becomes more accurate as the slope  $b$  becomes closer to zero.

The flux equation given by Blumberg<sup>4</sup> and Giddings<sup>16</sup> is of the form

$$\frac{\partial c(z,t)}{\partial t} = \frac{\partial}{\partial z} \left( D_T \frac{\partial c(z,t)}{\partial t} \right) - \frac{\partial}{\partial z} u_z c(z,t) \quad (3-20)$$

In theory we can solve Equation 3-20 when we assume  $c(z,t)$  as Gaussian (Equation 3-25, below). However, in the current case the moving temperature gradient solution to Equation 3-20 will result in a non-separable partial differential equation. In the following, we give some simple assumptions that can be used to create two ordinary differential equations. Although these approximations yield only an approximate solution for  $\mu_t$  and  $\sigma_t$ , behavior of these as we change  $b$  or  $t$  can be examined using these equations.

To obtain an appropriate, conservative solution, we propose approximating both for the dispersion due to longitudinal diffusion,  $D_M$ , and resistance to mass transfer,  $D_A$ , as a function of temperature. First we assume that the dispersion due to resistance to mass transfer can be approximated by

$$\tilde{D}_A = \frac{\gamma_2 u_m^2}{T^{*1+\eta}} \quad (3-21)$$

Since  $T^*$  is the lowest temperature gradient value we will use, this assumption results in an overstatement of the total dispersion,  $D_T$ .

The longitudinal diffusion term at any point  $z$  in dispersion can be written as

$$D_M = \gamma_1 (T^* + b \delta(z - z_o)) \quad (3-22)$$

However, if  $\mu_t$  represents the mean of the peak, relative to  $z_o$ , then we can approximate

$D_M$  with the value

$$\tilde{D}_M = \gamma_1 (T^* + b \delta(\mu_t - z_o)) \quad (3-23)$$

Here we have assumed that the different diffusion models are determined by the constant  $\gamma_1$  scaled by a function of the temperature,  $T_{eq}$ , where  $\gamma_1 = \gamma T_{eq}^\eta$

The overall approximation dispersion term  $\tilde{D}_T$  will be given by

$$\tilde{D}_T = \tilde{D}_M + \tilde{D}_A \quad (3-24)$$

The resolution determined for the moving temperature gradient using  $\tilde{D}_T$  will be lower than the actual resolution. As noted in the literature, with a linear temperature gradient, the peak shape is approximately Gaussian

$$c(z, t) = \frac{1}{\sqrt{2\pi\sigma_t^2}} \exp\left(-\frac{(z - \mu_t)^2}{2\sigma_t^2}\right) \quad (3-25)$$

Using this expression for the peak shape in Equation 3-20 and differentiating, we obtain

$$c(z, t) \left[ \Delta_z \mu_t' + \Delta_z^2 \sigma_t \sigma_t' - \frac{\sigma_t'}{\sigma_t} \right] = c(z, t) \left( b\delta - \frac{\tilde{D}_T}{\sigma_t^2} + \Delta_z [v_z - b\delta(\mu_t - z_o)] + \Delta_z^2 (D_T - b\delta\sigma_t^2) \right) \quad (3-26)$$

where  $\Delta = \frac{z - \mu_t}{\sigma_t^2}$ . Since this equation must hold for all values of  $z$ , we can equate

coefficients of  $\Delta z$ . After cancelling the term  $c(z, t)$ , we obtain two ordinary differential equations

$$\mu_t' = v_{z_o} + b\delta z_o - b\delta \mu_t \quad (3-27)$$

$$\sigma_t \sigma_t' = \tilde{D}_T - \delta\sigma_t^2 \quad (3-28)$$

At time  $t = 0$ , we assume that injection produces a peak at point  $x = 0$  with a width of  $\sigma_o$ .

Thus, the center of the peak at  $t = 0$  is at  $z_o$ . Using this as an initial condition, we solve the first of these two equations to obtain an expression for  $\mu_t$

$$\mu_t = z_o + \frac{v_{z_o}}{b\delta} (1 - \exp(-2b\delta t)) \quad (3-29)$$

Using this solution for  $\mu_t$  and the initial width of the peak,  $\sigma_o$ , at injection, a preliminary solution of the second equation for  $\sigma_t^2$  can be obtained using Matlab. However, the resultant equation without evaluation of the initial conditions was long, a complicated equation. Therefore, simulation of the behavior of the widths of the peaks was done using the GC model discussed previously.

The result given in Equation 3-29 indicate that eventually the peak will reach a steady state at its  $T_{eq}$  value. The rate at which this is approximated depends on the value of  $b$ . It is important to note that the linear approximation of the peak velocity (Equation 3-16) is only nominal since the solution given in Equation 3-29 is not at the point at which the temperature reaches equilibrium as described above. To correct this, a more extensive expansion of the velocity is needed. However, the equations obtained were too difficult to solve analytically.

### 3.6 VALIDATION OF THE MODEL

To evaluate Equation 3-13 for calculating  $T_{eq}$ , experimental separations of normal alkanes (n-C<sub>11</sub> to n-C<sub>14</sub>) were performed using different axial temperature gradients (Figure 3-2). The custom-built instrument description is given in Chapters 5 and 6. For the calculation of  $T_{eq}$ , the thermodynamic parameters used are listed in Table 3-1. A comparison between the measured and calculated values is given in Table 3-2. In this table, the absolute percent relative standard deviation (%RSD) is relatively small (< 9.5 %RSD). The differences can be attributed to experimental error in measurements of the mobile phase flow, as well as in the axial temperature gradient profile. Therefore, these

results confirm the separation model approach as well as Equation 3-13 for calculating the  $T_{eq}$  values for compounds traveling with the moving temperature gradient.

Since Equation 3-29 provides the positions of the peaks in a moving temperature gradient, it was verified by direct comparison with the  $T_{eq}$  Equation 3-13. Assuming that equilibrium was reached ( $t \gg 0$ ) and rearranging Equation 3-29, we obtain

$$\mu_t - z_o = \frac{v_{z_o}}{b\delta} \quad (3-30)$$

where the exponential component in Equation 3-29 goes to zero at high values of  $t$ .

Knowing that  $b$  is the slope of the gradient (temperature / length), we can rewrite

Equation 3-30 as

$$(\mu_t - z_o)b = \frac{v_{z_o}}{\delta} = T_{eq} - T^* \quad (3-31)$$

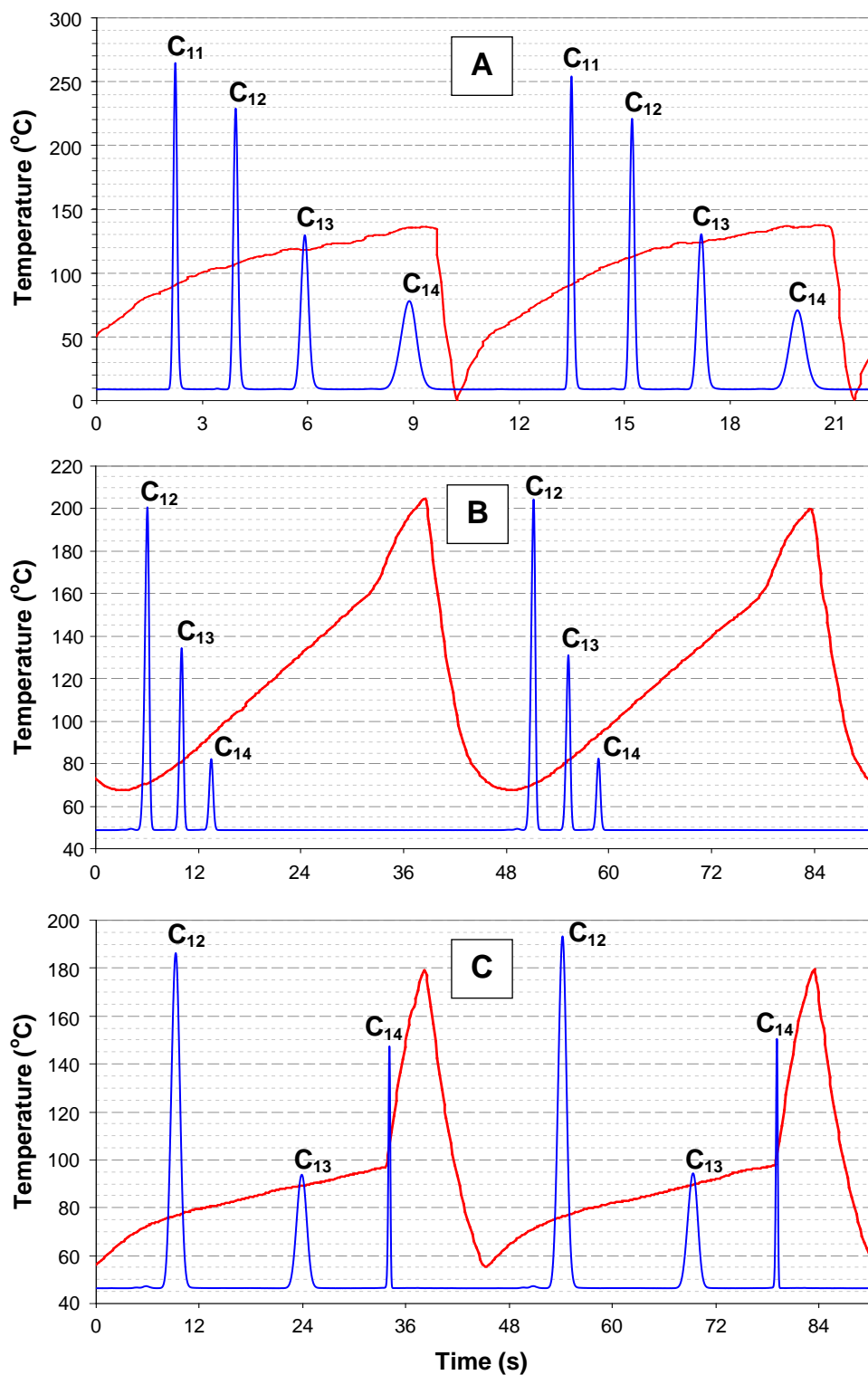
Using Equations 3-7, 3-13 and 3-19 to verify Equation 3-31, and the thermodynamic parameters in Table 3-1 for n-C<sub>14</sub>, assuming  $T^* = 50^\circ\text{C}$ ,  $w = 2 \text{ cm/s}$  and  $u_m = 130 \text{ cm/s}$  with  $b = 2^\circ\text{C/cm}$ , we obtain

$$\frac{v_{z_o}}{\delta} = 16.1^\circ\text{C} \quad \neq \quad T_{eq} - T^* = 47.4^\circ\text{C} \quad (3-32)$$

This difference indicates that the expression used to approximate the velocities of the peaks relative to the gradient must be expanded.

### 3.7 APPLICATIONS OF THE EQUATIONS

From Equation 3-11, it can be observed that for given  $u_m$  and  $w$  values, and once  $T_{eq}$  is reached, all of the analytes will travel along the column at a constant retention factor and, hence, partition coefficient (Equation 3-3). This characteristic is not observed in any of the conventional GC separation methods. In the case of isothermal GC (ITGC),



**Figure 3-2. Temperature profiles of a moving sawtooth axial temperature gradient and resultant repetitive chromatograms for continuous sampling of normal alkane vapors performed under different conditions. (A)  $u_m = 96.3$  cm/s,  $w = 9.09$  cm/s, (B)  $u_m = 155.1$  cm/s,  $w = 22.2$  cm/s. (C)  $u_m = 138.3$  cm/s,  $w = 22.2$  cm/s.**

**Table 3-2. Characteristic equilibrium temperatures for alkanes separated with sawtooth moving gradients, and their experimental and calculated  $T_{eq}$  values.**

Plot	Analytes	$T_{eq}$ Experimental	$T_{eq}$ Calculated	%RSD Difference
<b>A</b>	<i>n</i> -C <sub>11</sub>	91.4	98.3	7.49
	<i>n</i> -C <sub>12</sub>	110.3	113.9	3.21
	<i>n</i> -C <sub>13</sub>	127.5	128.7	0.89
	<i>n</i> -C <sub>14</sub>	138.9	142.4	2.55
<b>B</b>	<i>n</i> -C <sub>12</sub>	71.1	68.0	-4.38
	<i>n</i> -C <sub>13</sub>	81.9	82.4	0.62
	<i>n</i> -C <sub>14</sub>	94.1	95.9	1.91
<b>C</b>	<i>n</i> -C <sub>12</sub>	77.7	70.4	-9.46
	<i>n</i> -C <sub>13</sub>	90.0	84.8	-4.67
	<i>n</i> -C <sub>14</sub>	99.3	98.4	-2.62

the distribution coefficient is constant along the column; however, it increases with less volatile compounds, producing broad peaks. In the case of temperature programmed GC (TPGC), the distribution coefficients of the analytes decrease as the column temperature increases with time, allowing the separation of compounds with a broad range of boiling points. However, in TPGC when high heating rates are used, the last portion of the column is not utilized for separation as the analyte distribution coefficients become very small due to the high temperatures.<sup>6-7</sup> High values of retention factors produce broad peaks; on the other hand, low values reduce interactions of analytes with the stationary phase, decreasing separation. With the moving TGGC method, the desired retention factor values for all analytes can be tailored by choosing appropriate values of  $u_m$  and  $w$ . Controlling the time an analyte interacts with the stationary phase can provide fine control over the selectivity. In TPGC, the selectivity can change by using different heating rates, which also affects the total analysis time. In TGGC from Equation 3-11, we can observe that the retention factors and, hence, the selectivity can be changed by

modifying  $u_m$  while maintaining constant the total analysis time. This fundamental characteristic should be further tested experimentally using a variety of compounds instead of only n-alkanes, as the separation between the latter will remain proportional, and hence, a difference in selectivity will not be observed.

Using Equation 3-13 and the thermodynamic values in Table 3-1, a plot of the retention factor as a function of  $T_{eq}$  for a gradient velocity of 2.22 cm/s (45 s/loop) was constructed for normal alkanes (n-C<sub>8</sub> to n-C<sub>15</sub>) (Figure 3-3). This plot has several applications. From Equation 3-11, it was determined that all peaks move along the gradient with constant retention factors. Therefore, the intersections of horizontal lines in Figure 3-3 with the  $k$  plots of the n-alkanes allow determination of the  $T_{eq}$  values for the analytes as a function of the mobile phase velocity by tracing a horizontal line from the  $u_m$  used. This information can be utilized to determine the maximum and minimum temperature limits of the moving gradient for separation of selected analytes. Figure 3-3 can also be used to determine the  $u_m$  values that place the  $T_{eq}$  values of the analytes inside the available temperature gradient range. This plot can greatly facilitate the use of the moving TGGC technique by quickly providing the  $T_{eq}$  values of the analytes under given conditions.

Equation 3-13 was also used to determine the effect of measurement accuracy of the mobile phase velocity on calculations of the  $T_{eq}$  values for normal alkanes (Figure 3-4). From Figure 3-4, it can be observed that the mobile phase velocity accuracy does not have a major impact on calculations  $T_{eq}$ . In this figure, it can be observed that deviations of 10% in the mobile phase velocity produce deviations between 2 to 8% in the  $T_{eq}$  values of the n-alkanes. The deviations observed for  $T_{eq}$  values were smaller for



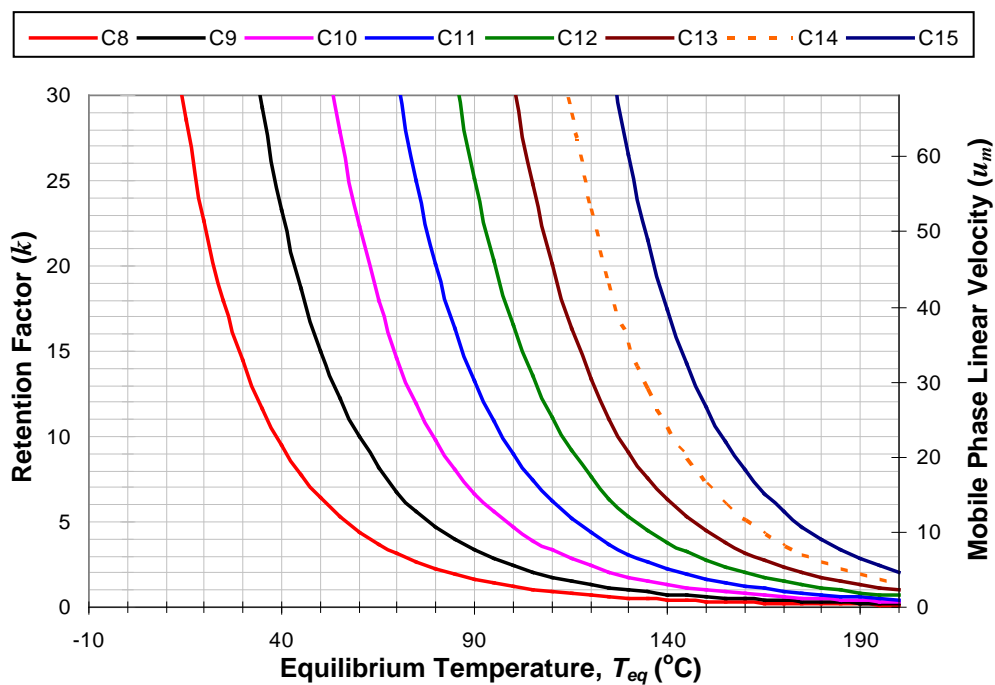


Figure 3-3. Retention factor and mobile phase velocity as a function of  $T_{eq}$  for normal alkanes.

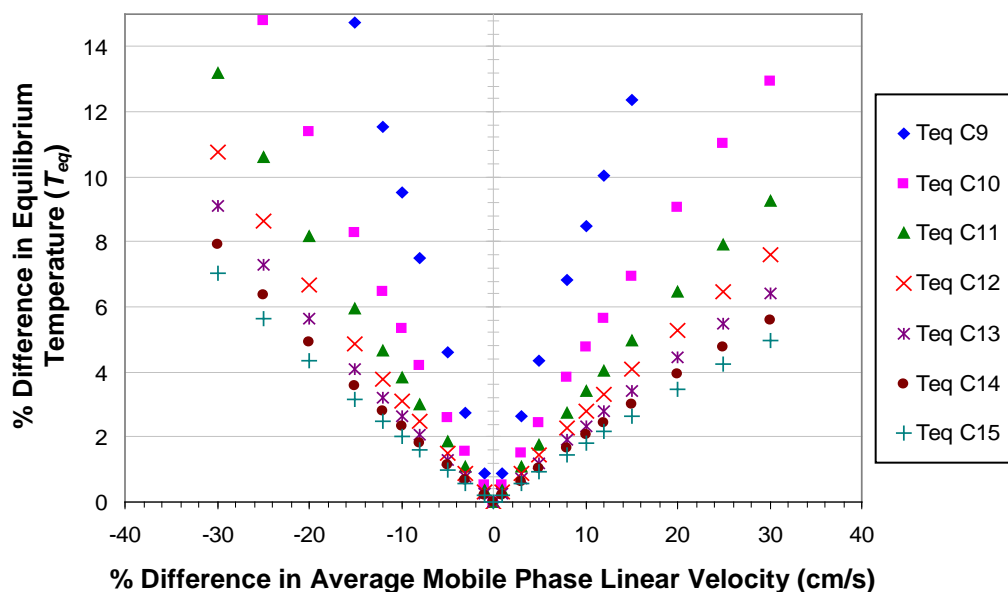


Figure 3-4. Effect of the mobile phase linear velocity on calculations of the  $T_{eq}$  values for various normal alkane compounds for  $u_m = 120$  cm/s.

the higher boiling point compounds. These results demonstrate that small changes in the mobile phase velocity will not significantly affect the  $T_{eq}$  values.

### 3.8 CONCLUSIONS

A mathematical model that incorporates the various components that affect the behavior of peaks in moving TGGC has been described. The equation obtained for the calculation of  $T_{eq}$  (Equation 3-13) showed that for a given mobile phase velocity and minimum achievable gradient temperature ( $T^*$ ), there is a gradient velocity range where the analytes can reach their  $T_{eq}$  values. The Giddings flux equation was used to generate partial differential equations to describe the position and broadening of the peaks in a moving temperature gradient. In an effort to simplify the equations, we made several assumptions about the dispersion and velocity of the peaks in the gradient, which resulted in two separate differential equations: one which is analytically solvable and the second one which must be solved using iterative techniques. Comparison of the  $T_{eq}$  equation with solutions of the solvable differential equation indicates that the expression used for the peak velocity relative to the gradient must be refined.

The  $T_{eq}$  equation proved to adequately determine the  $T_{eq}$  values of analytes in moving TGGC separations. Validation of the equation was performed by comparing experimental results with calculated values. The model was capable of predicting the  $T_{eq}$  values with a relative error of less than 9.5 %. Using the characteristic equilibrium temperature equation, the maximum potential of the TGGC technique can be exploited by rapidly determining the  $T_{eq}$  information that can be used for optimizing the temperature gradient profile. Plots of retention factor and mobile phase velocity versus  $T_{eq}$  could be a powerful tool for application of the moving TGGC technique, since it provides quick

information regarding the conditions required (*i.e.*,  $u_m$  and gradient profile) to separate selected analytes. This equation would be of particular interest when applying feedback control for the moving TGGC technique to perform optimum separations in short times and with minimum intervention.

### 3.9 REFERENCES

1. Blumberg, L. M., Outline of a Theory of Focusing in Linear Chromatography. *Anal. Chem.* **1992**, *64* (20), 2459-2460.
2. Blumberg, L. M., Variance of a Zone Migrating in a Linear Medium .2. Time-Varying Nonuniform Medium. *J. Chromatogr.* **1993**, *637* (2), 119-128.
3. Blumberg, L. M., Focusing Cannot Enhance Resolution or Speed Limit of a GC Column. *J. Chromatogr. Sci.* **1997**, *35* (9), 451-454.
4. Blumberg, L. M.; Berger, T. A., Variance of a Zone Migrating in a Nonuniform Time-Invariant Linear Medium. *J. Chromatogr.* **1992**, *596* (1), 1-13.
5. Blumberg, L. M., Limits of Resolution and Speed of Analysis in Linear Chromatography With and Without Focusing *Chromatographia* **1995**, *40* (3-4), 218-218.
6. Grall, A., *et al.*, Peak Capacity, Peak-Capacity Production Rate, and Boiling Point Resolution for Temperature-Programmed GC with Very High Programming Rates. *Anal. Chem.* **2000**, *72*, 591-598.
7. Harris, W. E.; Habgood, H. W., *Programmed Temperature Gas Chromatography*. John Wiley & Sons: New York, 1966; p 305.
8. Berezkin, V. G., *et al.*, Temperature Gradients in Gas Chromatography. *J. Chromatogr.* **1986**, *373*, 21-44.
9. Fenimore, D. C., Gradient Temperature Programming of Short Capillary Columns. *J. Chromatogr.* **1975**, *112*, 219-227.
10. Kaiser, R., Temperature Gradient Chromatography. *Chromatographia* **1968**, *1*, 199-207.
11. Nerheim, A. G., Gas-Liquid Chromatography. *Anal. Chem.* **1960**, *32*.
12. Tudge, A. P., Studies in Chromatographic Transport III. Chromatography. *Can. J. Phy.* **1961**.
13. Zhukhovitskii, A. A., Some Developments in Gas Chromatography in the U.S.S.R. In *Gas Chromatography 1960*, Scott, R. P. W., Ed. Butterworths: Edinburgh, 1960; pp 293-300.
14. Zhukhovitskii, A. A., *et al.*, New Method of Chromatographic Analysis. *Doklady Akademii Nauk SSSR* **1951**, *77*, 435-8.
15. Ettre, L. S.; Hinshaw, J. V., *Basic Relationships of Gas Chromatography*. Advanstar Communications: Cleveland, 1993.
16. Giddings, J. C., *Unified Separation Science*. Wiley Interscience New York, 1991.

17. Snijders, H., *et al.*, Optimization of Temperature-Programmed Gas Chromatographic Separations I. Prediction of Retention Times and Peak Widths from Retention Indices. *J. Chromatogr. A* **1995**, 718, 339-355.
18. Ohline, R. W.; DeFord, D. D., Chromathermography, the Application of Moving Thermal Gradients to Gas Liquid Partition Chromatography. *Anal. Chem.* **1963**, 35 (2), 227-234.

## 4 PEAK SWEEPING AND GATING USING THERMAL GRADIENT GAS CHROMATOGRAPHY

### 4.1 INTRODUCTION

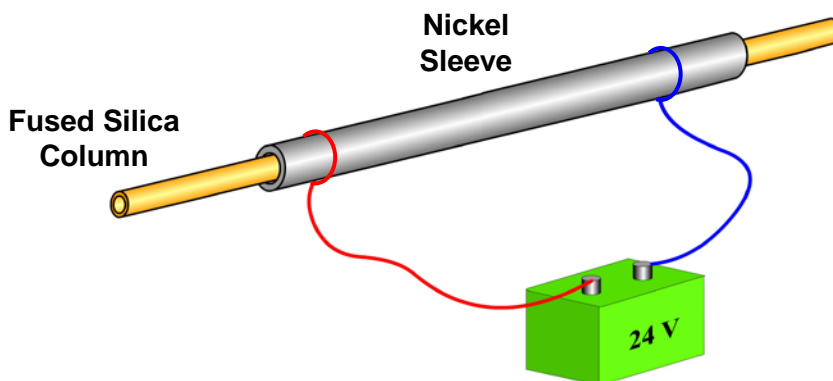
In thermal gradient gas chromatography (TGGC), the temperature along the separation column changes simultaneously in time and position,  $T(t,x)$ ,<sup>1-2</sup> unlike in isothermal and temperature programmed GC operations (ITGC and TPGC), where the column temperature is uniform along the column length at any given time,  $T(t)$ . The use of axial temperature gradients in GC was first introduced by Zhukhovitskii in 1951<sup>3</sup> and studied over the years by various scientists.<sup>4-10</sup> More recently, it was further explored by Rubey<sup>1</sup> and Phillips<sup>2</sup> in the 1990s, and by Zhao<sup>11</sup> and Contreras<sup>12</sup> in the early 2000s. In TGGC, the column temperature typically decreases from the injector to the detector, causing peaks to experience a focusing effect, as the front of the peaks will always be at lower temperatures and moving slower than the rear of the peaks. This behavior is markedly different from what is experienced in conventional GC, where the chromatographic bands continuously spread with migration distance.

The thought of controlling the temperature along the column to produce a focusing effect on the peaks has intrigued scientists since the technique was introduced. However, the use and evaluation of this technique has been hindered by technical difficulties involved in construction of the instrumentation and control of temperature. Controversy has arisen over the years regarding separation expectations and actual capabilities of TGGC.<sup>13</sup> Previous work has suggested that TGGC can provide superior performance in resolution and speed of analysis compared to conventional GC separation

modes.<sup>1-2, 6, 14-15</sup> On the other hand, theoretical work by Blumberg and Ohline<sup>5, 16-17</sup> has shown that under ideal chromatographic conditions, an increase in the gradient slope for a moving linear gradient produces an overall resolution decrease. Unfortunately, no experimental work has been performed to confirm either point of view. The controversy around TGGC and instrumentation difficulties have discouraged further development, overlooking the separation potential of the technique. Even though TGGC has been around for a long time, it is still considered to be in its infancy. The technique offers new possibilities for controlling the movement and elution of compounds that have not been fully explored to date. Current technology can facilitate the development of new TGGC instruments that can take advantage of the separation potential of the technique. In this chapter, a simple laboratory instrument for generating stationary axial temperature gradients is presented, and a comparison of the different GC separation modes is provided. Furthermore, a new method for selectively releasing analyte peaks from the column, TGGC gating, is introduced.

## **4.2 MATERIALS AND METHODS**

A simple laboratory apparatus based on a tubular heat exchanger was used to generate the axial temperature gradients. The heat exchanger was based on resistance heating and convection cooling. The system was constructed using a direct resistively-heated nickel sleeve inside a custom-made adhesive polyimide tube. The polyimide tube served as a heat exchanger along which the temperature gradient was generated. A 1.3 m x 0.1 mm ID x 0.4  $\mu$ m DB-5 fused silica column from Agilent (Santa Clara, CA, USA) was used for the separations. Direct resistive heating of the fused silica column was performed by placing the column inside an electroformed nickel sleeve (0.024" OD x



**Figure 4-1. Configuration for resistively heating the fused silica capillary column.**

0.017" ID ) from VICI (Houston, TX, USA ) (Figure 4-1). Heating was achieved by applying a voltage across the Ni sleeve.

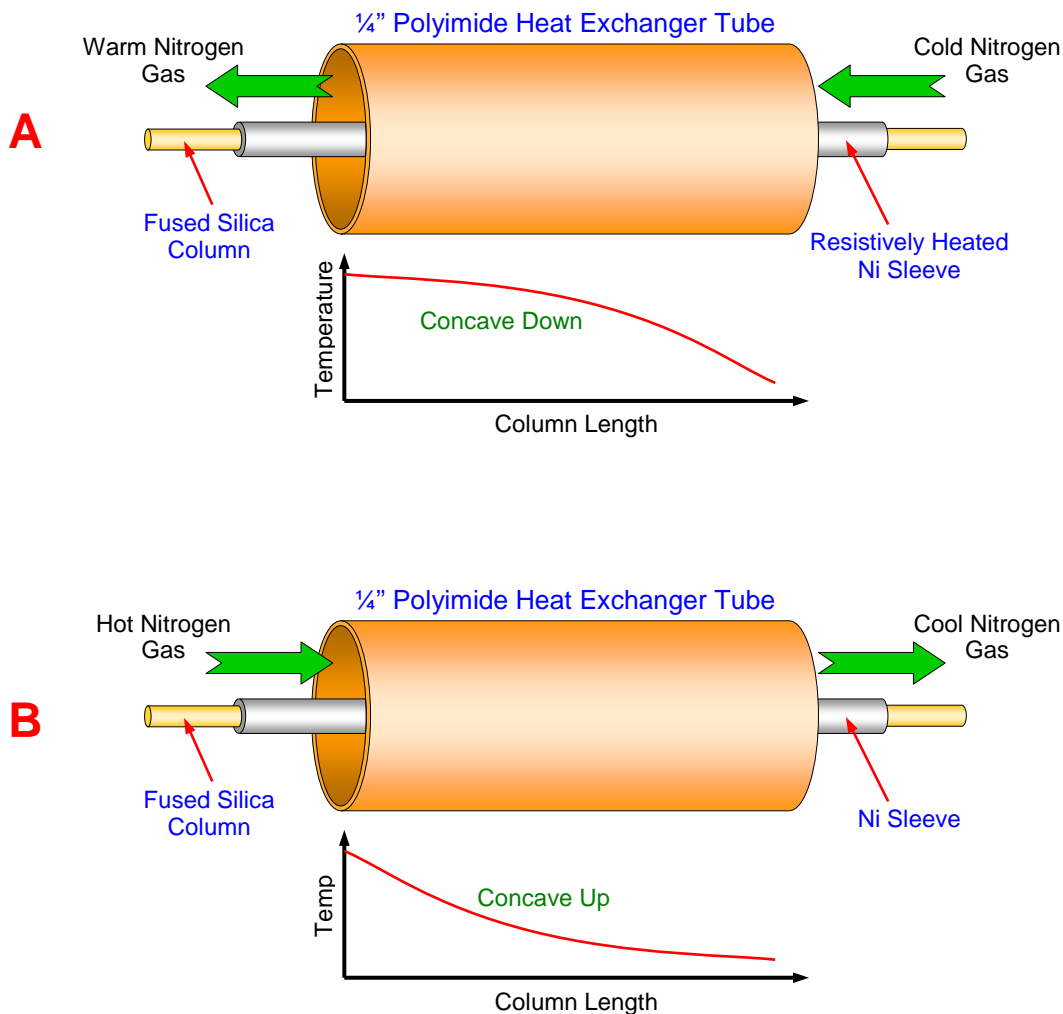
For generating a gradient, the fused silica column and Ni sleeve arrangement was inserted inside a 1 m x 1/4" ID custom-made polyimide tube (Figure 4-2), and kept coaxially inside by coiled wire with alternating diameters of 1/4" and 1/16".<sup>12</sup> Axial temperature gradients were generated by heat transfer when flow of nitrogen gas passed through the polyimide tube while the column was being resistively heated (Figure 4-2A). Another method for generating a gradient profile was achieved when externally heated nitrogen gas was cooled as it traveled along the polyimide tube (Figure 4-2B); no resistive heating was applied in this case. Although the temperature gradient profile generated with both system configurations were usually curved, linear gradients could be achieved by using a large flow rate, which produced a shallower gradient slope. The column temperature was monitored through time at three different positions (Figure 4-4). Small (0.005" ID) type K thermocouples from Omega (Stamford, CT, USA) were used, and the temperature was recorded using a USB National Instruments data acquisition

system and a custom-made LabVIEW program (Austin, TX, USA). The polyimide tube had a low thermal mass to allow fast changes in temperature; the tube was made from a ½” wide x 0.0025” thick polyimide tape with silicone adhesive from McMaster-Carr (Los Angeles, CA, USA).<sup>12</sup> To construct the polyimide tube, a ¼” ID stainless steel tube was carefully wrapped with polyimide tape with the non-adhesive part of the tape facing the metal tube. The edges of the tape windings were positioned next to each other. The tube was finished by winding another layer of polyimide tape over the first with the adhesive side down, covering the gaps of the first wrapping.<sup>12</sup>

The column temperature was controlled with a simple custom-made linear power amplifier circuit (Figure 4-3), allowing a LabVIEW program to control the voltage applied to the Ni sleeve. The use of Ultra Reliable Power Transistors in parallel reduced the risk of over-heating the column due to a transistor failure, since these transistors contain an internal current and thermal limiting circuit that cuts the power in the case of fast voltage variations. Two 12 VDC 250 W power supplies from Digi-Key (PN: 271-2147, Thief River Falls, MN, USA) connected in series were used to supply the power to heat the Ni sleeve, which had a resistance of 1 Ω/m at room temperature. The maximum voltage applied to the Ni sleeve was 15 V.

A liquid nitrogen heat exchanger bath was used to cool the nitrogen gas down to – 20 °C. The heat exchanger bath consisted of a coiled ¼” copper tube inside a Dewar flask. For heating the nitrogen gas, a heater was fabricated from a 10” x ¼” ID copper tube packed with stainless steel wool and heated with 1” wide heating tape from Omega. The heater was typically set at 350°C. The nitrogen gas flow was regulated with a needle valve. A Gilmont direct reading rotameter was used for measuring the flow (Cole-

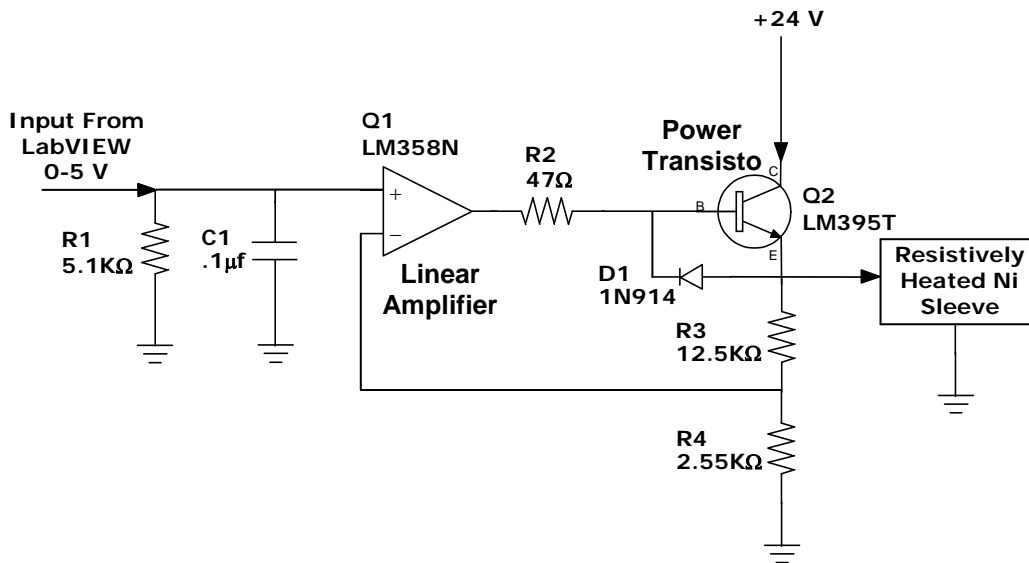




**Figure 4-2. Heat exchanger configuration for generating (A) concave down and (B) concave up profiles.**

Parmer, Vernon Hills, IL, USA). The flows varied between 3 to 13 L/min. Solenoid valves from ASCO (PN: 8262G210, Florham Park, NJ, USA) were used to quickly turn on/off the flow of nitrogen gas using the custom-written LabVIEW program. The TGGC system used an injector and flame ionization detector (FID) from an Agilent 6890 GC system (Santa Clara, CA, USA). The FID detector was set at an acquisition rate of 200 Hz, and chromatographic data were acquired and handled using Agilent ChemStation

software (version D.01.00). Figure 4-4 shows the overall diagram of the TGGC system used to generate the axial temperature gradients.



**Figure 4-3. Power circuit that controlled the voltage of the resistively heated Ni sleeve through a custom LabVIEW program.**

Normal alkanes from nonane to tetradecane ( $C_9$ - $C_{14}$ ), and a standard EPA 624 sample were used to evaluate the separation capabilities of the TGGC system. Solid phase microextraction (SPME) was the extraction and injection method used in the experiments. A 65  $\mu\text{m}$  film thickness polydimethylsiloxane-divinylbenzene (PDMS-DVB) SPME fiber from Supelco (Bellefonte, PA, USA) was used. The injector temperature and detector were maintained at 250°C. Injections were performed in the split mode (500:1) and constant head pressure was used. Helium was used as the mobile phase for all the separations. An Agilent 6890/5973N GC-MSD system was used to aid in the identification of the EPA 624 standard compounds. A 5 m x 0.1 mm x 0.4  $\mu\text{m}$  DB-5 column, was used for the GC-MS analysis.

All chemicals used were commercially available. n-Nonane (99%) was obtained from Acros (Morris Plains, NJ, USA). n-Decane (99%) was obtained from Spectrum Chemicals (Gardena, CA, USA). n-Undecane (99%), n-dodecane (99%), n-tridecane (99%), n-tetradecane (99%), and methanol (99.9%) were obtained from Sigma-Aldrich (Milwaukee, WI, USA). The 624 EPA volatile halocarbon mixture (Volatiles MegaMix, 2000  $\mu\text{g}/\text{mL}$  in methanol) was obtained from Restek (Bellefonte, PA, USA).

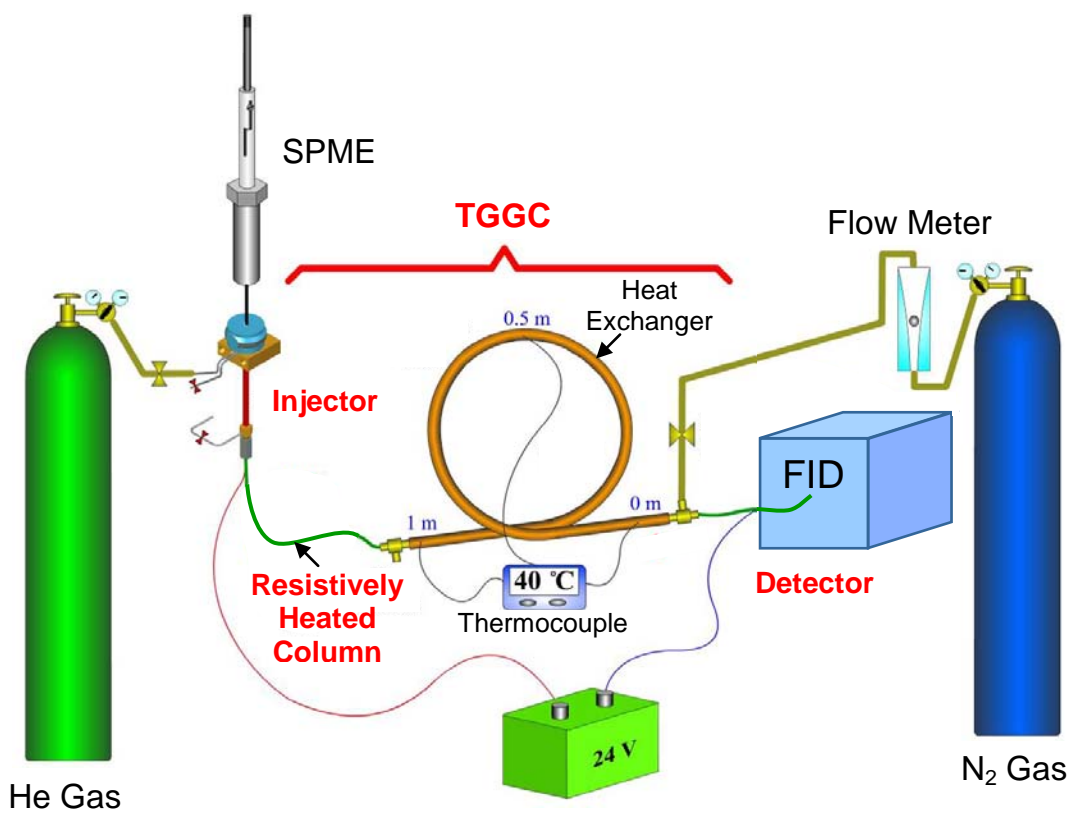


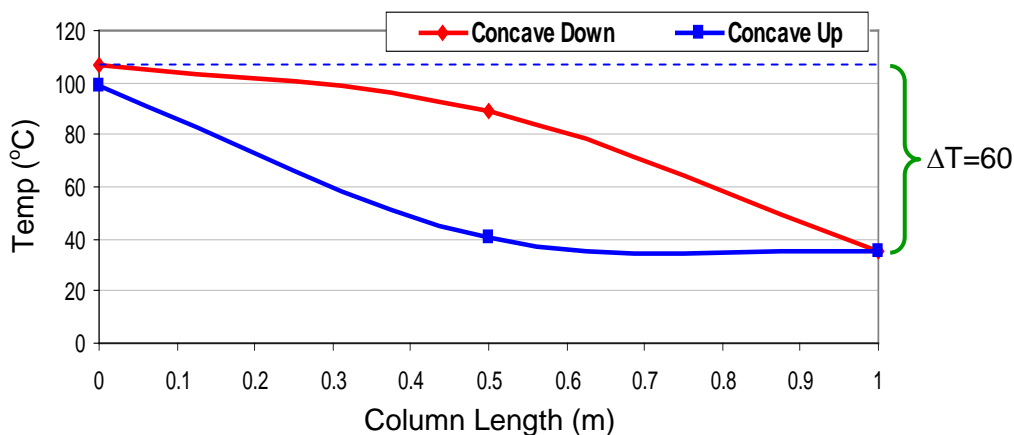
Figure 4-4. TGCC system for generating concave down axial temperature gradient profiles.

## 4.3 RESULTS AND DISCUSSION

### 4.3.1 Generation of Axial Temperature Gradients

Testing of the heat exchanger system was performed by generating concave down and concave up temperature gradient profiles, following the flow configurations of Figure

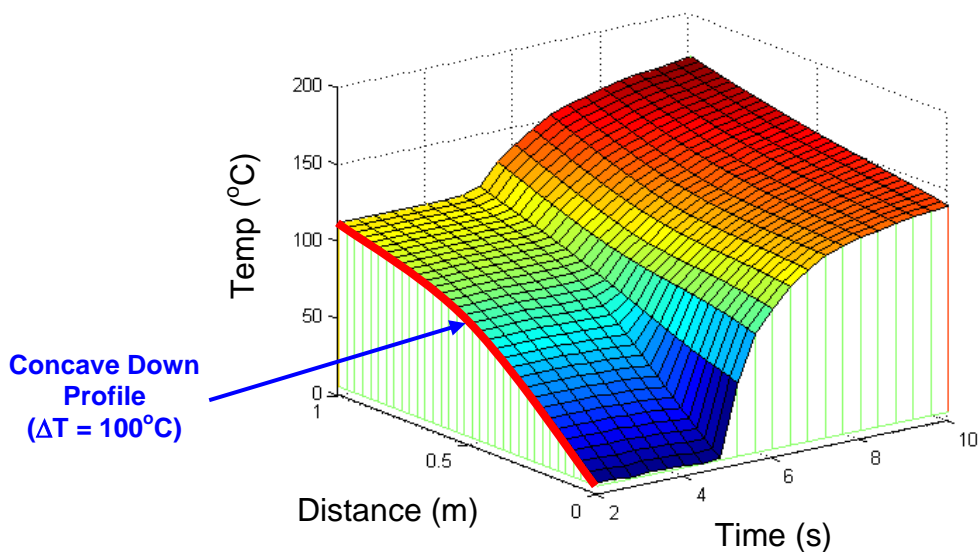
4-2. The capability of the system for creating axial temperature gradients along a 1 m column was confirmed with the gradients shown in Figure 4-5. A concave down profile was achieved using room temperature nitrogen gas in combination with resistive heating of the Ni sleeve, while the concave up gradient was formed using preheated nitrogen gas that cooled as it traveled along the heat exchanger (Figure 4-5).



**Figure 4-5. Example of axial temperature gradient profiles generated with the TGGC heat exchanger system. Concave down profile: 8 L/min room temperature nitrogen while 2.5 V was applied to the Ni sleeve. Concave up profile: 8 L/min preheated nitrogen gas with no resistive heating of the Ni sleeve.**

Another way of representing the axial temperature gradients in TGGC was suggested by Rubey,<sup>1</sup> in which three-dimensional plots called thermal fields are used to represent the simultaneous changes of temperature with respect to both time and position. An example of a thermal-field generated with the previously described TGGC system is shown in Figure 4-6. In this figure, it can be seen how the temperature changes along the column length, forming a concave down profile, and how the profile changes in time as it is heated. Figure 4-6 also shows that analytes traveling inside the column will always encounter a negative temperature gradient, even during the heating stage, a characteristic

of this technique that aids in reducing band broadening of the peaks as they migrate through the column. The axial temperature gradients of Figures 4-5 and 4-6 validate the heat exchanger arrangement for producing a suitable thermal gradient environment for TGGC separations.



**Figure 4-6. Thermal field showing heating of a concave down axial temperature gradient. Cold nitrogen at a flow of 10 L/min in combination with 4 V potential applied to the Ni sleeve. Heating at 2300°C/min was achieved by turning off the nitrogen flow and increasing the voltage to 12 V.**

### 4.3.2 Peak Sweeping

With a negative axial temperature gradient, as chromatographic peaks move in the direction toward lower temperatures along the column, they not only focus, but they also slow down as they become more retained. Eventually, there is a need to release the peaks to the detector. Releasing the peaks can be achieved by moving the gradient towards the detector (non-stationary or moving gradient),<sup>4, 18</sup> increasing the gradient temperature

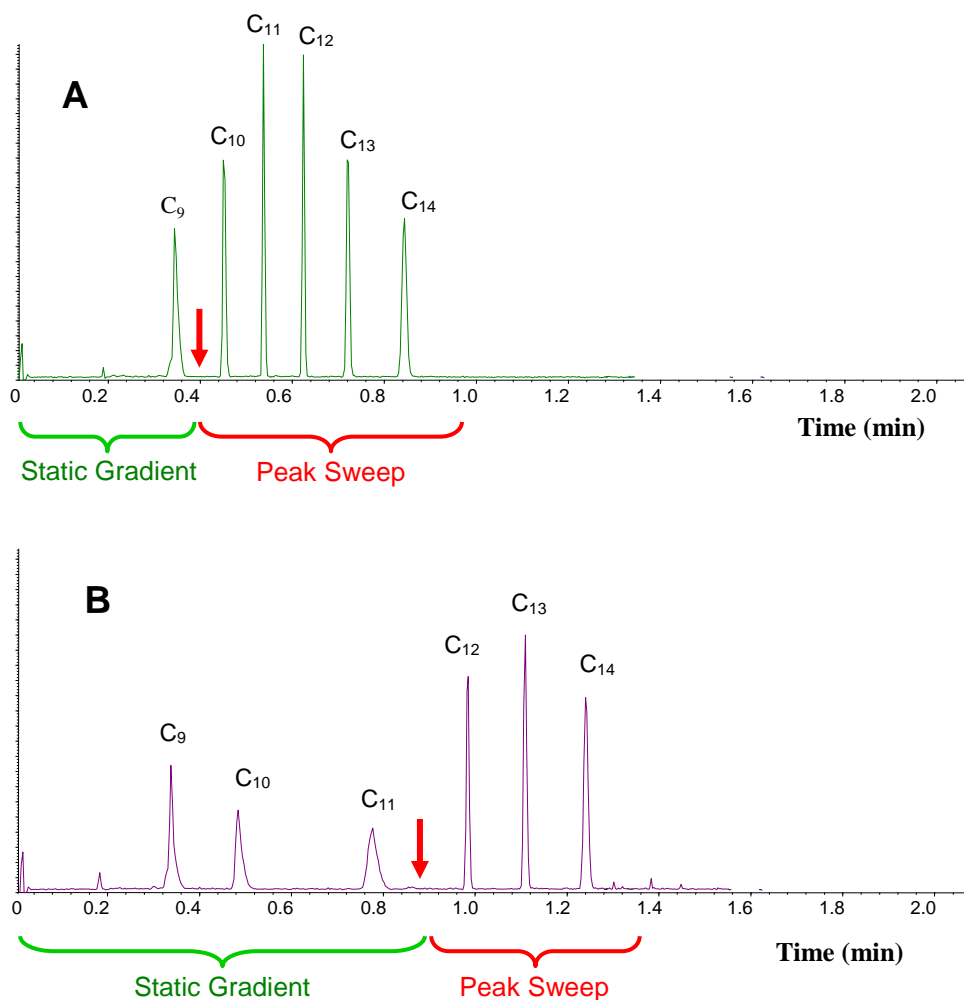
(gradient temperature programming),<sup>2, 7-8, 19</sup> or by raising the cold side temperature of the gradient (which we call sweeping).<sup>1, 12, 20-21</sup> All of these operations are special cases of the TGGC technique. Using the TGGC instrument (Figure 4-4), releasing of peaks can be performed using the sweeping or gradient temperature programming operation. For the concave down profile, sweeping was achieved by simultaneously stopping the flow of nitrogen and increasing the voltage of the resistively heated Ni sleeve (Figure 4-6).

The sweeping operation was demonstrated with the concave down gradient and an n-alkane sample (n-C<sub>9</sub> to n-C<sub>14</sub>). Figure 4-7A shows a typical TGGC separation, which involves introducing a sample into a column with a decreasing temperature gradient, waiting for a short time until the sample separates along the gradient, and then releasing the peaks. In Figure 4-7, the point of release is indicated by arrows, which indicates the moment when the gradient temperature was rapidly increased (heating rate of 130°C/min) and the focused peaks were released. The more volatile analytes may also elute in a negative gradient (static gradient separation), however, slow elution produces wide peaks since the detector signal is recorded as a function of time, as seen in Figure 4-7B. Furthermore, the peak signals decrease as a result of the small amount of analytes moving to the detector. For this reason, it is important to rapidly release the peaks into the detector to take advantage of the focusing effect that is attained in the column.

A static gradient can be applied in combination with sweeping to improve the separation of the less retained analytes in the gradient. Static gradient separations resemble isothermal operation in which compounds elute at a constant temperature, and later eluting peaks broaden and spread exponentially in time, as seen in Figure 4-7B. The focusing effect of the gradient can be clearly seen in Figure 4-7; all peaks released (past

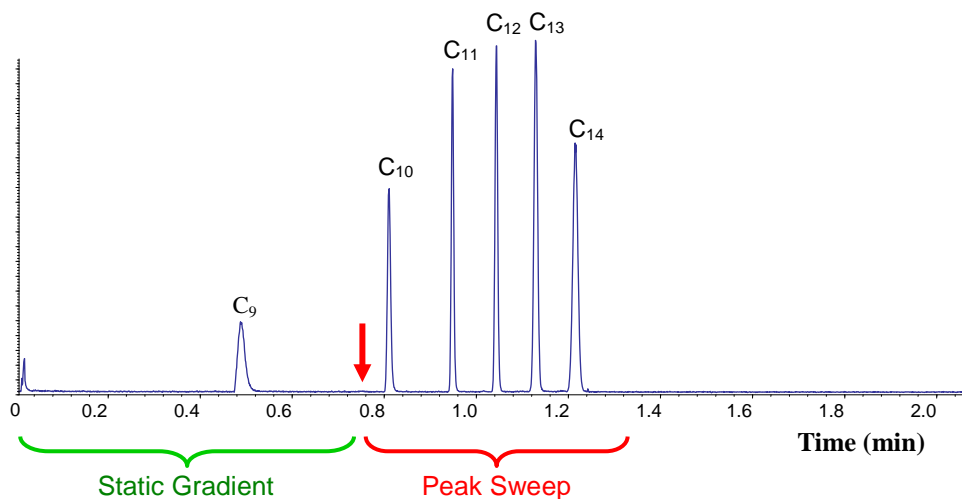
the arrow) were narrow, without any noticeable broadening with elution time as typically observed in isothermal separations (Figure 4-7B). In addition, this figure shows how the detection limit improves by increasing the signal-to-noise ratios of the peaks due to the focusing effect.

Figure 4-8 shows the separation of n-alkanes using the concave up profile in



**Figure 4-7. TGGC separations of n-alkanes using a concave down profile and sweeping operation at different different times (A and B) (arrows represent the times when the column was heated at 130°C/min to release the analytes). The gradient profile used is shown in Figure 4-5. The mobile phase flow rate was 0.35 mL/min.**

Figure 4-5. Sweeping using the concave up temperature profile was achieved by resistively heating the column without stopping the flow of hot nitrogen gas. Narrow peaks were obtained with the concave up profile following the release of the analytes (Figure 4-8). However, with the concave up profile, the elution times of the alkanes differed from those obtained with the concave down profile (Figure 4-7A). The first difference observed was that the overall elution of the compounds in the concave up profile occurred later. This is a result of the lower temperatures associated with the concave up profile (Figure 4-5), which increased the retention times. Furthermore, in Figure 4-8, it can be seen that the later eluting peaks ( $C_{13}$  and  $C_{14}$ ) elute closer to each other as compared with the more separated analytes observed in Figure 4-7A. This characteristic is a direct result of the temperature gradient profile. In the concave down gradient, the early eluting compounds experience a temperature gradient with a higher slope than the later compounds, thus bringing the first peaks closer together (Figure 4-



**Figure 4-8. TGGC separation of n-alkanes using a concave up profile and sweeping operation (arrow represents the time when the column was heated to release the analytes at a heating rate of  $130^{\circ}\text{C}/\text{min}$ ). The temperature profile used is shown in Figure 4-5. The mobile phase flow rate was  $0.35\text{ mL}/\text{min}$ .**



7A). In the concave up profile, the steepest part of the temperature gradient where compounds elute close together, is at the injector side of the gradient where later eluting compounds focus. The concave down profile provides better separation of mixtures with a higher fraction of heavier compounds, while the concave up profile is more suitable for separating mixtures with a higher fraction of volatile compounds.

#### **4.4 EXPERIMENTAL COMPARISON OF THE DIFFERENT GC SEPARATION MODES**

The TGGC system not only can generate negative axial temperature gradients, but it can also perform isothermal and programmed temperature separations. For this reason, the TGGC system was used to compare the separation capabilities of the different separation modes, while employing the same GC column and system arrangement. Comparison of the different GC separation modes was performed by adjusting the operating conditions of each mode for the analytes to be separated in the same time period (Figure 4-9). The sample used was a mixture (100 ppm each in methanol) of normal alkanes (n-C<sub>9</sub> to n-C<sub>13</sub>). Isothermal GC separation was achieved by keeping the entire column at a constant temperature of 165°C, while GC temperature programming was performed by increasing the temperature of the entire column from 80°C to 200°C at a rate of 25°C/s (1500°C/min) without an initial hold time. The thermal gradient GC separation was performed with a concave down gradient from 80°C to -20°C, followed by sweeping after 2.4 s of injection to 200°C at 58°C/s (3500°C/min). The negative temperature gradient was generated with a 13 L/min flow of cold nitrogen gas with simultaneous heating of the column by applying 3 V to the resistively heated Ni Sleeve. The total analysis time for the alkane sample was performed in less than 7 s, with peak

widths as narrow as 100 ms. A constant 22 psig column head pressure was employed. Resolution and peak capacity (maximum number of resolved peaks per time)<sup>22-24</sup> were used to compare the different separation modes. Three separations for each operational mode were performed to determine the separation reproducibility (Table 4-1). The relative standard deviation obtained for peak areas was below 5%, indicating reproducible sample collection and introduction. The retention time reproducibility for all separation modes was also low, with a standard deviation of less than 3.5% (Table 4-1).

**Table 4-1. Relative standard deviations obtained from three separations performed for each GC operation mode.**

Analytes	ITGC % RSD		TPGC % RSD		TGGC % RSD	
	Retention Time	Peak Area	Retention Time	Peak Area	Retention Time	Peak Area
C <sub>9</sub>	-	-	2.53	2.36	2.32	4.95
C <sub>10</sub>	3.00	3.39	3.09	1.21	2.62	3.38
C <sub>11</sub>	2.55	4.55	3.48	0.90	2.24	2.35
C <sub>12</sub>	1.57	5.03	2.22	1.87	1.93	3.13
C <sub>13</sub>	1.53	3.22	2.53	3.21	1.64	5.06

Figure 4-9 shows a comparison of n-alkane chromatograms obtained using the TGGC system in the different GC operational modes. The separation window was defined as the time between the n-C<sub>9</sub> and n-C<sub>13</sub> peaks for the TGGC separation (segmented lines in Figure 4-9). From this figure, the ITGC separation clearly shows the general elution problem (GEP), where the first peaks are narrow and cluster together, while the later eluting compounds are broader and further apart. An improved separation of the n-alkane mixture was obtained with TPGC, as expected, since it is well known that TPGC is a solution to the GEP. TGGC also provided a good solution for the GEP, as seen in Figure 4-9.<sup>1,5</sup> From Figure 4-9, it is clear that TPGC and TGGC separations similarly resolves the GEP observed in ITGC. However, it is more difficult to compare TPGC and

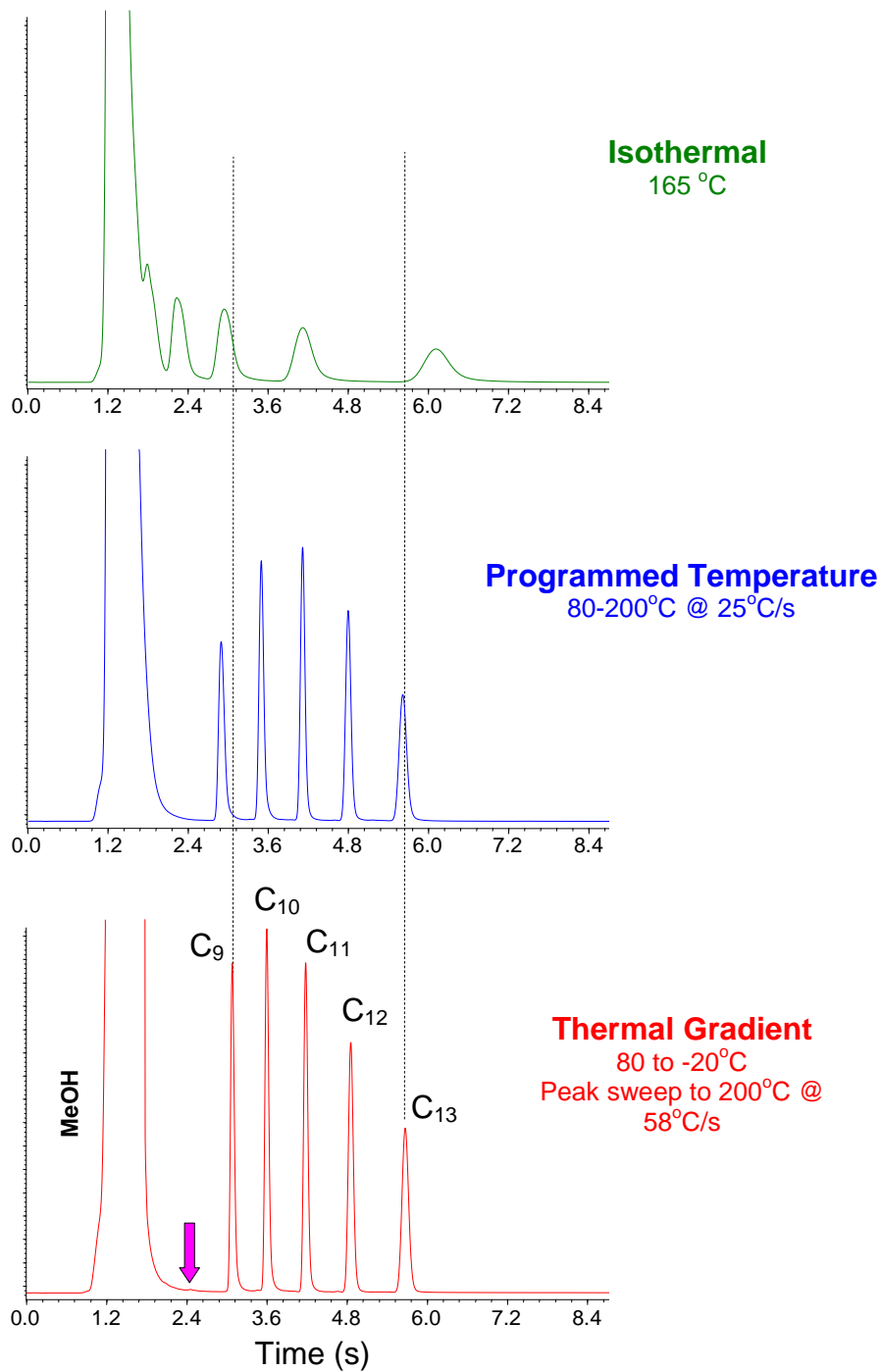
TGGC. The average peak capacities as listed in Table 4-2 for ITGC, TPGC and TGGC separations were 7.61, 17.56 and 20.60, respectively. These results show that TGGC provided 17% higher peak capacity compared to TPGC. A higher peak capacity was obtained even though the TGGC separation was performed in a 2% smaller separation window than the TPGC separation. This result demonstrates the potential that negative temperature gradients can produce on separations.

A graphical comparison of the resolution of the alkanes for all separations performed is shown in Figure 4-10. In this figure, it can be observed that the ITGC resolution increases with later eluting peaks, a typical behavior for ITGC separations. However, the resolution trends for the TPGC and TGGC separations were very similar, with the exception of the first peaks in the TGGC method, which showed better resolution. Narrower and higher signal-to-noise peaks were obtained in the TGGC separation (Figure 4-9). The narrow peaks are a result of the focusing effect of the gradient. However, one can argue that the TGGC method generally used lower temperatures than the TPGC separation, which aided in obtaining narrow peaks. A lower starting temperature for the TPGC method and a faster heating rate could be used. However, it is known that high heating rates in TPGC decreases the overall peak capacity of the system due to inefficient utilization of the down-stream portion of the column as the retention of the analytes becomes very small.<sup>25</sup> The goal was to use the lowest heating rate for TPGC that provides separation in the same amount of time. These constraints reflect the problem encountered when establishing temperature limits for comparing TPGC and TGGC for fast separations. The separations in Figure 4-9 represent operating

parameters for each separation mode that allowed the separation of the n-alkane mixture in the same time period.

The modest increase in peak capacity obtained with the TGGC method suggests that this technique can provide slightly better separation than TPGC. However, taking into account experimental error, one can conclude that the TGGC method can provide separations comparable to TPGC.

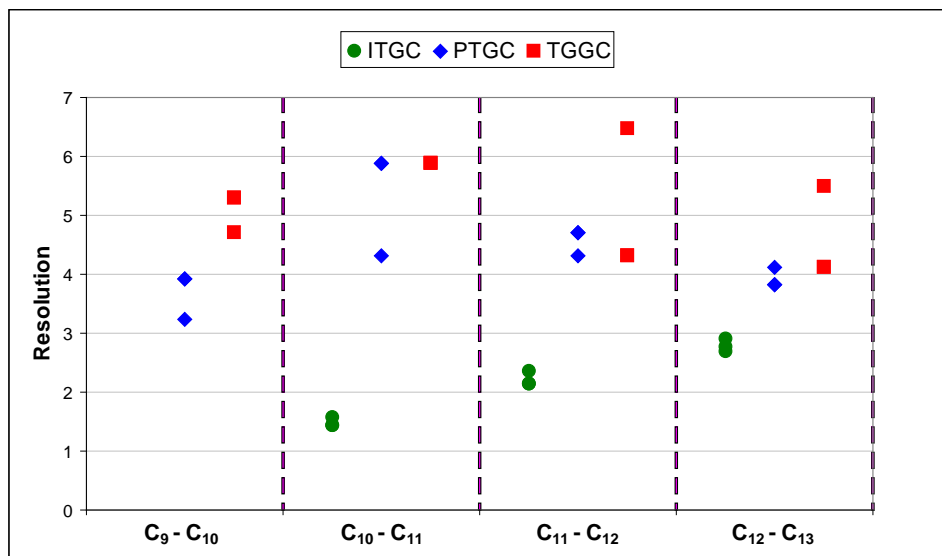
A standard mixture of EPA Method 624 volatile halocarbon compounds was used as well to compare separations from the TPGC and TGGC methods. The EPA 624 standard was diluted to 20 ppm in water, and SPME sampling was performed. The TGGC separations were performed using a concave up gradient profile from 80 to 35°C. The negative temperature gradient was generated with 13 L/min flow of hot nitrogen gas without resistively heating the column. Heating was performed after 14.5 s at a heating rate of 116°C/min. The 26 compounds were not completely resolved using the 1-m TGGC column (Figure 4-11); therefore, an MSD was used to aid in peak identification. As previously discussed, the parameters of the TPGC and TGGC separation modes can be adjusted to achieve separations in the same period of time. An example of this is shown in Figure 4-11 for a complex mixture, where two different TPGC separations and a TGGC separation are compared. Figure 4-11A shows a TPGC separation of the EPA Method 624 mixture for which the column was initially at 35°C (0 s hold) and ramped to 200°C (0 s hold) at a heating rate of 38°C/min. This TPGC separation shows low resolution for the most volatile compounds, and good separation for the later eluting ones. Figure 4-11B, on the other hand, shows a TGGC separation of the sample using a concave up profile, showing an overall improvement compared to the TPGC separation



**Figure 4-9.** GC analysis of normal alkanes using different separation modes. The arrow indicates when the temperature gradient was increased (sweeping).

**Table 4-2. Peak capacities obtained from n-alkane separations using different GC operation modes.**

	ITGC	TPGC	TGGC
Separation 1	7.65	18.34	19.62
Separation 2	7.74	15.99	19.03
Separation 3	7.45	18.34	23.15
<b>Average</b>	7.61	17.56	20.60



**Figure 4-10. Resolution comparison of the different separation modes.**

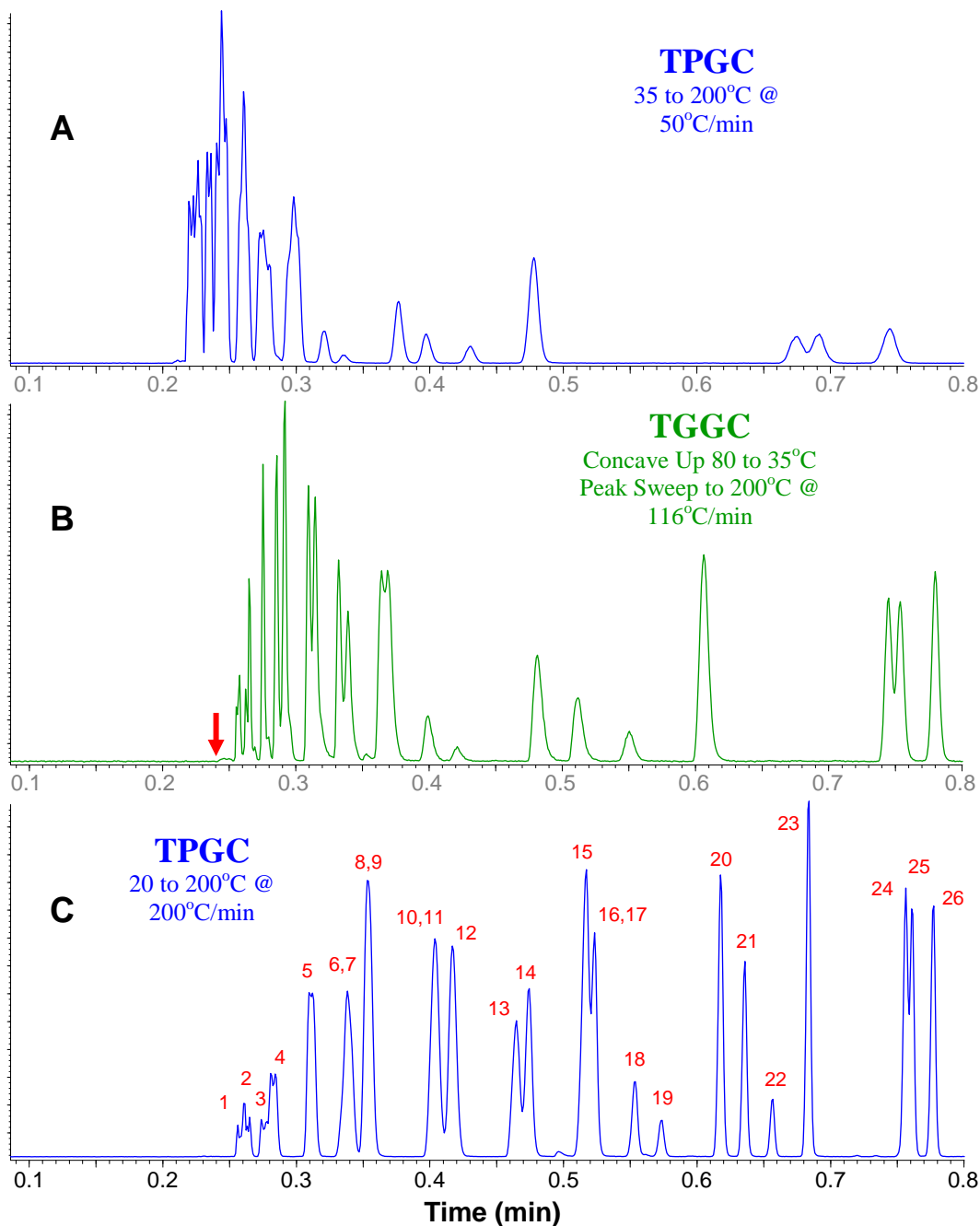
(Figure 4-11A). Even though the initial temperature of the TPGC method (Figure 4-11A) and the lower temperature of the TGGC profile were the same, better separation of the volatile compounds was achieved with the concave up negative gradient. This improvement comes as a result of the focusing effect of the gradient and the longer times that analytes spend at colder temperatures, interacting more with the stationary phase. The narrower late eluting peaks are also due to the focusing effect of the gradient, as well as to the higher elution temperatures. However, better separation in the same period of time was achieved (Figure 4-11C) when the TPGC separation was performed with an

initial temperature of 20°C (0 s hold) and temperature program to 200°C (0 s hold) at a heating rate of 200°C/min. Even distribution of the analytes and improvement in separation of compounds can be observed. However, for the later eluting compounds, the resolutions achieved with TGGC and TPGC were equivalent. In any case, comparison of TPGC and TGGC methods is difficult since a variety of conditions can be used to achieve the same separation window. Although the TPGC separation (Figure 4-11C) produced the overall best resolution, the use of a gradient that extends to lower temperatures could likely improve the TGGC separation. Unfortunately, a concave up gradient with lower temperatures was difficult to generate with the TGGC system.

These experiments demonstrate the difficulty in comparing TPGC and TGGC methods. The results show that, in general, separations obtained with the peak sweep TGGC method are comparable to those from TPGC.

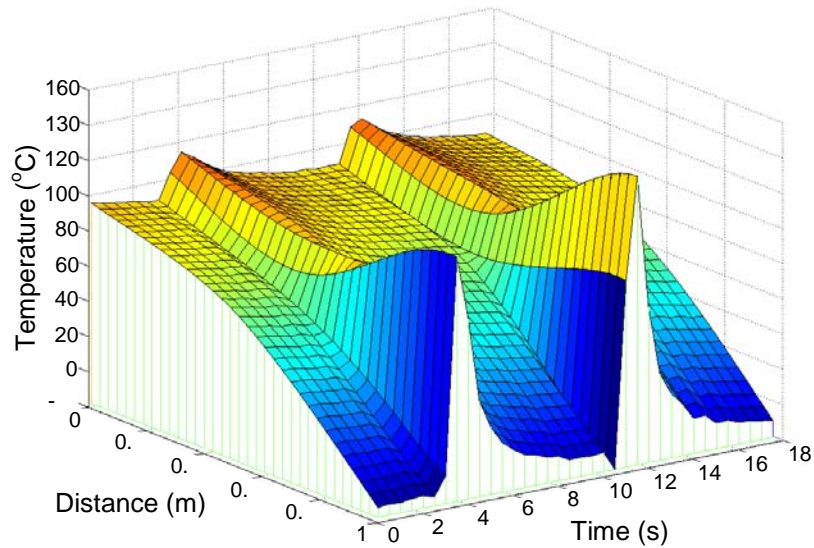
## **4.5 PEAK GATING**

A new separation strategy was developed as a result of the low thermal mass of the TGGC design that allowed heating and cooling rates as high as 4000 °C/min (67 °C/s) and 3500 °C/min (58 °C/s), respectively. The fast heating rates were achieved by simultaneously increasing the voltage of the resistively heated Ni sleeve and by flowing preheated nitrogen gas through the heat exchanger (detector end). Fast heating and cooling rates, are achievable, not only because of the low thermal mass of the system, but also because only one portion of the column needs to be heated and cooled. A thermal field with these fast heating and cooling rates can be seen in Figure 4-12. The elevated temperatures at the end of the gradient (1 m point) in the thermal field are due to the high temperatures of the gas being introduced into the heat exchanger.



**Figure 4-11.** GC analyses of a 26 component EPA Method 624 volatile halocarbon mixture using different separation modes. The red arrow indicates when the gradient was heated in **B**. Peak identifications: (1) 1,1-dichloroethane, (2) methylene chloride, (3) *trans*-1,2-dichloroethene, (4) 1,1-dichloroethane, (5) chloroform, (6) 1,2-dichloroethane, (7) 1,1,1-trichloroethene, (8) benzene, (9) carbon tetrachloride, (10) 1,2-dichloropropane, (11) trichloroethylene, (12) bromodichloromethane, (13) 2-chloroethylvinyl ether, (14) *cis*-1,3-dichloropropene, (15) *trans*-1,3-dichloropropene, (16) toluene, (17) 1,1,2-trichloroethene, (18) dibromochloromethane, (19) tetrachloroethene, (20) chlorobenzene, (21) ethyl benzene, (22) bromoform, (23) 1,1,2,2-tetrachloroethane, (24) 1,3-dichlorobenzene, (25) 1,4-dichlorobenzene, (26) 1,2-dichlorobenzene.





**Figure 4-12. Concave down thermal field for a typical peak gating operation, where heating and cooling rates as high as 4000 and 3500°C/min, respectively, can be achieved.**

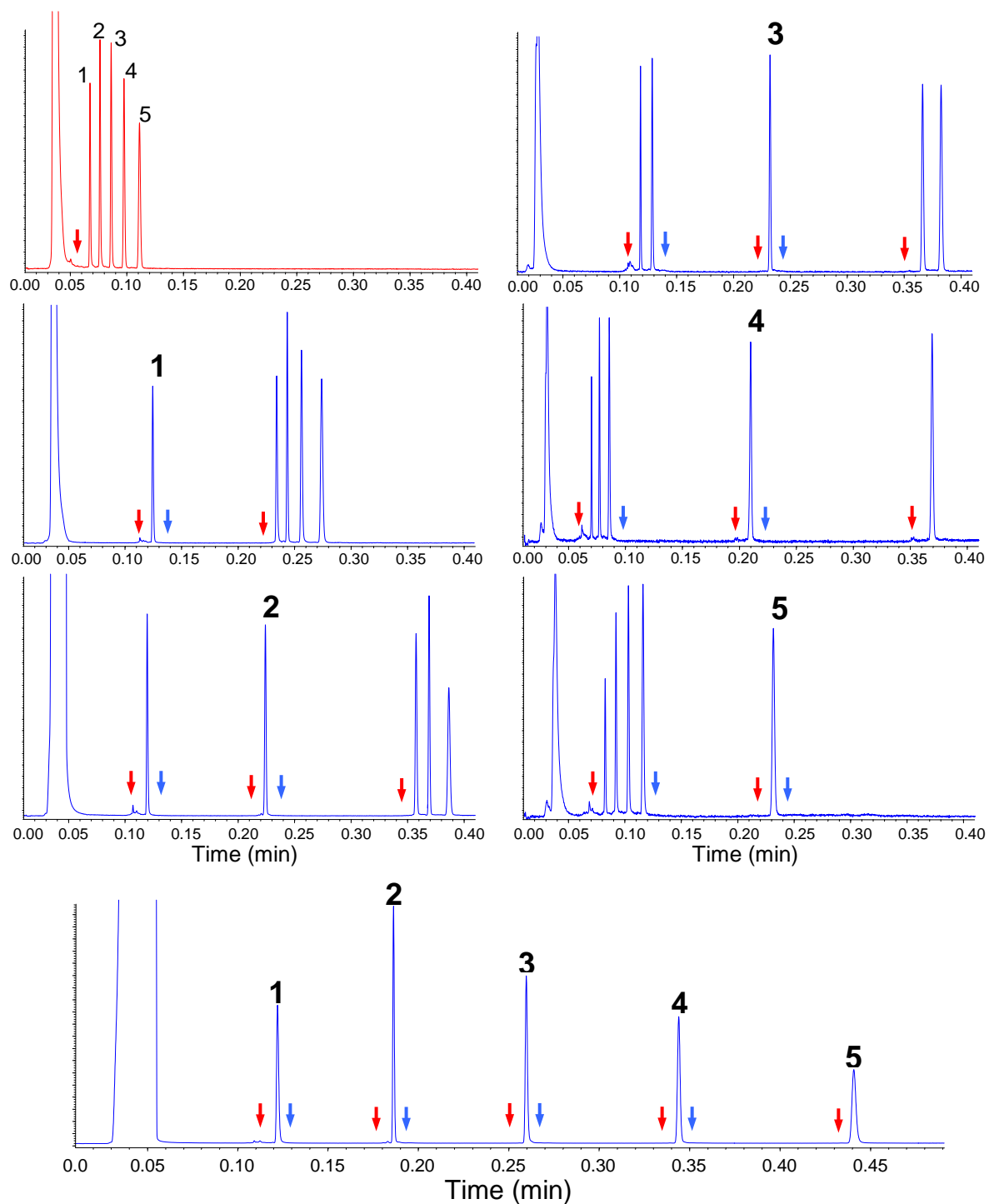
The TGGC design permitted the selective elution of an analyte or a group of analytes in a mixture without sacrificing resolution. We have called this method “peak gating”, where one peak is allowed to elute while the remaining peaks inside the column are retained. Examples of peak gating can be seen in Figure 4-13. A concave down gradient was used in these separations by using 13 L/min of cold nitrogen gas simultaneously with heating by applying 3 V to the Ni sleeve (Figure 4-12). The compounds are initially separated and “parked” in the column due to the axial temperature gradient. Peaks can be released one at a time by rapidly raising the column temperature followed by re-establishing the gradient (Figure 4-12). The negative gradient aids by keeping the peaks focused inside the column, reducing any band broadening due to diffusion while each isolated peak is being eluted. Figure 4-13 clearly shows how selective isolation of one peak from the others can be achieved with the gating operation. This process is of great interest for target analysis, where peaks of interest can be

individually isolated, facilitating their analysis. Peak gating can also be used as in heart cutting<sup>26</sup> and flow modulation,<sup>27</sup> in which a region of a chromatogram is transferred into another column for further separation using a different stationary phase. Peak gating offers the ability to select as many heart cuts as desired, by stopping the separation in the first column at any time without degrading the separation. Parking of the peaks inside the column is dependent on the analytes and the gradient temperatures used. Current methods cannot stop the ongoing separation without degrading the separation.

Timing is an important factor in gating, since multiple peaks of a single compound may be generated if the fast cooling divides a chromatographic band. Gating has the potential to be used as a multidimensional modulator to transfer focused sections from the first column into the second column. Although gating was tested with a short column, applications with longer columns should not be disregarded. In GC×GC, stopping the entire first dimension using the gating method would allow thorough analysis in the second dimension by using longer columns and TPGC or TGGC. Furthermore, the fast heating and cooling rates achieved with the TGGC system make it ideal as a separation method in the second dimension of a GC×GC system,<sup>12</sup> where current separations are performed isothermally.<sup>28</sup>

#### **4.6 APPLICATION OF TGGC TO A COMPLEX SAMPLE**

The standard EPA Method 624 volatile halocarbon mixture was used to test the different peak releasing operations of TGGC (*i.e.*, static gradient and gating) for the separation of a complex sample. TGGC separations were performed using a concave up gradient profile from 80 to 35°C. Figure 4-14 shows chromatograms of a peak sweep separation (Figure 4-14B) and two separations (Figure 4-14A and C) obtained using static



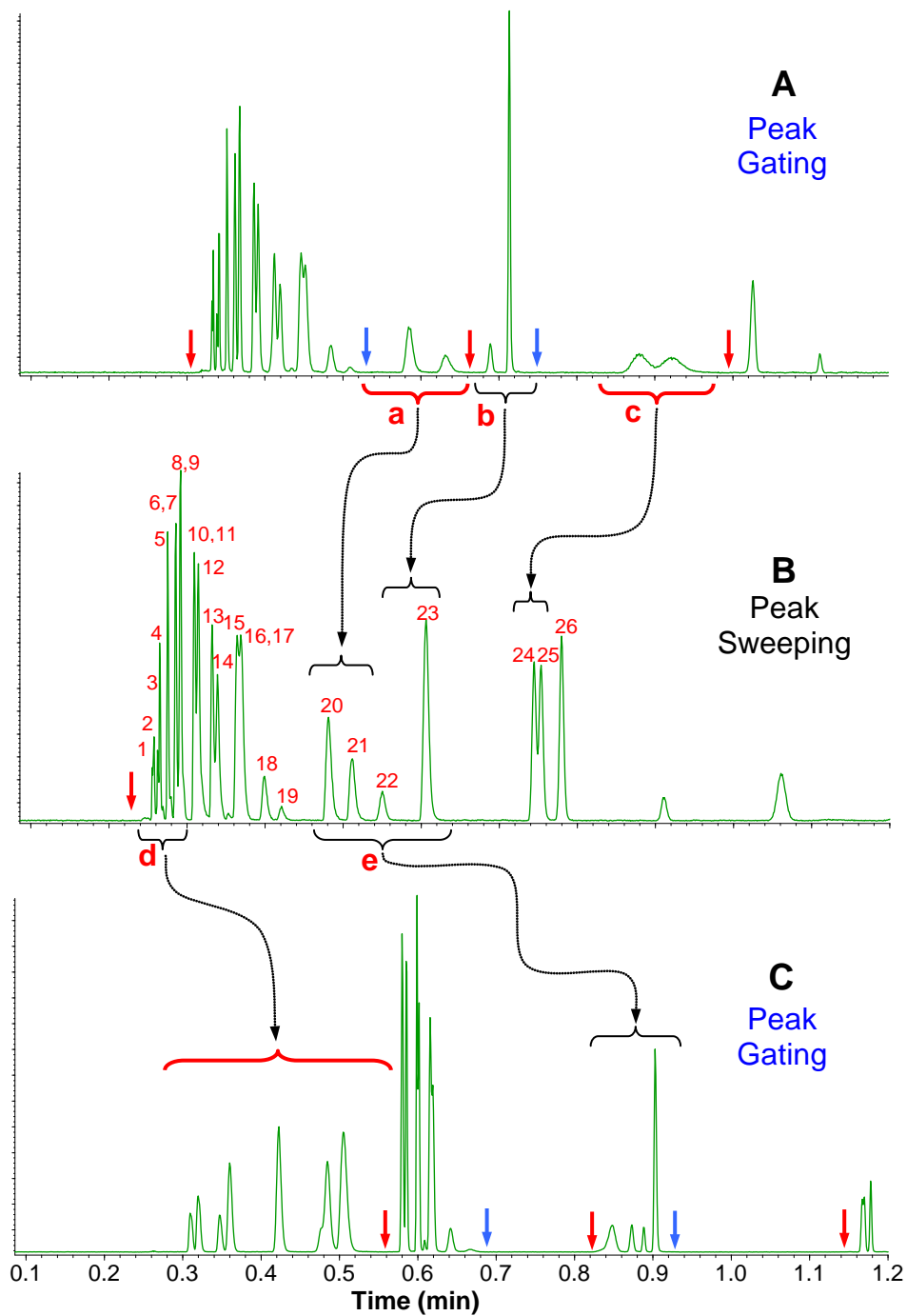
**Figure 4-13. Application of TGGC gating to selectively separate the n-alkanes. Red and blue arrows indicate when the gradient was heated and cooled, respectively. Peak identifications: (1) n-C<sub>9</sub>, (2) n-C<sub>10</sub>, (3) n-C<sub>11</sub>, (4) n-C<sub>12</sub>, and (5) n-C<sub>13</sub>.**

gradient and gating operations to further analyze individual regions of the chromatogram. The red and blue arrows in the chromatograms represent the times when the gradient was heated or cooled, respectively. Figure 4-14B shows a rapid TGGC separation of the complex sample. The 26 analytes were not completely resolved; thus, GC-MS was necessary for identification of the peaks.

A more detailed analysis of the mixture could be performed using various peak releasing operations. As can be seen in Figure 4-14A and C, improvements in the separation of peaks in regions (a), (c) and (d) were over 100%, 30% and 30%, respectively. This improvement was a result of using a static gradient and allowing the compounds to elute from the constant gradient, providing isothermal-like separation. For region (b), gating of the peaks allowed selective refocusing and, hence, an increase in signal-to-noise as observed in Figure 4-14A, where peak 23 became the tallest in the chromatogram. Gating was also used with the complex sample to show its ability to isolate a group of peaks, as seen in region (e) (Figure 4-14C). The separation of the compounds from the rest of the chromatogram can facilitate automated qualitative and quantitative analysis. These separations show how the TGGC technique in combination with different peak releasing methods can be used to selectively improve the separation, detection limit, and target analysis of a complex sample.

## **4.7 CONCLUSIONS**

The results in this chapter show that the developed TGGC system can successfully produce axial temperature gradients along a 1 m column. Concave down and up gradient profiles can be generated. A direct comparison between ITGC, TPGC and TGGC separations was performed. The TPGC and TGGC modes proved to be a solution



**Figure 4-14.** Application of different TGGC operations for separation of a 26 component EPA Method 624 volatile halocarbon mixture. The red and blue arrows indicate when the gradient was heated and cooled at a heating rate of 4000 and 3500°C/min, respectively. The red brackets indicate static gradient separation of the analytes. For peak identifications, see Figure 4-11.

to the general elution problem commonly observed in ITGC separations of compound mixtures with a wide range of volatilities. However, the comparison between TPGC and TGGC proved to be difficult, since a wide range of temperature conditions can be applied in each method so that the analysis can be performed in the same time window. The overall results of the comparison show that, in general, the TGGC method can provide equivalent separations to TPGC. However, TGGC offers unique possibilities to improve the separation of compounds. The low thermal mass of the TGGC system allowed fast heating and cooling of the column to as high as 4000 and 3500°C/min, respectively. This characteristic permitted the development of a new TGGC separation strategy, *i.e.*, gating, that allows the selective separation of compounds in a complex mixture with minimum effect on the resolution of the remaining compounds inside the column.

The TGGC technique in combination with different peak releasing methods (static gradient, peak sweeping and gating) proved to improve the separation, detection limit, and target analysis of selective chromatographic regions in a complex sample. Fast turnaround times and separation equivalence to TPGC makes TGGC an attractive alternative method for the second dimension separation in GC×GC analysis, in which short isothermal columns are used. Implementation GC×TGGC should greatly enhance the peak capacity of the GC×GC technique by performing fast TGGC separations in the second dimension. Preliminary work with a different TGGC instrument has been reported,<sup>12</sup> showing promising results. However, further work should be performed to improve the TGGC sweeping system to provide more control over the gradient temperature profile and to take advantage of the separation potential that the TGGC technique can offer.

## 4.8 REFERENCES

1. Rubey, W. A., A Different Operational Mode for Addressing the General Elution Problem in Rapid Analysis Gas Chromatography. *J. High Resol. Chromatogr.* **1991**, *14*, 542-548.
2. Phillips, J. B.; Jain, V., On-Column Temperature Programming in Gas Chromatography Using Temperature Gradients Along the Capillary Column. *J. Chromatogr. Sci.* **1995**, *33*, 543-550.
3. Zhukhovitskii, A. A., *et al.*, New Method of Chromatographic Analysis. *Doklady Akademii Nauk SSSR* **1951**, *77*, 435-8.
4. Tudge, A. P., Studies in Chromatographic Transport III. Chromathermography. *Can. J. Phy.* **1961**.
5. Ohline, R. W.; DeFord, D. D., Chromathermography, the Application of Moving Thermal Gradients to Gas Liquid Partition Chromatography. *Anal. Chem.* **1963**, *35* (2), 227-234.
6. Nerheim, A. G., Gas-Liquid Chromathermography. *Anal. Chem.* **1960**, *32*.
7. Vergnaud, J. M., Gas Phase Chromatography: The Application of Gas Flow Variation and Backflushing. *J. Chromatogr. A.* **1965**, *19*, 495-503.
8. Fenimore, D. C., Gradient Temperature Programming of Short Capillary Columns. *J. Chromatogr.* **1975**, *112*, 219-227.
9. Kaiser, R., Temperature Gradient Chromatography. *Chromatographia* **1968**, *1*, 199-207.
10. Berezkin, V. G., *et al.*, Temperature Gradients in Gas Chromatography. *J. Chromatogr.* **1986**, *373*, 21-44.
11. Zhao, H., *et al.*, Characteristics of TGPGC on short micro packed capillary column. *Anal. Sci.* **2002**, *18* (1), 93-95.
12. Contreras, J. A. Design and Application of Thermal Gradient Programming Techniques for Use in Multidimensional Gas Chromatography-Mass Spectrometry (MDGC-MS) University of Dayton, Dayton, 2004.
13. Blumberg, L. M., Focusing Cannot Enhance Resolution or Speed Limit of a GC Column. *J. Chromatogr. Sci.* **1997**, *35* (9), 451-454.
14. Rubey, W., Operational Theory and Instrumental Implementation of the Thermal Gradient Programmed Gas Chromatography (TGPGC) Mode Analysis. *J. High Resol. Chromatogr.* **1992**, *15*, 795-799.
15. Jain, V.; Phillips, J. B., High-Speed Gas Chromatography Using Simultaneous Temperature Gradient in Both Time and Distance along Narrow-Bore Capillary Columns. *J. Chromatogr. Sci.* **1995**, *33*, 601-605.
16. Blumberg, L. M., Outline of a Theory of Focusing in Linear Chromatography. *Anal. Chem.* **1992**, *64*, 2459-2460.
17. Blumberg, L. M., Limits of Resolution and Speed of Analysis in Linear Chromatography With And Without Focusing. *Chromatographia* **1994**, *39* (11-12), 719-728.
18. Zhukhovitskii, A. A., Some Developments in Gas Chromatography in the U.S.S.R. In *Gas Chromatography 1960*, Scott, R. P. W., Ed. Butterworths: Edinburgh, 1960; pp 293-300.

19. Bellabes, R., *et al.*, Gas Chromatography with Backflushing: Isothermal during the First Step, Programming of Longitudinal Temperature Gradient during the Second Step. *Sep. Sci. Technol.* **1982**, 17 (9), 1177-1182.
20. Rubey, W. A. Gas Chromatography Methods and Apparatus US Patent 5028243, 1991.
21. Rubey, W. A., Theory of Constrained Migration Behavior in Open-Tubular Gas Chromatography Columns with Various Operational Modes. In *23<sup>rd</sup> International Symposium on Capillary Chromatography*, Riva del Garda, Italy 2000.
22. Giddings, J. C., *Anal. Chem.* **1984**, 56, 1258A.
23. Bertsch, W., Two-Dimensional Gas Chromatography. Concepts, Instrumentation, and Applications – Part 1: Fundamentals, Conventional Two-Dimensional Gas Chromatography, Selected Applications *J. High Resol. Chromatogr.* **1999**, 22, 647-665.
24. Giddings, J. C., *Unified Separation Science*. Wiley Interscience New York, 1991.
25. Grall, A., *et al.*, Peak Capacity, Peak-Capacity Production Rate, and Boiling Point Resolution for Temperature-Programmed GC with Very High Programming Rates. *Anal. Chem.* **2000**, 72, 591-598.
26. Deans, D. R., A New Technique for Heart Cutting in Gas Chromatography. *Chromatographia* **1968**, 1 (1-2), 18-22.
27. Examining Comprehensive Flow-Modulated Two-Dimensional Gas Chromatography. [www.agilent.com](http://www.agilent.com).
28. Marriott, P.; Shellie, R., Principles and Applications of Comprehensive Two-Dimensional Gas Chromatography. *TrAC Trends in Analytical Chemistry* **2002**, 21 (9-10), 573-583.

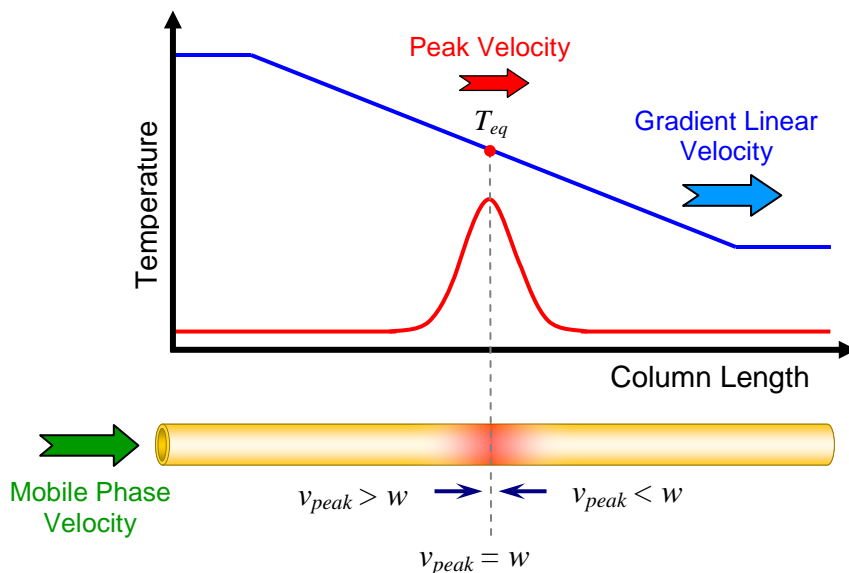


## 5 MOVING THERMAL GRADIENT GAS CHROMATOGRAPHY

### 5.1 INTRODUCTION

In thermal gradient gas chromatography (TGGC) the column temperature changes simultaneously in time and position. Typical separations are performed in a decreasing column temperature from the injector to the detector.<sup>1-2</sup> As the analytes move along the column into lower temperatures, their retention increases, slowing them down. For this reason, the trapped analytes must be released from the column into the detector. This is achieved by either moving the gradient towards the detector (non-stationary or moving gradient),<sup>3-4</sup> increasing the gradient temperature (gradient temperature programming),<sup>1, 5-7</sup> or eliminating the gradient by raising the whole column length to a high temperature (sweeping).<sup>2, 8-10</sup> In this chapter, a novel approach for generating a moving axial temperature gradient is discussed, and a unique axial temperature gradient operating method is introduced. The new TGGC method is based on a moving sawtooth temperature gradient profile that allows for continuous sampling and separation.

In a moving temperature gradient, analytes that are separated along the gradient are swept along the column at the speed of the gradient. The analytes reach their steady states along the moving temperature gradient, where their elution velocities all equal the velocity of the gradient as shown in Figure 5-1.<sup>3</sup> If a compound is initially at a lower or higher temperature than its  $T_{eq}$ , it will move along the column at lower or higher velocity, respectively, until it reaches its  $T_{eq}$  (Figure 5-1). Separated compounds will then travel



**Figure 5-1.** Diagram of the movement of an analyte in a moving temperature gradient.  $T_{eq}$  = characteristic equilibrium temperature,  $v_{peak}$  = peak linear velocity and  $w$  = gradient linear velocity.

isothermally along the column with the gradient velocity at their specific  $T_{eq}$  values, a behavior that is unique to this separation technique. The  $T_{eq}$  depends on the analyte, the gradient ( $v_m$ ) and the mobile ( $w$ ) phase linear velocity, which can be determined by

$$T_{eq} = \frac{\Delta H}{R \left( \ln(v_m - w) - \ln\left(\frac{a}{\beta} w\right) \right)} \quad (5.1)$$

where  $\beta$  is the mobile phase ratio,  $\Delta H$  is the molar enthalpy, and  $a$  is a molar entropy related term. Both thermodynamic terms can be experimentally determined (see Chapter 2). The only requirement to reach  $T_{eq}$  is that the mobile phase velocity must be greater than the linear velocity of the temperature gradient. However, the only analytes that escape this process are those whose  $T_{eq}$  values are either lower (not retained) or higher (strongly retained) than the moving temperature gradient limits. Therefore, in a sawtooth temperature gradient profile, separation takes place in each tooth for a set of compounds

with  $T_{eq}$  values that are contained within the temperature gradient limits. Another unique characteristic of a moving gradient is the focusing effect that takes place as a result of the sample being forced to its  $T_{eq}$  (Figure 5-1), a behavior not encountered in conventional GC. For this reason, the injection method becomes less critical than in other GC methods, and continuous sampling can be performed.

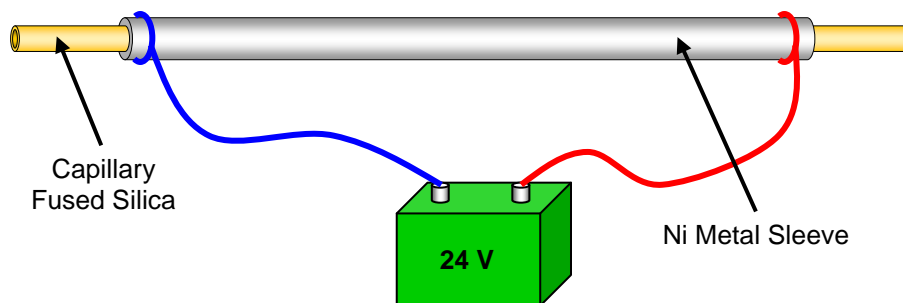
A moving TGGC system, based on resistive heating column technology and convective cooling was designed, constructed and evaluated. Testing of the system was performed by continuous analysis of a mixture of normal alkanes. The unique characteristics of the moving TGGC system for fast, continuous analysis makes it also an attractive alternate as a modulator and second dimension separation method for improving the separation performance in comprehensive GC×GC. A kerosene sample was used for testing a home-built comprehensive GC×TGGC system, as well as for evaluating the separation of a complex sample. The separation features of the new technique are highlighted and discussed in this chapter.

## **5.2 MATERIALS AND METHODS**

### **5.2.1 Construction and Operation of the Moving TGGC System**

Previous moving gradient systems were based on a moving coaxial oven that contained an axial temperature gradient in close contact with the column.<sup>4, 11-15</sup> However, this approach of generating a gradient proved to be cumbersome and difficult to implement. Furthermore, it required that the oven be moved back to the injector end of the column to start another separation, which decreases its throughput capability. Furthermore, since the separation took place inside the oven length, and since the oven

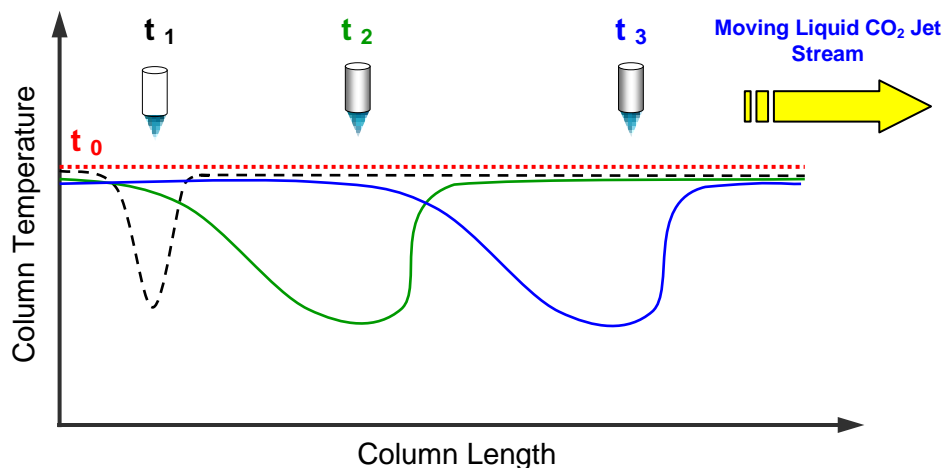
covered a short length of the column, only a small fraction of the column was used for the separation at any given time. A novel approach based on resistance heating technology and convective cooling was used to develop a sawtooth moving temperature gradient generator. The system was constructed using a direct resistively-heated nickel sleeve as the column heater. A 3 m x 0.1 mm ID x 0.4  $\mu\text{m}$  DB-5 fused silica column from Agilent (Santa Clara, CA, USA) was used for the separations. Direct resistive heating of the fused silica column was performed by placing the column inside an electroformed nickel sleeve (0.024" OD x 0.017" ID) from VICI (Houston, TX, USA ) (Figure 5-2). Heating of the Ni sleeve was achieved by applying a voltage across the length of the nickel sleeve.



**Figure 5-2. Configuration for resistively heating the fused silica capillary column.**

The moving axial temperature gradient was generated when a liquid  $\text{CO}_2$  cold jet stream moved along the heated column in the direction of the mobile phase. A diagram showing the generation of a temperature gradient can be seen in Figure 5-3. The entire resistively heated column was maintained at the upper temperature before the jet was turned on ( $t_0$ , dotted line). When the liquid  $\text{CO}_2$  jet stream was turned on ( $t_1$ , dashed line), the resistively heated column that was under the jet stream was cooled. The jet stream was then moved along the column ( $t_3$ , green line). As the jet moved forward downstream,

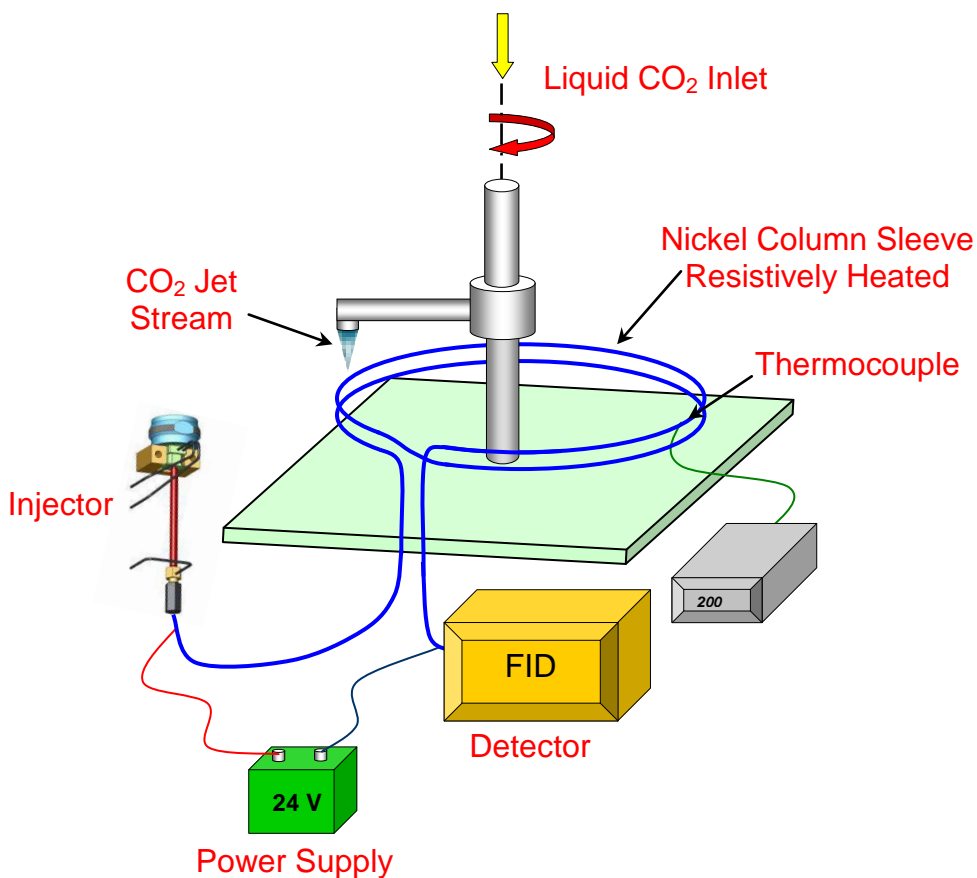
the column behind started to heat back up, generating the temperature gradient. As the jet stream continued to move, a moving concave down temperature gradient was formed (blue line).



**Figure 5-3. Diagram illustrating the generation of a moving temperature gradient by the application of a liquid CO<sub>2</sub> jet stream.  $t_0$  = initial column status at high temperature (red dotted line),  $t_1$  = nitrogen jet stream on (dashed line),  $t_2$  &  $t_3$  = moving jet stream and formation of the moving temperature gradient (green and blue lines, respectively).**

A continuous moving gradient was achieved by moving the cold CO<sub>2</sub> jet stream in a circle. Figure 5-4 shows a diagram of the configuration of the moving TGGC system. The resistively heated nickel column was configured in a circle, and the liquid CO<sub>2</sub> jet stream was positioned directly above the column (Figure 5-4). The jet stream rotated along the column, following the direction of the mobile phase gas. To generate the sawtooth temperature gradient profile, two or more cold CO<sub>2</sub> jet streams could be used at the same time. The downside of this option is that the sawtooth length would be limited by the number of jet streams employed. Another alternative, which was used in this work, was to simultaneously cool two or more loops of the resistively heated column (Figure 5-4). The advantage of using this method is that the sawtooth length is the entire

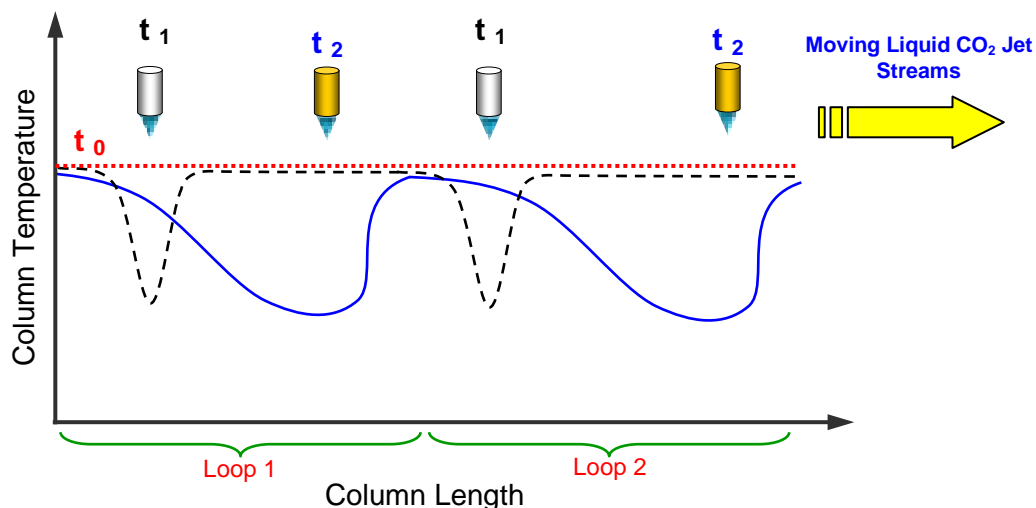
perimeter of the circle, instead of a fraction of the perimeter, as in the case when various cooling jets are used to form the sawtooth gradient.



**Figure 5-4. System configuration for generating a moving sawtooth temperature gradient for TGGC.**

Figure 5-5 shows the generation of a moving sawtooth temperature gradient by configuring the column in two loops. At the initial time ( $t_0$ , dotted line), the resistively heated column was maintained at a high temperature. As the liquid  $\text{CO}_2$  jet stream was turned on ( $t_1$ , dashed line), the two resistively heated columns that were under the jet stream were cooled, forming simultaneously two cold temperature wells (Figure 5-5). As the jet stream moved forward down stream, the column started to heat up, generating a

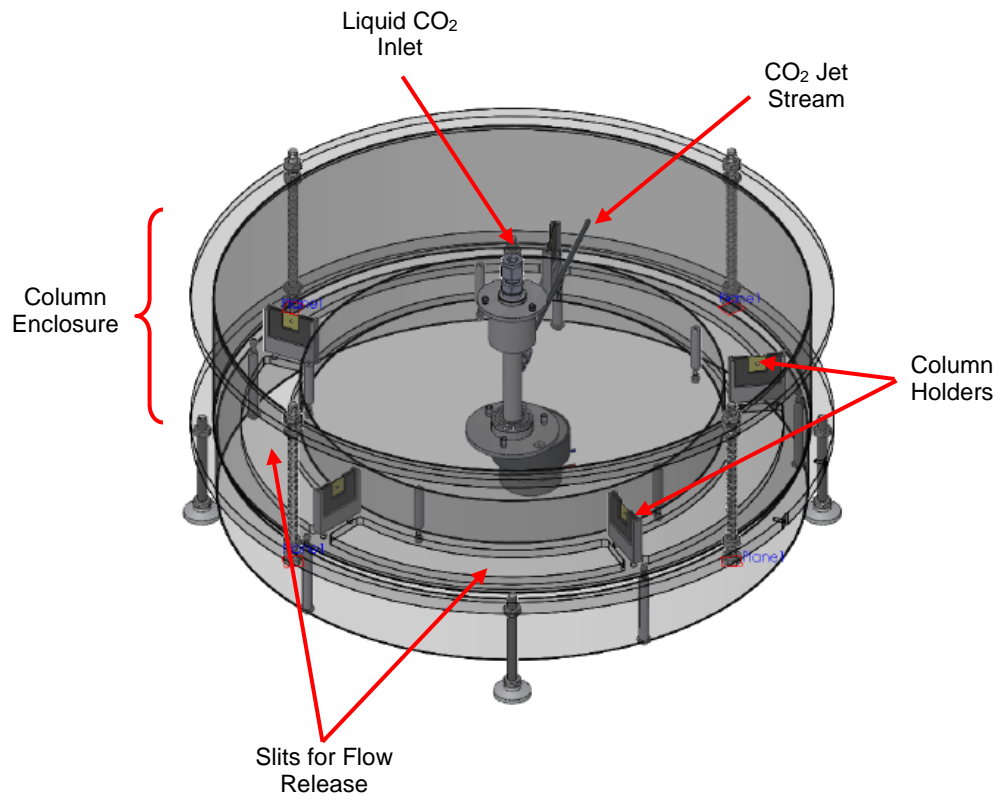
moving sawtooth temperature gradient ( $t_2$ , blue line). Each loop became a separate tooth in the sawtooth gradient as seen in Figure 5-5.



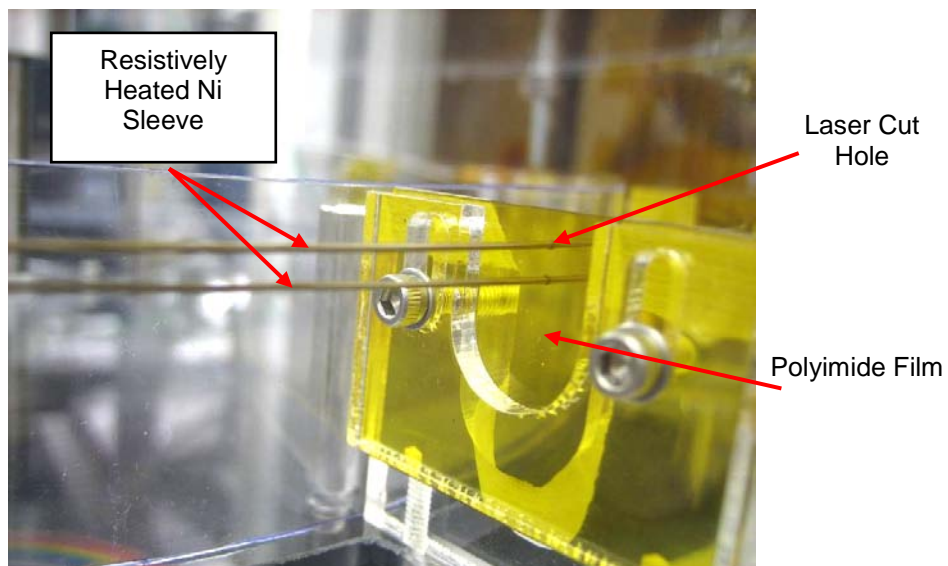
**Figure 5-5. Diagram of temperature gradient generation for a sawtooth type profile by simultaneously cooling two resistively heated loops.  $t_0$  = initial column status at high temperature (dotted line),  $t_1$  = the two nitrogen jet streams on (dashed line),  $t_2$  = moving jet stream and formation of the saw-tooth profile along the column (blue line).**

Figure 5-6 shows a cad design indicating the different components of the moving TGGC system. Key components that allowed the proper function of the system were the column holders. Suspension of the column in the air without creating cold spots was essential for the design to permit GC separations. The solution was to use thin (0.005”) polyimide film from McMaster-Carr (Los Angeles, CA, USA) with laser cut holes, at positions where the resistively heated column arrangement was suspended (Figure 5-7). The tiny contact area, combined with low thermal conductivity and high operating temperature of the polyimide film, made it an ideal column support to allow minimum loss of heat and, hence, reduction of any cold spots.

Another important component of the moving TGGC system is the column enclosure. The enclosure cover was designed to reduce temperature fluctuations along



**Figure 5-6. Cad drawing of the moving TGGC system.**



**Figure 5-7. Photograph of the column support structure.**



the resistively heated column due to any room air convection. The system was positioned 1.5' above the bench top to reduce the turbulent air formed from the CO<sub>2</sub> jet stream bouncing from the bench top and entering the system through the bottom slits, causing temperature fluctuations along the column. Figure 5-8 shows a photograph of the moving TGGC system, indicating all of the instrument components. Upchurch PEEK tubing (0.02" ID, Oak Harbor, WA, USA) was used as the restrictor and liquid CO<sub>2</sub> jet nozzle. A tee connection was used to divide the liquid CO<sub>2</sub> flow into two streams to provide a longer cooling length of 0.5" to provide adequate cooling of the resistively heated column (Figure 5-8). Condensation of water vapor from the environment on the nozzle disrupted the uniformity of the jet stream. Adding a resistively heated metal tube on top of the PEEK nozzle (not shown in Figure 5-8) proved to be the solution.

Continuous sampling was performed by direct introduction of the head space of a mixture of normal alkanes. Helium was used as the head space sweep gas through a tee above a modified ¼" Swagelok (Solon, OH, USA) cap fitting connection (Figure 5-9). The head pressure of the continuous sampling system was maintained at 2 psig higher than the column head pressure to ensure flow of sample into the injector.

The diameter of the resistively heated column coil was 32 cm, for a perimeter of 100.5 cm. This size was chosen since previous results with the TGGC sweeping method showed good separations using temperature gradients of 1 m in length. The outside temperature of the Ni sleeve was lower than the inside; therefore, a correction factor was used to determine the right value. The column temperature was controlled with a simple custom-made linear power amplifier circuit, previously described in Chapter 4, allowing the LabVIEW program to control the amount of voltage applied to the Ni sleeve. The

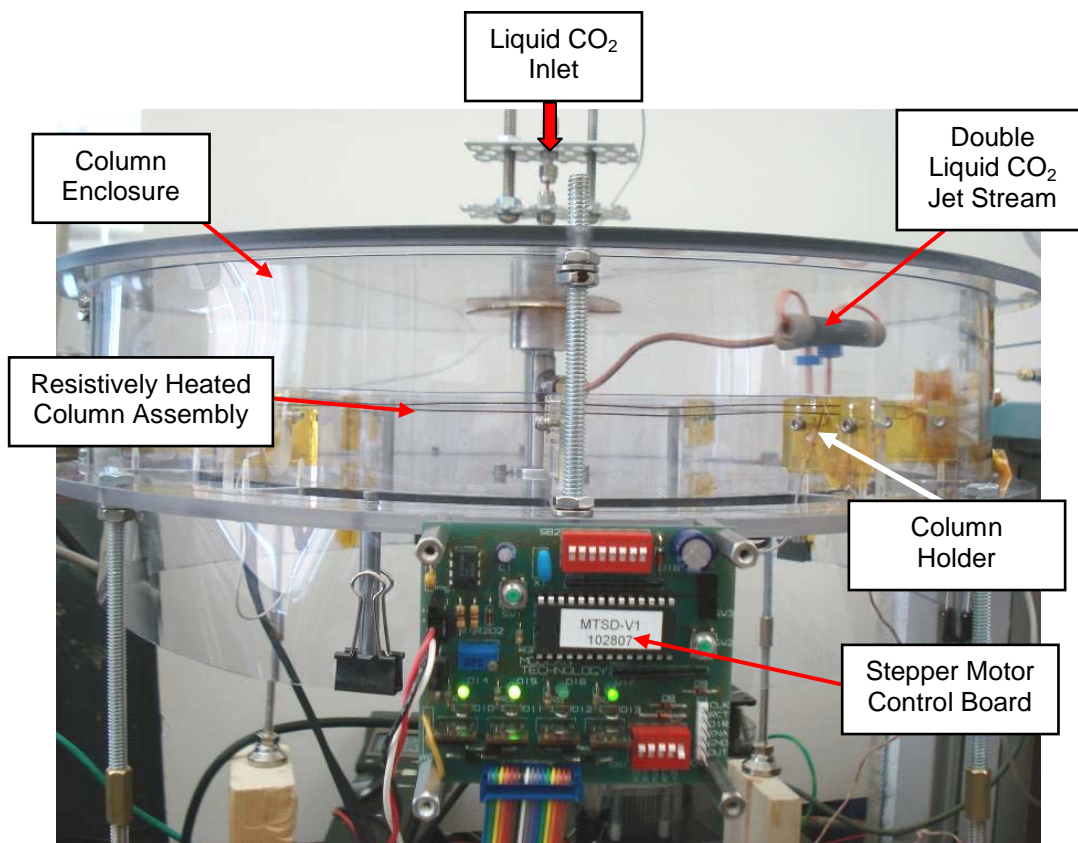


Figure 5-8. Photograph of the moving TGGC system.

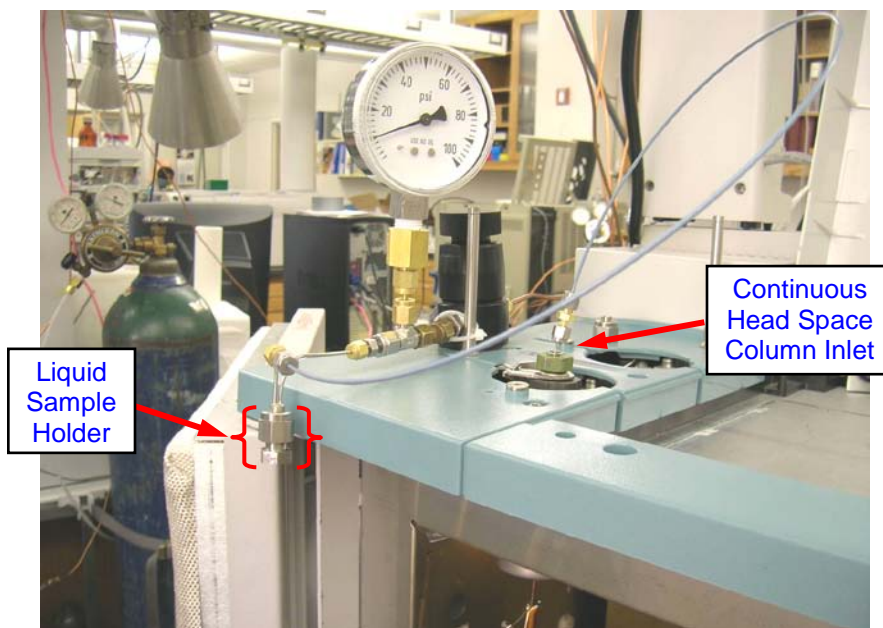


Figure 5-9. Configuration of the continuous head space sampling system.

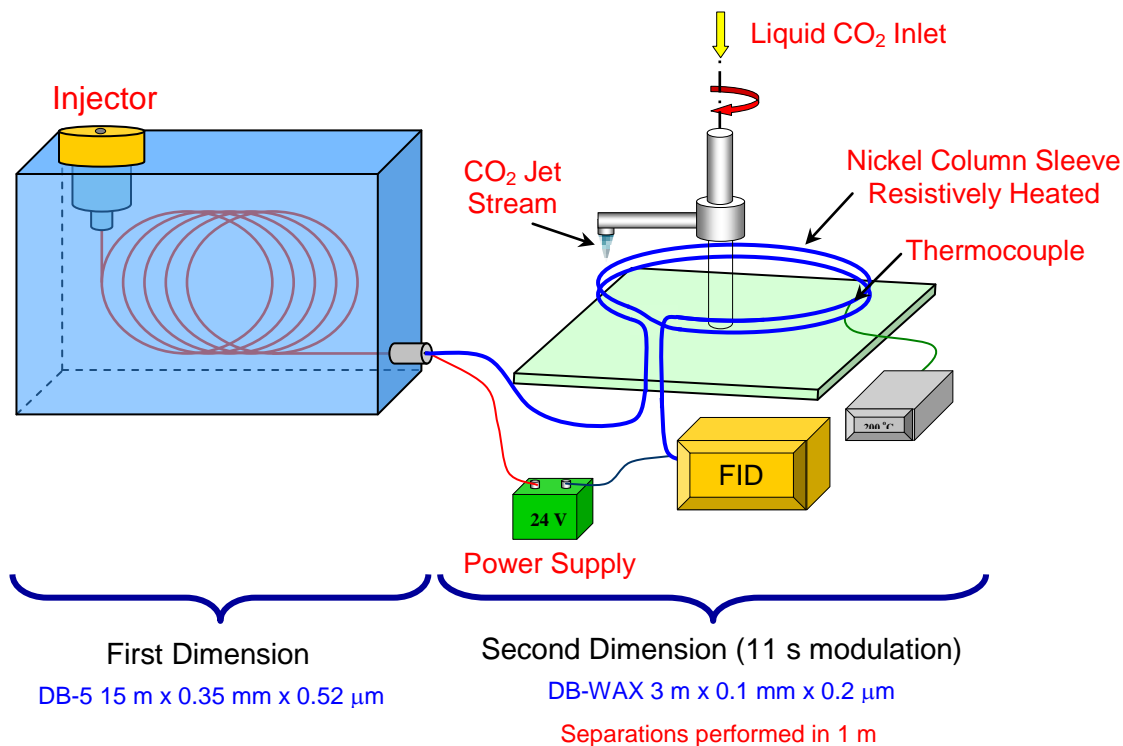
rotation velocity of the jet stream was controlled with a stepper motor board controller from DigiKey (Thief River Falls, MN, USA) (Figure 5-8). Two 12 VDC 250 W power supplies from Digi-Key (part number: 271-2147) connected in series were used to supply the power to heat the Ni sleeve which had a resistance of 1  $\Omega$ /m at room temperature. Since two loops were used for the moving TGGC system, the 1 m left over was used for transfer lines (50 cm each for connection to the injector and detector). These transfer lines were heated to 200°C separately using coiled 29 AWG Nichrome 80 resistive heating wire from Pelican (Naples, FL, USA). Two Variac Autotransformers from Staco Energy Products (Dayton, OH, USA) provided the power for the transfer lines. The TGGC system used the injector and flame ionization detector (FID) of an Agilent 6890 GC system (Santa Clara, CA, USA). The injector temperature and detector were maintained at 250°C. Injections were performed in the split mode (100:1), and constant head pressure was used for the analysis. Helium was used as the mobile phase for all the separations. The FID detector was set at a scanning rate of 200 Hz, and the chromatographic data were handled using the Agilent ChemStation software (version D.01.00).

All chemicals used were commercially available. n-Undecane (99%), n-dodecane (99%), n-tridecane (99%), n-tetradecane (99%), methanol (99.9%), and kerosene were obtained from Sigma-Aldrich (Milwaukee, WI, USA).

### **5.2.2 Construction and Operation of the Comprehensive GC×TGGC System**

A comprehensive GC×TGGC system was constructed by interfacing an Agilent 6890 GC-FID system with the previously described moving TGGC system (Figure 5-10). For the primary column, a non-polar 15 m x 0.35 mm x 0.52 mm DB-5 column was used, and for the second dimension, a polar 3 m x 0.1 mm x 0.2 mm DB-WAX column was

utilized, both columns from Agilent. Testing of the GC×TGGC system was performed with a methanol sample containing 1000 ppm kerosene. The primary column conditions for the temperature program was 30°C (hold 6 min) to 160°C (hold 10 min) at a heating rate of 2°C/min. The injector pressure program was 55 psig (hold 6 min) to 61 psig (hold 10 min) at a pressure program rate of 0.09 psig/min. An injection of 0.5 μL with a split of 300:1 was performed. The linear velocity in the moving TGGC system was 9.09 cm/s (11 s/rev), and the program voltage for the Ni sleeve was 2.8 V (hold 6 min) to 10.3 V (hold 1 min) at a heating rate of 0.1 V/min. Data were obtained with the ChemStation software, and reconstruction of two and three dimensional chromatograms was performed with a custom written Matlab program (version 7.4, Natic, MA, USA).



**Figure 5-10. Diagram of the comprehensive GC×TGGC system.**

## 5.3 RESULTS AND DISCUSSION

### 5.3.1 TGGC System Development

In the design of the moving TGGC system, the first step was to perform simulations using the simple mathematical plate model discussed in Chapter 2 to determine the feasibility of using a moving sawtooth temperature profile to carry out separations. Figure 5-11 shows a typical simulation, assuming a concave down sawtooth temperature gradient profile with 1 tooth/m from 110 to 10°C, a gradient linear velocity of 2.22 cm/s, a mobile phase linear velocity of 116.8 cm/s, and 500 segments/m. The ability of the moving sawtooth temperature gradient to perform continuous sampling and separation was first demonstrated using simulations (Figure 5-11), which provided the theoretical support for a moving sawtooth temperature profile TGGC separation concept.

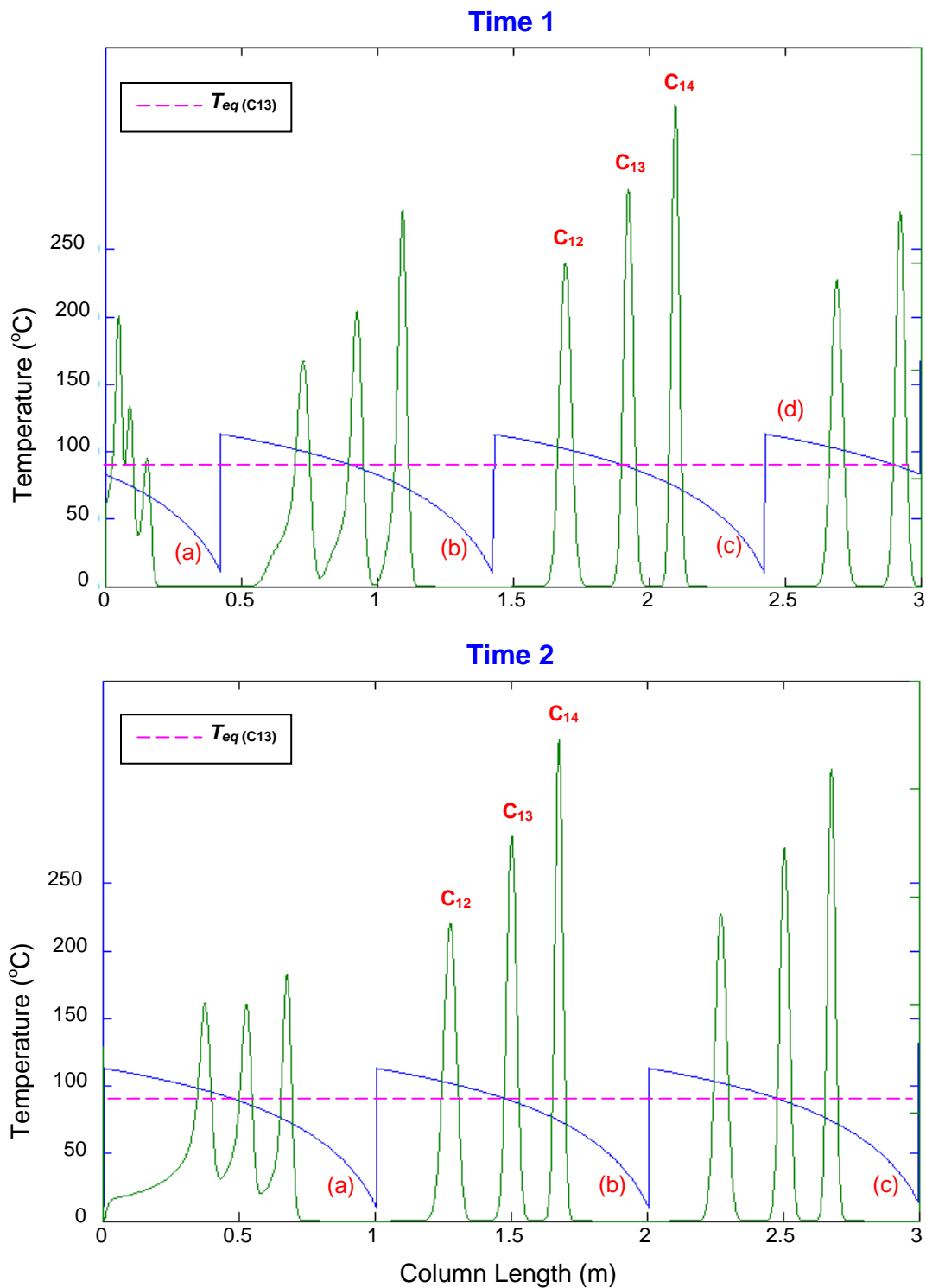
The simulations also helped in the development and design of the moving TGGC system by offering unique insights as the separation proceeded (Figure 5-11). The number of loops required in the system was chosen from results of moving gradient simulations. Figure 5-11 shows separations at a given “time 1”, and at some later “time 2”. Four teeth can be seen at time 1, showing how simultaneous sampling and separation take place in the first tooth (a). During the second tooth (b), the focusing process can be observed with narrowing peaks (Figure 5-11, times 1 and 2), as the rear of the peaks start to move towards their characteristic equilibrium temperatures. By the third tooth (c), the peaks are completely separated and developed, so no gain in separation is observed. Therefore, it was decided to use two teeth (or loops), since they provided the best separation in the least amount of time. The simulations showed that once the peaks

reached their characteristic equilibrium temperatures, a third (c) and fourth (d) tooth did not significantly contribute to improving the separations.

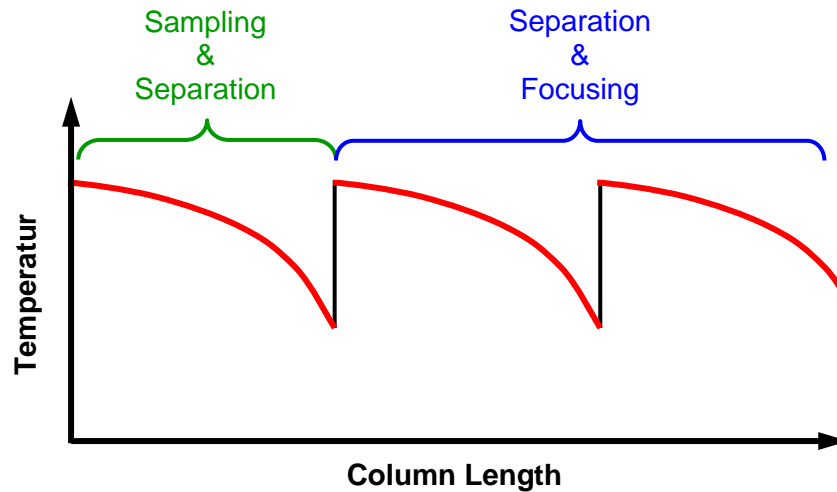
The continuous moving sawtooth temperature gradient analysis process can be summarized in Figure 5-12, where simultaneous sampling and separation take place in the first tooth, and further separation and focusing of the peaks are achieved in the following teeth.

### **5.3.2 Generation of Axial Temperature Gradients**

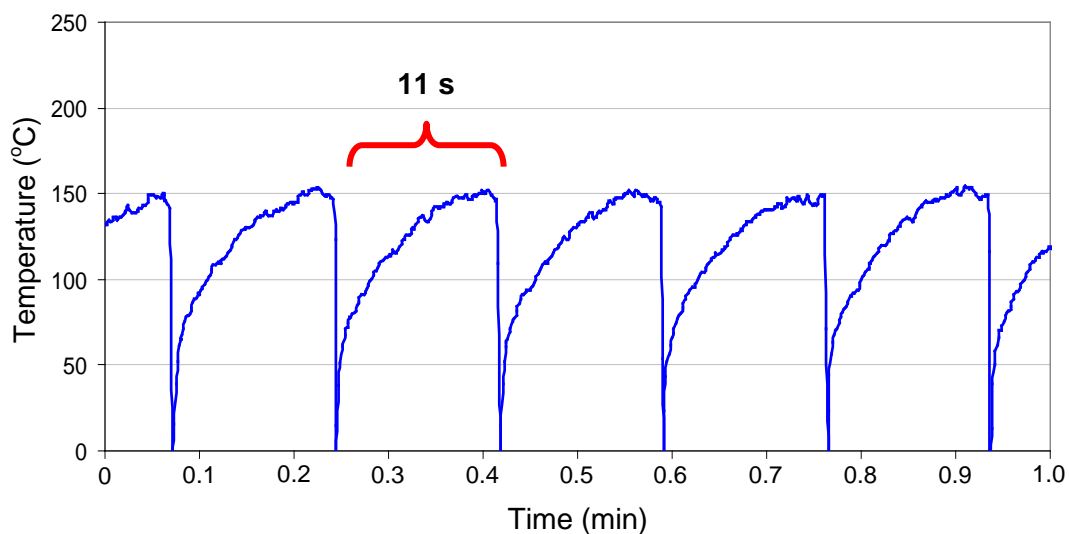
Testing of the gradient generation system was performed by producing moving axial temperature gradients. For generating a moving gradient, the Ni column was resistively heated with 15.3 V and the jet stream moved at 11 s/rev, which meant that the linear velocity of the gradient was 9.09 cm/s, since each loop was equal to 1 m. For these conditions, a concave down profile from 150 to 0°C was obtained. Figure 5-13 shows the sawtooth temperature gradient profile generated with the moving TGGC system as a function of time. The appearance of the gradient profile is the reverse of the profiles presented as a function of length or position (Figures 5-3, 5-5, 5-11, and 5-12), because it plotted as a function of time. The temperature data plotted in Figure 5-13 are unfiltered; therefore, the roughness of the gradient profile is mostly due to system noise. With the use of liquid CO<sub>2</sub> in combination with the low thermal mass of the resistively heated Ni sleeve, cooling rates as high as 11,000°C/min could be achieved. The temperature difference across the gradient was controlled by the amount of voltage applied across the Ni sleeve, as well as by the linear speed of the moving gradient. Smaller temperature differences would be obtained if the voltage of the Ni sleeve was decreased (Figure 5-14) or if the linear velocity of the gradient was increased. However, because of the design,



**Figure 5-11.** Snapshots at two different times from a simulation of the separation of normal alkanes as they travelled and separated along the column during a concave down moving sawtooth temperature gradient operation with continuous sample injection. The temperature gradient profile is also plotted.



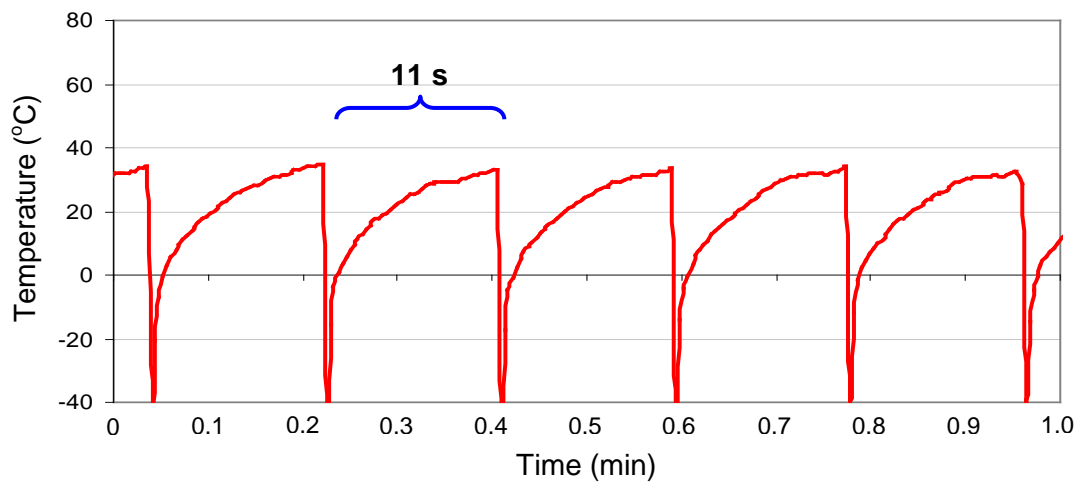
**Figure 5-12. Diagram of the moving sawtooth temperature gradient GC process.**



**Figure 5-13. Moving sawtooth temperature gradient profile. Ni sleeve voltage of 15.3 V, 11 s/loop or 9.09 cm/s gradient linear velocity.**

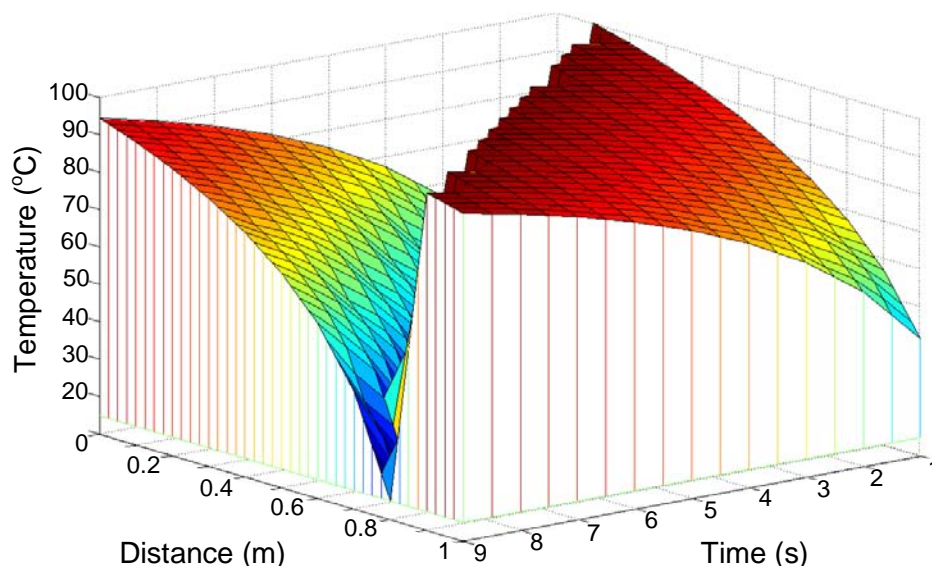
the faster the gradient moved, the smaller the available temperature range, since less time would be available for cooling as well as for heating the gradient. Furthermore, with this temperature gradient generation method, the profile would always be achieved with a concave down profile, as seen in Figures 5-13 and 5-14. Adequate temperature reproducibility was observed with the temperature gradient profile.





**Figure 5-14. Moving sawtooth temperature gradient profile. 3.8 V Ni sleeve voltage, 11 s/loop or 9.09 cm/s gradient linear velocity.**

A thermal field of a typical moving gradient is shown in Figure 5-15, where two teeth of a moving sawtooth gradient can be observed, showing a wave-like profile. Figure 5-15 also shows that analytes traveling inside the column will always encounter a



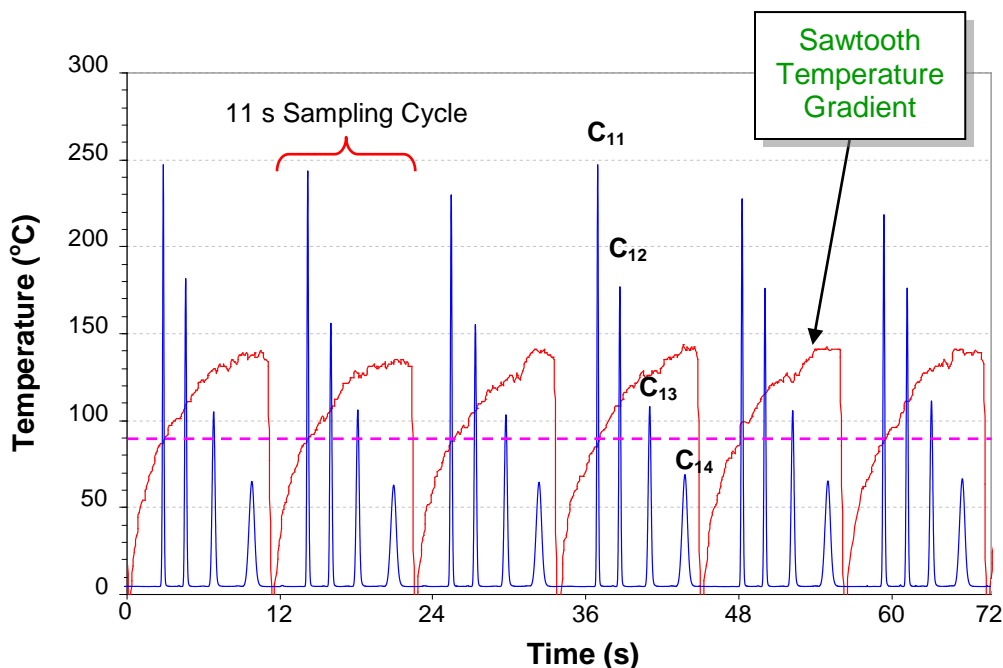
**Figure 5-15. Thermal field of a moving sawtooth axial temperature gradient.**

negative temperature gradient, ensuring that the peaks will be continuously focusing at their respective characteristic equilibrium temperatures. The lower temperature of the sawtooth moving wave gradient prevents peaks with higher  $T_{eq}$  from moving into the next tooth, allowing continuous sampling to occur without disrupting separations in the following teeth.

### 5.3.3 Continuous Analysis of Normal Alkanes

Testing of the moving TGGC system was performed with continuous introduction of a mixture of normal alkanes from undecane to tetradecane ( $C_{11}$ - $C_{14}$ ). Figure 5-16 shows the sawtooth temperature gradient and repetitive alkane chromatograms as a result of continuous sampling and separation of the sample. The absence of broad tailing peaks and the presence of Gaussian shaped narrow peaks in the chromatogram validates the two-loop (two teeth) design approach of the moving TGGC system. Figure 5-16 shows the interesting phenomena that underline the fundamental importance of the moving TGGC technique. It can be observed in this figure that the peaks elute at their characteristic equilibrium temperatures (pink dashed line for  $C_{11}$ ). These compounds move through the column and elute at their respective isothermal temperatures. Looking at the separation in time and space, the peaks appear to be surfing on a thermal wave (Figure 5-15) or in other words, surfing the temperature gradient (Figure 5-16).

The measured and calculated characteristic equilibrium temperatures from equation 5-1 are listed in Table 5-1. From this table, it can be observed that each normal alkane eluted at a constant temperature, since the percent relative standard deviation (%RSD) is below 4.6%, demonstrating that a steady state was reached in the moving negative gradient at  $T_{eq}$ . Also, it can be observed that the calculated  $T_{eq}$  values were in



**Figure 5-16.** Temperature profile of a moving sawtooth axial temperature gradient (i.e., thermal wave) and resultant repetitive chromatograms for continuous sampling of normal alkane vapors. The pink dashed line represents the characteristic equilibrium temperature of  $C_{11}$ . The average resolutions are  $C_{11}$ - $C_{12} = 6.4$ ,  $C_{12}$ - $C_{13} = 5.6$ , and  $C_{13}$ - $C_{14} = 4.1$ . The separation conditions were: 52.6 psig head pressure, 1.44 mL/min mobile phase flow, 9.09 cm/s gradient linear velocity and 15 V Ni sleeve voltage.

close agreement with the experimental values; the differences between them were within the %RSD obtained for the measured values. These results indicate that equation 5.1 can be used to estimate the  $T_{eq}$  of analytes separated in a moving gradient if their thermodynamic properties, and mobile phase and gradient linear velocities are known.

**Table 5-1.** Average characteristic equilibrium temperatures for alkanes separated with the sawtooth moving gradient, and their  $T_{eq}$  values.

Compound	$T_{eq}$ Measured	%RSD	$T_{eq}$ Calculated	$\Delta H/R$ (K)	$\ln(a/\beta)$
<i>n</i> -C11	91.4	4.51	97.7	5318.4	-12.058
<i>n</i> -C12	110.3	3.52	113.3	5672.75	-12.397
<i>n</i> -C13	127.5	2.29	128.1	6088.61	-12.892
<i>n</i> -C14	138.9	2.18	141.8	6500.43	-13.382

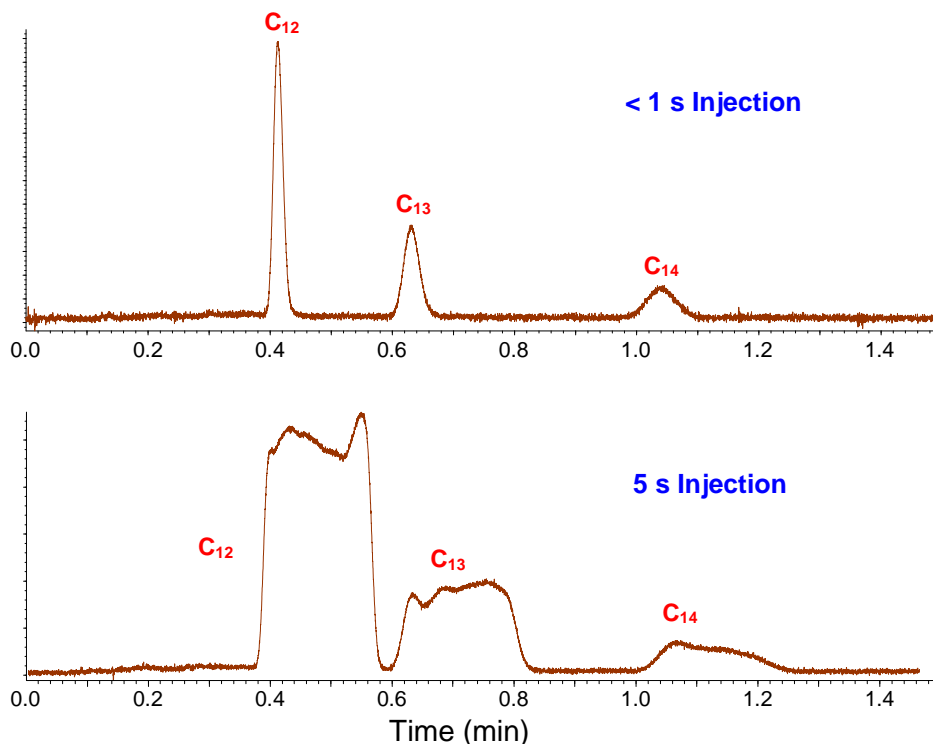
In Table 5-2, high reproducibility of the peak areas (< 2.4% RSD) can be observed, which demonstrates the sampling uniformity of the moving TGGC system and, hence, the potential of this separation technique for quantitative analysis. The peak width %RSD for all of the alkanes was relatively low, with the exception of C<sub>11</sub>. This indicates some non-uniformity in the sawtooth temperature profile. However, one must consider that the peak width variation is exaggerated for narrow peaks as a result of the minimum time scale that the data analysis system can measure. For the case of the ChemStation software used, this limit was 60 ms, which represents between 33% of the peak width at half height maximum for C<sub>11</sub>.

**Table 5-2. Peak widths and standard deviations obtained from continuous analysis of normal alkanes.**

Analyte	Peak Width (ms)	%RSD		Gradient Slope (°C/cm)
		Peak Width	Peak Area	
C <sub>11</sub>	229	22.22	0.56	1.54
C <sub>12</sub>	306	0.00	0.70	1.32
C <sub>13</sub>	484	10.53	0.58	0.67
C <sub>14</sub>	867	6.79	2.31	0.35

Sampling was performed in the first loop of the system as observed in Figure 5-11. Therefore, the sample injection time was 11 s. Even though the sample band was wide, narrow peak widths in the range of 230 and 870 ms were achieved (Table 5-2), demonstrating the focusing effect of the moving axial negative gradient. The peak widths obtained were directly related to the gradient slope, as can be seen in Table 5-2. The steeper gradient provided narrower peaks (C<sub>11</sub>) and the shallower gradient generated broader peaks (C<sub>14</sub>). The focusing effect of the peaks is a function of the temperature

gradient slope, since the greater the temperature changes with respect to  $T_{eq}$ , the smaller the region in which the analyte can spread. The focused peaks gave resolution values of 6.4, 5.6 and 4.1 for high to low slopes, respectively, between  $C_{11}$  and  $C_{14}$ . Such a large sample volume injection would not have provided acceptable results in the isothermal mode, as seen in Figure 5-17, since narrow injection bands are generally required to allow good separations. The moving TGGC system on the other hand does not require narrow band injections to achieve high efficiency separations (Figure 5-16) as needed by conventional GC techniques, especially in fast analysis.<sup>16</sup> In GC, sample introduction has a great effect on the separation efficiency, as observed in Figure 5-17. Therefore, the simplicity of sample introduction in moving TGGC makes it very attractive, especially for continuous analysis.



**Figure 5-17. Isothermal separations of normal alkanes for different injection times. The column temperature was 170°C.**

Large sample introduction achieved with the moving TGGC system allows the signal-to-noise to increase and, hence, the detection limit to go down, which is a result of allowing more sample into the column, as well as providing focusing of the bands. Large sample introduction can be viewed as on-column sample pre-concentration, making moving TGGC suitable for trace analysis.<sup>14</sup>

Another advantage of applying a moving sawtooth temperature gradient for continuous analysis is that no sampling time is lost during cooling; the system is continuously sampling and separating the analytes within successive moving gradients.<sup>17-</sup>  
<sup>19</sup> With conventional temperature programmed GC (TPGC) methods, continuous analysis of a stream is not possible, since there is a need to inject narrow bands. Although focusing takes place in TPGC, it only occurs at the initial separation temperature; thus, during the cooling step, sampling is either stopped or sample concentration is conducted in a different system. Even so, fast TPGC separations have been achieved (< 1 s) by directly resistively heating GC metal columns.<sup>16</sup> Such systems require long cooling times (~100 s) to be ready to conduct another run.<sup>1, 16</sup> The unique sampling and separation characteristics of the moving TGGC technique allows it to have the highest sample throughput of any GC separation mode. This is of great importance for industrial applications that require routine analysis or constant process monitoring, such as in monitoring reactors. Furthermore, from Figure 5-16, it can be observed that the overall moving TGGC separation resembles a TPGC operation, since the normal alkane peaks (C<sub>11</sub>-C<sub>13</sub>) are narrow and evenly spaced. This similarity would have been even greater if the sawtooth profile was linear.

These results highlight the advantages and potential that a moving gradient, especially a moving sawtooth gradient, can offer. In a moving gradient GC separation for constant mobile phase and gradient velocity, the positions of the peaks and their peak widths are a function of the temperature gradient profile. This characteristic is of fundamental importance, since by controlling the profile of the temperature gradient, one can easily manipulate the separation of the analytes and, hence, the separation power of the system.

### **5.3.4 Use of Moving TGGC as Modulator and Second Dimension Separation Technique in Comprehensive GC×GC Separations**

Comprehensive two-dimensional GC, or GC×GC, is a powerful technique for the analysis of complex mixtures. In GC×GC, the sample is separated in two different columns connected in series. The separated sample in the primary column is sliced into small fractions that are then transferred into the secondary column for a second, independent separation.<sup>20-22</sup> The high separation power of this technique is a result of the high peak capacity achieved, which can be estimated as the product of the individual peak capacities of each column dimension.<sup>23</sup> The fractional amount of sample transferred from the primary column to the secondary column is dependant on the speed of analysis of the secondary column, since the analysis in the second dimension must be completed before the next fraction is injected. The goal is to avoid any overlap of successive fractions at the detector (*i.e.*, wraparound), which destroys the separation achieved in the second dimension and complicates the reconstruction of the two dimensional chromatogram. For this reason, the secondary column separations are currently performed under isothermal conditions and typically achieved in a few seconds (1 to 12

s)<sup>24-27</sup> to preserve the separation already attained in the primary column. Longer second dimension analysis can be performed, however, it comes at the cost of increasing the total GC×GC analysis time. Because of the use of isothermal separation in the secondary column, typical two dimensional GC×GC chromatograms show the elution problem in the second dimension, where the first peaks are not resolved and the later eluting peaks are spread and broad.<sup>24-25, 28-29</sup> As a result, the separation in the secondary column does not take advantage of the entire second dimension space. The total peak capacity of the GC×GC technique can be greatly improved with the application of TPGC operation in the second dimension. However, even though fast TPGC separations have been achieved (< 1 s), the long cooling times (~100 s) have limited its application in the second dimension of GC×GC separations.<sup>1, 16</sup>

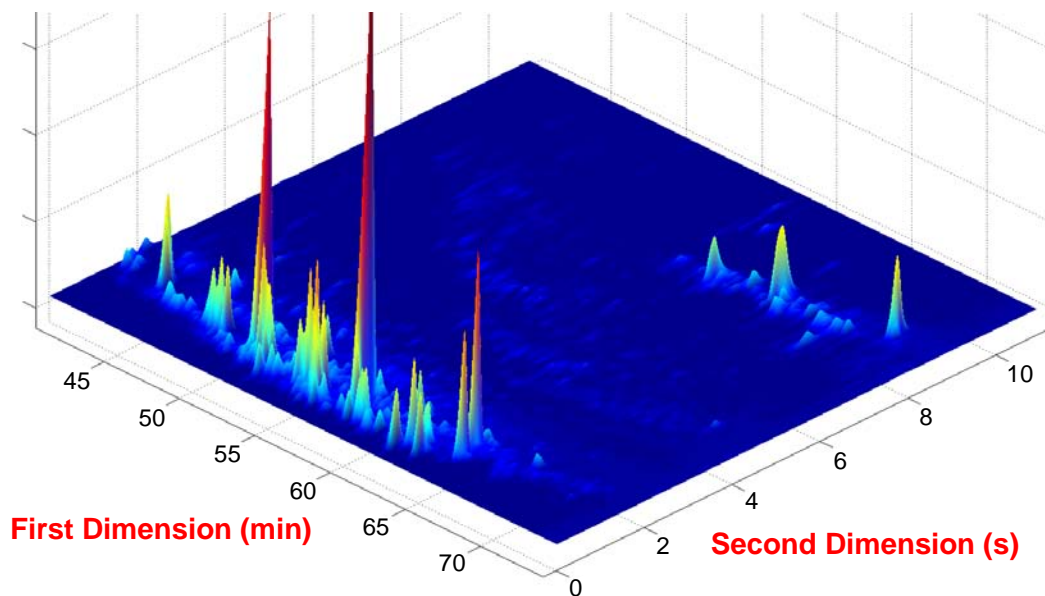
On the other hand, the moving TGGC technique offers some unique capabilities that make it a very attractive alternative as a separation method for the second dimension in GC×GC analysis. As previously demonstrated, it can accommodate continuous sampling and analysis using a moving sawtooth gradient. Furthermore, it produces separations similar to TPGC, demonstrated by the observation that normal alkanes were evenly separated. It can be used as a solution to the GEP for mixtures with a wide range of volatilities (*i.e.*, retention factors), which is important to improve separations in the GC×GC second dimension and, hence, the total peak capacity of the system. In moving TGGC, compounds separate on the slopes of the teeth of a sawtooth gradient, without interfering with separations occurring in the following teeth, a very attractive feature to eliminate wrap around problems in GC×GC. Furthermore, since compounds in the moving TGGC travel along the column at the linear velocity of the temperature gradient,



longer columns with faster gradient velocities can be used to improve the peak capacity of the system without sacrificing separation time. Modulation or slicing of the eluting peaks from the primary column can be achieved with the sawtooth gradient itself, reducing the need for a separate modulator. In fact, moving TGGC resembles the moving thermal modulator introduced by Phillips.<sup>22, 26</sup> Actually, the thermal modulator can be considered to be a temperature gradient with a very steep slope that moves in a very short column, producing narrow band injections. These unique characteristics of the moving TGGC method makes it a very attractive alternative as a modulator and separation method to improve the second dimension separation and overall peak capacity of GC×GC separations.

The potential of moving TGGC as modulator and second dimension separation method in a comprehensive GC×GC system can be visualized in Figures 5-18 and 5-19. Figure 5-18 shows a three-dimensional plot of the GC×TGGC separation of a kerosene sample, in which peaks can be seen distributed along the second dimension separation, demonstrating the two-dimensional separation ability of the system.

Furthermore, a more orthogonal separation is obtained in the second dimension, and the “roof-tile” effect, or diagonal sub-bands corresponding to groups of isomers that are commonly observed in GC×GC separations, is absent.<sup>27</sup> This is desirable, since a more efficient utilization of the second dimension space can be performed and, hence, an increase in the total peak capacity can be obtained. The single second dimension chromatogram in Figure 5-19, shows that in 11 s of the first dimension, over 13 peaks were not resolved. This chromatogram not only shows the need for the GC×GC technique in separating complex samples, but it also demonstrates the separation capability of the



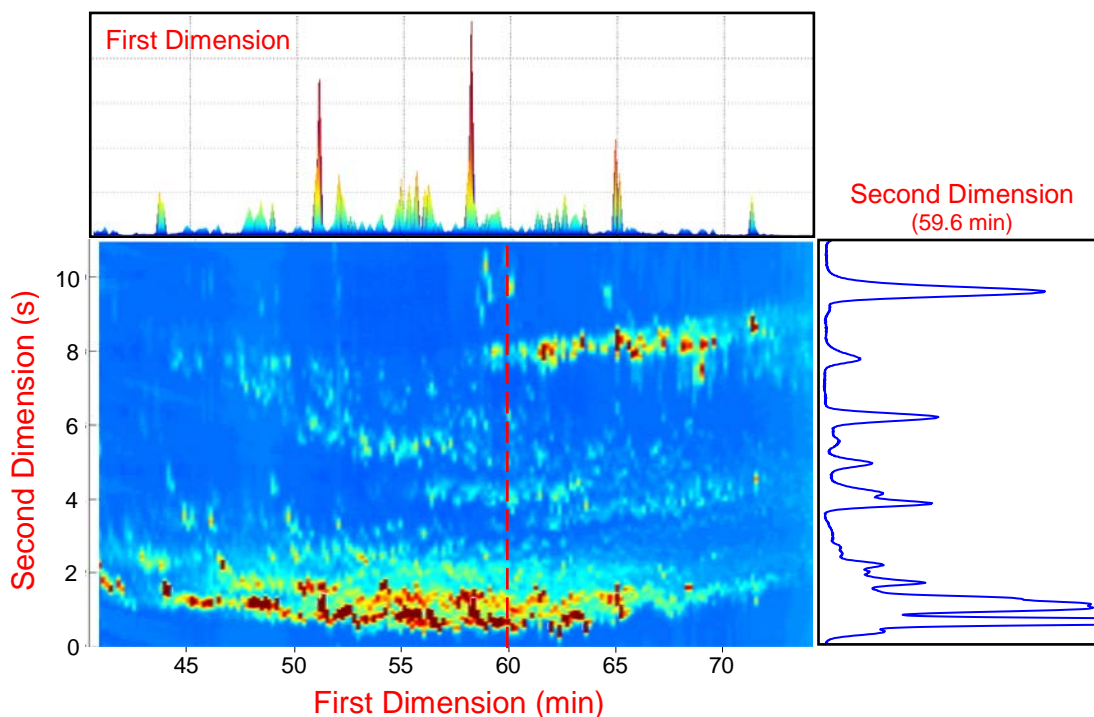
**Figure 5-18. Three dimensional view of a GCxTGGC separation of kerosene.**

moving TGGC system for complex mixtures. It is noteworthy to mention that narrower focused peaks are distributed along the second dimension, even for the later eluting compounds, which is not generally observed in conventional GC×GC separations.<sup>25, 27</sup>

The later narrow peaks can also be observed in the three dimensional chromatogram (Figure 5-18). No wraparound problems were observed, since elevated temperature at the end of each tooth in the moving sawtooth gradient removed any compounds remaining inside the second dimension column. Even though the column in the second dimension was 3 m in length, the separation was performed in only 1 m, which was the length of the thermal gradient (*i.e.*, tooth) where the separation took place. This result provides evidence of the possibility of using longer columns in the second dimension, which is desirable to improve the peak capacity of the system. Since the compounds travel at the speed of the gradient, longer columns with faster gradient velocities could be used to

improve the peak capacity of the system, without affecting the second dimension analysis time and without wraparound problems.

The home-built GCxTGGC system shows great potential to improve the separation power of comprehensive GC×GC separations. However, careful optimization of the GCxTGGC parameters must be done to take full advantage of this system.



**Figure 5-19. 2D chromatogram of a GCxTGGC kerosene separation, showing the one-dimensional chromatogram separation on top and a second dimension chromatogram obtained at a retention time of 59.6 min (segmented line) on the right.**

## 5.4 CONCLUSIONS

The moving TGGC system was capable of producing moving sawtooth temperature gradient profiles. The two-loop design allowed continuous analysis of a normal alkane mixture (C<sub>11</sub> to C<sub>14</sub>). The normal alkane peaks eluted at their characteristic

temperatures of equilibrium, a distinctive behavior that underlines the fundamental importance of the moving TGGC technique. Moving TGGC showed separations comparable to TPGC. This was observed in the separation of C<sub>11</sub> to C<sub>13</sub> normal alkanes, in which narrow and evenly spaced peaks were produced. This technique can be used to separate mixtures of compounds with wide ranges of volatilities. The focusing effect of the moving gradient could be observed by the narrow peaks obtained after sampling for a long time period. This is important for improving the detection limits of the system for use in trace analysis. The effect of the gradient slope on peak widths showed that steeper gradients provided narrower peaks as a result of reducing the region where the analytes can spread, due to the higher temperature differences around  $T_{eq}$ . The high reproducibility of the peak areas (< 2.4%RSD) demonstrated that the system could be used for quantitative analysis. Fast separations and continuous analysis possible, because no time was lost during cooling; the system was continuously sampling and cooling at the same time throughout the sawtooth temperature profile, allowing high throughput. This characteristic allowed TGGC to be used for comprehensive GC×GC, which was demonstrated with the separation of a kerosene sample with TGGC as the second dimension and modulator in the comprehensive arrangement. The moving TGGC system allowed good distribution of peaks in the second dimension and narrow peaks for late eluting compounds. The system more efficiently utilized the second dimension space, producing orthogonal separations and eliminating wraparound problems. The results reported in this chapter demonstrate the potential separation capabilities of the moving TGGC method, which must be further explored to take full advantage of the technique.

This work also demonstrates how this technology, even though introduced in the early 1950s,<sup>4, 13</sup> can provide new possibilities and interesting solutions to current problems.

## 5.5 REFERENCES

1. Phillips, J. B.; Jain, V., On-Column Temperature Programming in Gas Chromatography Using Temperature Gradients Along the Capillary Column. *J. Chromatogr. Sci.* **1995**, *33*, 543-550.
2. Rubey, W. A., A Different Operational Mode for Addressing the General Elution Problem in Rapid Analysis Gas Chromatography. *J. High Resolut. Chromatogr.* **1991**, *14*, 542-548.
3. Tudge, A. P., Studies in Chromatographic Transport III. Chromathermography. *Can. J. Phy.* **1961**.
4. Zhukhovitskii, A. A., Some Developments in Gas Chromatography in the U.S.S.R. In *Gas Chromatography 1960*, Scott, R. P. W., Ed. Butterworths: Edinburgh, 1960; pp 293-300.
5. Fenimore, D. C., Gradient Temperature Programming of Short Capillary Columns. *J. Chromatogr.* **1975**, *112*, 219-227.
6. Vergnaud, J. M., Gas Phase Chromatography: The Application of Gas Flow Variation and Backflushing. *J. Chromatogr. A* **1965**, *19*, 495-503.
7. Bellabes, R., *et al.*, Gas Chromatography with Backflushing: Isothermal during the First Step, Programming of Longitudinal Temperature Gradient during the Second Step. *Sep. Sci. Technol.* **1982**, *17* (9), 1177-1182.
8. Rubey, W. A. Gas Chromatography Methods and Apparatus US Patent 5028243, 1991.
9. Rubey, W. A., Theory of Constrained Migration Behavior in Open-Tubular Gas Chromatography Columns with Various Operational Modes. In *23<sup>rd</sup> International Symposium on Capillary Chromatography*, Riva del Garda, Italy 2000.
10. Contreras, J. A. Design and Application of Thermal Gradient Programming Techniques for Use in Multidimensional Gas Chromatography-Mass Spectrometry (MDGC-MS) University of Dayton, Dayton, 2004.
11. Nerheim, A. G., Gas-Liquid Chromathermography. *Anal. Chem.* **1960**, *32*.
12. Ohline, R. W.; DeFord, D. D., Chromathermography, the Application of Moving Thermal Gradients to Gas Liquid Partition Chromatography. *Anal. Chem.* **1963**, *35* (2), 227-234.
13. Zhukhovitskii, A. A., *et al.*, New Method of Chromatographic Analysis. *Doklady Akademii Nauk SSSR* **1951**, *77*, 435-8.
14. Kaiser, R., Temperature Gradient Chromatography. *Chromatographia* **1968**, *1*, 199-207.
15. Vigdergauz, M. S., The Early Period of the Development of Gas Chromatography in the U.S.S.R. *Chromatographia* **1978**, *11* (11), 627-633.
16. Reid, V. R., *et al.*, Investigation of High-Speed Gas Chromatography Using Synchronized Dual-Valve Injection and Resistively Heated Temperature Programming. *J. Chromatogr. A* **2007**, *1148*, 236-243.

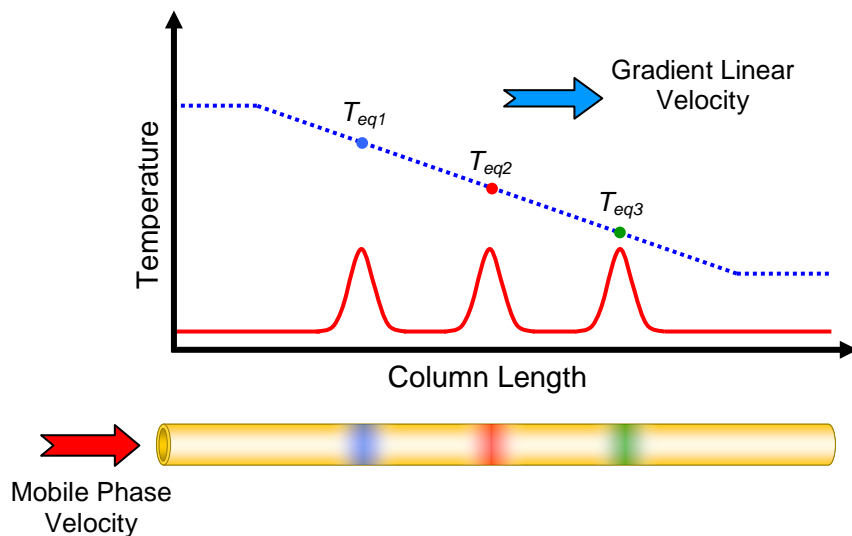
17. Contreras, J. A., *et al.* In *Theoretical and Practical Justification of Thermal Gradient Gas Chromatography*, PITTCON, Chicago, IL, March; 2009.
18. Contreras, J. A.; Lee, M. L. In *Analytical Gradient Focusing Separation Techniques*, 236th American Chemical Society Philadelphia, PA, August; 2008.
19. Contreras, J. A., *et al.* In *Moving Wave Temperature Gradient Gas Chromatography*, 32<sup>nd</sup> International Symposium on Capillary Chromatography and 5<sup>th</sup> GC×GC Symposium, Riva del Garda Italy, May; 2008.
20. Bertsch, W., Two-Dimensional Gas Chromatography. Concepts, Instrumentation, and Applications – Part 1: Fundamentals, Conventional Two-Dimensional Gas Chromatography, Selected Applications *J. High Resolut. Chromatogr.* **1999**, *22*, 647-665.
21. Bertsch, W., Two-dimensional Gas Chromatography. Concepts, Instrumentation, and Applications - Part 2: Comprehensive Two-dimensional Gas Chromatography. *J. High Resolut. Chromatogr.* **2000**, *23* (3), 167-181.
22. Phillips, J. B.; Xu, J. Z., Comprehensive Multidimensional Gas-Chromatography. *J. Chromatogr. A.* **1995**, *703* (1-2), 327-334.
23. Kinghorn, R. M.; Marriott, P. J., Comprehensive Two-Dimensional Gas Chromatography Using a Modulating Cryogenic Trap. *J. High Resolut. Chromatogr.* **1998**, *21* (11), 620-622.
24. Marriott, P.; Shellie, R., Principles and Applications of Comprehensive Two-Dimensional Gas Chromatography. *TrAC* **2002**, *21* (9-10), 573-583.
25. Adahchour, M., *et al.*, Recent Developments in the Application of Comprehensive Two-dimensional Gas Chromatography. *J. Chromatogr. A* **2008**, *1186* (1-2), 67-108.
26. Geus, H.-J. d., *et al.*, Comprehensive Two-Dimensional Gas Chromatography with a Rotating Thermal Desorption Modulator and Independently Temperature-Programmable Columns. *J. High Resolut. Chromatogr.* **2000**, *23* (3), 189-196.
27. Beens, J., *et al.*, Proper Tuning of Comprehensive Two-Dimensional Gas Chromatography (GC×GC) to Optimize the Separation of Complex Oil Fractions. *J. High Resolut. Chromatogr.* **2000**, *23* (3), 182-188.
28. Examining Comprehensive Flow-Modulated Two-Dimensional Gas Chromatography. [www.agilent.com](http://www.agilent.com).
29. Panic, O.; Gorecki, T., Comprehensive Two-Dimensional Gas Chromatography (GC×GC) in Environmental Analysis and Monitoring. *Anal. Bioanal. Chem.* **2006**, *386* (4), 1013-1023.

## 6 MOVING THERMAL GRADIENT GC WITH CUSTOM TEMPERATURE PROFILES

### 6.1 INTRODUCTION

In moving thermal gradient gas chromatography (TGGC), separations are achieved when a decreasing temperature gradient from the injector to the detector moves along the column in the direction of the mobile phase.<sup>1-8</sup> As the analytes move along the column into lower temperatures, their retention increases, slowing them down; however, the movement of the gradient along the column increases the temperature around the analytes and causes them to move with greater velocity (Figure 6-1). Eventually, a steady state condition is reached for each analyte, where it moves at the same velocity as the gradient at a characteristic equilibrium temperature ( $T_{eq}$ ) (Figure 6-1). If an analyte is initially at a lower or higher temperature than its  $T_{eq}$ , it will move along the column at lower or higher velocity, respectively, until it reaches its  $T_{eq}$ . This characteristic produces a focusing effect, counteracting the broadening observed in conventional GC by retarding the leading edges of the peaks while accelerating their trailing edges.<sup>2-3</sup>

In moving TGGC, the more volatile compounds are eluted in the cooler region of the gradient, while less volatile compounds travel in the hotter region. Therefore, the  $T_{eq}$  is a function of the analyte as well as the gradient and mobile phase linear velocities. Since analytes travel with the gradient at their respective  $T_{eq}$  values, it is obvious that the temperature gradient profile has the greatest influence on the separation process. These attributes underline the fundamental importance of this technique, since unparalleled

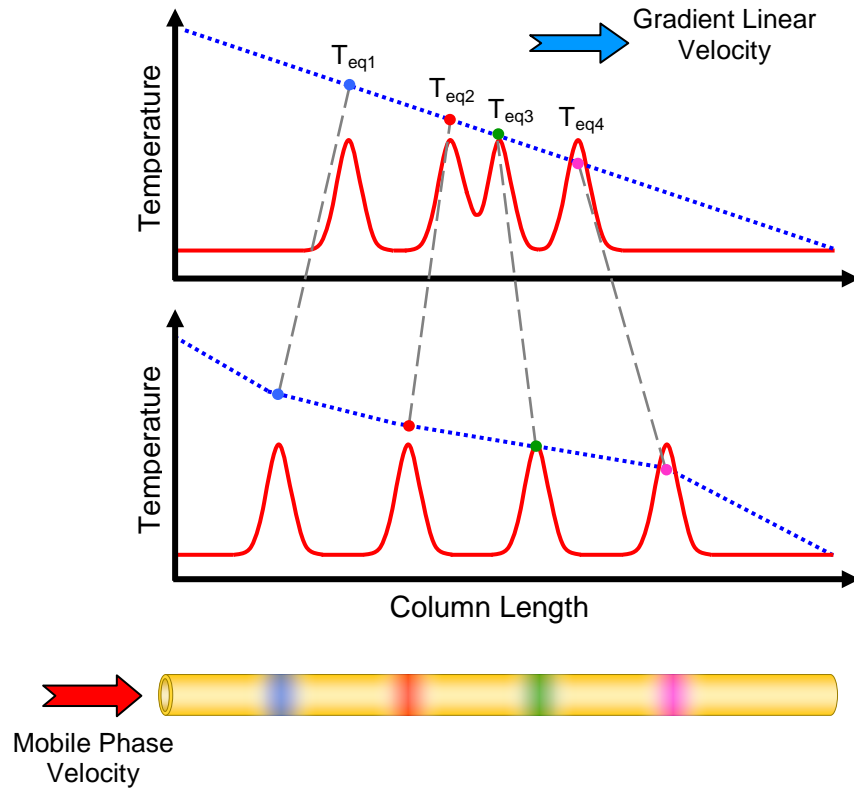


**Figure 6-1. Diagram illustrating analytes traveling in a moving temperature gradient.**

separation flexibility can be achieved by customizing the temperature gradient profile (Figure 6-2). Adjusting the temperature profile offers intriguing possibilities that have not been explored before for improving and optimizing separations. Changing the temperature profile allows unique control of the movement and elution of sample components.<sup>9</sup> Figure 6-2 shows a diagram illustrating the separation potential of the technique, where the separation of analytes in a linear gradient are improved with a custom temperature profile that moves apart the  $T_{eq}$  values of the analytes. Custom temperature profiles allow more efficient utilization of the column space and, hence, overall improvement in the separation.

The moving TGGC technique with custom profiles has the potential to uniquely optimize separations rapidly producing narrow peaks and improving the peak capacity (maximum number of resolved peaks per unit time)<sup>10</sup> of the column. Currently, method development in GC is tedious and time-consuming. The moving TGGC technique can greatly reduce the optimization time by using custom temperature profiles.





**Figure 6-2. Diagram showing the unique separation potential of the moving TGGC technique that allows optimization of separations by customizing the gradient profile.**

To the best of our knowledge, previous TGGC studies have only utilized linear<sup>1-3, 5, 11-13</sup> and concave down<sup>14-15</sup> temperature gradients with limited control over the profile shape. As a result, the separation potential of TGGC has not been fully exploited. Understanding the effects that axial temperature gradient profiles have on separation performance is of great importance in optimizing moving TGGC. However, the main challenge is development of instrumentation for generating and controlling the desired temperature gradient profiles. Lack of suitable instrumentation has limited the use and evaluation of TGGC. In this chapter, the design, development, and testing of a moving TGGC instrument capable of generating custom sawtooth temperature gradient profiles is described. The effects of the gradient profiles as well as the different factors that affect

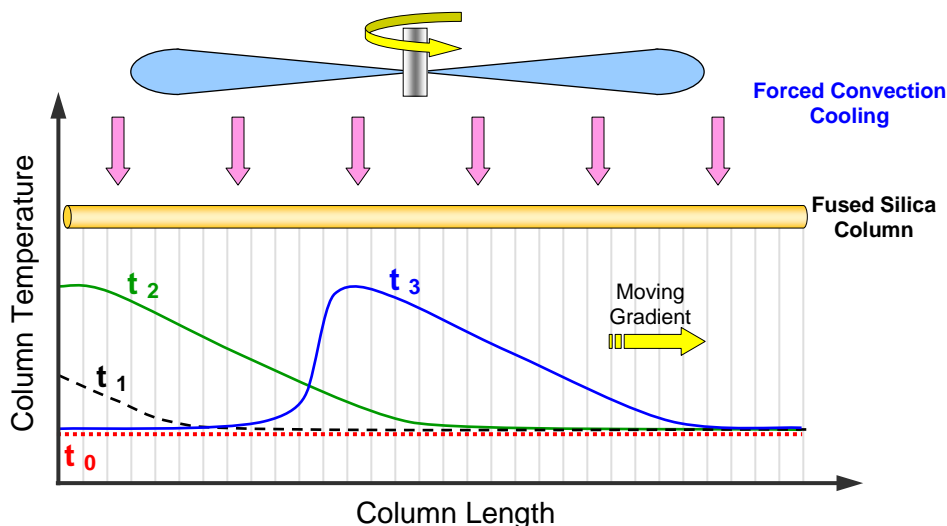
the separation performance in a moving gradient are discussed. A new low thermal mass resistive heating assembly for fast TPGC is also described, and a comparison between the different GC separation methods is presented.

## **6.2 MATERIALS AND METHODS**

### **6.2.1 Construction and Operation of the Moving TGGC System**

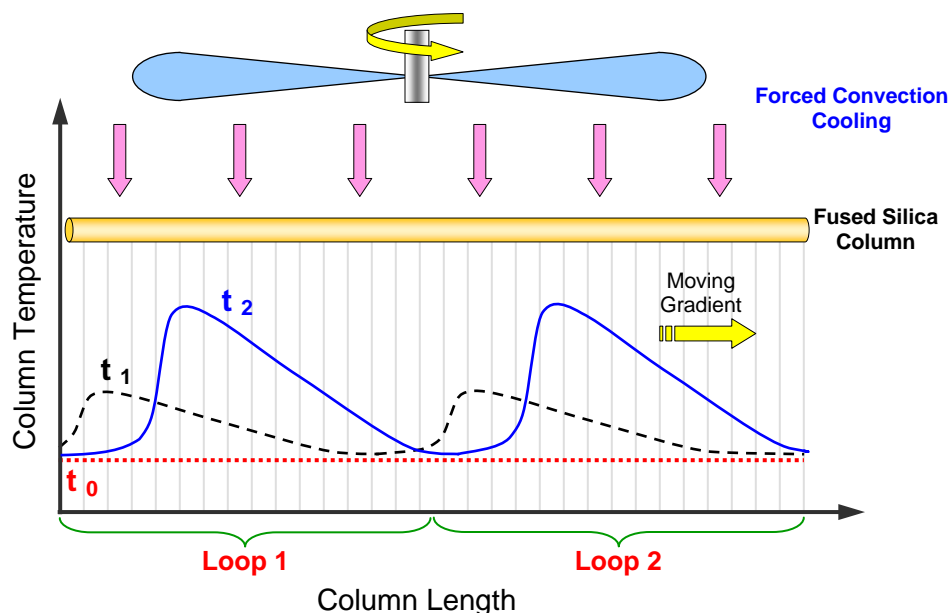
The moving TGGC system was constructed according to the design discussed in Chapter 5, where a sawtooth temperature profile was generated when a cold jet stream continuously moved along a resistively heated column, arranged in a circle. The moving cold jet approach did not have the ability for modifying the axial temperature gradient profile required for exploring the separation potential of this technique. To allow flexibility in gradient profile shape forced air convection cooling combined with a series of individually resistively heated sections was used. In this new approach for generating the temperature gradient, the column was kept at a low temperature by continuous forced air convection, while resistively heated sections were individually controlled to form the desired moving temperature profile (Figure 6-3). A similar approach was previously proposed by Fenimore;<sup>1</sup> however, in his design no forced air convection was used and his studies were limited to linear gradients with different slopes. A diagram showing the generation of the temperature gradient can be seen in Figure 6-3. The entire column was initially maintained at a low temperature ( $t_0$ , dotted line). When the voltage to the resistively heated sections was gradually increased ( $t_1$ , dashed line), the temperature gradient started to form. The profile of the temperature gradient was a function of the voltage applied to each of the resistively heated sections; in this case a linear gradient is

depicted ( $t_2$ , green line). After the desired gradient was formed and moving downstream, the resistively heated sections behind the gradient were turned off to allow cooling, producing a tooth of the sawtooth temperature profile (blue line).



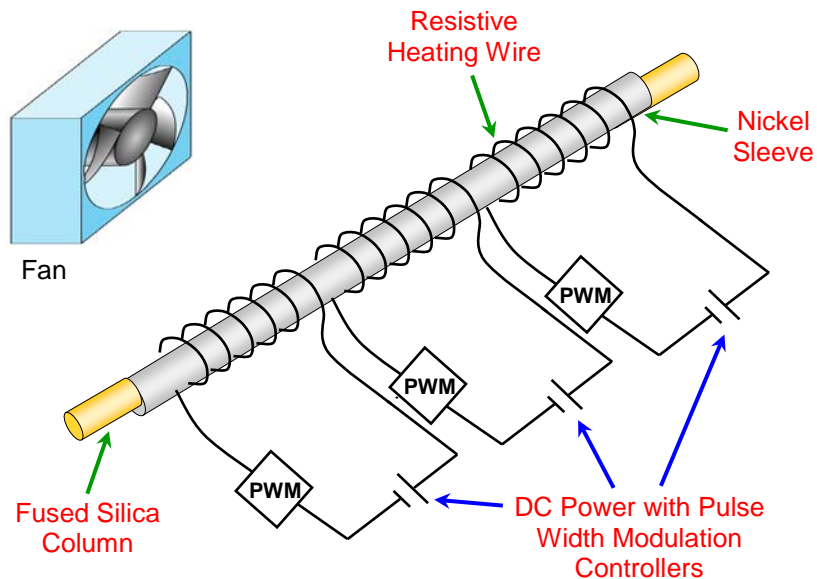
**Figure 6-3. Diagram illustrating the generation of a moving temperature gradient by resistively heating individual sections of the column with forced convection cooling. Grey lines represent the separation between individual resistively heated sections.  $t_0$  = initial column status at a low temperature (red dotted line),  $t_1$  = gradually resistively heating the first segments of the column (dashed line),  $t_2$  &  $t_3$  = fully developed moving temperature gradient (green and blue lines, respectively).**

For generating the sawtooth temperature profile, two column loops were simultaneously heated, following the previous moving TGGC design, such that each loop became a separate tooth in the sawtooth gradient (Chapter 5). Figure 6-4 shows the generation of a moving sawtooth temperature gradient by configuring the column in a coil with two loops. The column was maintained initially at a low temperature ( $t_0$ , dotted line). When the power to the individual resistively heated sections increased according to a given profile (linear), two temperature gradients were formed as the two column loops were simultaneously heated ( $t_1$ , dashed line). Once the temperature gradient was fully developed, a moving sawtooth temperature profile was generated (blue line).

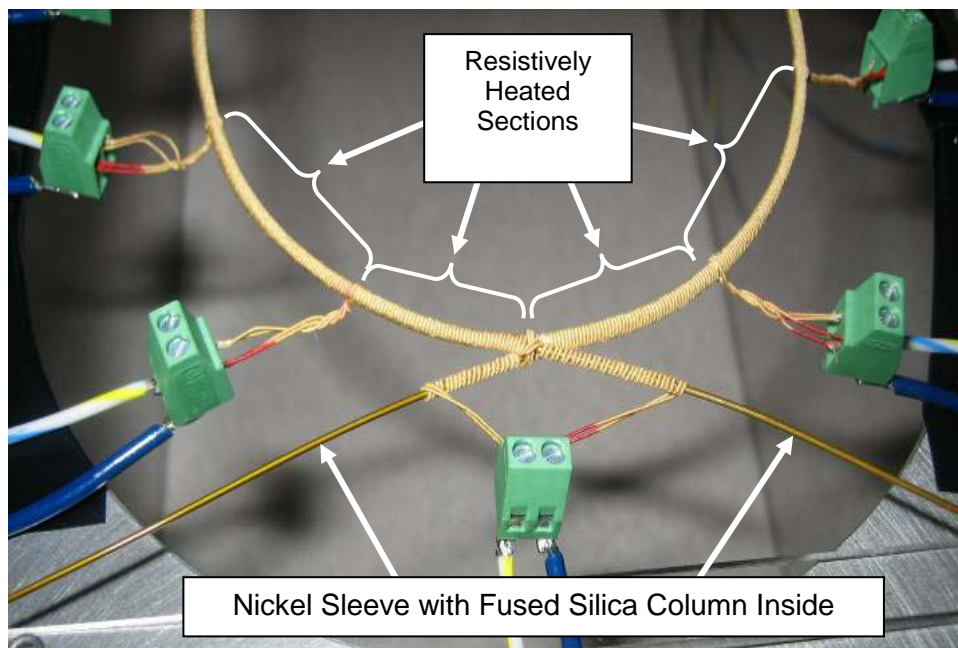


**Figure 6-4. Diagram illustrating the generation of a moving sawtooth temperature gradient by simultaneously heating two column loops using individually resistively heated segments in combination with forced convection cooling. Grey lines represent the separation between individual resistively heated sections.  $t_0$  = initial column status at a low temperature (red dotted line),  $t_1$  = beginning of the formation of the temperature gradients (dashed line),  $t_2$  = fully developed moving sawtooth temperature gradient (blue line).**

The column loop with a perimeter of 1 m was heated by 40 individual resistively heated sections of 1" in length. This length was chosen since previous results with the moving TGGC system showed good separations using temperature gradients of 1 m in length. The column used was a 3 m x 0.1 mm ID x 0.4  $\mu$ m DB-5 (5%-phenyl-methylpolysiloxane) fused silica column from Agilent (Santa Clara, CA, USA). The fused silica column was inserted inside an electroformed nickel sleeve (0.024" OD x 0.017" ID) from VICI (Houston, TX, USA) to serve as a structural support as well as to allow a smooth temperature change between the individual heated sections. Various techniques were considered for heating each section, including direct resistive heating of the nickel sleeve itself. However, this method required the use of large step-down transformers which made this method difficult to implement. Each of these sections was



**Figure 6-5. Configuration of the individual resistively heated coils with pulse modulation control for the generation of custom temperature gradient profiles.**



**Figure 6-6. Photograph of the tightly wind Nichrome 80 wires, showing the individual resistively heated sections.**

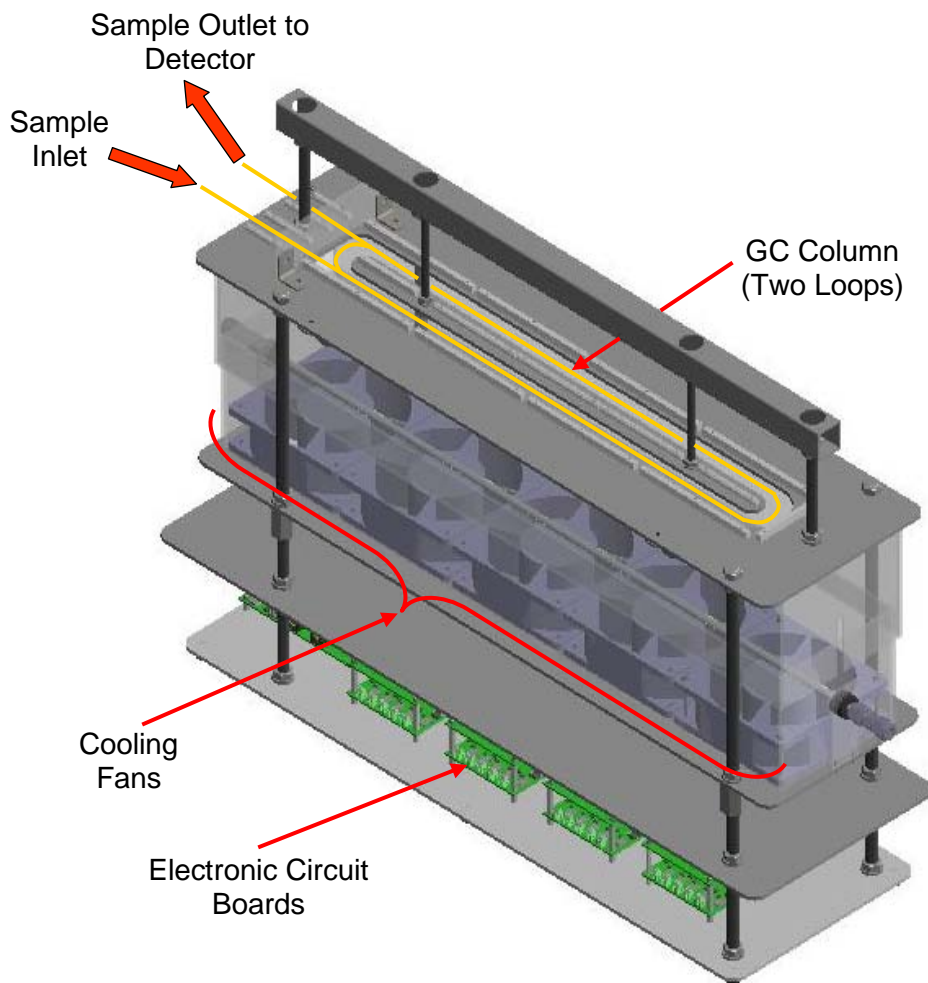
heated using a tightly coiled 38 AWG Nichrome 80 resistive heating wire from Pelican (Naples, FL, USA) (Figures 6-5 and 6-6). A pair of resistive heating wires in parallel

were used to decrease the total resistance of the heated sections to  $12 \Omega$  (Figure 6-6). The use of thin wires maintained the low thermal mass of the system. Each coil was independently heated under computer control with a custom-designed circuit board, making the instrument design flexible for generating a wide variety of moving temperature gradient profiles.

Figure 6-7 shows a diagram of the configuration of the new moving TGGC system. The column loop was arranged longitudinally instead of in a circle to reduce the system dimensions and facilitate cooling with the use of 5" x 5" square fans. The column was kept in place by the resistively heated wire connections (Figure 6-6). A series of fans placed below the column provided continuous cooling by forced air convection (Figure 6-7), which allowed rapid cooling of the resistively heated sections for generating the moving sawtooth temperature profile. To reduce fluctuations in the column temperature due to turbulence in the convective air flow, a 1" thick aluminum honeycomb sheet from McMaster-Carr (Los Angeles, CA, USA) was placed on top of the fans (Figure 6-8). To further reduce any turbulence in the air, the fans were operated by drawing air instead of blowing air from the top where the column was placed (Figure 6-7).

Heating of each individual section was achieved by pulse-width modulation (PWM) of a DC voltage applied to the system, which allowed simple electronics (Figure 6-8). Each resistively heated element was controlled by a custom circuit board, which used C++ programming to control the profile and the linear velocity of the moving sawtooth gradient. The gradient specifications were easily downloaded to the boards using a custom-written computer program. A 13.8 VDC 550 W power supply from Digi-Key (Thief River Falls, MN, USA) was used to heat all of the resistively heated sections

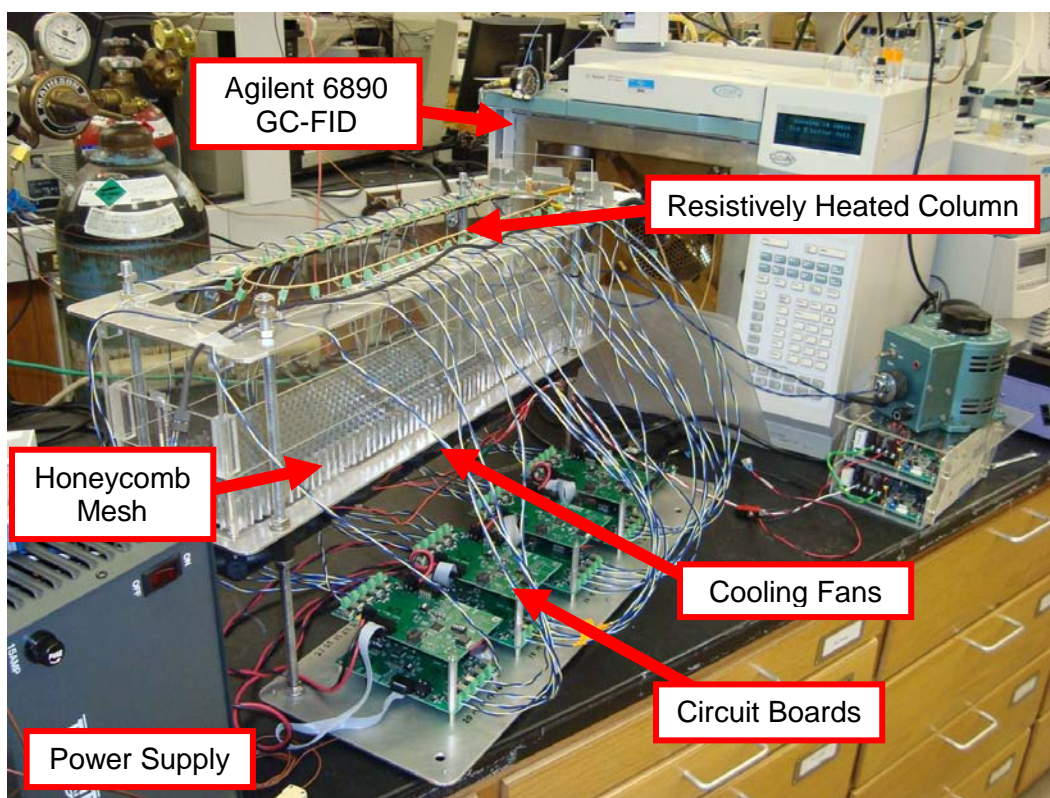
(Figure 6-8). A photograph of the complete moving TGGC system can be seen in Figure 6-8, with labels to identify the principal components of the system.



**Figure 6-7. System configuration for generating custom moving sawtooth temperature gradient profiles.**

The column temperature was monitored using small (0.005" OD) type K thermocouples from Omega (Stamford, CT, USA) positioned at the inlet of the column loop. Temperature data were recorded at 100 Hz using a USB National Instruments data acquisition system and a custom-written LabVIEW program (Austin, TX, USA). The outside temperature of the Ni sleeve was lower than the inside; therefore, a correction

factor was used to record the correct value. A dummy column with 5 resistively heated sections was used as well to record the inside temperature. An infrared camera SC500 from FLIR (Santa Barbara, CA, USA) was also used to monitor the moving temperature gradient along the resistively heated sections.



**Figure 6-8. Photograph of the moving TGGC system with individual resistively heated sections for the generation of custom temperature gradients.**

The moving TGGC system was connected to a GC injector and flame ionization detector (FID) using two 50 cm transfer lines from the 1 m column length leftover, after using 2 m of the column in the resistively heated loops. These transfer lines were heated to 200°C separately using coiled 29 AWG Nichrome 80 resistive heating wire from Pelican (Naples, FL, USA). Two Variac autotransformers from Staco Energy Products (Dayton, OH, USA) provided the power for the transfer lines. The moving TGGC system



used the injector and FID of an Agilent 6890 GC system (Santa Clara, CA, USA), as shown in Figure 6-8. The injector and detector temperatures were maintained at 250°C. Continuous sampling was performed by direct introduction of the headspace of a mixture of n-alkanes, following the method described in Chapter 5. Headspace injections using gastight syringes from Hamilton (Reno, NV, USA) were also performed. Injections were performed in the split mode (100:1), and constant head pressure was used for the analysis. Helium was used as the mobile phase for all the separations. The FID was set at a frequency of 200 Hz, and the chromatographic data were handled using the Agilent ChemStation software (version D.01.00).

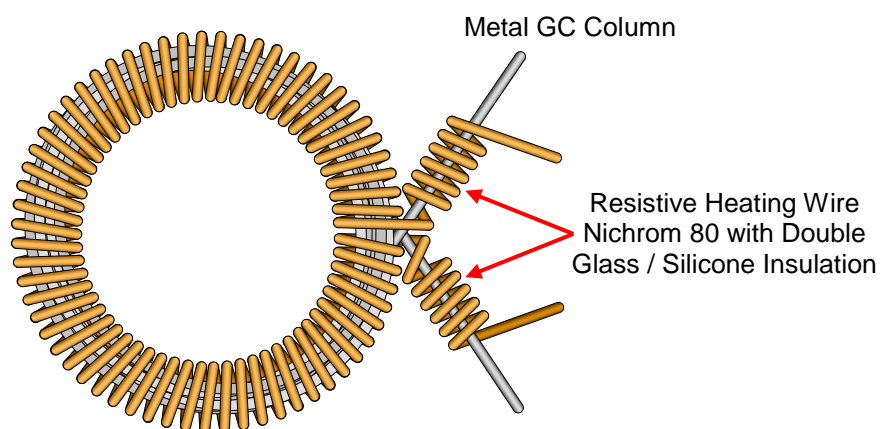
All chemicals used were commercially available. n-Dodecane (99%), n-tridecane (99%), n-tetradecane (99%), nonylamine (97%), decylamine (95%), and methanol (99.9%) were obtained from Sigma-Aldrich (Milwaukee, WI, USA). Frankincense (India) essential oil was obtained from Native American Nutritionals (Ava, MO, USA).

### **6.2.2 Development of a Resistively Heated TPGC Column Assembly**

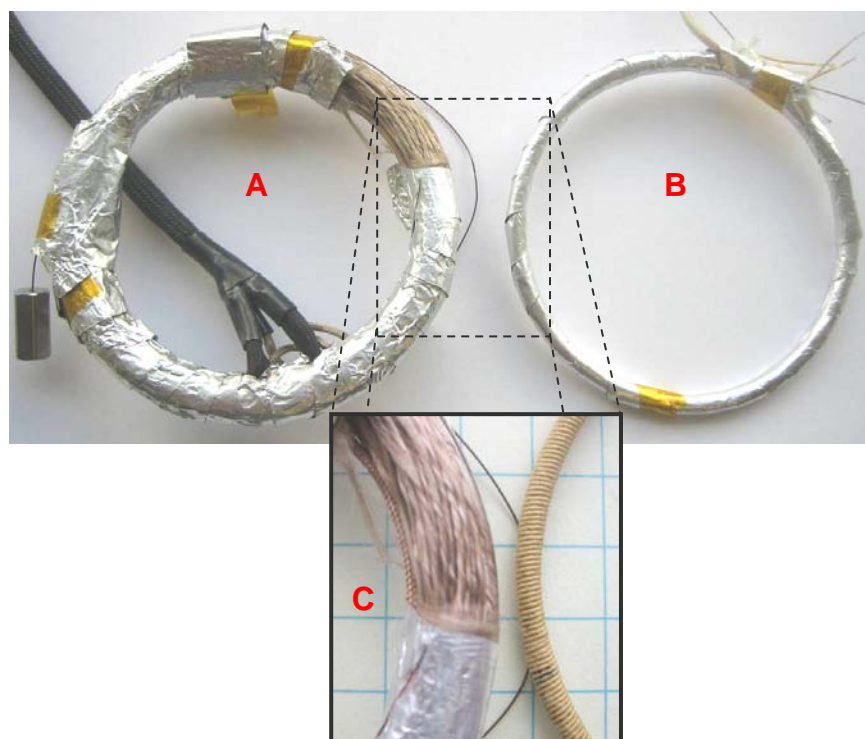
Although the moving TGGC system had a 3 m column, the separation was performed in only 1 m, which was the maximum length of the gradient. For this reason, in order to perform a comparison between moving TGGC, ITGC, and TPGC separations, a GC system with 1 m column was required. As previously reviewed in Chapter 1, there are different column heating approaches for performing ITGC and TPGC analysis. However, due to the relatively fast separations obtained with the moving TGGC system, heating rates greater than 200°C/min were required for TPGC analysis for a reasonable comparison with moving TGGC. Conventional GC systems are not capable of achieving such high rates. For this reason, a new resistive heating approach was developed to allow

fast heating rates for short columns. A simple column assembly was developed that consisted of coiling a 1.4 m x 0.1 mm x 0.4  $\mu\text{m}$  RTX-5 (5% -phenyl/95% dimethylpolysiloxane) metal column from Restek (Bellefonte, PA, USA) in a 0.5" radius, and tightly winding it with 38 AWG Nichrom 80 resistive heating wire with double glass silicon electrical insulation (Figure 6-9). The column was then wrapped with fiber glass and aluminum foil to improve the heating efficiency. The low thermal mass of the assembly allowed for fast heating and cooling rates. The resistive heating wire was also used to reduce any cold spots along the column ends that extended out of the loop (Figure 6-9); this minimized temperature gradients along the transfer lines into the column assembly. Longer resistive heating wires could be used to form a one piece column assembly and transfer lines to the injector and detector, simplifying the system. The column temperature was monitored using a small (0.005" ID) type K thermocouple from Omega, placed within the column coil to provide accurate reading. The resistive heating assembly was combined with a small fan that continuously drew air over the column to reduce temperature fluctuations due to natural convection and lack of feedback control.

Although wrapping a coiled column with resistive heating wire seems to be straightforward, to the best of my knowledge, it has not been reported before. Resistive heating of fused silica capillary columns by this new method may not be as successful as heating metal columns due to thicker capillary wall thickness and lower thermal conductivity of fused silica [1.38 W/(mK)] compared to stainless steel [16 ~ 45 W/(mK)]. Excellent deactivation methods for metal GC have been developed during the last decade. Most previous work, therefore, on resistive heating (see Chapter 1) has mainly focused on fused-silica columns or direct resistive heating of metal columns. The higher thermal



**Figure 6-9. Diagram of the resistively heated assembly for TPGC and ITGC separations.**



**Figure 6-10. Photographs showing (A) 5 m commercially available LTM-GC assembly, (B) 3.5 m resistive heating assembly described in this work, and (C) close up showing both columns side by side.**

conductivity of stainless steel and thinner wall thickness facilitate the resistive heating approach. The resistively heated GC system assembly and a commercially available

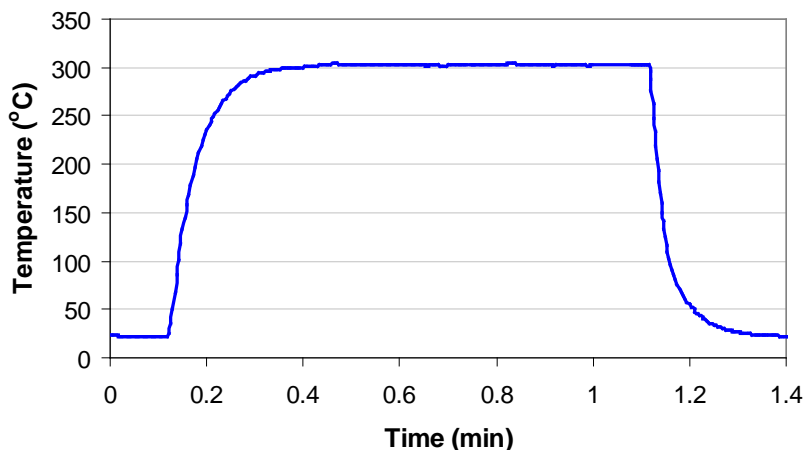
resistive heating approach (Agilent low thermal mass (LTM-GC) assembly)<sup>16-20</sup> are shown in Figure 6-10. In this photograph, it can be appreciated that the new resistive heating approach is significantly smaller. The smaller size of the new heating assembly emphasizes its potential to be used in portable GC instrumentation.

## **6.3 RESULTS AND DISCUSSION**

### **6.3.1 Generation of Temperature Gradients**

The heating and cooling capabilities of the individually resistively heated sections were first studied to establish how fast the temperature can be varied to form a moving temperature gradient. The low thermal mass of the resistively heated sections in combination with continuous cooling by forced air convection allowed the system to achieve heating rates as high as 1200°C/min and cooling times from 300 to 50°C in less than 6 s (Figure 6-11). These high heating rates and short cooling times allowed the temperature of the individual resistive heating sections to be quickly adjusted, providing the system with ample flexibility for producing temperature gradients with different profiles. The moving TGGC system was tested by producing sawtooth temperature gradients with different profiles.

The ability of the system to produce custom temperature gradients can be observed in Figure 6-12, where a series of sawtooth linear temperature profiles with different slopes are shown. In this figure, the high reproducibility of the sawtooth temperature profile produced with the moving TGGC instrument can be seen. The minimum temperature achieved for the sawtooth temperature gradients was room temperature, as a result of using ambient air for cooling. The temperature of the air flow

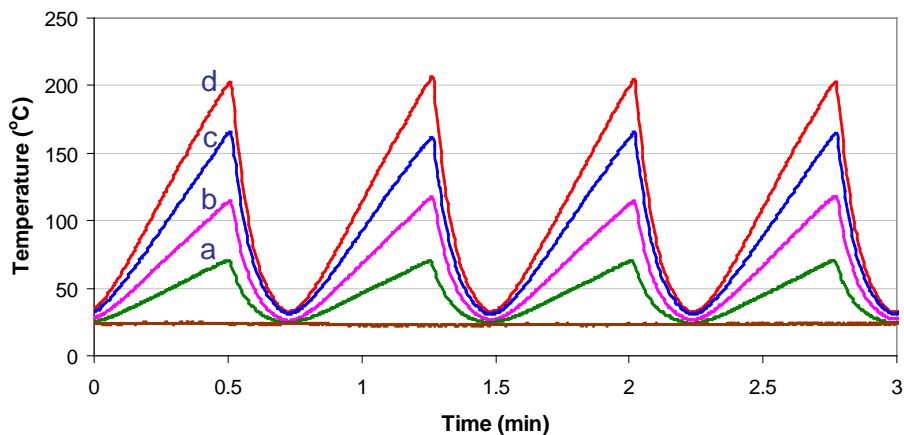


**Figure 6-11. Heating and cooling capabilities of the resistively heated sections with continuous forced air convection cooling. A heating rate of 1200°C/min and cooling from 300 to 50°C in less than 6 s was typical.**

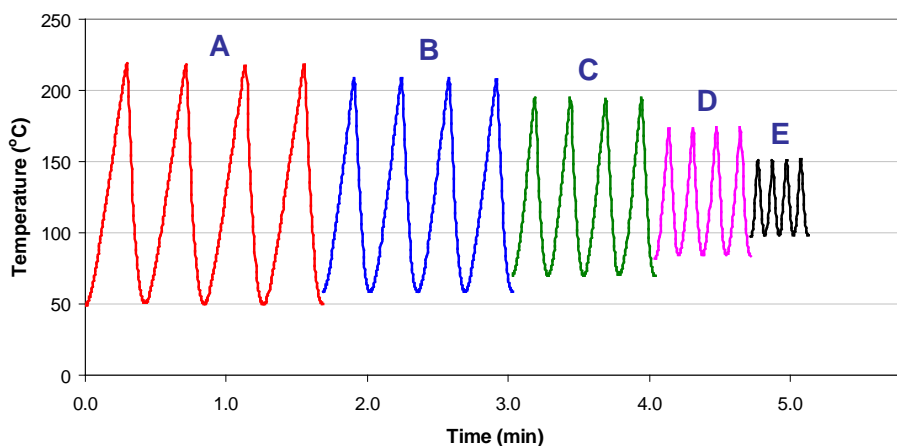
had a significant effect on the cooling speed and on the minimum and maximum gradient temperature limits. The gradient linear velocity also played an important role in the temperature range that the gradient could achieve (Figure 6-13). If the gradient speed was increased, less time was available for cooling and heating and, thus producing a smaller temperature range. This can be clearly seen in Figure 6-13, where the temperature range decreased as the linear velocity of the sawtooth temperature gradient increased.

Although, the system was capable of producing sawtooth gradients with a broad range of gradient linear velocities, only a small temperature difference of 50°C was achieved for the fastest gradient (Figure 6-13). Since the analytes move with the gradient at their  $T_{eq}$ , a gradient with a large temperature range is desirable to include a broad volatility range of compounds.

The limiting factor for achieving fast moving gradients with a wide temperature ranges in the current design is the temperature of the convective cooling fluid. High heating rates could be easily achieved by increasing the heating voltage, which also



**Figure 6-12. Sawtooth linear temperature gradient profiles with different slopes. (a)  $0.73^{\circ}\text{C}/\text{cm}$ , (b)  $1.44^{\circ}\text{C}/\text{cm}$ , (c)  $2.07^{\circ}\text{C}/\text{cm}$  and (d)  $2.75^{\circ}\text{C}/\text{cm}$ . The gradient velocity was  $2.22\text{ cm/s}$  ( $45\text{ s/rev}$ ).**



**Figure 6-13. Sawtooth linear temperature profiles as a function of gradient linear velocity; the heating voltage and times for heating and cooling were kept constant. (A)  $25\text{ s/rev}$ , (B)  $15\text{ s/rev}$ , (C)  $10\text{ s/rev}$  and (D)  $5\text{ s/rev}$ .**

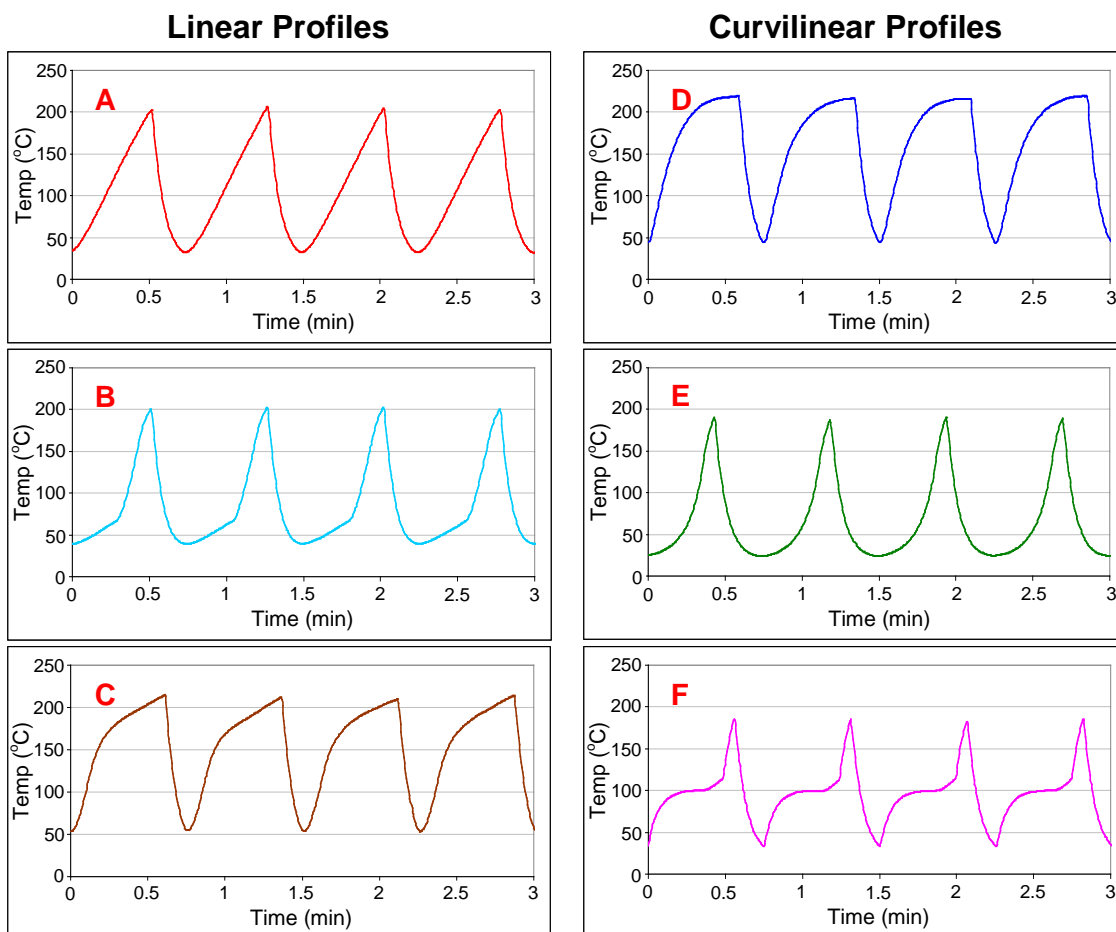
raised the upper temperature limit of the gradient. However, achieving lower temperatures required cooling the air (*i.e.*, air conditioner) or placing the resistively heated coil arrangement inside a cold environment, such as in a conventional GC oven with cryogenic cooling. Lower convective air temperatures broaden the temperature

range of the gradient by reducing the cooling time. With the current system, cooling from 200°C to 30°C requires 11 s (Figure 6-12). This implies, that for a gradient moving at 22 s/rev with a cooling time of 11 s, 50% of the time must be used for cooling. As a result, the gradient was generated in only 50 cm of the column. A compromise between separation time and the length of column used for separation had to be made. A gradient velocity of 2.22 cm/s (45 s/rev) was chosen for the separations in this work, since it provided a wide temperature range [30°C to 200°C (Figure 6-12)] and a relatively fast separation (every 45 s). At this speed, the cooling time represented 25% of the total separation time and, hence, separations were performed in 75 cm of the 100 cm available in the temperature gradient for each tooth. Increasing the length of column used for separation above 75 cm came at a cost of longer separation times.

The ability of the moving TGGC instrument to generate custom temperature gradient profiles was tested using a gradient velocity of 2.22 cm/s (45 s/rev). Figure 6-14 shows a variety of sawtooth temperature profiles in which linear (Figures 6-14A, B and C), and curvilinear (Figures 6-14D, E and F) gradients were created. In this figure, adequate reproducibility of the temperature gradient was observed for the different profiles. As seen in Figure 6-14, the moving TGGC system design not only created linear gradients with several slopes (Figures 6-14B and C), but also curvilinear gradients with challenging profile designs, such as the one in Figure 6-14F. A gradient slopes of 8.7°C/cm for the steepest region in Figure 6-14F, and cooling rates over 1000°C/min were observed. The TGGC system was capable of achieving gradient slopes as high as 16°C/cm. The temperature gradients shown in Figure 6-14, and their combination, such as in Figure 6-14F, encompasses a wide range of possibilities, demonstrating the ability

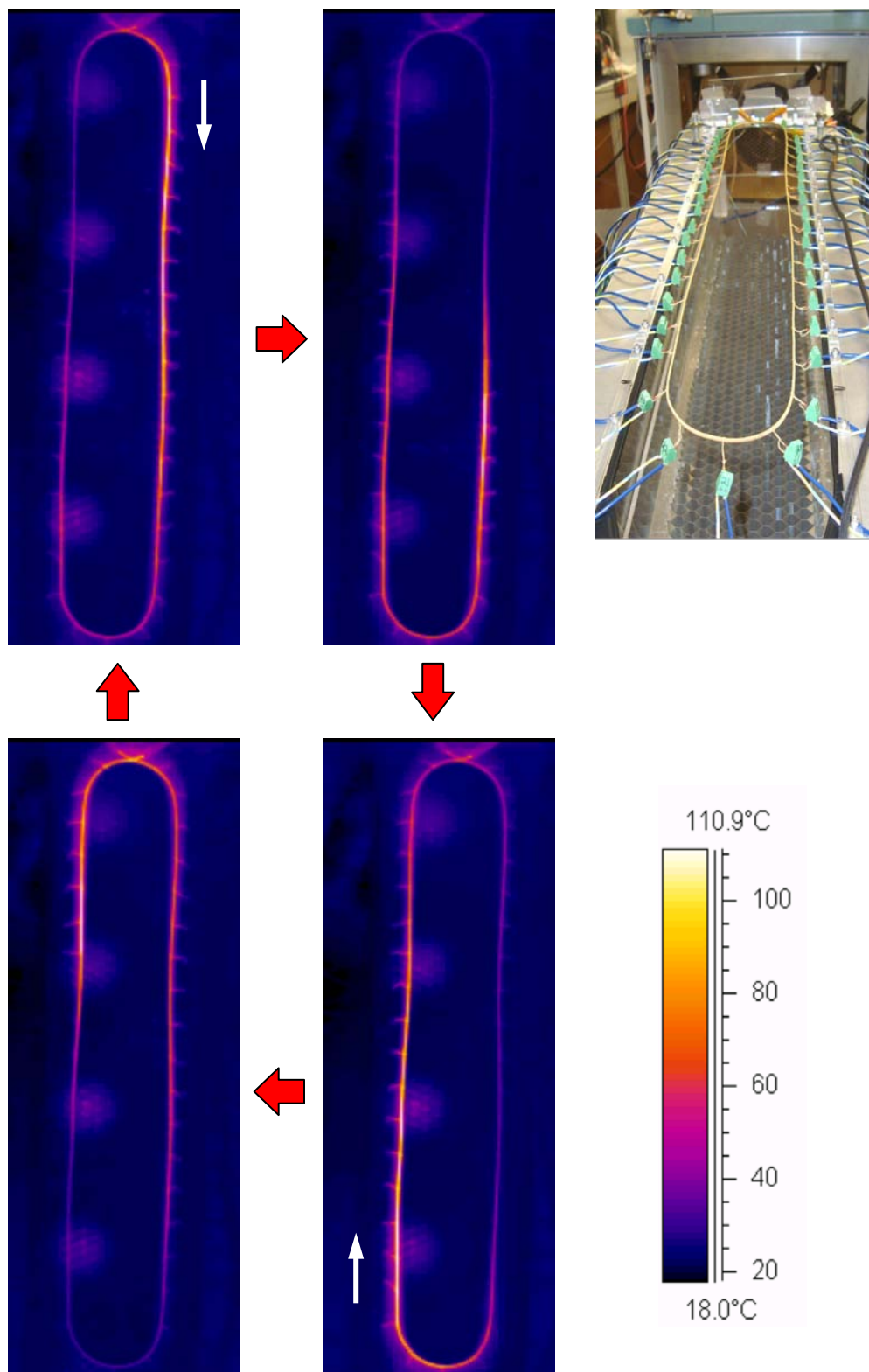
of the moving TGGC system to produce custom temperature profiles. This unique system flexibility allowed exploration of the separation potential of the moving TGGC technique.

The moving temperature gradient along the column was monitored with an infrared (IR) camera to ensure the proper operation of all resistive heating sections. Figure 6-15 shows a cycle of a moving linear gradient along the column loop in a series of IR photographs. In this figure, the resistively heated column regions can be seen heating and cooling to form the moving gradient profile.



**Figure 6-14. Different sawtooth temperature gradient profiles generated with the moving TGGC system. (A) Linear, (B) two slopes low-high, (C) two slopes high-low (D) concave down, (E) concave up, and (F) combination of concave up and down profiles. A gradient velocity of 2.22 cm/s (45 s/rev) was used.**



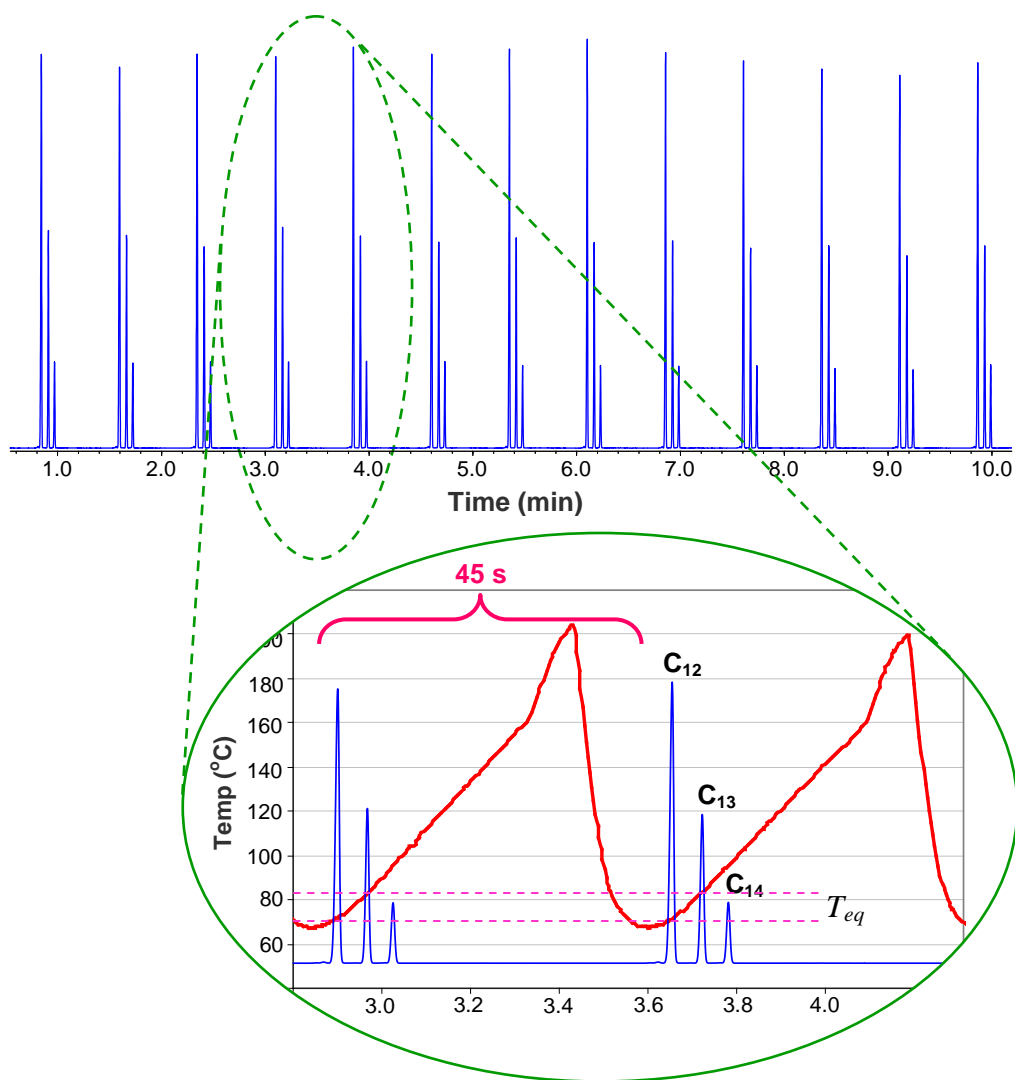


**Figure 6-15. Infrared photographs of the moving TGGC system showing a linear temperature gradient moving around the column loop. The white arrows indicate the clockwise rotation direction of the moving gradient.**

The smooth temperature transition between the individual resistively heated sections can be observed in Figure 6-15, demonstrating good temperature conduction as a result of using the Ni sleeve. Infrared measurements verified that the system generated custom moving temperature profiles (Figure 6-15).

### 6.3.2 Testing of the Moving TGGC System

For testing the moving TGGC system, continuous introduction of the headspace of a mixture of normal alkanes from dodecane to tetradecane ( $C_{12}$ - $C_{14}$ ) was performed. A series of chromatograms, as a result of continuous sampling and separation by the moving sawtooth temperature gradient, can be seen in Figure 6-16. The repetitive chromatograms in this figure validate the system design and demonstrate the separation capability of the moving TGGC system. Even though the injected bands were 45 s wide, narrow peaks with good resolution were obtained (Table 6-1), demonstrating the focusing effect of moving axial negative temperature gradients. In Figure 6-16, it can be observed that each normal alkane eluted at its  $T_{eq}$  ( $C_{12} = 72^{\circ}\text{C}$ ,  $C_{13} = 84^{\circ}\text{C}$ , and  $C_{14} = 96^{\circ}\text{C}$ ), a characteristic that is unique to this separation technique. The higher resolution between  $C_{12}$ - $C_{13}$  can be attributed to the slightly shallower slope where  $C_{12}$  is located, positioning its  $T_{eq}$  farther apart from the  $T_{eq}$  of  $C_{13}$ . The shallower slope also explains the wider peak width of  $C_{12}$  given in Table 1-1. In this table, it can also be observed that a low percent relative standard deviation (%RSD) for peak widths and peak areas were obtained (< 2.3%), which indicates the high reproducibility of the generated sawtooth temperature profiles, and high sampling uniformity. These results show that the resistively heated moving TGGC instrument operated properly and allowed the continuous analysis of a mixture of normal alkanes.



**Figure 6-16.** Continuous analysis of n-alkane vapors using a moving sawtooth temperature profile, with resultant repetitive chromatograms. Zoom of the chromatogram shows the temperature gradient profile used. The average resolution values are  $C_{12}$ - $C_{13} = 4.1$ , and  $C_{13}$ - $C_{14} = 3.8$ . The separation conditions were: 70 psig head pressure, 2.88 mL/min mobile phase flow, 2.22 cm/s (45 s/rev) gradient velocity, and 1.64°C/cm gradient slope for the largest linear temperature region.

**Table 6-1.** Peak widths and percent relative standard deviations obtained from continuous analysis of normal alkanes.

Compound	Peak Width (s)	%RSD	
		Peak Width	Peak Area
<i>n</i> -C12	1027	2.75	0.69
<i>n</i> -C13	935	4.10	2.51
<i>n</i> -C14	925	3.05	2.19

### 6.3.3 Effect of Axial Temperature Gradients on Separation

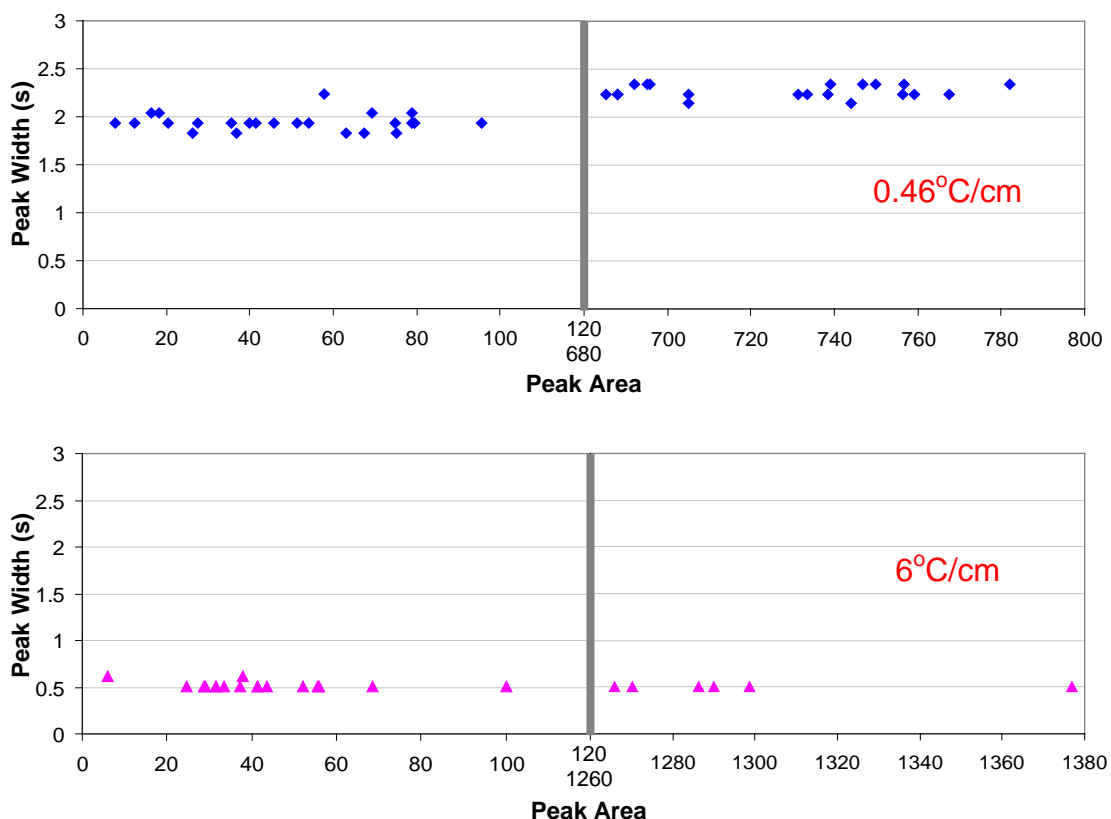
The capability of the moving TGGC system to accurately control the temperature gradient profiles provided the opportunity to evaluate experimentally the effect of axial temperature gradients on separation.

#### 6.3.3.1 Effect of Sample Size on Peak Width

For these experiments, a linear gradient profile was maintained and the amount of sample injected was varied. The test was performed with only n-tridecane ( $C_{13}$ ) to avoid coelution and to allow adequate measurements of the peak width when steep gradients were used. To provide a wide range of sample sizes, the head space above liquid analyte was injected using a gastight syringe, and the continuous sampling system described in Chapter 5 was used. Figure 6-17 shows the peak width of  $C_{13}$  for a shallow ( $0.46^{\circ}\text{C}/\text{cm}$ ) and a steeper ( $6^{\circ}\text{C}/\text{cm}$ ) gradient slope. From this figure, it can be observed that the sample amount has little effect on the peak width. This is more evident for the steeper slope where even an increase in an order of magnitude of the sample amount did not cause a significant change in the peak width. On the other hand, a small increase of 16.8% was observed for the shallower slope (Table 6-2).

These results demonstrate the focusing effect of the moving TGGC technique; a greater temperature difference with respect to the  $T_{eq}$  (steeper gradient) provides a stronger focusing effect, allowing peak widths to be less affected by the amount of sample introduced. This characteristic of the moving TGGC technique allows for long injection times (45 s) that can be used to concentrate analytes in the column (on-column sample pre-concentration).<sup>2</sup> The large sample introduction ability combined with focusing of the analytes leads to enhancement of the detection limits of the system as

narrower and taller peaks are produced, which is of great interest for performing trace analysis. The amount of sample proved to have little effect on peak width; however, the gradient slope, on the other hand, showed the opposite. This was evident with a decrease in peak widths of over 70% with a steeper temperature gradient (Figure 6-17).



**Figure 6-17. Peak width of C<sub>13</sub> as a function of the amount of sample injected for two different gradient slopes. To the right of the horizontal line in the plots, the effect of a larger amount of sample is shown. Separation conditions: 60 psig head pressure, 2.28 mL/min mobile phase flow, and 2.22 cm/s (45 s/rev) gradient velocity.**

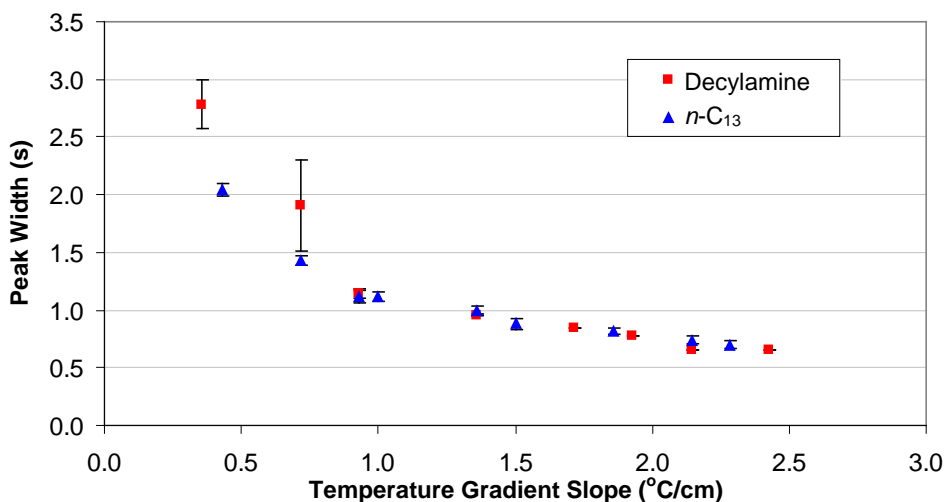
**Table 6-2. Peak widths and relative standard deviations obtained for n-tridecane at two different gradient slopes and various concentrations.**

	0.46°C/cm		6°C/cm	
	Average	%RSD	Average	%RSD
Lower concentration	1.94	4.61	0.519	5.66
Higher concentration	2.27	2.96	0.51	0

### 6.3.3.2 *Effect of Gradient Slope on Peak Width and Peak Symmetry*

In moving TGGC, the gradient slope has a great impact on the peak width of analytes, as observed in Figure 6-17. Thus, understanding its effect can help to maximize the separation power of the technique. The gradient slope was evaluated for its effect not only on the peak widths of analytes, but also on peak symmetry. Peak tailing, which is evident when the later eluting half of the peak is wider than the front half, can significantly affect the quality of the separation and the system detection limit. However, the focusing effect of the moving TGGC technique can be a solution to this problem.<sup>5</sup> Polar compounds commonly exhibit peak tailing in columns coated with nonpolar stationary phases due to surface activity from adsorption sites such as silanol groups and metal oxide sites.<sup>21-25</sup> Even commercial capillary columns show some surface activity, since there are always residual active sites after surface passivation.<sup>26</sup> For this reason, separation of samples containing compounds with wide polarity can be challenging. Polar compounds that are very sensitive to surface activity are amines.<sup>26-28</sup> Therefore, the effect of the gradient slope on peak widths was evaluated for polar (decylamine) and nonpolar (C<sub>13</sub>) compounds (Figure 6-18). The effect of the gradient slope on the peak width can be clearly seen in Figure 6-18, where a 5 times increase in the gradient slope produced over a 65% decrease in the peak widths for C<sub>13</sub> and decylamine. The focusing strength in moving TGGC increases with gradient slope, producing narrower peaks as observed in Figure 6-18. Although wider peak widths for the polar compound were observed for gradient slopes below 1°C/cm, at steeper slopes, both polar and non-polar analyte peak widths were comparable. These results suggest that the focusing effect is to some extent independent of the analyte type, which is beneficial for the analysis of mixtures

containing both polar and nonpolar compounds. The minimum achievable peak width is a function of the band broadening process, as well as the temperature gradient resolution in the column (currently 1" sections). Further tests using different stationary phase film thicknesses and columns with improved temperature gradient resolution will be required to determine the factors that affect the minimum peak width.



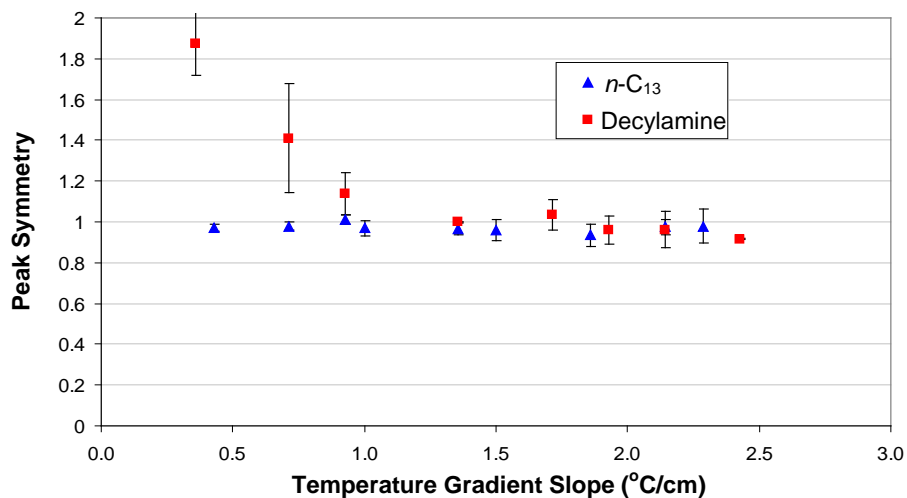
**Figure 6-18. Peak width of polar (decylamine) and nonpolar ( $n\text{-C}_{13}$ ) compounds as a function of the gradient slope. Separation conditions: 60 psig head pressure, 2.28 mL/min mobile phase flow, and 2.22 cm/s (45 s/rev) gradient velocity.**

The peak symmetries of decylamine and  $\text{C}_{13}$  were determined by<sup>10</sup>

$$As = \frac{\text{actual peak width}}{\text{width of symmetrical peak}} = \frac{a+b}{2a} \quad (1)$$

where  $a$  is the width of the front half of the peak and  $b$  is the width of the back half of the peak measured at 10% of the peak height from the leading or trailing edges of the peak to a line dropped perpendicularly from the peak apex. The peak symmetry value of a symmetrical peak is 1; tailing and fronting peaks give values above and below 1, respectively. Figure 6-19 shows the peak symmetries for  $\text{C}_{13}$  and decylamine for various

gradient slopes. For the case of  $C_{13}$ , the gradient slope did not have a major effect on its peak symmetry (Figure 6-19). However, most of the peaks had narrower front peak halves as a result of the gradient itself, which slows down the leading edge of the peak and accelerates the tailing edge, making the peak apex move closer to the front edge. On the other hand, a significant improvement of peak symmetry for decylamine was observed (Figure 6-19) with an increase in the gradient slope.

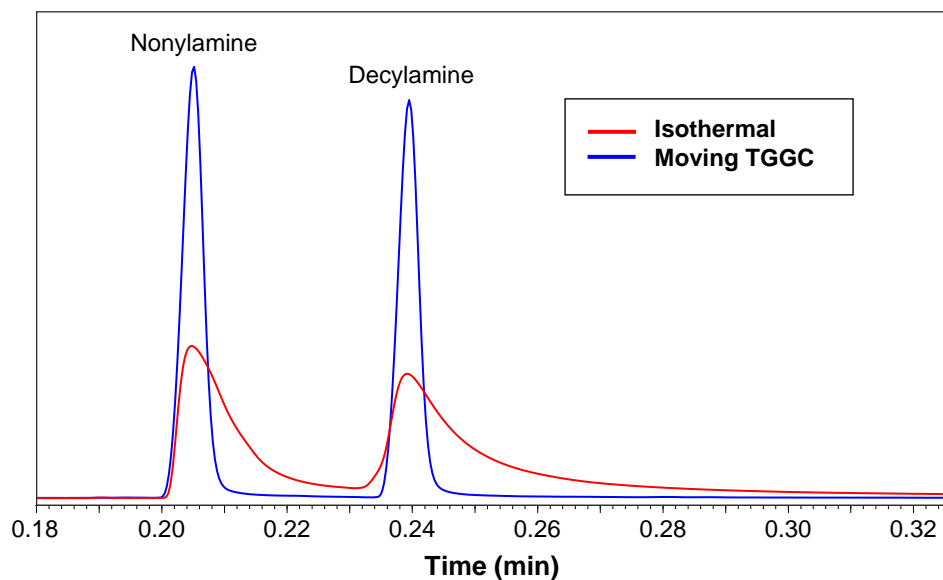


**Figure 6-19. Peak symmetry of polar (decylamine) and nonpolar ( $n-C_{13}$ ) compounds as a function of gradient slope for a column coated with a slightly polar stationary phase (5% diphenyl, 95% dimethyl polysiloxane). Separation conditions: 60 psig head pressure, 2.28 mL/min mobile phase flow rate, and 2.22 cm/s (45 s/rev) gradient velocity.**

Under gradient conditions, the trailing fraction of a peak is always at higher temperature than its  $T_{eq}$  and, hence, it constantly moves faster than the velocity of the peak apex to catch up to its  $T_{eq}$ . For decylamine, tailing was overcome after a gradient of  $1^{\circ}\text{C}/\text{cm}$  (Figure 6-19), gradient velocity of 2.22 cm/s and mobile flow rate of 2.28 mL/min.

Figure 6-20 shows a comparison of peak symmetries between isothermal and moving TGGC separation of nonylamine and decylamine, where a considerable





**Figure 6-20. Peak shape comparison of isothermal and moving TGGC separations of nonylamine and decylamine. For the isothermal separation,  $As_{\text{nonylamine}} = 6.3$  and  $As_{\text{decylamine}} = 6.8$ , with a resolution of 1.5. For the moving TGGC separation,  $As_{\text{nonylamine}} = 1.0$  and  $As_{\text{decylamine}} = 0.9$ , with a resolution of 5.1. Separation conditions: 195°C for the isothermal separation, 20 psig head pressure, 0.34 mL/min mobile phase flow, 3.28°C/cm gradient slope, and 2.22 cm/s (45 s/rev) gradient velocity.**

improvement in peak symmetry (*i.e.*, reduced tailing) is observed for the moving TGGC method. The peak shape improvement not only provided a threefold increase in the resolution, but also doubled the signal-to-noise. Peak shape plays an important role in resolution and detection (Figure 6-19), especially in trace analysis, since tailing peaks often overlap, limiting quantification. Tailing peaks can also become a problem when minor peaks are covered by the tail. The moving TGGC technique proved to be a good solution to improve tailing. These results show that for a given gradient and mobile phase linear velocity, the peak width in moving TGGC is somewhat independent of analyte concentration and type (*i.e.*, polar or nonpolar), and mostly dependent on the gradient slope. This characteristic can be used to optimize the peak widths of individual analytes

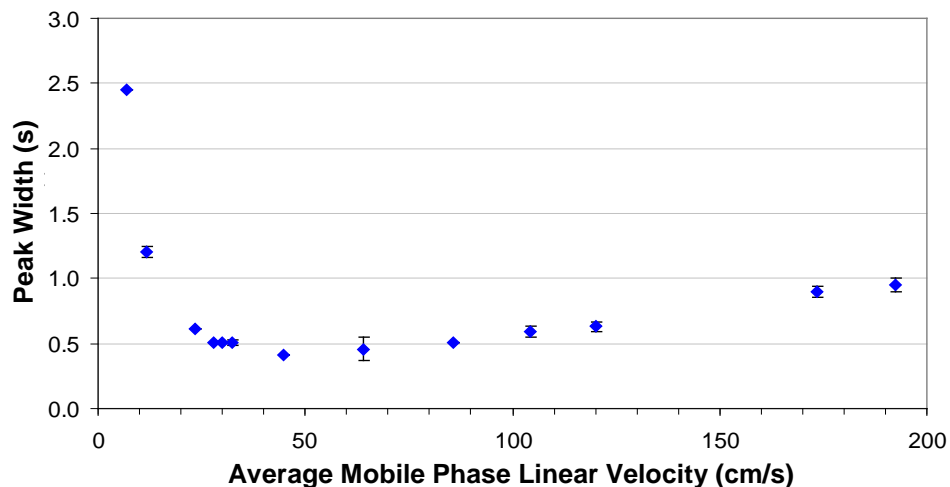
by modifying the gradient slope under the peaks, improving separation, signal-to-noise, and tailing.

### ***6.3.3.3 Effect of Mobile Phase Linear Velocity on Peak Width***

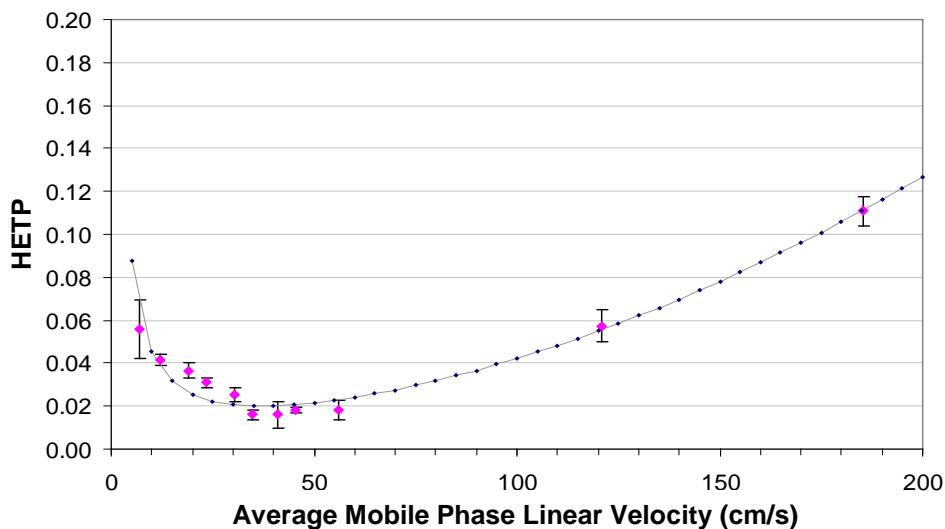
The focusing effect in moving TGGC aids in counteracting band broadening due to longitudinal diffusion and resistance to mass transfer, as can be seen in Figure 6-21. In this figure, the peak width of C<sub>13</sub> was measured for various mobile phase linear velocities while keeping the moving TGGC gradient slope and velocity constant (Figure 6-21). The plot obtained was similar to a van Deemter curve<sup>10</sup> with a minimum band width at an optimal velocity. For comparison, the van Deemter plot for C<sub>13</sub> was determined using the moving TGGC column under isothermal conditions at 125°C (Figure 6-22). The van Deemter curve obtained is similar to Figure 6-21, with optimum linear velocity around 40 cm/s for both plots. These results demonstrate peak broadening effects in moving TGGC.

At the optimum linear velocity, peak widths as narrow as 200 ms were obtained for a gradient slope of 11.26°C/cm with resistive heating sections of 1". Smaller peaks should be possible using a system with higher axial temperature gradient resolution (< 1" wide heated sections).

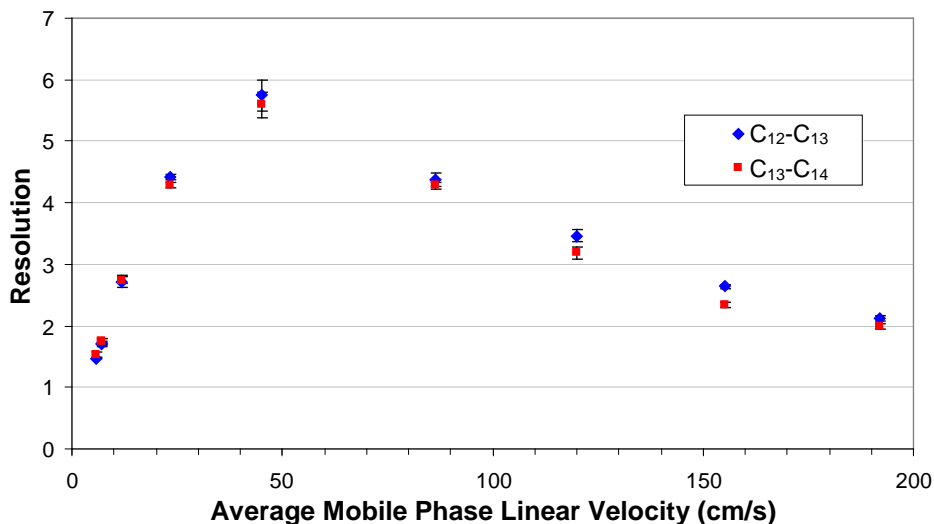
The effect of the mobile phase linear velocity on separations in moving TGGC can be seen in Figure 6-23. In this figure, the resolution between normal alkanes (C<sub>12</sub>-C<sub>13</sub> and C<sub>13</sub>-C<sub>14</sub>) is plotted as a function of the mobile phase linear velocity. As can be observed in this figure, maximum resolution is achieved near the optimum linear velocity. Regardless of the focusing effect of moving TGGC, the broadening processes still affect chromatographic performance.



**Figure 6-21.** Peak width as a function of the mobile phase linear velocity for constant gradient slope and velocity. Separation conditions: 60 psig head pressure, 2.28 mL/min mobile phase flow, 2.22 cm/s (45 s/rev) gradient velocity, and 2.75°C/cm gradient slope. The linear sawtooth profile used is plot d in Figure 6-12.



**Figure 6-22.** Van Deemter plot for  $C_{13}$  where HETP is the height equivalent to a theoretical plate.<sup>10</sup> For isothermal separations, the entire TGGC column length was held constant at 125°C.



**Figure 6-23. Resolution of 2 normal alkane pairs (C<sub>12</sub>-C<sub>13</sub> and C<sub>13</sub>-C<sub>14</sub>) as a function of the mobile phase linear velocity for a constant moving TGGC gradient slope. Separation conditions: 2.22 cm/s (45 s/rev) gradient velocity and 2.75°C/cm gradient slope. The linear sawtooth profile used is plot d in Figure 6-12.**

#### 6.3.3.4 Effect of the Gradient Slope on Separation

From the previous discussion, it was determined that increasing the gradient slope produced narrower peaks; however, its effect on separation must also be evaluated. For this purpose, a mixture of normal alkanes (C<sub>12</sub>-C<sub>14</sub>) was separated using various linear gradient slopes (Figure 6-24). Evenly spaced peaks in all of the chromatograms in Figure 6-24 demonstrate the linearity of the gradients used. With an increase in gradient slope, the peaks became closer faster than they become narrower, thus, decreasing their resolution. A broader view of this effect can be seen in Figure 6-25 where plots of resolution of two n-alkane pairs as a function of the gradient slope up to 11°C/cm are shown. In this figure, an overall decrease in resolution is observed as the gradient slope increases. The slower decrease in rate of resolution loss at higher gradient slopes is a result of the axial temperature gradient resolution of the system. Since analytes elute at

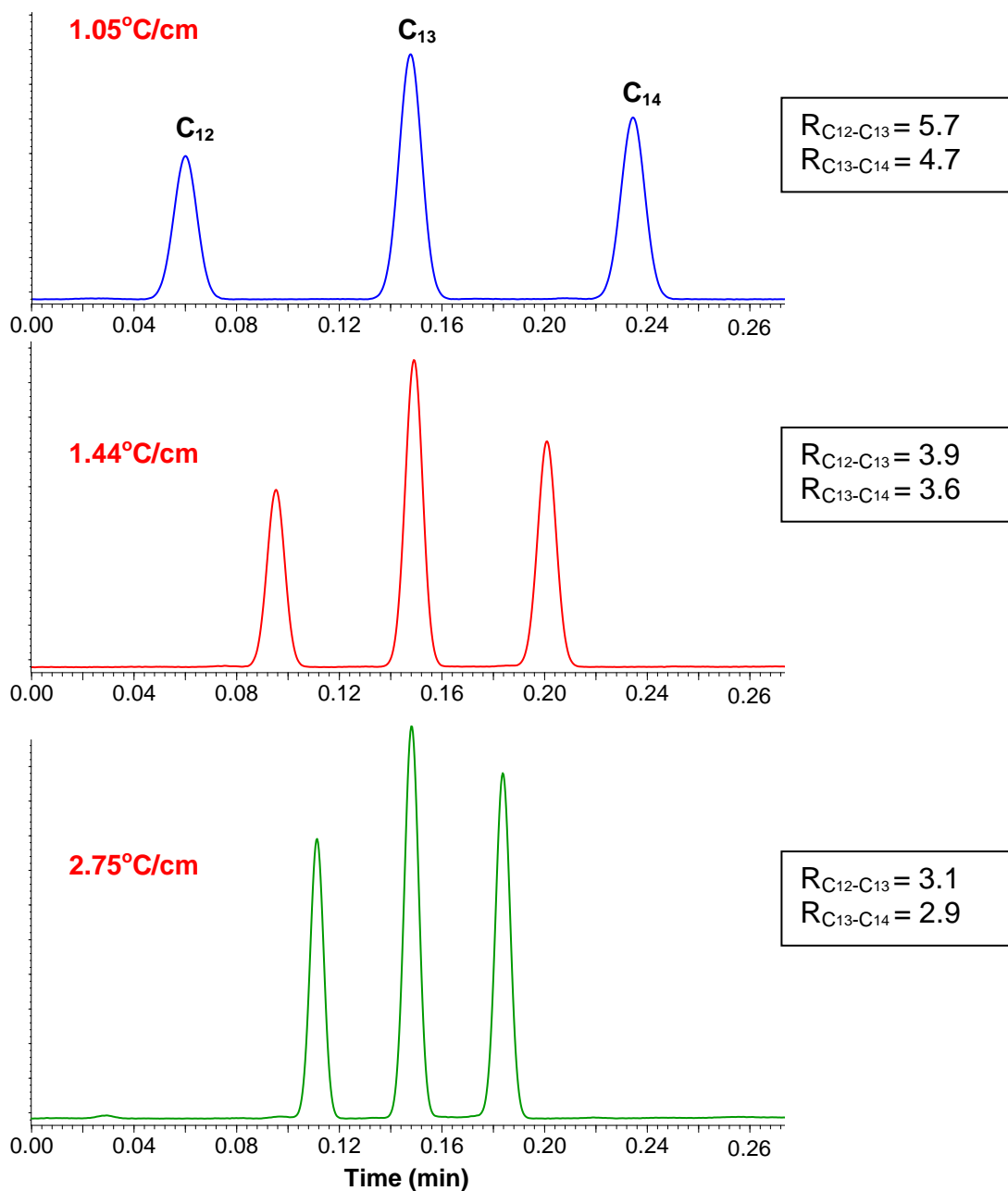
their  $T_{eq}$  values in moving TGGC, steeper linear temperature gradients should place the  $T_{eq}$  values of the analytes closer to each other. However, smooth steep gradients are difficult to generate with our current system, since the resistively heated sections are 1” (2.54 cm) in length. From Figure 6-25, the resolution rate slows down after 3°C/cm; therefore, this must be close to the best gradient achievable for this system. Further experiments using a system with higher axial temperature resolution should be performed to determine the factors affecting the minimum resolution observable. These results show that band broadening plays an important role in moving TGGC.

#### **6.3.4 Use of Custom Gradient Profiles**

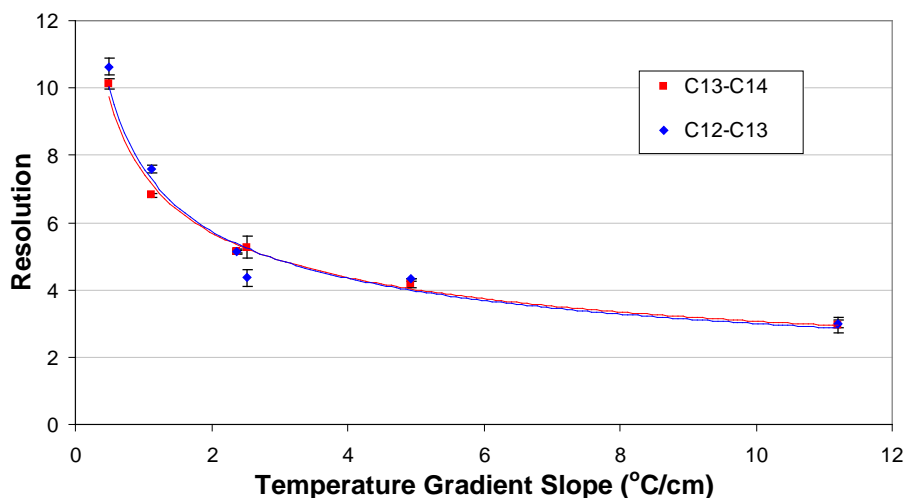
In moving TGGC, since the analytes migrate at their specific  $T_{eq}$  values (Figure 1-1), the temperature gradient profile determines the elution positions of the analytes and, hence, their separation. This is a unique and fundamental characteristic of the technique that has not been exploited before. The ability of the moving TGGC system to generate different sawtooth temperature gradient profiles has allowed us to explore this intriguing possibility. The resultant repetitive chromatograms from continuous sampling of three normal alkane vapors ( $C_{12}$ - $C_{14}$ ) obtained with custom temperature gradients are shown in Figure 6-26.

The high reproducibility of the peak areas and widths obtained (Table 6-3) demonstrates the uniformity of the custom sawtooth temperature profiles generated and the potential for sample quantification using this technique. Manipulating the moving gradient profile has allowed unique control of the separation power, improving separations of analytes, as well as selectively increasing peak capacity and signal-to-noise (S/N) due to the focusing effect of the negative temperature gradient. All of these effects

can be seen in Figure 6-26. Figure 6-26A shows the results of a steep gradient ( $6^{\circ}\text{C}/\text{cm}$ ), which placed all  $T_{eq}$  values close together and reduced the peak capacity (Table 6-3). In



**Figure 6-24. Separation of normal alkanes ( $\text{C}_{12}\text{-C}_{14}$ ) using different gradient slopes. Linear sawtooth profiles were used. Separation conditions: 60 psig head pressure, 2.28 mL/min mobile phase flow, 2.22 cm/s (45 s/rev) gradient velocity.**



**Figure 6-25. Resolution of two pairs of normal alkanes (C<sub>12</sub>-C<sub>13</sub> and C<sub>13</sub>-C<sub>14</sub>) as a function of the temperature gradient slope. Separation conditions: 20 psig head pressure, 0.34 mL/min mobile phase flow, 2.22 cm/s (45 s/rev) gradient velocity, and 2.75°C/cm gradient slope.**

Figure 6-26B, the temperature profile used was shallower (0.5°C/cm), increasing the usage of the column space, which resulted in an overall separation improvement. This can be seen in the total peak capacity achieved (Table 6-3).

The shallow temperature profile evenly spread the  $T_{eq}$  of the analytes which resulted in equal resolution between the peaks (Table 6-3). Figure 6-26C shows how improvement in the peak capacity between C<sub>13</sub>-C<sub>14</sub> can be achieved using a customized temperature profile. An improvement of 80% in peak capacity was achieved compared to Figure 6-26B (Table 6-3). Although an improvement in peak capacity was achieved between C<sub>13</sub>-C<sub>14</sub>, the total peak capacity only increased slightly. Customized gradients allow efficient management of the column separation space by providing more column space for the section of the chromatogram that requires additional resolution. Another capability that custom temperature profiles offer can be seen in Figure 6-26D, where selective improvement of the S/N is shown for C<sub>14</sub>. As previously discussed, the peak width of the analyte in the moving TGGC technique is a function of the gradient slope.

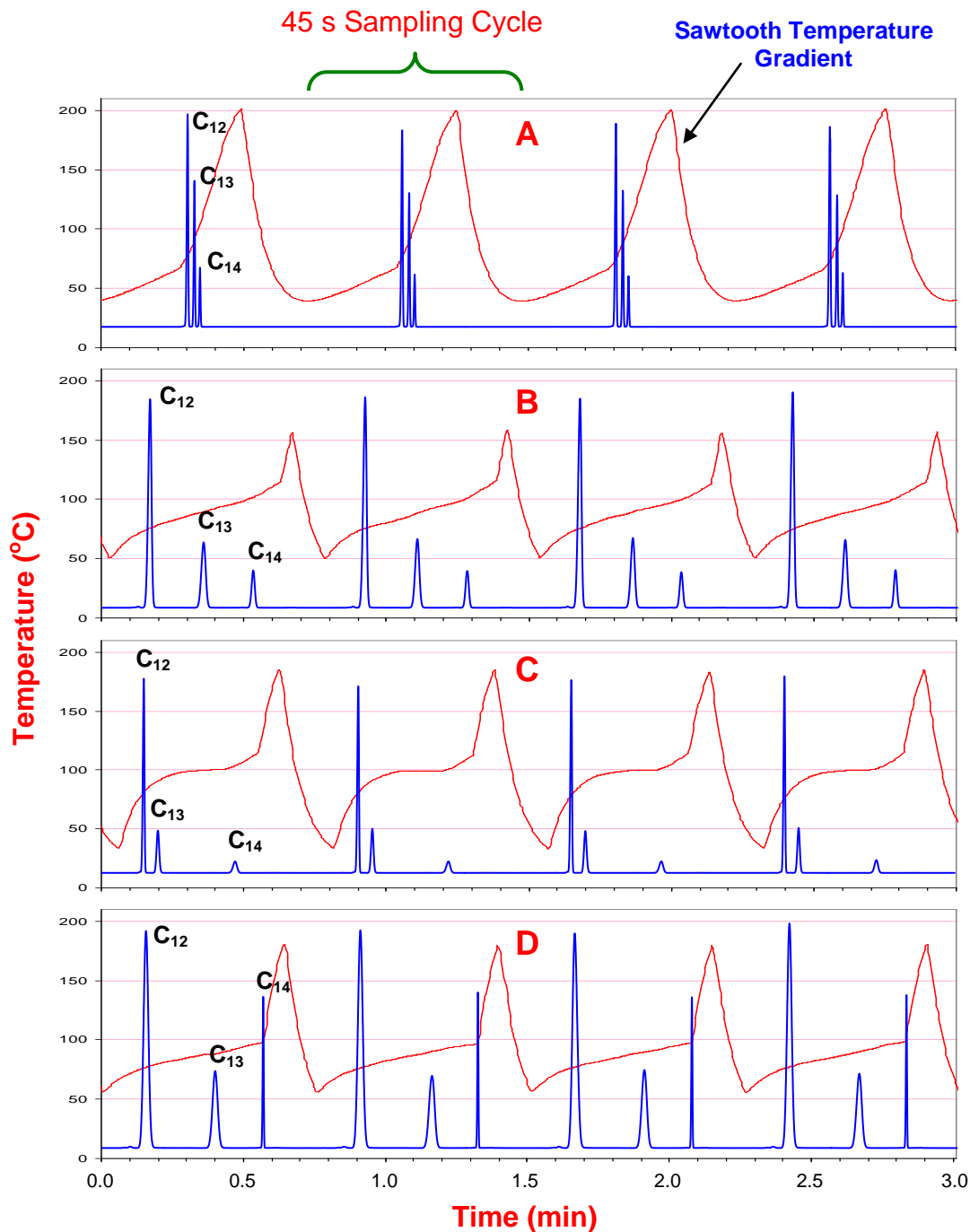
However, it was also discussed that steeper gradients provided less resolution, and this remains true when both compounds are subjected to a linear gradient.

In a customized gradient profile, the gradient slope under a peak can be selectively adjusted, improving S/N without decreasing resolution as shown in Figures 6-26D and 6-27. In Figure 6-27, a resolution as high as 46 was achieved with a peak width of 300 ms, demonstrating the capability of the technique to selectively optimize the peak width. The use of a more precise temperature gradient could limit the steeper gradient slope change to the band width of the targeted peak. The separations shown in Figures 6-26 and 6-27 demonstrate the unparallel separation flexibility of the moving TGGC technique that allows unique control of the movement and elution of compounds and, hence, their separation. The separations in Figure 6-26 could probably be performed by TPGC using a GC system with fast heating and cooling rates, and a multi-ramp program, which takes a long time to optimize. In contrast, in moving TGGC, the optimized profile can be determined after the first separation is performed, since it provides the  $T_{eq}$  values of the analytes. The temperature profile can be then be adjusted to produce the most efficient separation. This characteristic makes moving TGGC an appealing technique for facilitating method development and, potentially, automated optimization of separations through feedback control.

### **6.3.5 Experimental Comparison of Moving TGGC with TPGC Separations**

For performing TPGC, a different GC system was required, since the moving TGGC instrument was not programmed for simultaneously heating all of the resistively heated sections at the same temperature. Furthermore, in order to make a good comparison between the two separation methods, the column lengths needed to be the

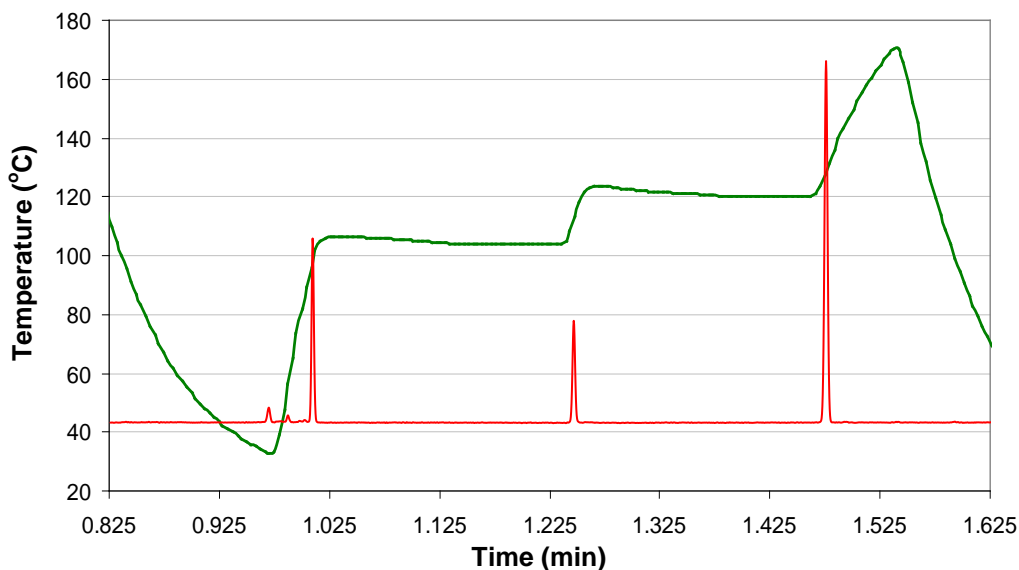




**Figure 6-26.** Chromatograms resulting from four different custom moving sawtooth axial temperature gradient profiles for continuous sampling of three normal alkane vapors. The chromatograms show the unique control of selectivity using the TGGC technique. Separation conditions: 60 psig head pressure, 2.28 mL/min mobile phase flow, and 2.22 cm/s (45 s/rev) gradient velocity. The  $T_{eq}$  for the alkanes were C<sub>12</sub> = 77.7°C, C<sub>13</sub> = 90.0°C, and C<sub>14</sub> = 99.3°C.

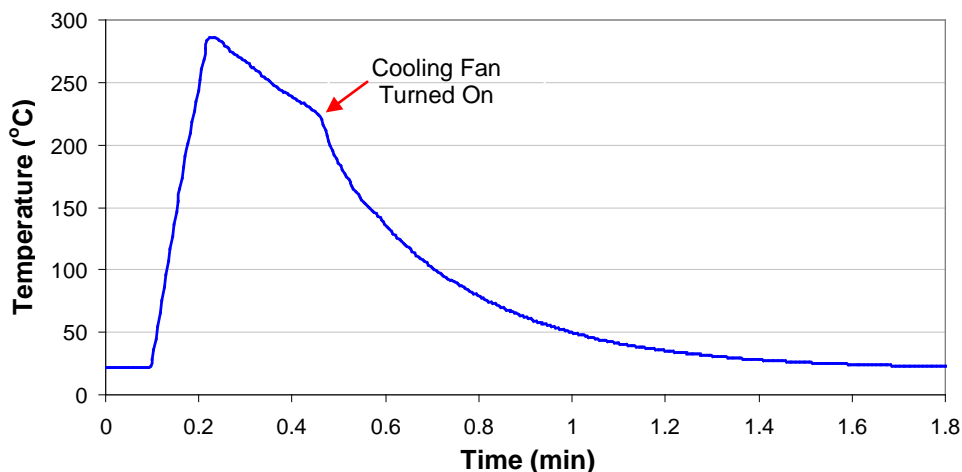
**Table 6-3. Peak widths, resolution, peak capacity and relative standard deviations obtained for the normal alkanes (C<sub>12</sub>-C<sub>14</sub>) separated using different gradient profiles.**

Plot	Analytes	Peak Width (s)	% RSD Peak Width	% RSD Peak Area	Resolution	Peak Capacity
<b>A</b>	C <sub>12</sub>	0.61	0.00	2.15	C <sub>12-13</sub> = <b>2.68</b> C <sub>13-14</sub> = <b>2.29</b>	C <sub>12-13</sub> = <b>1.7</b>
	C <sub>13</sub>	0.51	0.00	1.07		C <sub>13-14</sub> = <b>1.3</b>
	C <sub>14</sub>	0.51	0.00	1.69	<b>Total = 4.0</b>	
<b>B</b>	C <sub>12</sub>	1.43	0.00	1.49	C <sub>12-13</sub> = <b>6.91</b> C <sub>13-14</sub> = <b>6.61</b>	C <sub>12-13</sub> = <b>5.9</b>
	C <sub>13</sub>	1.84	2.82	0.73		C <sub>13-14</sub> = <b>5.6</b>
	C <sub>14</sub>	1.33	3.77	0.94	<b>Total = 12.5</b>	
<b>C</b>	C <sub>12</sub>	0.71	0.00	0.76	C <sub>12-13</sub> = <b>3.27</b> C <sub>13-14</sub> = <b>11.22</b>	C <sub>12-13</sub> = <b>2.2</b>
	C <sub>13</sub>	1.12	4.65	0.41		C <sub>13-14</sub> = <b>10.3</b>
	C <sub>14</sub>	1.73	6.06	1.14	<b>Total = 13.5</b>	
<b>D</b>	C <sub>12</sub>	2.04	4.08	1.10	C <sub>12-13</sub> = <b>6.81</b> C <sub>13-14</sub> = <b>7.32</b>	C <sub>12-13</sub> = <b>5.8</b>
	C <sub>13</sub>	2.24	2.25	1.16		C <sub>13-14</sub> = <b>6.2</b>
	C <sub>14</sub>	0.51	10.53	0.77	<b>Total = 13.0</b>	



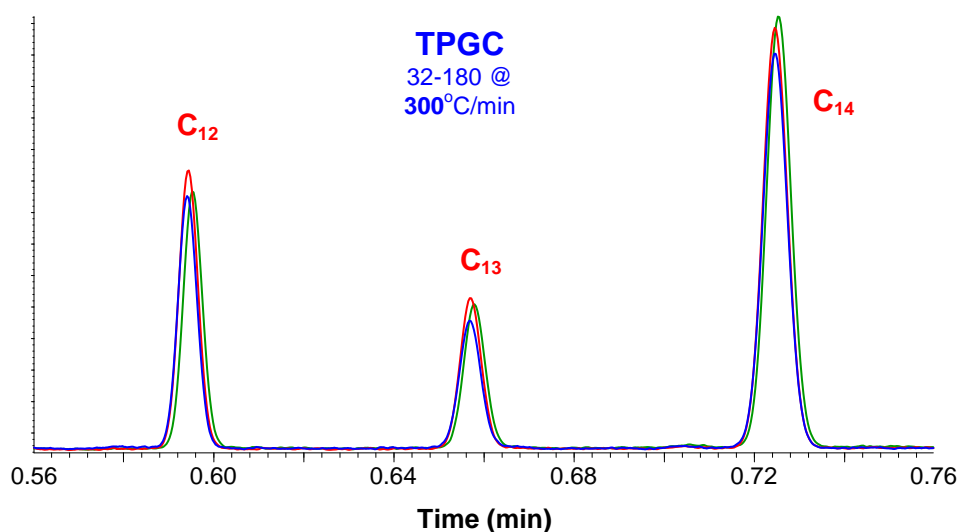
**Figure 6-27. Separation of normal alkanes (C<sub>12</sub>-C<sub>14</sub>) using a custom gradient profile for maximizing resolution and S/N. Separation conditions: 20 psig head pressure, 0.34 mL/min mobile phase flow, 8.2°C/cm gradient slope where the  $T_{eq}$  values of the peaks were located, and 2.22 cm/s (45 s/rev) gradient velocity. The  $T_{eq}$  for the alkanes were C<sub>12</sub> = 99°C, C<sub>13</sub> = 111°C, and C<sub>14</sub> = 128°C. Resolution: C<sub>12</sub>-C<sub>13</sub> = 46.5 and C<sub>13</sub>-C<sub>14</sub> = 41.5.**

same. In moving TGGC, the separation takes place in the length of column where the gradient is generated. For our TGGC instrument, even though the column used was 3 m in length, the maximum gradient length was 1 m. For this reason TPGC separations were also performed using a 1 m column. However, due to the fast separations obtained with the moving TGGC system, heating rates greater than 200°C/min were required. This high heating rate cannot be achieved with conventional GC systems; therefore, a new resistive heating approach was developed for fast TPGC separations. The column assembly was described in Section 6.2.2. Heating rates as high as 2100°C/min and cooling times of 30 s from 250 to 50°C were possible (Figure 6-28). High reproducibility of analyte retention time (< 0.3 %RSD) under TPGC operations, can be seen in Figure 6-29. Gaussian peak shapes and linear temperature heating rates validated the resistive heating assembly for comparison of the TGGC and TPGC separation modes.



**Figure 6-28.** Heating and cooling temperature ramp of the new 1 m resistively heated TPGC assembly with heating rates as high as 2100°C/min and a cooling rate from 200 to 50°C in 32 s.

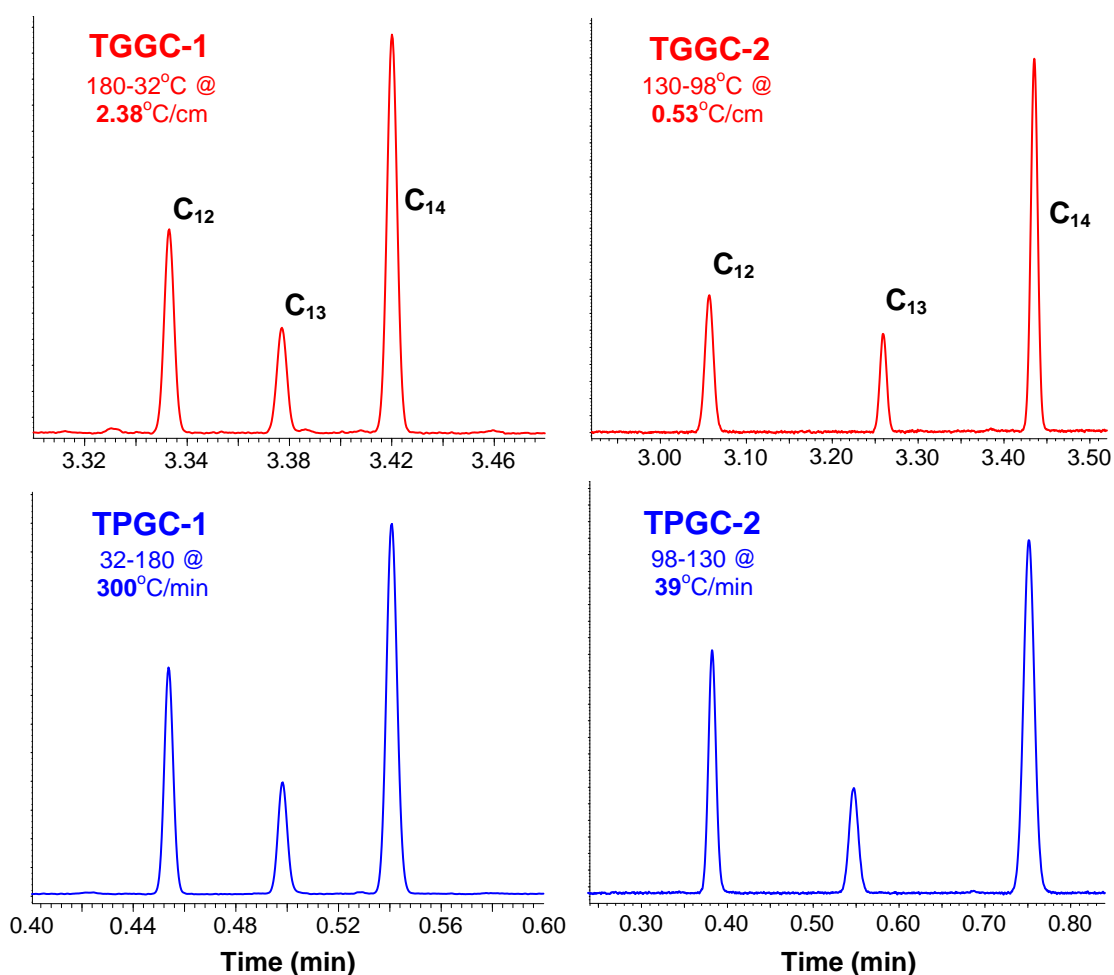
Comparison of the GC separation modes was performed by adjusting the operating conditions of each mode for the analytes to be separated in the same time period (Figure 6-30). Samples used for the experiments were the headspace of a normal alkane mixture (C<sub>12</sub>-C<sub>13</sub>) and an essential oil (Frankincense, India). Peak capacity and resolution were used to compare the different separation methods. The initial and final temperatures used in the TPGC separations were the minimum and maximum



**Figure 6-29. Reproducibility of the separation of normal alkanes (C<sub>12</sub>-C<sub>14</sub>) using the new resistively heated TPGC column assembly.**

temperatures of the moving TGGC profile, and as many variables as possible between the two separation modes were maintained the same. Figure 6-30 shows analyses of the normal alkane mixture using linear moving gradient profiles, with equivalent TPGC separations underneath. The separation window used for comparison was defined as the time between the C<sub>12</sub> and C<sub>14</sub> peaks for the TGGC separation. The separation of alkanes was first performed with a moving temperature gradient from 180 to 32°C, and then compare

ed with its equivalent TPGC separation (Figure 6-30). For TGGC-1 and TPGC-1, the separations of alkanes were very similar, with evenly spaced peaks and peak widths. However the TPGC-1 separation produced narrower peaks for C<sub>12</sub> and C<sub>13</sub>, which led to a higher peak capacity compared to the moving TGGC-1 separation (Table 6-4). Focusing by the low initial temperature in TPGC-1 allowed it to produce narrow peaks. However, even though the minimum temperature of the moving gradient was 32°C, the  $T_{eq}$  values of the analytes were much higher (C<sub>12</sub>=99°C, C<sub>13</sub>=111°C and C<sub>14</sub>=128°C), as seen in



**Figure 6-30. GC analysis of normal alkanes (C<sub>12</sub>-C<sub>14</sub>) using different separation modes. Separation conditions for TGGC: 20 psig head pressure (for both methods), 0.34 mL/min mobile phase flow, and 2.22 cm/s (45 s/rev) gradient velocity. For the TPGC separations, no hold times for the initial and final temperatures were used.**

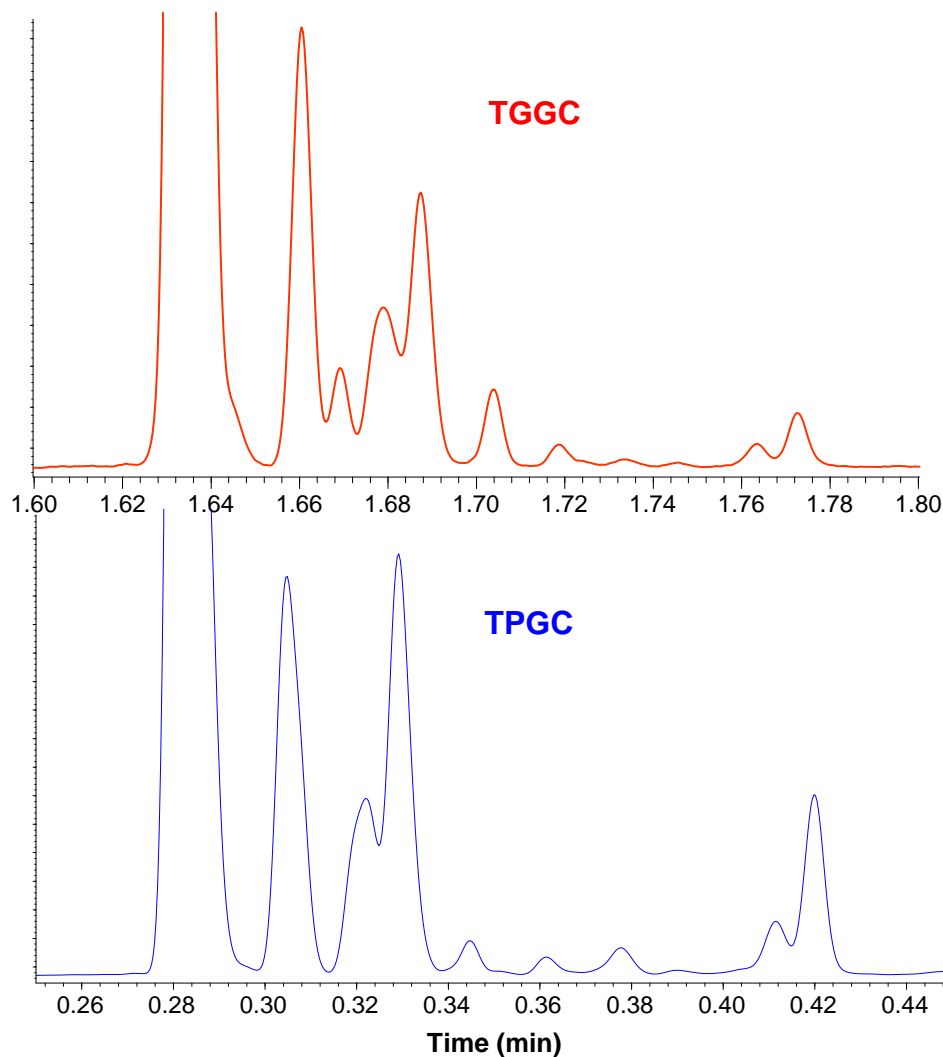
Figure 6-27 (where the separation conditions were the same). Therefore, a shallower temperature gradient which included the  $T_{eq}$  values of the alkanes was used.

A comparison with the shallow gradient is shown on the right side of Figure 6-30. With a shallower gradient, the peaks in the moving TGGC-2 separation were narrower than in the TPGC-2 separation (Table 6-4). Furthermore, a higher peak capacity was also achieved with moving TGGC-2 (Table 6-4). The peaks in the TPGC-2 chromatogram showed isothermal behavior, since the peaks became broader and farther apart as they eluted, possibly as a result of the high initial temperature and slow heating rate of the TPGC-2 method. The conditions used in TPGC-2 limited the range of compounds that could be separated, which was not the case for moving TGGC.

**Table 6-4. Peak widths, resolution and peak capacities of the normal alkanes using different separation methods.**

Separation	Analytes	Peak Width (s)	Resolution	Peak Capacity
<b>TGGC-1</b>	C <sub>12</sub>	0.51	C <sub>12-13</sub> = <b>5.15</b> C <sub>13-14</sub> = <b>5.12</b>	C <sub>12-13</sub> = <b>4.2</b>
	C <sub>13</sub>	0.51		C <sub>13-14</sub> = <b>4.1</b>
	C <sub>14</sub>	0.51		
				<b>Total = 9.3</b>
<b>TPGC-1</b>	C <sub>12</sub>	0.41	C <sub>12-13</sub> = <b>6.47</b> C <sub>13-14</sub> = <b>5.62</b>	C <sub>12-13</sub> = <b>5.5</b>
	C <sub>13</sub>	0.41		C <sub>13-14</sub> = <b>4.6</b>
	C <sub>14</sub>	0.51		
				<b>Total = 10.1</b>
<b>TGGC-2</b>	C <sub>12</sub>	1.20	C <sub>12-13</sub> = <b>10.88</b> C <sub>13-14</sub> = <b>10.27</b>	C <sub>12-13</sub> = <b>9.9</b>
	C <sub>13</sub>	0.99		C <sub>13-14</sub> = <b>9.3</b>
	C <sub>14</sub>	1.02		
				<b>Total = 20.2</b>
<b>TPGC-2</b>	C <sub>12</sub>	1.12	C <sub>12-13</sub> = <b>8.06</b> C <sub>13-14</sub> = <b>8.56</b>	C <sub>12-13</sub> = <b>8.1</b>
	C <sub>13</sub>	1.33		C <sub>13-14</sub> = <b>8.6</b>
	C <sub>14</sub>	1.53		
				<b>Total = 17.7</b>

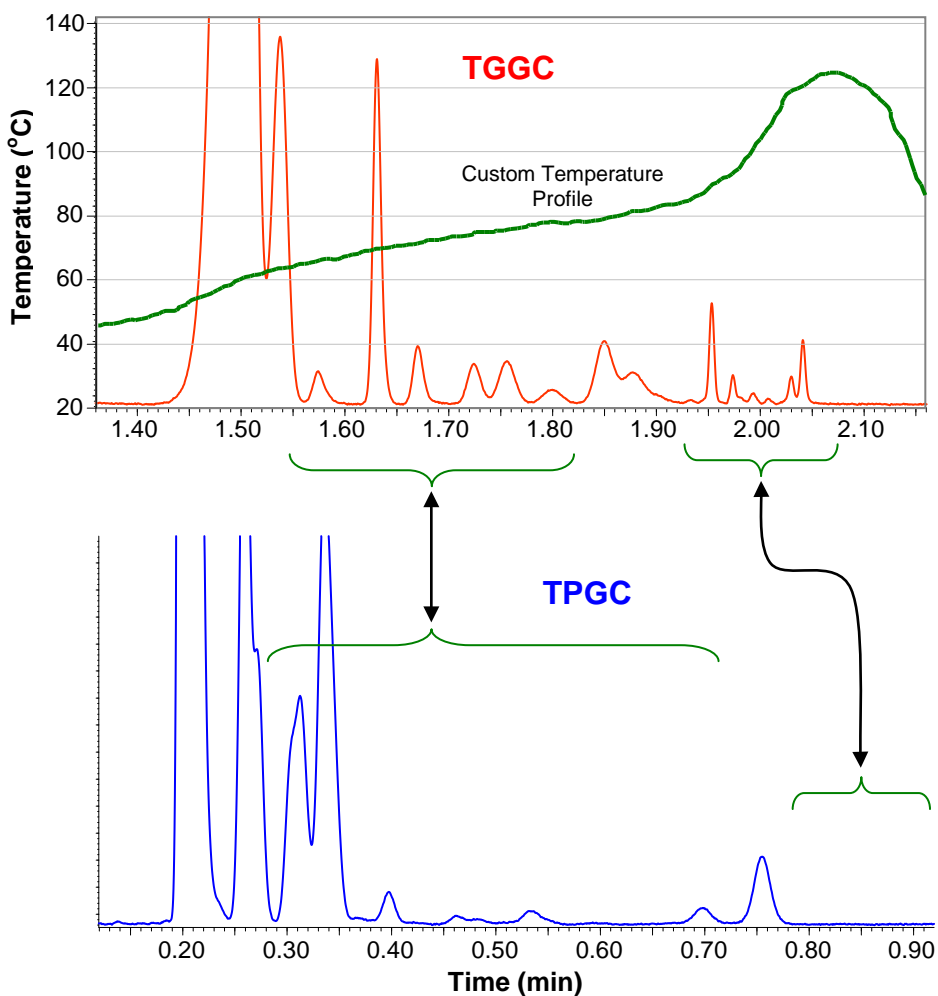
The moving TGGC method was also compared to TPGC using a more complex sample. Figure 6-31 shows the headspace analysis of an essential oil using the moving TGGC and TPGC methods. In this figure, both separations appear to be very similar, with the exception of an extra resolved peak eluting at 1.67 min for the TGGC separation. Besides the extra peak in the TGGC separation, peak height differences were also observed. Further tests are required to establish which separation method provides the



**Figure 6-31. GC analysis of the headspace of frankincense (India) essential oil using different separation modes. Separation conditions for TGGC: 20 psig head pressure, 0.34 mL/min mobile phase flow, 180-32°C linear gradient, 2.39°C/cm gradient slope, and 2.22 cm/s (45 s/rev) gradient velocity. For TPGC: initial temperature 28°C (0 s hold) to 180°C (0 s hold) @ 70°C/min, 20 psig head pressure.**

best separation. Overall the separations produced by the moving TGGC method were very similar to the TPGC method. Further evaluation using complex samples and a mass spectrometer would allow a better comparison.

Figure 6-32 shows the effect of a custom temperature gradient profile on the separation of the essential oil sample, and compares it with a TPGC separation. In this figure, the separation improvement that a custom moving temperature gradient profile



**Figure 6-32. GC analysis of the head space of frankincense (India) essential oil by moving TGGC with a custom temperature profile and by TPGC. The brackets indicate the areas where the separation was improved. Separation conditions for TGGC: 20 psig head pressure, 0.34 mL/min mobile phase flow, 180-32°C linear gradient, 2.39°C/cm gradient slope, and 2.22 cm/s (45 s/rev) gradient velocity. For TPGC: initial temperature 88°C (0 s hold) to 120°C (0 s hold) @ 26°C/min, 20 psig head pressure.**



can provide is clearly seen. This improvement was achieved by adequately distributing the peaks along the gradient. The overall S/N of the peaks was improved. Later broad eluting peaks not seen in the TPGC separation were focused, and their S/N was improved with a steeper gradient in the custom temperature profile of the moving TGGC. However, further optimization of the profile is still required, since some resolution was lost for the first two peaks. These results show the potential that custom gradient profiles can provide to optimize separations of complex samples.

## 6.4 CONCLUSIONS

The moving TGGC system based on continuous forced air convection cooling and individually resistively heated sections proved to adequately produce moving sawtooth temperature gradients with custom profiles. The flexibility of the system for customizing the temperature profiles allowed a more in-depth analysis of the effects of axial temperature gradients in separations, as well as allowing the exploration of potential applications. In moving TGGC, peak width was found to be mostly dependent on the gradient slope. The sample concentration and injection band width had little to no effect on peak width, a characteristic that allowed the use of the technique for continuous sampling. It was also observed that peak width was, to some extent, independent of analyte type (polar/nonpolar). Tailing of peaks was greatly reduced with a steep gradient slope, which led to improved separation of tailing compounds.

Increasing the slope for a linear gradient resulted in an overall decrease in resolution of compounds. This was a result of the peaks becoming closer faster than they become narrow. This phenomenon is similarly observed in ITGC and TPGC, when the column temperature and heating column rate, respectively, are increased, producing an

overall decrease in resolution. Proper application of each technique is required to maximize its separation potential.

To compare moving TGGC with TPGC, a new resistive heating approach for TPGC was developed to allow fast heating rates. Reproducible retention times, Gaussian peaks, and linear heating rates up to 2100°C/min validated the system design. The overall results of the comparison showed that moving TGGC separations with linear gradients were equivalent to TPGC separations, producing narrow, evenly spaced peaks. However, TGGC offers unique possibilities to improve the separation of selected compounds.

In moving TGGC, since the peaks elute at their  $T_{eq}$  values, the gradient profile determines their resolution. Manipulating the moving gradient profile has allowed unique control of the separation power, improving separations of analytes, as well as selectively increasing peak capacity and signal-to-noise (S/N) due to the focusing effect of the negative temperature gradient. With this technique, the movement and elution of compounds was accurately controlled. Furthermore, the S/N was also improved by changing the gradient slope at the peak position. Custom gradients allowed efficient management of the column separation space by providing more column space to the area of the chromatogram that required additional resolution, a characteristic that holds great promise for performing smart separations where the column space is efficiently utilized and optimal separations can be quickly achieved. This characteristic makes it very appealing for reducing method development time. Furthermore, this technology has the potential to be used in combination with feedback control to perform efficient separations with minimum user intervention.

This work has shown the unparalleled separation flexibility that moving TGGC with custom temperature gradient profiles offers. The fundamental separation principles of this technique have been highlighted. However, further work is still required to take full advantage of the separation potential of moving TGGC. The characteristics of this technique make it very appealing for use in other areas of GC, such as in micro-GC systems where its application could improve the separation performance.

## 6.5 REFERENCES

1. Fenimore, D. C., Gradient Temperature Programming of Short Capillary Columns. *J. Chromatogr.* **1975**, *112*, 219-227.
2. Kaiser, R., Temperature Gradient Chromatography. *Chromatographia* **1968**, *1*, 199-207.
3. Ohline, R. W.; DeFord, D. D., Chromathermography, the Application of Moving Thermal Gradients to Gas Liquid Partition Chromatography. *Anal. Chem.* **1963**, *35* (2), 227-234.
4. Tudge, A. P., Studies in Chromatographic Transport III. Chromathermography. *Can. J. Phy.* **1961**.
5. Zhukhovitskii, A. A., Some Developments in Gas Chromatography in the U.S.S.R. In *Gas Chromatography 1960*, Scott, R. P. W., Ed. Butterworths: Edinburgh, 1960; pp 293-300.
6. Zhukhovitskii, A. A., *et al.*, New Method of Chromatographic Analysis. *Doklady Akademii Nauk SSSR* **1951**, *77*, 435-8.
7. Contreras, J. A., *et al.* In *Moving Wave Temperature Gradient Gas Chromatography*, 32<sup>nd</sup> International Symposium on Capillary Chromatography and 5<sup>th</sup> GC×GC Symposium, Riva del Garda Italy, May; 2008.
8. Contreras, J. A., *et al.* In *Theoretical and Practical Justification of Thermal Gradient Gas Chromatography*, PITTCON, Chicago, IL, March; 2009.
9. Contreras, J. A.; Lee, M. L. In *Analytical Gradient Focusing Separation Techniques*, 236th American Chemical Society Philadelphia, PA, August; 2008.
10. Ettre, L. S.; Hinshaw, J. V., *Basic Relationships of Gas Chromatography*. Advanstar Communications: Cleveland, 1993.
11. Vergnaud, J. M., Gas Phase Chromatography: The Application of Gas Flow Variation and Backflushing. *J. Chromatogr. A.* **1965**, *19*, 495-503.
12. Berezkin, V. G., *et al.*, Temperature Gradients in Gas Chromatography. *J. Chromatogr.* **1986**, *373*, 21-44.
13. Jain, V.; Phillips, J. B., High-Speed Gas Chromatography Using Simultaneous Temperature Gradient in Both Time and Distance along Narrow-Bore Capillary Columns. *J. Chromatogr. Sci.* **1995**, *33*, 601-605.

14. Contreras, J. A. Design and Application of Thermal Gradient Programming Techniques for Use in Multidimensional Gas Chromatography-Mass Spectrometry (MDGC-MS) University of Dayton, Dayton, 2004.
15. Rubey, W. A., A Different Operational Mode for Addressing the General Elution Problem in Rapid Analysis Gas Chromatography. *J. High Res. Chromatogr.* **1991**, *14*, 542-548.
16. Agilent Low Thermal Mass (LTM) System for Gas Chromatography Data Sheet. [www.agilent.com](http://www.agilent.com).
17. Mustacich, R., *et al.*, Fast GC: Thinking Outside the Box. *American Lab.* **2003**.
18. Mustacich, R. V.; Everson, J. F. Reduced Power Consumption Gas Chromatograph System. US Patent 6217829, 2001.
19. Mustacich, R. V.; Richards, J. P. Electrically Insulated Gas Chromatograph Assembly and Method of Fabricating Same. US Patent 6209386, 2001.
20. Sloan, K. M., *et al.*, Development and Evaluation of a Low Thermal Mass Gas Chromatograph for Rapid Forensic GC-MS Analyses. *Field Anal. Chem.* **2001**, *5* (6), 288-301.
21. Lee, M. L., *et al.*, Fused Silica Capillary Columns Technology for Gas Chromatography. *J. Chromatogr. Sci.* **1984**, *22*, 136-142.
22. Markides, K. E., *et al.*, Deactivation of Fused Silica Capillary Columns with Phenylhydrosiloxanes. *J. High Res. Chromatogr. Comun.* **1985**, *8*, 378-384.
23. Woolley, C. L., *et al.*, Deactivation of Fused-Silica Capillary Columns with Polymethylhydrosiloxanes Optimization of Reaction Conditions. *J. Chromatogr.* **1986**, *367*, 9-22.
24. Woolley, C. L., *et al.*, Deactivation of Small Diameter Fused Silica Capillary Columns with Organosilicon Hydrides. *J. High Res. Chromatogr. Comun.* **1986**, *9*, 506-514.
25. Woolley, C. L., *et al.*, Static Coating of Phenyl and Biphenyl Polysiloxane Stationary Phases on Small-Diameter Capillary Columns. *J. High Res. Chromatogr. Comun.* **1988**, *11*, 113-118.
26. Serrano, G., *et al.*, Assessing the reliability of wall-coated microfabricated gas chromatographic separation columns. *Sensors and Actuators B-Chemical* **2009**, *141* (1), 217-226.
27. Radadia, A. D., *et al.*, Micromachined GC Columns for Fast Separation of Organophosphonate and Organosulfur Compounds. *Anal. Chem.* **2008**, *80* (11), 4087-4094.
28. Nishino, M., *et al.*, Development of  $\mu$  GC (Micro Gas Chromatography) with High Performance Micromachined Chip Column. *IEEJ Trans.* **2009**, *4* (3), 358-364.

## 7 CONCLUSIONS AND FUTURE WORK

### 7.1 CONCLUSIONS

The focus of the research work described in this dissertation was understanding the effects that axial temperature gradients have on GC separations, and exploring the separation potential that TGGC can offer. These goals were achieved through the development of mathematical models and instrumentation that allowed study of the effects of axial temperature gradients. A simple mathematical model based on the plate and rate models for GC was developed, and a computer program was written. The model was validated with experimental measurements, from which accurate retention times and overall peak broadening behavior were achieved. The use of the mathematical model facilitated evaluation of different gradient profiles and separation strategies prior to development of the instrumentation, providing a theoretical proof of concept.

Three instruments capable of generating axial temperature gradients were developed and evaluated. The first instrument was based on a heat exchanger concept with forced convection cooling and direct resistive heating of the column using a nickel sleeve. The low thermal mass of the instrument provided high heating and cooling rates that allowed selective elution of compounds (gating). The system versatility also allowed direct comparison of the TGGC method with ITGC and TPGC separations, showing that TGGC separations were equivalent to TPGC. The second instrument was based on resistive heating and a moving cold jet stream of liquid CO<sub>2</sub>. The unique design allowed the generation of a moving sawtooth temperature profile that permitted continuous sample analysis. The focusing effect of moving TGGC permitted wide injection bands

(45 s) with little degradation of compound resolution. The analysis of normal alkanes showed how the peaks eluted at their  $T_{eq}$  values, and the similarity of the separation to TPGC. Moreover, the unique characteristics of the system made it attractive for use as modulator and second dimension of a GC×GC system. Results of the comprehensive GC×TGGC separation of kerosene showed that the moving sawtooth gradient should enhance the peak capacity of GC×GC separations by eliminating wraparound and minimizing the general elution problem observed in the second dimension. Finally, a third instrument based in continuous forced air convection and resistively heated independent sections was developed. The high flexibility of the system for customizing temperature profiles allowed full exploitation of the separation capabilities of moving TGGC. Results from the analysis of normal alkanes showed that the peak widths of compounds were mostly dependent on the slope of the gradient, and their separation was dependent on the gradient profile. The use of custom temperature profiles allowed unique control over the separation power of the system, improving separations, as well as selectively increasing the peak capacity and S/N of the analytes. A new resistively heated assembly for TPGC separations was developed to allow comparison between moving TGGC and TPGC. The comparison showed again that TGGC separations were equivalent to TPGC separations, with the exception that TGGC offers unparalleled separation flexibility that cannot be found in any other separation method.

This work highlights the fundamental principles of axial temperature gradients, and explores the separation potential of the TGGC technique. Much work is still required, especially in designing simple instruments capable of controlling the temperature profile along the column. This technology holds great promise for performing smart separations

where the column space is efficiently utilized and optimal separations can be quickly achieved. Moreover, unique control of the movement and elution of compounds can be used to greatly reduce method development time in GC. This feature can be automated using feedback to develop efficient separations with minimum user intervention. This technology is of special interest in micro-GC technology, which allows easier incorporation of resistive heating elements in the micro-column design.

## **7.2 RECOMMENDATIONS FOR FUTURE RESEARCH**

### **7.2.1 Effects of Axial Temperature Gradient Resolution and Stationary Phase Film Thickness on Peak Width**

In this dissertation, several instruments capable of generating axial temperature gradients were developed. However, the design that provided the most flexibility to control the gradient profiles and, hence, allow detailed study of the effects of axial temperature gradients, was the system that used individually resistively heated sections in combination with continuous forced air convection cooling.

Using this instrument, several studies of the effects of axial temperature gradients on separation were performed. However, smooth gradients were difficult to generate with the system, since the resistively heated sections were 1" (2.54 cm) in length. From experiments, it was determined that at gradient slopes higher than 3°C/cm, the gradient slope was no longer uniform, limiting use of the system to adequately evaluate the effects of steeper gradient slopes. Therefore, further experiments using a system with improved axial temperature gradient resolution (~ 1 cm/section) should be performed to determine the factors affecting the minimum peak width and resolution.

From the results obtained in Chapter 6, it was determined that the minimum achievable peak width was a function of the mobile phase linear velocity (due to band broadening processes), the gradient slope, and the axial temperature gradient resolution in the column. Further tests using different stationary phase film thicknesses will provide better understanding of peak broadening due to resistance to mass transfer. Tests in columns without stationary phase should be performed to provide a complete picture of the effects of axial temperature gradients in separation. The results will allow better understanding of the effects of axial temperature gradients, and allow design of instruments capable of taking full advantage of the separation potential of TGGC.

### **7.2.2 Retention Indices in TGGC for the Identification of Analytes**

Since in TGGC, for a given gradient and mobile phase velocity, peaks elute at given  $T_{eq}$  values, this behavior can be used to help identify compounds through the use of the retention index system. The Kovat's retention index ( $I$ ) is based on normalizing the logarithm of retention time of a compound ( $i$ ) with respect to the logarithm of retention times of adjacent eluting members of a homologous series (normal alkanes) in isothermal separations.<sup>1</sup> The normalized value is then related to the carbon number of the adjacent n-alkanes. The retention index allows the identification of compounds by comparing the measured retention indices with tabulated values that are readily available. This is possible because even though the elution times of compounds vary with the column length, film thickness and mobile phase velocity, the relative retention time between adjacent n-alkane peaks for a given stationary phase remains constant. In TPGC, a similar retention index ( $I^T$ ) value can be calculated by<sup>1</sup>

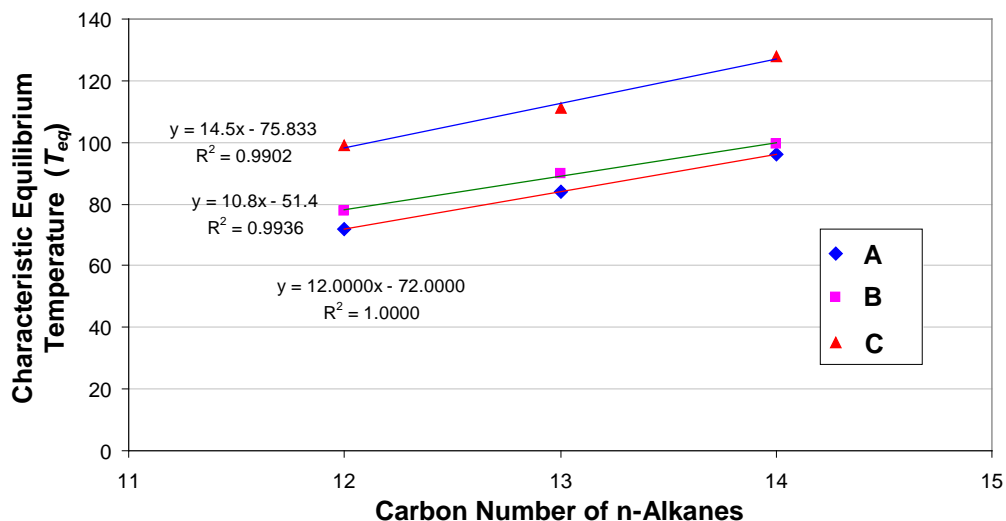


$$I^T = 100 \left[ \frac{t_{R(i)} - t_{R(z)}}{t_{R(z+1)} - t_{R(z)}} + z \right] \quad (7.1)$$

where  $z$  is the carbon number and the various  $t_R$  symbols represent the retention times of the analyte and the bracketing n-alkanes. The validity of the retention index depends on the linearity of the retention times of the n-alkanes with carbon number when temperature programming is used. For TGGC, a high degree of linearity was observed between the  $T_{eq}$  values and carbon numbers of the n-alkanes, as seen in Figure 7-1. This linearity was observed regardless of the gradient profile used. Therefore, due to the linearity observed with regard to the  $T_{eq}$  values, we can write a similar equation to the retention index Equation 7.1.

$$I^{T_{eq}} = 100 \left[ \frac{T_{eq(i)} - T_{eq(z)}}{T_{eq(z+1)} - T_{eq(z)}} + z \right] \quad (7.2)$$

The use of Equation 7.2 would not only facilitate the identification of compounds by their calculated retention indices, but it could also be used to aid in the design and optimization of the gradient profile by calculating the  $T_{eq}$  values of target compounds from their tabulated retention indices. This equation would be a simple tool for the determination of the  $T_{eq}$  values and identification of analytes. However, the accuracy of Equation 7.2 will depend on the accuracy of the  $T_{eq}$  measurements. This equation needs to be further proven by separating more normal alkanes in the gradient and determining the  $T_{eq}$  linearity with respect to carbon number for a wider range of normal alkanes. Furthermore, retention indices should be calculated and compared with measured values using Equation 7.2.



**Figure 7-1. Linearity of measured  $T_{eq}$  values with respect to the carbon number of n-alkanes, demonstrating that they could be used for the calculation of retention indices. The  $T_{eq}$  values were obtained from separations shown in Chapter 6. (A) Values from Figure 6-27. (B) Values from Figure 6-26. (C) Values from Figure 6-16.**

### 7.2.3 Improvement of the Simulation Model

The Mathematical model and simulation program, presented in Chapter 2, proved to be a very useful tool for evaluating different separation strategies and temperature gradient profiles for the optimization of separations. Further work is required to improve the prediction of the peak widths and to optimize the simulation to reduce the simulation time. Another important improvement would be to make it more user friendly since it can also be used for simulating ITGC and TPGC separations and, hence, has the potential for use as a teaching tool, since it allows visualization of the separation as the analytes travel along the column.

### 7.2.4 Use of Feedback Control with Moving TGGC

Unique control of the movement and elution of compounds by controlling the temperature gradient profile in moving TGGC would greatly facilitate rapid optimization

of separations. Currently, considerable time is wasted for method development in conventional chemical separation techniques, such as chromatography.<sup>2</sup> When compounds elute together, it is usually desirable to optimize the operating parameters and perform another separation with better selectivity. Since this process is typically time-consuming, it would be highly desirable to have rapid (*i.e.*, real time or near real time), automatic feedback control of the operating parameters so that subsequent separations are improved.

Automatic feedback control can be implemented for both peak sweeping (Chapter 4) and moving sawtooth gradient operations (Chapter 6). However it could be more easily applied to the moving temperature gradient profile, since the peaks elute from the column at constant  $T_{eq}$  values. Figure 7-2 shows schematically how starting with a linear gradient, the gradient profile can be changed in subsequent separations to provide different separations and, ultimately, the optimum separation. After the first separation, the  $T_{eq}$  values for all separated compounds can be easily determined. Knowing the  $T_{eq}$  values allows the temperature profile to be modified to improve the separation performance by moving the  $T_{eq}$  positions of the coeluting compounds farther apart, or moving them closer together if they are overly resolved.

The best separation can be achieved very quickly using the moving TGGC method. Feedback from a fast, continuous analysis (for example a moving sawtooth gradient) can automatically modify the temperature gradient profile to improve the resolution of coeluting peaks. Figure 7-3 shows a schematic diagram of a computerized system that would automatically optimize the separation. The first gradient could be a simple linear gradient; the computer would analyze the chromatographic data and check

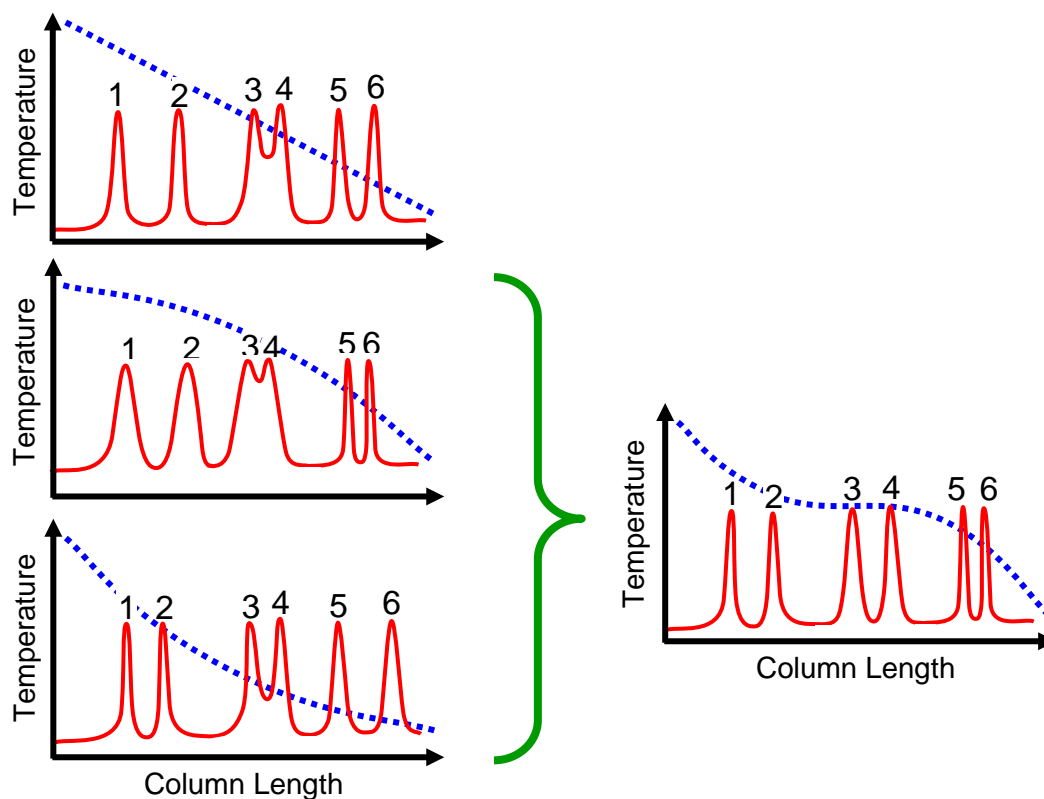


Figure 7-2. Schematic diagram showing how different temperature gradient profiles result in different chromatographic resolution. The right chromatogram shows the optimum profile.

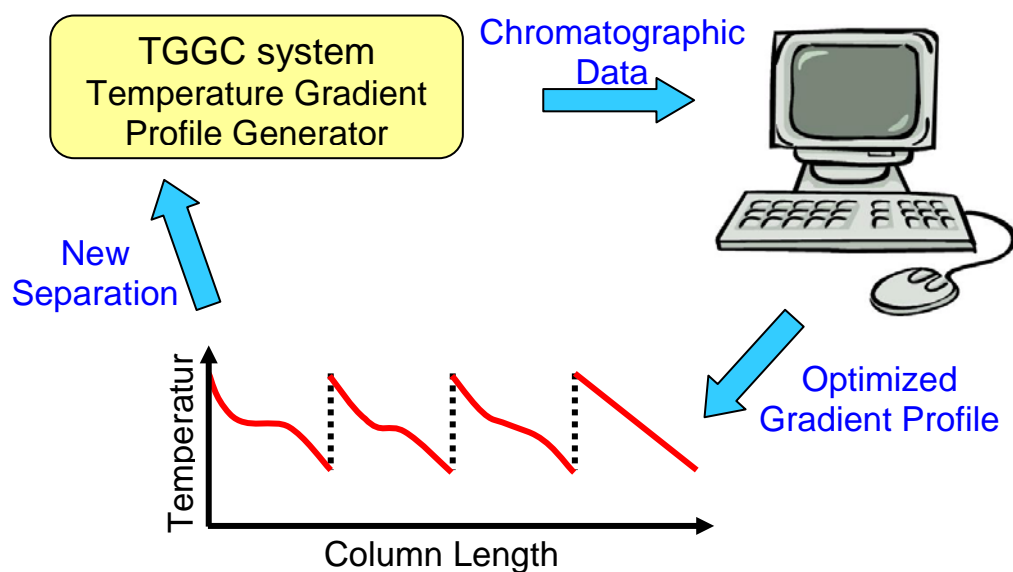


Figure 7-3. Schematic diagram showing computer control of the feedback system for optimizing a separation.

for coeluting peaks. Then it would determine how to modify the second or third temperature gradient profiles to achieve optimum separation of the compounds (i.e., resolution of all components in minimum time). The addition of feedback control to the moving TGGC system would greatly enhance its separation power.

### **7.2.5 Use of Moving TGGC as Modulator and Second Dimension Separation in Comprehensive GC×GC Separations**

The second dimension separation in current comprehensive GC×GC systems is usually isothermal.<sup>3-6</sup> Typical GC×GC chromatograms show the general elution problem where the first peaks are not resolved and the later eluting peaks are broad.<sup>5,7</sup> Due to the requirement to perform second dimension separations in seconds, isothermal separations in short columns are used. Fast temperature programming has not been possible in the second dimension of GC×GC due to the long cooling times of fast TPGC systems.<sup>8-9</sup> In contrast, moving TGGC would be very attractive as a modulator and separation method for the second dimension in GC×GC, since sequential analysis in short analysis times can be performed. Furthermore, as has been demonstrated, separations in a moving gradient are equivalent to temperature programmed separations. Preliminary results are promising (Chapter 5), showing improved distribution and separation of analytes in the second dimension, and elimination of wraparound problems. Another advantage that this technique offers is that longer columns can be used, since compounds travel along the column at the linear velocity of the gradient. Application of the moving TGGC technique showed a more efficient utilization of the second dimension space, which translates into an increase in the overall peak capacity of the system.

The moving sawtooth gradient used to gather preliminary results had a concave down profile, which limited the second dimension separation. The use of moving gradients with linear profiles or even customized temperature profiles should greatly improve the peak capacity. The current system for customized temperature gradients cannot generate fast moving gradients as a result of the considerably long cooling times due to the temperature of the cooling fluid. However, fast moving gradients can be achieved by placing the resistively heated coil inside a cold environment, such as a conventional GC oven with cryogenic cooling. Lower convective air temperatures would allow fast moving customized sawtooth profiles.

Currently, GC×GC is considered to be a hot topic in the separation science community, and the general elution problem in the second dimension is a well known problem with no adequate solution available. The use of moving TGGC as modulator and second dimension separation for enhancing the overall peak capacity of GC×GC would be of great interest and, therefore, should be further explored.

### **7.2.6 Application of Moving TGGC in Micro-GC Technology**

Interest in microfabricating GC systems stems from inherent performance gains that arise when analytical systems are downsized to the micron scale.<sup>10</sup> The benefits include, but are not limited to, parallel manufacturing for low production costs, small thermal mass for low power consumption, compact and robust systems, short analysis times and field applicability.

The first attempts to produce microfabricated columns for GC date back to the late 1970s at Stanford University, where Terry *et al.* first reported the use of photolithography and chemical etching techniques to fabricate a rectangular cross section

separation column in a silicon wafer.<sup>11</sup> Subsequent to this ground-breaking work, ongoing research on prototype micro-GCs has continued in several laboratories, including the national laboratories.<sup>12-19</sup> Even though several microchip GCs have been developed recently, full utilization of their potential performance has not yet been realized.

Miniaturization of GC involves some technical challenges, as first reported by Terry. The most critical challenge is the difficulty of coating a microfabricated column due to Raleigh instability,<sup>20</sup> and uneven coating in sharp corners because of surface tension of the coating solution, resulting in relatively poor column performance.<sup>11, 21</sup> As the analyte band travels along the separation column, it will be broadened and diluted. The extent of this band spreading is related to the separation efficiency. Relatively poor column performance in current microchip GC systems,<sup>13, 16-18, 22-26</sup> such as broad bands and non-Gaussian peak shapes (tailing) are attributed to well known factors:

1. Non-uniformities in the distribution of stationary phase due to pooling in sharp corners create thicker coatings where analytes spend longer time, which broadens the chromatographic peaks.<sup>14, 27-28</sup>
2. Active sites on the silica surfaces such as silanol groups and metal oxide residues cause unwanted adsorption and peak tailing. This effect is more dramatic in microfabricated columns where the surface to volume ratio is much higher.<sup>20, 23-24, 29-30</sup>
3. Extra-column band broadening due to connections to the microfabricated column, as well as other dead volumes, and non-uniform flows along the microchip channels can completely destroy any resolution achieved by the column.<sup>13, 17</sup>

4. Band dispersion can occur from unequal analyte path lengths due to inside and outside trajectories at curves in the microchips (race-track effect).<sup>14</sup>
5. Broad band injections can limit the maximum separation power of the column, especially for miniaturized channels characteristic of microfluidic systems.<sup>9, 31</sup>

Current micro-column GC technology alternatives produce low separation performance from stationary phase pooling, non-uniformities in the stationary phase coating, and surface activity.<sup>13, 16-18, 22-23, 25</sup> Another restriction when using micro-GC systems is the need for narrow band injections. This is currently achieved by sophisticated injection systems which are not easily miniaturized.<sup>8-9, 18, 31</sup>

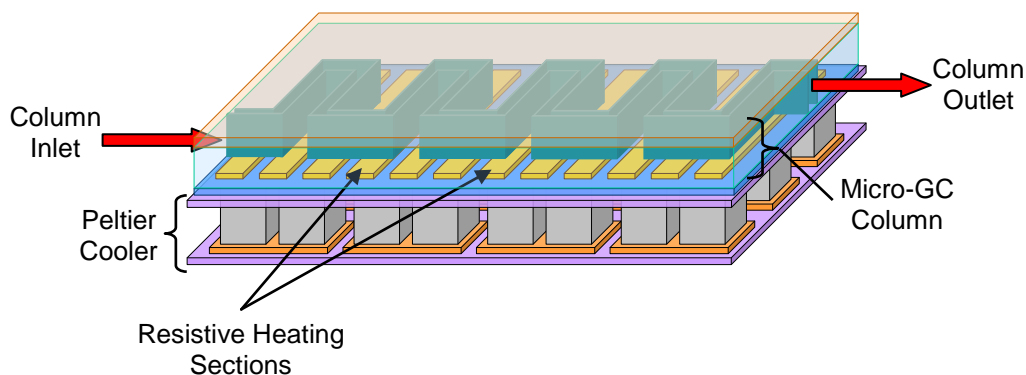
TGGC can aid in overcoming these hurdles.<sup>32-34</sup> In moving TGGC, analyte bands are focused as they travel through the column, allowing on-column concentration and less stringent requirements for sample introduction and detection. Furthermore, since TGGC is a focusing technique, it will also reduce band broadening due to non-uniform stationary phase coatings, extra-column effects and dead volumes along the column. The use of moving TGGC reduces peak tailing as demonstrated in Chapter 6, which greatly increases the separation performance of microfabricated GC systems.

The design of microfabricated TGGC systems could stem from our work with lab-size TGGC systems, where resistive-heating technology in combination with thermoelectric cooling (Peltier cooler) could be used to generate flexible axial temperature gradients in a miniaturized format. To achieve this, individual resistively heated sections could be incorporated in microfabricated GC columns. Convective and thermoelectric cooling could also be used in the micro-GC system to provide a wider temperature range than achieved with the current TGGC design. A Peltier cooler in

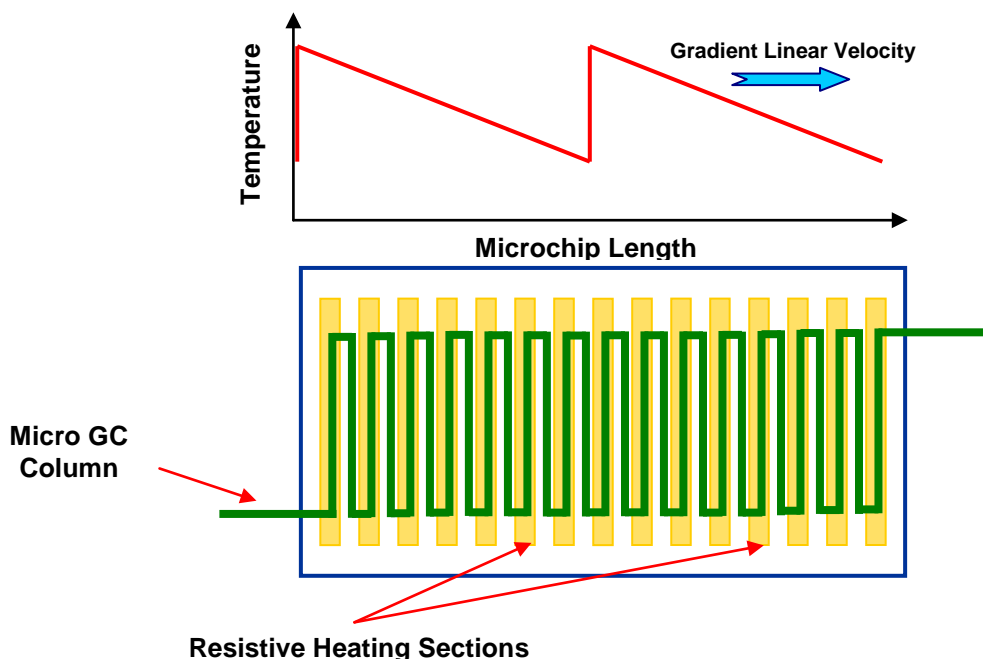


conjunction with the resistively heated sections could provide rapid cooling for generating a moving sawtooth temperature profile along the microfabricated column (Figure 7-4). In order to emulate the resistively heated sections along the capillary column (Chapter 6), the microfabricated column can be formed in a serpentine design parallel to the resistively heated sections (Figures 7-4 and 7-5). This is the key for generating axial temperature gradients along a microfabricated GC column. A diagram showing this can be seen in Figure 7-5.

The versatility of the resistive heating design in a micro-GC system will allow ITGC, TPGC and TGGC separations. This has the potential to utilize the first part of the column as an integrated in-column sample preconcentrator, reducing extra-column band broadening effects from interfacing different devices. Furthermore, the system also has the potential to perform comprehensive multidimensional GC analysis in a single chip, greatly increasing the separation power of the system.<sup>35</sup> For GC×GC, the first ¾ of the column can be coated with a non-polar stationary phase, and a slow TPGC can be applied. The remaining ¼ of the column can be coated with a polar stationary phase, and



**Figure 7-4. Diagram of a microfabricated GC column design that incorporates resistively heated sections to implement the TGGC technique for improving the separation performance of current micro-GC systems.**

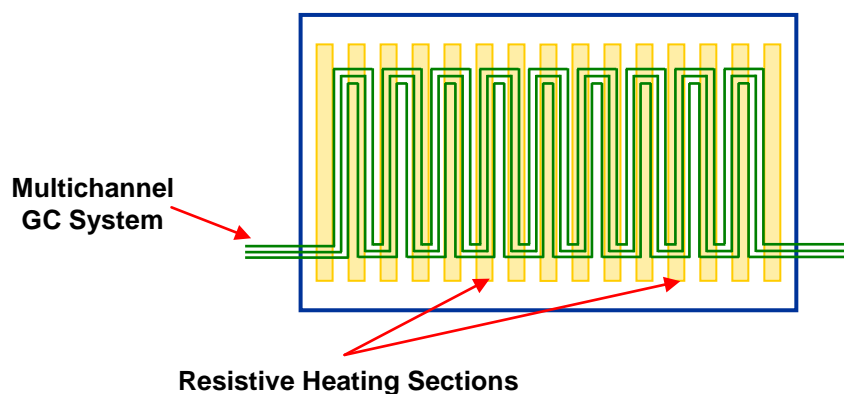


**Figure 7-5. Diagram showing a temperature gradient profile that may result from a microfabricated GC column design that incorporates the use of resistively heated sections to implement the TGGC technique.**

a fast sawtooth moving gradient can be used in this section as a modulator and second dimension separation. The advantage of using a moving sawtooth gradient as the modulator is the simplicity of the system, which reduces the need for a modulator between two column sections. Another possibility is to perform not only GC×TGGC but also GC×TGGC×TGGC<sup>36</sup> to further enhance the separation.

An increase in sample capacity for micro-GC systems is of great interest when using miniature detectors, which are normally less sensitive than conventional detectors.<sup>15-16</sup> A method for increasing the sample capacity of a micro-GC system and, hence, its sensitivity is by using multiple chromatographic channels. The use of multi-capillary columns to increase the capacity of the GC system while maintaining the separation efficiency has been reported previously.<sup>37-38</sup> The use of multiple channels can greatly increase the sample capacity and sensitivity of the micro-GC system and, hence,

facilitate the use of current miniature detector technology. This idea, to the best of our knowledge, has never been incorporated in micro-GC systems. However, having two or more channels with slight variations in the stationary phase coatings can decrease the separation efficiency by producing broad peaks due to elution time differences between the channels.<sup>38</sup> Since analytes move along the separation column at the velocity of the temperature gradient profile at their respective temperatures of equilibrium in TGGC, this problem can be eliminated, allowing the development of multicapillary micro-GC systems (Figure 7-6).<sup>32-33, 39</sup>

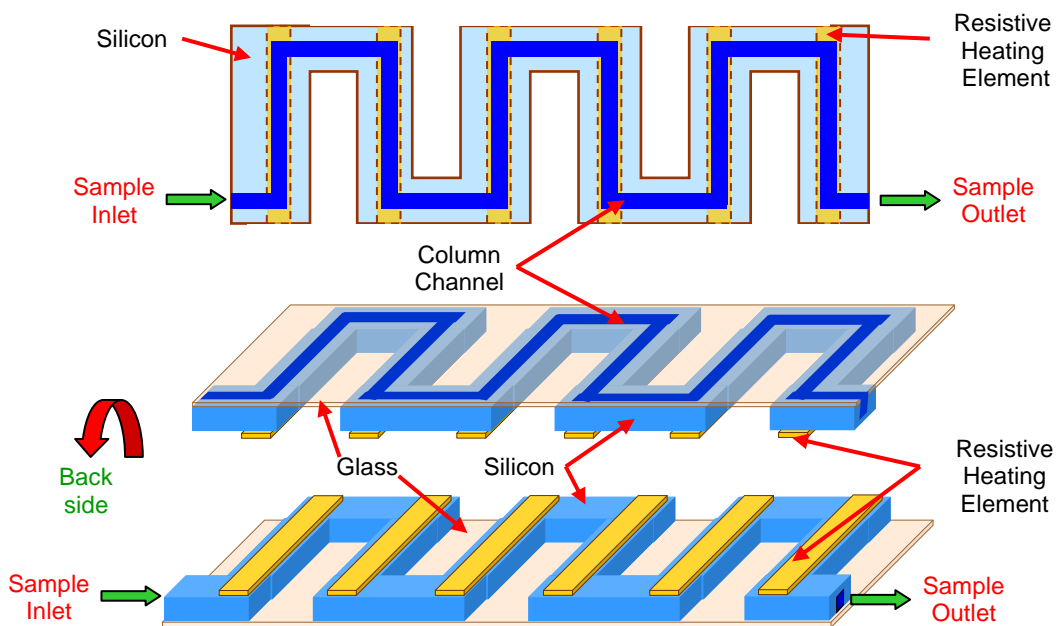


**Figure 7-6. Diagram of a multichannel microfabricated GC system to improve the sample capacity and sensitivity of the system.**

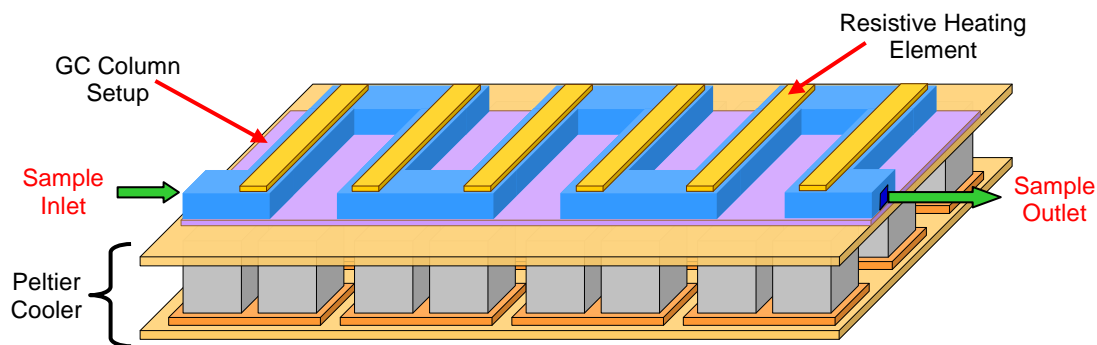
In our work, we have demonstrated that injection bands as wide as 45 s have been possible using the moving TGGC method. This would be very useful for sample introduction in microchip-GC technology, which requires narrow band injections to take advantage of the separation power of micro-GC columns.<sup>8-9, 18, 31</sup> TGGC can concentrate analytes in large injections, which is of great importance in micro-GC systems, since the typical preconcentrator before the microfabricated column can be eliminated.<sup>16</sup> Furthermore, the unique selectivity achieved with the use of custom gradient profiles would be of great benefit to micro-GC systems for overcoming the compromised

separation efficiency due to the previously mentioned factors. The use of the TGGC technique in a micro-GC system would allow the maximum performance of microfabricated columns, bringing closer to reality the total miniaturization of a GC system.

Preliminary work has shown that the high thermal conductivity of silicon (Si) [148 W/(mK)] prevents the generation of temperature gradients. However, the use of glass with a 100-fold smaller thermal conductivity [1.3 W/(mK)] has given promising results. Therefore, the first tests of TGGC in a microchip format should be performed in glass. Figure 7-8 shows another possible design that can facilitate the generation of axial temperature gradients in micro-GC systems. This alternative design reduces the heat conduction between the serpentine column segments, facilitating the establishment of the axial temperature gradient along the micro-GC column. The complete micro-column GC assembly is shown in Figure 7-8.



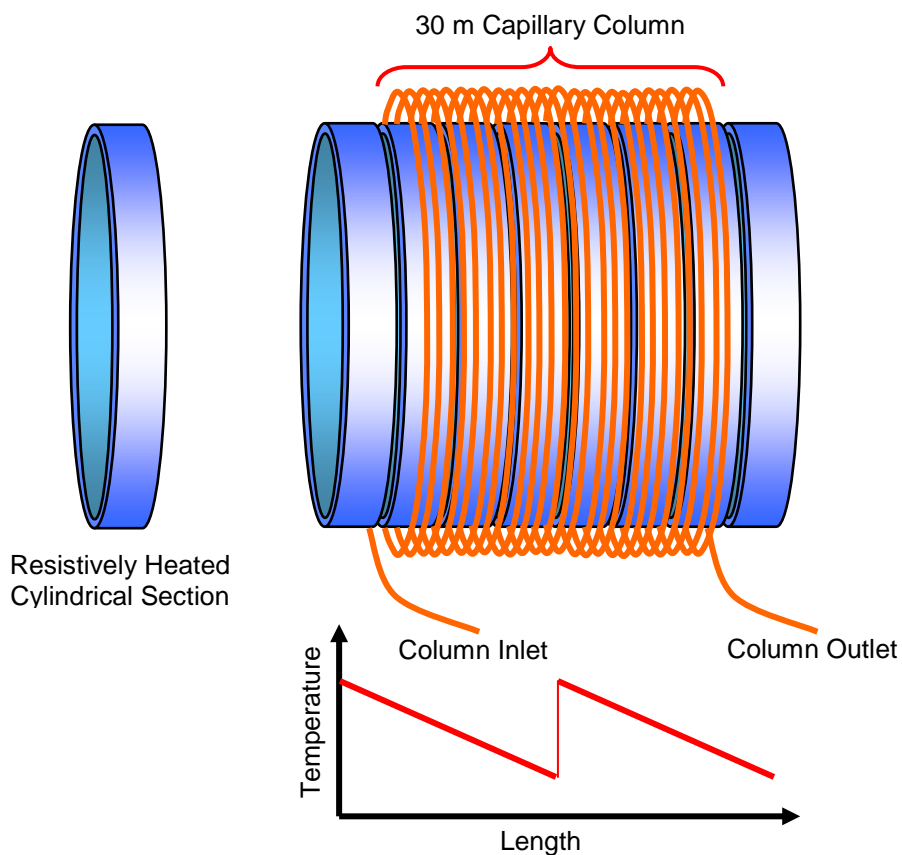
**Figure 7-7. Diagram showing different views of a micro-GC column.**



**Figure 7-8. Diagram showing a micro-GC assembly including Peltier cooler.**

### 7.2.7 Lab-size TGGC System for Long Columns

In this dissertation, we showed the separation principles of TGGC and its future potential using systems with short columns. The prototype systems constructed in this work were directed towards fast separations and, thus, short column lengths were chosen. However, the use of longer columns with TGGC should not be disregarded. What is required is an instrument capable of generating gradients in longer columns. Based on the design with individually resistively heated sections, Figure 7-9 shows the use of resistively heated cylindrical sections (thin ceramic or polyimide resistive heating elements) to generate a negative axial temperature gradient for columns as long as 30 m in length. The sections would be placed together, forming a long cylinder around which the GC column could be wrapped.<sup>40</sup> This fixture can be placed inside a conventional convective GC oven, which can be held at low temperatures (room temperature down to -20°C). The system would operate according to the same principles as the system previously described in Chapter 6. This system has the potential to greatly increase the separation power of the TGGC system.



**Figure 7-9. Diagram of a TGGC instrument to accommodate a 30 m capillary column.**

### 7.2.8 Extended Moving TGGC: a Leap into the Future of Portable GC Systems

As demonstrated in this work, the resolution in moving TGGC can be uniquely controlled by modifying the temperature gradient profile. However, the maximum resolution that can be achieved between compounds is limited by the actual physical length of the temperature gradient profile. Shallower temperature gradients place the  $T_{eq}$  values of analytes farther apart, improving the separations. However, the use of shallower gradients in a fixed column length produces temperature gradients with small temperature ranges, limiting the boiling point ranges of compounds that can be separated. The use of individually resistive heated sections arranged linearly in a straight column offers a

unique solution to this problem. Instead of limiting the gradient profile to the length of column that is within the resistively heated sections, a gradient longer than the heated column can be implemented (Figure 7-10).

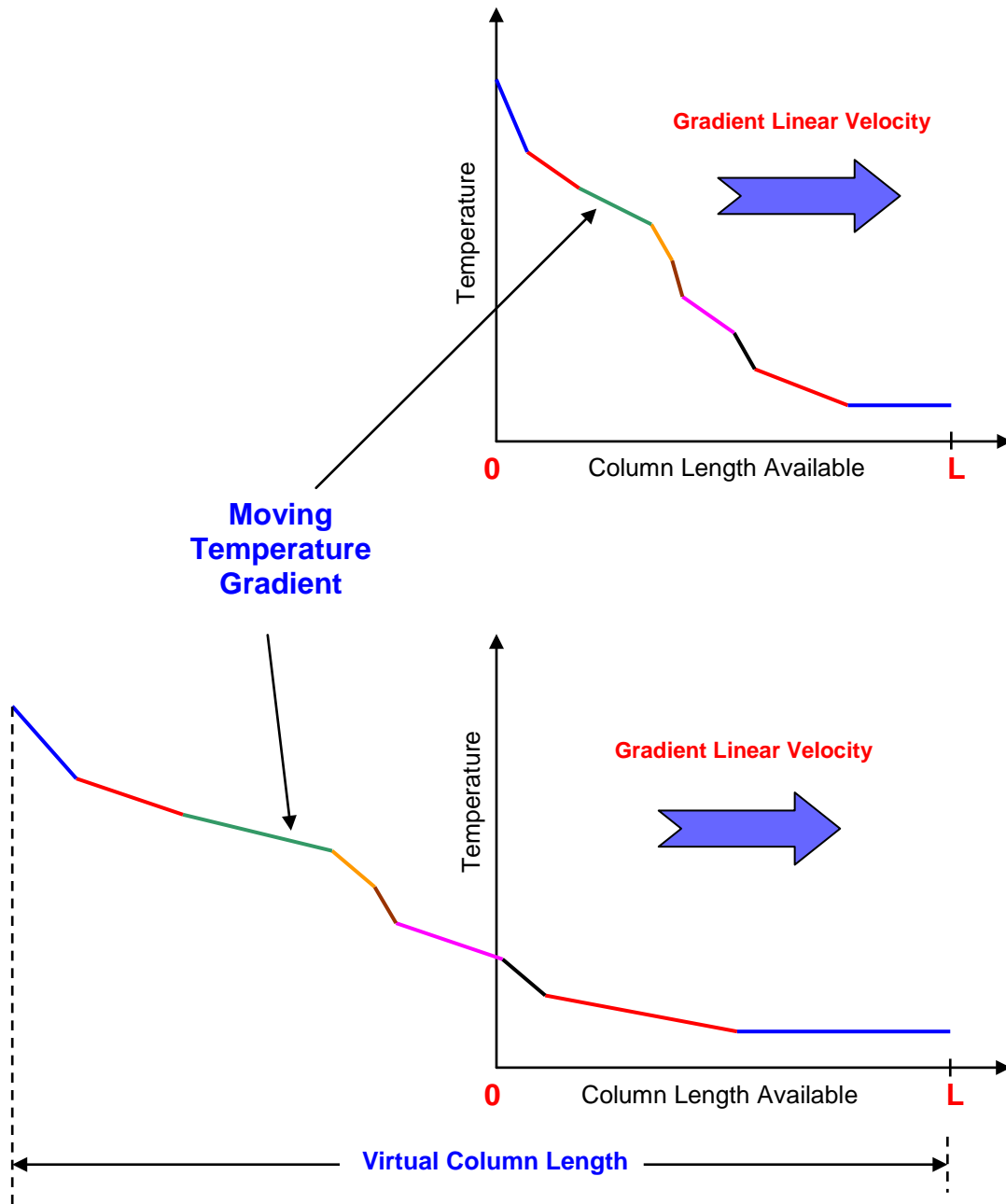
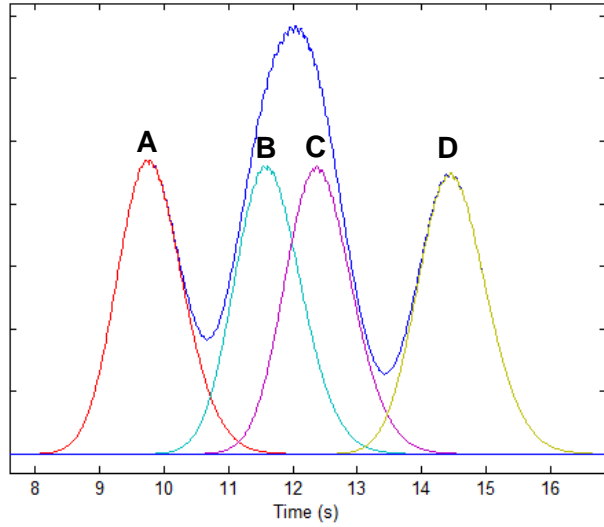


Figure 7-10. Diagram of the TGGC virtual column concept.

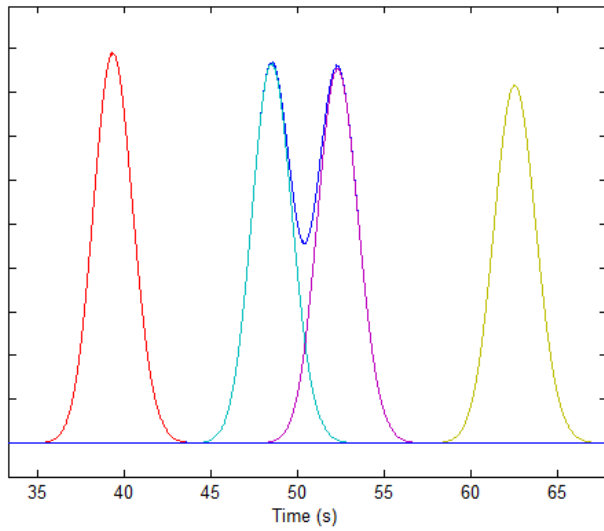
To test this concept, simulations using the model and computer program described in Chapter 2 were performed (Figure 7-11). The simulations consisted of comparing separations performed using a 1 m column and gradients corresponding to longer column lengths with simulated separations performed using an actual longer column. For comparison, the gradient and mobile phase velocities were kept constant for each case, and a linear moving gradient with constant temperature range was used. Figure 7-11 shows a separation obtained using the 1 m column with a 1 m gradient length compared to separations obtained using a 1 m column with an extended gradient length of 5 m, and a simulation of the separation using a 5 m column with a 5 m gradient length. From this figure, we can observe that by using the extended gradient concept, an increase in resolution can be obtained. Table 7-1 lists the simulated resolutions obtained using the 1 m column with extended lengths of 2, 3 and 5 m, compared with simulated separations using actual columns lengths of 2, 3 and 5 m. From this table, we can observe that between 45 to 120% increase in resolution can be achieved by using the extended gradient length concept. However, with longer extended gradient lengths, the percent difference in the resolution with respect to separations using actual column lengths increased. This is as result of compounds eluting before they reach their  $T_{eq}$  points, thereby limiting the maximum extended gradient length. Further simulations and experimental work are required to prove this idea. These preliminary results show that even though separations with the extended gradients were not equal to using the actual column length, a considerable increase in resolution was obtained. The potential separation capabilities of the extended gradient would be of great interest in micro-column GC technology, where the column lengths in the micro-GC devices are limited.



1 m Column



5 m Gradient Length in a 1 m Column



5 m Column

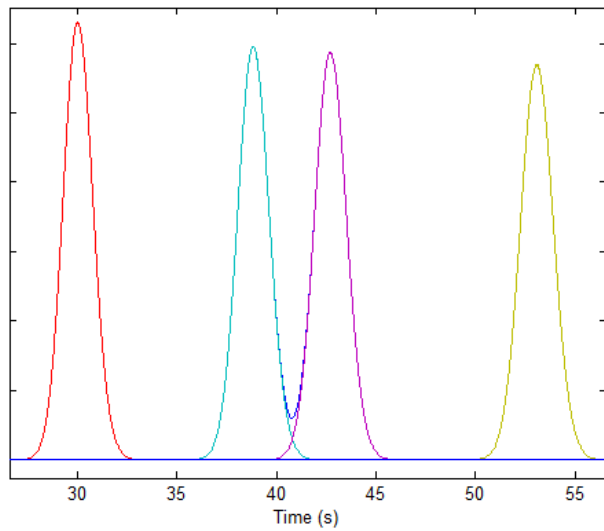


Figure 7-11. Simulations showing the effect on resolution of using temperature gradients equivalent to longer column lengths.

**Table 7-1. Resolution of simulated separations showing the comparison between the virtual column length of a 1 m column with respect to separations obtained with actual column lengths.**

Compound Pairs	RESOLUTION				
	1 m		2 m		
	Actual	Actual	Virtual	% Difference	% Increase
A-B	0.88	1.48	1.32	11.00	49.10
B-C	0.37	0.63	0.55	12.22	47.34
C-D	0.98	1.65	1.45	12.19	48.06

Compound Pairs	1 m		3 m		
	Actual	Actual	Virtual	% Difference	% Increase
	A-B	0.88	2.00	1.61	19.28
B-C	0.37	0.85	0.67	21.16	78.50
C-D	0.98	2.22	1.75	21.02	79.70

Compound Pairs	1 m		5 m		
	Actual	Actual	Virtual	% Difference	% Increase
	A-B	0.88	2.88	1.97	31.41
B-C	0.37	1.22	0.81	34.01	115.06
C-D	0.98	3.20	2.12	33.66	117.30

### 7.2.9 Applications of Axial Temperature Gradients in Other Separation Areas

The use of axial temperature gradients has been discussed in considerable detail with respect to GC. However, the technique can be potentially employed in high performance liquid chromatography (HPLC), supercritical fluid chromatography (SFC), capillary electrochromatography (CEC), and in equilibrium gradient methods such as temperature gradient focusing (TGF).

### 7.2.9.1 *Liquid Chromatography*

HPLC is the most widely used analytical technique for the analysis of nonvolatile organic compounds. The separation process in HPLC relies on partitioning of the analyte between the mobile and stationary phases. In HPLC, the solvent strength of the mobile phase is the major variable for controlling the selective retention of solutes in the column. Although temperature is traditionally considered to be a variable that has a minor effect on HPLC separations, in the last decade, studies have shown that its effect can play a significant role.<sup>41-43</sup> An increase in temperature increases the solvating power of the liquid mobile phase, decreases its viscosity and increases solute diffusivity, resulting in improved mass transfer and an increase in column efficiency.<sup>44</sup> Also, as a result of increasing the temperature, the pressure drop of the column decreases, which allows the use of smaller particles or longer columns to obtain higher total plate numbers.<sup>44</sup> Furthermore, shorter analysis times can be achieved without sacrificing resolution since the dispersion due to resistance to mass transfer is decreased at higher temperatures; hence, higher than optimal mobile phase velocities can be used.<sup>43</sup>

Studies have shown that the solvent strength, a major variable for controlling retention in HPLC, can be affected by temperature.<sup>45</sup> Tran *et al.* directly compared the effects of changing the solvent composition and the column temperature. The results showed that second to the percent of organic modifier, the temperature exerted the greatest effect on the retention of neutral, acidic and basic components in a reversed phase system.<sup>45</sup> In another study, Sander *et al.* evaluated the effect of temperature on selectivity; the authors observed that changes in the selectivity occurred with changes in temperature for a wide variety of stationary phases.<sup>46</sup> Also, results showed that lower

column temperatures improved the separation of isomers. The increased interest in the use of temperature as an active tool for optimizing liquid chromatography separations in the last decade has led to the application of temperature programming in liquid chromatography separations (temperature gradient capillary liquid chromatography).<sup>47-49</sup>

The use of axial temperature gradients could improve both peak shape and resolution in conventional HPLC. However, its impact on resolving power would be more evident in microchip HPLC systems, where the miniaturization of column dimensions allows for easier control of temperature. The trend in analytical instrumentation in the last decade has been towards miniaturization. The development of new techniques in microelectromechanical systems (MEMS) has allowed the micro fabrication of various analytical techniques such as chip-based capillary electrophoresis<sup>50-53</sup> (CE) as well as chip-based GC systems.<sup>15, 54-55</sup> However, most microchip based separation techniques developed up to now have focused on electrophoretic over chromatographic techniques due to difficulties in integrating on-chip injectors and mechanical valves, and the lack of easy flow control.<sup>53, 56</sup> Especially for HPLC micro devices, flow control has proven to be very challenging.<sup>56</sup> Miniaturization and integration of solvent pumps capable of generating high pressures with smoothly changing flow rates and uniform solvent gradient profiles have been difficult.<sup>57-60</sup> The low likelihood of generating high quality solvent gradients in microchip HPLC systems compromises chromatographic performance.

To overcome these challenges, the design of a microchip system could be simplified by using only one pump<sup>57</sup> with a single solvent composition in combination with a moving axial temperature gradient to generate a solvent strength gradient profile.

As previously mentioned, solvent strength and selectivity can be easily modified by changing the temperature of the chromatographic column. However, previous work has focused on changing the entire column temperature in time,<sup>45-46</sup> which creates a change in the solvent strength throughout the entire column instead of creating a solvent strength gradient as commonly used in HPLC. Axial temperature gradients (a change in temperature along the column) in miniaturized HPLC systems could be used as a simple way to control the solvent strength along the LC column. The microchip HPLC system temperature control could resemble that described for a microchip GC system. The main difference in instrumentation would be the requirement of a liquid pump in the microchip HPLC system.

Temperature programming in a microchip HPLC system without a gradient in solvent composition has been tested, and a successful chromatographic separation of derivatized amino acids was obtained.<sup>59-60</sup> These results showed that temperature programming is a feasible alternative to solvent gradient elution in certain cases. Although the separation was successful, the chromatographic performance was relatively poor, showing wide peaks with low signal to noise.

The implementation of a moving axial temperature gradient in a microchip HPLC system would enhance the separation performance by generating a solvent gradient profile in the column that resembles conventional gradient elution. In a reversed-phase HPLC system, lower temperatures would cause the mobile phase to behave as a more polar solvent, while higher temperatures would decrease the polarity.<sup>61</sup> In an axial temperature gradient, the inlet temperature of the column would be higher than the outlet

temperature, simulating solvent gradient elution. The solvent gradient strength generated with the axial temperature gradient would focus peaks and improve the detection limits.

Furthermore, all of the advantages observed in the use of axial temperature gradients in GC could be extrapolated to HPLC. Among these advantages are:

1. Large volume sample enrichment could be achieved by maintaining the initial temperature of the column low during injection, decreasing the detection limits of the system.<sup>47</sup>
2. Continuous analysis and separation could be performed using a moving sawtooth temperature profile.
3. Unique control of the separation selectivity would be possible by tailoring the temperature gradient profile and, hence, the solvent gradient strength profile in the column, maximizing the resolution.
4. Higher temperatures would reduce the pressure drop and, hence, longer columns could be used, increasing the separation power.
5. Comprehensive separations or LCxLC could be performed in a single microchip. For this, the secondary column would have a smaller diameter than the primary column to allow faster mobile phase velocities, and it most likely would contain a different stationary phase.
6. Miniaturization typically involves a decrease in sample capacity; however, moving gradient multicapillary LC could be performed without degrading the separation performance.

### **7.2.9.2 Temperature Gradient Focusing (TGF)**

Temperature gradient focusing (TGF) is a technique that simultaneously concentrates and separates ionic species in solution within microchannels or capillaries.<sup>62</sup> TGF is a counter-flow gradient focusing method that operates by balancing the electrophoretic migration of analyte molecules against the bulk flow of solution in a separation channel. In TGF, the buffer ionic strength is dependent on temperature.<sup>63</sup> When a temperature is applied to the system, the electrical conductivity of the buffer changes; a higher temperature results in higher buffer conductivity and, therefore, a lower electric field. The electrophoretic velocity of an analyte is dependent on the electric field strength, so a temperature gradient along the separation channel would result in an electric field gradient and, hence, a gradient in electrophoretic velocity.<sup>64</sup> The analytes would focus at unique locations (zero-velocity points) along the channel where the bulk solution velocity against the electrophoretic velocity of the analyte is balanced.<sup>62, 65</sup>

In microfluidic systems, sample preconcentration is a critical operation due to the extremely small quantities of analytes that can be injected onto the separation column and the very short (10-100  $\mu\text{m}$ ) optical detection path length.<sup>66</sup> TGF offers a simple solution to decrease the detection limits of trace compounds, showing concentration of greater than 10,000-fold for dilute analytes.<sup>62, 65</sup> However, one drawback of TGF is the limited peak capacity; only a small number of analyte peaks (i.e., 2 or 3) can be simultaneously focused and separated.<sup>62, 67</sup> A solution to this problem is to vary the bulk flow over time, keeping the temperature gradient constant to sequentially focus and elute analytes past a fixed detection point. This method received the name “scanning” TGF.<sup>67</sup> Although scanning TGF provided an increase in the peak capacity, this improvement came at the

expense of separation time. The use of narrow temperature gradients (2 and 5 mm<sup>64-68</sup>) in a scanning TGF mode meant that every adjustment in the bulk flow required time to concentrate a new band in the temperature gradient.

Current micro-fluidic TGF systems only use linear temperature gradients, limiting the separation power and, hence, the peak capacity of the system.<sup>64-68</sup> In theoretical work by Tolley *et al.*,<sup>69</sup> it was suggested that the peak capacity of equilibrium gradient methods, such as TGF, could be increased by using a nonlinear field (temperature) gradient.<sup>69-71</sup> Furthermore, it was demonstrated that by modifying the electric field gradient profile in equilibrium concentration techniques, closely coeluting analytes could be separated.<sup>72</sup>

Longer columns with longer axial temperature gradients would allow not only an increase in the peak capacity, but also a decrease in the analysis time, by simultaneously concentrating a wide range of analytes instead of only 2 or 3. The focused analytes would then be moved into the detection window by moving the temperature gradient along the separation column. Furthermore, unique control of the selectivity and signal to noise of the analytes would be achieved by controlling the temperature gradient profile as previously described for GC applications. After moving an analyte inside the detection window, a sharper gradient slope in the detection window could be established to further focus the band.

A microchip TGF system would follow the same design to control the axial temperature along the channel as previously described for a microchip GC system. The column design could be either straight or follow a serpentine pattern. Accurate control of the gradient temperature profile and bulk flow would allow much more flexibility and



increased separation power. The flexibility of the system would allow feed-back control to perform real time optimization of the concentration and separation of the analytes.

### ***7.2.9.3 Capillary Electrochromatography (CEC)***

Axial temperature gradients could also be applied in CEC to improve separation performance, since CEC and HPLC are similar techniques. In CEC, mobile phase transport is achieved by electrosmotic flow instead of by a pressure gradient as in HPLC. However, the separation of neutral compounds in CEC is achieved by partitioning between mobile and stationary phases as in HPLC. The difference is that separation of charged analytes is accomplished by a combination of partitioning and differential electromigration. The effect of temperature in CEC separations has been previously studied, showing that the separation performance can be modified.<sup>73-75</sup> For this reason, axial temperature gradients in CEC microchip based systems could provide an improvement in the resolution of compounds.

### ***7.2.9.4 Supercritical Fluid Chromatography (SFC).***

Axial temperature gradients could also be applied in SFC to improve separation performance, since SFC is considered to be a hybrid between GC and LC. Although pressure is the variable that has the greatest effect on the separation, temperature can also change the solvating power of the mobile phase.<sup>76-78</sup> Therefore, the use of axial temperature gradients in SFC could be considered as a means to enhance the separation performance.

### 7.3 REFERENCES

1. Ettre, L. S.; Hinshaw, J. V., *Basic Relationships of Gas Chromatography*. Advanstar Communications: Cleveland, 1993.
2. Phillips, J. B., Reducing GC Method Development Time - GC-SOS. *Anal. Chem.* **1995**, *67* (11), A360-A361.
3. Adahchour, M., *et al.*, Recent Developments in the Application of Comprehensive Two-dimensional Gas Chromatography. *J. Chromatogr. A* **2008**, *1186* (1-2), 67-108.
4. Bertsch, W., Two-dimensional Gas Chromatography. Concepts, Instrumentation, and Applications - Part 2: Comprehensive Two-dimensional Gas Chromatography. *J. High Resolut. Chromatogr.* **2000**, *23* (3), 167-181.
5. Blomberg, J., *et al.*, Comprehensive Two-dimensional Gas Chromatography (GC×GC) and Its Applicability to the Characterization of Complex (Petrochemical) Mixtures. *J. High Resolut. Chromatogr.* **1997**, *20* (10), 539-544.
6. Marriott, P.; Shellie, R., Principles and Applications of Comprehensive Two-Dimensional Gas Chromatography. *TrAC* **2002**, *21* (9-10), 573-583.
7. Beens, J., *et al.*, Proper Tuning of Comprehensive Two-Dimensional Gas Chromatography (GC×GC) to Optimize the Separation of Complex Oil Fractions. *J. High Resolut. Chromatogr.* **2000**, *23* (3), 182-188.
8. Phillips, J. B.; Jain, V., On-Column Temperature Programming in Gas Chromatography Using Temperature Gradients Along the Capillary Column. *J. Chromatogr. Sci.* **1995**, *33*, 543-550.
9. Reid, V. R., *et al.*, Investigation of High-Speed Gas Chromatography Using Synchronized Dual-Valve Injection and Resistively Heated Temperature Programming. *J. Chromatogr. A* **2007**, *1148*, 236-243.
10. Manz, A., *et al.*, Miniaturized Total Chemical Analysis Systems: A Novel Concept for Chemical Sensing. *Sens. Actuators B* **1990**, *1*, 244-248.
11. Terry, S. C.; Herman, J. C., A Gas Chromatographic Air Analyzer Fabricated on a Silicon Wafer. *IEEE Trans. Electron Devices* **1979**, *26*, 1880-1886.
12. Bhushan, A., *et al.*, Fabrication and Preliminary Results for LiGA Fabricated Nickel Micro Gas Chromatograph Columns. *J. Microelectromech. Syst.* **2007**, *16* (2), 383-393.
13. Bhushan, A., *et al.*, Fabrication of Micro-gas Chromatograph Column for Fast Chromatography. *Microsyst. Technol.* **2007**, *13*, 361-368.
14. Lambertus, G., *et al.*, Design, Fabrication, and Evaluation of Microfabricated Column for Gas Chromatography. *Anal. Chem.* **2004**, *76*, 2629-2637.
15. Lambertus, G., *et al.*, Silicon Microfabricated Column with Microfabricated Differential Mobility Spectrometer for GC Analysis of Volatile Organic Compounds. *Anal. Chem.* **2005**, *77* (23), 7563-7571.
16. Lu, C.-J., *et al.*, First-Generation Hybrid MEMS Gas Chromatograph. *Lab Chip* **2005**, *5*, 1123-1131.
17. Pai, R. S., *et al.* In *Microfabricated Gas Chromatograph for Trace Analysis*, Technologies for Homeland Security, Waltham, MA, 12-13 May; 2008; pp 150-154.

18. Reid, V. R., *et al.*, High-Speed, Temperature Programmable Gas Chromatography Utilizing a Microfabricated Chip With an Improved Carbon Nanotube Stationary Phase. *Talanta* **2009**, *77*, 1420-1425.
19. Stadermann, M., *et al.*, Ultrafast Gas Chromatography on Single-Wall Carbon Nanotube Stationary Phases in Microfabricated Channels. *Anal. Chem.* **2006**, *78* (15), 5639-5644.
20. Bartle, K. D., *et al.*, Rayleigh Instability of Stationary Phase Films in Capillary Column Chromatography. *J. High Res. Chromatogr. Chromatogr. Commun.* **1987**, *10*, 128-136.
21. Sumpter, R. S.; Lee, M. L., Enhanced Radial Dispersion in Open Tubular Column Chromatography. *J. Microcol. Sep.* **1991**, *3*, 91-113.
22. Radadia, A. D., *et al.*, The fabrication of All-silicon Micro Gas Chromatography Columns Using Gold Diffusion Eutectic Bonding. *J. Micromech. Microeng.* **2010**, *20* (1).
23. Radadia, A. D., *et al.*, Micromachined GC Columns for Fast Separation of Organophosphonate and Organosulfur Compounds. *Anal. Chem.* **2008**, *80* (11), 4087-4094.
24. Nishino, M., *et al.*, Development of  $\mu$  GC (Micro Gas Chromatography) with High Performance Micromachined Chip Column. *IEEJ Trans.* **2009**, *4* (3), 358-364.
25. Serrano, G., *et al.*, Assessing the Reliability of Wall-coated Microfabricated Gas Chromatographic Separation Columns. *Sensors and Actuators B-Chemical* **2009**, *141* (1), 217-226.
26. Nakai, T., *et al.*, Micro-fabricated Semi-packed Column for Gas Chromatography by Using Functionalized Parylene as a Stationary Phase. *J. Micromech. Microeng.* **2009**, *19* (6).
27. Reid, V. R.; Synovec, R. E., High-Speed Gas Chromatography: The Importance of Instrumentation Optimization and the Elimination of Extra-Column Band Broadening. *Talanta* **2008**, *76*, 703-717.
28. Radadia, A. D., *et al.*, Partially Buried Microcolumns for Micro Gas Analyzers. *Anal. Chem.* **2009**, *81* (9), 3471-3477.
29. Lee, M. L., *et al.*, Fused Silica Capillary Columns Technology for Gas Chromatography. *J. Chromatogr. Sci.* **1984**, *22*, 136-142.
30. Woolley, C. L., *et al.*, Deactivation of Small Diameter Fused Silica Capillary Columns with Organosilicon Hydrides. *J. High Res. Chromatogr. Chromatogr. Commun.* **1986**, *9*, 506-514.
31. Gross, G. M., *et al.*, High-speed Gas Chromatography Using Synchronized Dual-valve Injection. *Anal. Chem.* **2004**, *76*, 3517-3524.
32. Contreras, J. A., *et al.* In *Theoretical and Practical Justification of Thermal Gradient Gas Chromatography*, PITTCON, Chicago, IL, March; 2009.
33. Contreras, J. A.; Lee, M. L. In *Analytical Gradient Focusing Separation Techniques*, 236th American Chemical Society Philadelphia, PA, August; 2008.
34. Rubey, W. A., A Different Operational Mode for Addressing the General Elution Problem in Rapid Analysis Gas Chromatography. *J. High Resolut. Chromatogr.* **1991**, *14*, 542-548.

35. Lee, M. L., *et al.* In *New Frontiers in Gas Chromatography-Reincarnation of Old Ideas*, ISCCE, Portland, Oregon, May 18-19; 2009.
36. Watson, N. E., *et al.*, Comprehensive Three-dimensional Gas Chromatography with Parallel Factor Analysis. *Anal. Chem.* **2007**, *79*, 8270-8280.
37. Cooke, W. S., Multicapillary Columns: an Idea Whose Time has Come. *Today Chem. Work* **1996**, *1*, 16-20.
38. Rosenkranz, B.; Bettmer, J., Rapid Separation of Elemental Species by Multicapillary GC. *Anal. Bioanal. Chem.* **2002**, *373* (6), 461-5.
39. Contreras, J. A., *et al.* In *Moving Wave Temperature Gradient Gas Chromatography*, 32<sup>nd</sup> International Symposium on Capillary Chromatography and 5<sup>th</sup> GC×GC Symposium, Riva del Garda Italy, May; 2008.
40. Fenimore, D. C., Gradient Temperature Programming of Short Capillary Columns. *J. Chromatogr.* **1975**, *112*, 219-227.
41. Greibrokk, T., Heating or Cooling LC Columns. *Anal. Chem.* **2002**, *74* (13), 374A-378A.
42. Greibrokk, T.; Andersen, T., High-temperature Liquid Chromatography. *J. Chromatogr. A* **2003**, *1000* (1-2), 743-755.
43. Vanhoenacker, G.; Sandra, P., High Temperature and Temperature Programmed HPLC: Possibilities and Limitations. *Anal. Bioanal. Chem.* **2008**, *390* (1), 245-248.
44. Sheng, G. C., *et al.*, Elevated Temperature Liquid Chromatography Using Reversed-phase Packed Capillary Columns. *J. Microcol. Sep.* **1997**, *9* (2), 63-72.
45. Tran, B. Q., *et al.*, The Influence of Stop-flow on Band Broadening of Peptides in Micro-liquid Chromatography. *Chromatographia* **2006**, *64* (1-2), 1-5.
46. Sander, L. C.; Wise, S. A., The Influence of Column Temperature on Selectivity in Reversed-phase Liquid Chromatography for Shape-constrained Solutes. *J. Sep. Sci.* **2001**, *24* (12), 910-920.
47. Holm, A., *et al.*, Novel Column Oven Concept for Cold Spot Large Volume Sample Enrichment in High Throughput Temperature Gradient Capillary Liquid Chromatography. *J. Sep. Sci.* **2003**, *26* (12-13), 1147-1153.
48. Bruheim, I., *et al.*, Temperature-programmed Packed-capillary Liquid Chromatographic Separation of Polystyrenes. *Chromatographia* **2001**, *53*, S266-S270.
49. Molander, P., *et al.*, The Impact of Column Inner Diameter on Chromatographic Performance in Temperature Gradient Liquid Chromatography. *Analyst* **2003**, *128* (11), 1341-1345.
50. Padaruskas, A., CE Determination of Small Ions: Methods and Techniques. *Anal. Bioanal. Chem.* **2006**, *384* (1), 132-144.
51. Pumera, M., Analysis of Explosives Via Microchip Electrophoresis and Conventional Capillary Electrophoresis: A Review. *Electrophoresis* **2006**, *27* (1), 244-256.
52. Sinville, R.; Soper, S. A., High Resolution DNA Separations Using Microchip Electrophoresis. *J. Sep. Sci.* **2007**, *30* (11), 1714-1728.
53. Asensio-Ramos, M., *et al.*, Food Analysis: A Continuous Challenge for Miniaturized Separation Techniques. *J. Sep. Sci.* **2009**, *32* (21), 3764-3800.

54. Bruns, M. W., High-Speed Portable Gas-Chromatography - Silicon Micromachining. *Erdol & Kohle Erdgas Petrochemie* **1994**, 47 (3), 80-84.
55. Zampolli, S., *et al.*, Real-time Monitoring of Sub-ppb Concentrations of Aromatic Volatiles with a MEMS-enabled Miniaturized Gas-chromatograph. *Sensors and Actuators B-Chemical* **2009**, 141 (1), 322-328.
56. Hernandez-Borges, J., *et al.*, Recent Applications in Nanoliquid Chromatography. *J. Sep. Sci.* **2007**, 30 (11), 1589-1610.
57. Borowsky, J. F., *et al.*, Electroosmotic Flow-Based Pump for Liquid Chromatography on a Planar Microchip. *Anal. Chem.* **2008**, 80 (21), 8287-8292.
58. Lazar, I. M., *et al.*, Microfluidic Liquid Chromatography System for Proteomic Applications and Biomarker Screening. *Anal. Chem.* **2006**, 78 (15), 5513-5524.
59. Shih, C. Y., *et al.*, An Integrated System for On-chip Temperature Gradient Interaction Chromatography. *Sensor. Actuat. A-Phys.* **2006**, 127 (2), 207-215.
60. Shih, C. Y., *et al.*, On-chip Temperature Gradient Interaction Chromatography. *J. Chromatogr. A* **2006**, 1111 (2), 272-278.
61. Tran, J. V., *et al.*, Temperature Effects on Retention in Reversed Phase Liquid Chromatography. *J. Sep. Sci.* **2001**, 24 (12), 930-940.
62. Shackman, J. G.; Ross, D., Counter-flow Gradient Electrofocusing. *Electrophoresis* **2007**, 28 (4), 556-571.
63. Sommer, G. J., *et al.*, Theoretical and Numerical Analysis of Temperature Gradient Focusing Via Joule Heating. *Lab Chip* **2007**, 7 (7), 898-907.
64. Becker, M., *et al.*, Temperature Gradient Focusing in Miniaturized Free-flow Electrophoresis Devices. *Electrophoresis* **2009**, 30 (24), 4206-4212.
65. Ross, D.; Locascio, L. E., Microfluidic Temperature Gradient Focusing. *Anal. Chem.* **2002**, 74 (11), 2556-2564.
66. Matsui, T., *et al.*, Temperature Gradient Focusing in a PDMS/glass Hybrid Microfluidic Chip. *Electrophoresis* **2007**, 28 (24), 4606-4611.
67. Hoebel, S. J., *et al.*, Scanning Temperature Gradient Focusing. *Anal. Chem.* **2006**, 78 (20), 7186-7190.
68. Huber, D. E.; Santiago, J. G., Taylor-Aris dispersion in Temperature Gradient Focusing. *Electrophoresis* **2007**, 28 (14), 2333-2344.
69. Tolley, H. D., *et al.*, Equilibrium Gradient Methods With Nonlinear Field Intensity Gradient: A Theoretical Approach. *Anal. Chem.* **2002**, 74 (17), 4456-4463.
70. Sun, X. F., *et al.*, Performance Optimization in Electric Field Gradient Focusing. *J. Chromatogr. A* **2009**, 1216 (1), 159-164.
71. Sun, X. F., *et al.*, Bilinear Electric Field Gradient Focusing. *J. Chromatogr. A* **2009**, 1216 (37), 6532-6538.
72. Lin, S. L., *et al.*, Programed Elution and Peak Profiles in Electric Field Gradient Focusing. *Electrophoresis* **2008**, 29 (5), 1058-1066.
73. Lin, J. M., *et al.*, Temperature Effect on Chiral Recognition of Some Amino Acids with Molecularly Imprinted Polymer Filled Capillary Electrochromatography. *Biomed. Chromatogr.* **1997**, 11 (5), 298-302.
74. Lin, J. M., *et al.*, Enantiomeric Resolution of Dansyl Amino Acids by Capillary Electrochromatography Based on Molecular Imprinting Method. *Chromatographia* **1998**, 47 (11-12), 625-629.

75. Rathore, A. S., *et al.*, Joule Heating in Packed Capillaries Used in Capillary Electrochromatography. *Electrophoresis* **2002**, *23* (17), 2918-2928.
76. Baker, L. R., *et al.*, Density Gradients in Packed Columns: II. Effects of Density Gradients on Efficiency in Supercritical Fluid Separations. *J. Chromatogr. A* **2009**, *1216* (29), 5594-5599.
77. Baker, L. R., *et al.*, Density Gradients in Packed Columns I. Effects of Density Gradients on Retention and Separation Speed. *J. Chromatogr. A* **2009**, *1216* (29), 5588-5593.
78. Poe, D. P.; Schroden, J. J., Effects of Pressure Drop, Particle Size and Thermal Conditions on Retention and Efficiency in Supercritical Fluid Chromatography. *J. Chromatogr. A* **2009**, *1216* (45), 7915-7926.